Attachment 1
NRC3-10-0006

Response to RAI Letter No. 16
(eRAI Tracking No. 3913)

RAI Question No. 02.05.01-3

RAI 02.05.01-03

FSAR Sections 2.5.1.1.4.1.1 and 2.5.3.2.2 provide limited discussions on the effects of glacial isostatic adjustments (GIA). FSAR Section 2.5.1.1.4.1.1 states that GIA is "suspected to be a cause of deformation within continental plates and may be a trigger of seismicity in eastern North America and other formerly glaciated regions." Please provide additional discussion of the following:

a. The potential GIA effects that might impact the seismic hazard in the Fermi site region

b. The geodetic strain rates that are currently measured in the site region

c. Any unusual strain gradients in the region and if there is any indication of localized strain on or near potential seismogenic structures

d. Any deformed glacial shorelines and whether or not the shoreline deformation can be explained solely by GIA processes

Response

a. *The potential GIA effects that might impact the seismic hazard in the Fermi site region*

Mazzotti and Adams (Reference 2.5.1-293) state "The spatial distribution of areas of high Holocene seismicity in eastern North America is commonly explained by the isostatic stress perturbation in the lithosphere associated with the melting of the Laurentide ice sheet about 19,000 to 8,000 years ago." In support of this statement, they cite Reference 2.5.1-484; Reference 2.5.1-485; Reference 2.5.1-292; Reference 2.5.1-460; and Reference 2.5.1-480.

Mazzotti and Adams (Reference 2.5.1-293) provide a discussion of this hypothesis and conclude that it is likely that only a very small percentage of the elastic postglacial rebound deformation translates into plastic deformation to produce earthquakes. They note that although models of postglacial rebound adjustments can be used to predict three-dimensional velocity, strain, and stress fields in the lithosphere, recent analyses by various researchers show that the horizontal components appear to be quite sensitive to the model parameters (e.g., viscosity profiles of the mantle, ice load history, ambient tectonic stress), leading to significant variations in the predicted horizontal velocities, strain, and stress rates.

Modeling of the strain and resulting changes in seismic stress caused by GIA in other areas (e.g., New Madrid seismic zone [Reference 2.5.1-460] and eastern Canada [Reference 2.5.1-293]) indicates that the effects on seismicity rates are expected to remain essentially unchanged over a few hundred to thousands of years. Therefore, it is not expected that seismicity rates in the site region will vary significantly in the future due to GIA.

b. *The geodetic strain rates that are currently measured in the site region*

Motions from 360 Global Positioning System (GPS) sites in Canada and the United States yield a detailed image of vertical and horizontal velocity fields within the nominally stable interior of the North American Plate (Reference 2.5.1-291) (Figures 2.5.1-253 and 2.5.1-254). Sella et al. (Reference 2.5.1-291) note that by far the strongest signal is the effect of GIA due to ice mass unloading during deglaciation. Vertical velocities show present-day uplift (approximately 10 mm/yr) near Hudson Bay, the site of thickest ice at the last glacial maximum. The uplift rates generally decrease with distance from Hudson Bay and change to subsidence (1 to 2 mm/yr) south of the Great Lakes.

As previously noted in the Fermi 3 FSAR, Revision 1, Section 2.5.1.1.4.1.1:

> "...the hinge line marking the approximate boundary between regions of vertical rebound to the north and subsidence to the south lies close to the northern margin of the site region. The site lies at the southern margin of the region affected by GIA. The residual velocity field indicates subsidence (1 – 2 mm/yr) throughout most of the site region, with possible minor uplift near the western end of Lake Erie (Reference 2.5.1-291). Data from water level gauges along the Great Lakes show subsidence along the southern shores of the Great Lakes (Reference 2.5.1-298)."

c. *Any unusual strain gradients in the region and if there is any indication of localized strain on or near potential seismogenic structures*

There are no known anomalies or strain gradients in the site region that are inconsistent with the GIA deformation pattern or are of sufficient amplitude to be detected. Horizontal motions show outward motions from Hudson Bay with complex local variations, especially in the far field (Figure 2.5.1-254). Comparison of GIA model predictions using four different upper mantle viscosity models to residual horizontal motions created by removing rigid plate motion from the GPS data shows significant misfits that are likely due to uncertainties associated with the ice load history, and to the assumption of laterally homogeneous rheology (Figure 1). Some of the horizontal scatter may reflect a combination of local site effects (noise) and intraplate tectonic signal. (Reference 2.5.1-291)

Monitoring of present-day tilting of the Great Lakes region based on water level gauges illustrates uplift in the northeast and subsidence in the south, indicating a pattern of land tilting upward to the northeast consistent with expected GIA (Figure 2)(Reference 2.5.1-298). The data are consistent with the geodetic data that show the Fermi 3 site and surrounding region are not characterized by strong vertical gradients or anomalies.

d. *Any deformed glacial shorelines and whether or not the shoreline deformation can be explained solely by GIA processes*

Glacial and postglacial GIA in the study region is evidenced by deformation (tilting or warping) of glacial lake strandlines (relict shorelines). Detailed mapping of strandlines and

shoreline features related to glacial lakes provides information on the location of the 'zero isobase' (also referred to as the 'hinge line') for several individual relict lake strandlines (Reference 2.5.1-274; Reference 2.5.1-294; Reference 2.5.1-296). The zero isobase or hinge line represents the general location of the boundary between a 'zone of horizontality' and zones of warping or relative uplift. Early rebound concepts of immediate rebound north of a hinge line were eventually replaced, and it is now recognized that there was continued uplift and rebound over much of the region in the Holocene (Reference 2.5.1-295). Geodynamical models that predict how the viscous mantle of the earth moves under surface loads show that the glacioisostatic recovery with a northward migration of a collapsing forebulge for the Great Lakes is a more appropriate model (Reference 2.5.1-486).

Figure 2.5.1-251 shows a summary plot of elevation versus distance of raised and uplifted shorelines of Whittlesey and subsequent lake phases, as well as elevations of submerged features in the Lake Erie basin as compiled by Coakley and Lewis (Reference 2.5.1-296). Plotting of strand elevation points for Lake Whittlesey in the Lake Erie basin yields a direction of maximum differential uplift of N24°E (Figure 2.5.1-252) and suggests that post-Whittlesey uplift, relative to altitudes in the zone of horizontality, has been 52 m (171 ft) at Buffalo, New York. Similarily, relative uplift since the lowest Lake Warren time has been about 43 m (141 ft) at Buffalo and 66 m (217 ft) at its most northern point, 13 km north of Batavia, New York. (Reference 2.5.1-297)

In Michigan, the Lake Whittlesey, Lake Maumee, and Lake Arkona beaches were observed to rise northward from within an area located north of Detroit. The hinge line of the younger Lake Warren and Lake Wayne strands, and of Lakes Grassmere and Lundy were recognized in the Lake Huron basin about 20 km (12.4 mi) and 117 km (72.7 mi) north of the Lake Whittlesey hinge line. (Reference 2.5.1-297).

Holcombe et al. (Reference 2.5.1-487) provides a revised Lake Erie postglacial lake-level history based on new detailed bathymetry. Previous reconstructions (e.g., Reference 2.5.1-296; Reference 2.5.1-297) varied in detail and water levels, but shared the following salient features: (1) high lake level stages of proglacial lakes and Lake Algonquin followed by very low lake levels in early Holocene time; (2) isostatic rebound and concomitant gradual rise in lake levels in the early Holocene; (3) stable or slowly rising lake levels in Middle Lake Erie time; (4) rise in lake levels accompanying the Nipissing rise to slightly higher than at present; and (5) lowering of lake levels to just below present level following the Nipissing rise event. The reconstructions recognize that the lake level has been controlled since deglaciation by isostatically rebounding outlet sills of the Niagara River, and that the Nipissing rise accompanied a shift in upper Great Lakes drainage from the North Bay outlet to the Port Huron outlet. In the new model, Holcombe et al. (Reference 2.5.1-487) note that in an isostatically rebounding lake, lake level histories vary with location, especially as a function of distance from the outlet sill. A new feature of the model is a proposed extended period of low lake level in the middle Holocene (9 to 6 ka), when lake level was controlled not by the level of the outlet sill, but by climate and water budget. Also contributing to a low water level during this time was flooding of the central basin of Lake Erie as isostatic rebound continued, greatly increasing lake surface area and concomitantly increasing surface

evaporation. At the time of the Nipissing rise (5,400 to 3,600 years ago, water level in eastern Lake Erie was 4 to 5 m (13 to 16.4 ft) higher than present. The western subbasin was flooded, but water level was about 3 m (10 ft) below present lake level.

The FSAR Revision 1 incorrectly stated that

> The Port Huron shoreline (approximately 13,000 years BP) was uplifted approximately 197 ft (60 m) between 11,000 and 7,000 years BP (Reference 2.5.1-272),

This statement should have read that a geophysical model (a dynamic model of glacioisostatic recovery with northward migration of a collapsing forebulge) suggests that Port Huron outlet was uplifted about 60 m (197 ft) between 11,000 and 7,000 years BP (Reference 2.5.1-272). Lewis et al. (Reference 2.5.1-272) note that the model findings are not necessarily consistent with geological data and inferences of former shorelines and runoff drainage patterns at the Port Huron outlet, suggesting that additional reconsideration of the data was needed.

Farrand (Reference 2.5.1-295) discusses evidence for uplift at Port Huron, which is the major outlet for glacial lakes as well as present-day Lake Huron (Figure 3). The earliest shorelines recorded at Port Huron, which have been uplifted 18 m (59 ft) show no differential uplift from earliest to latest Maumee times. Glacial Lake Whittlesey, the next youngest glacial lake, has been uplifted about 8.2 m (27 ft), and the Warren beach at Port Huron now lies at 215 m (705 ft), suggesting about 5.2 m (17 ft) of uplift. The Grassmere, Lundy, and Algonquin beaches at Port Huron exhibit no uplift. Farrand (Reference 2.5.1-295) therefore concluded that the rate of postglacial uplift (rebound) was very great at the time of deglaciation but it decelerated rapidly toward the present day.

In conclusion, deformation of glacial lake strandlines (relict shorelines) in the site region described in the literature is consistent with GIA. It is proposed that the statement regarding the uplift at Port Huron will be deleted in a future revision.

Figure 1. Comparison of GIA Model Predictions to Horizontal GPS Data

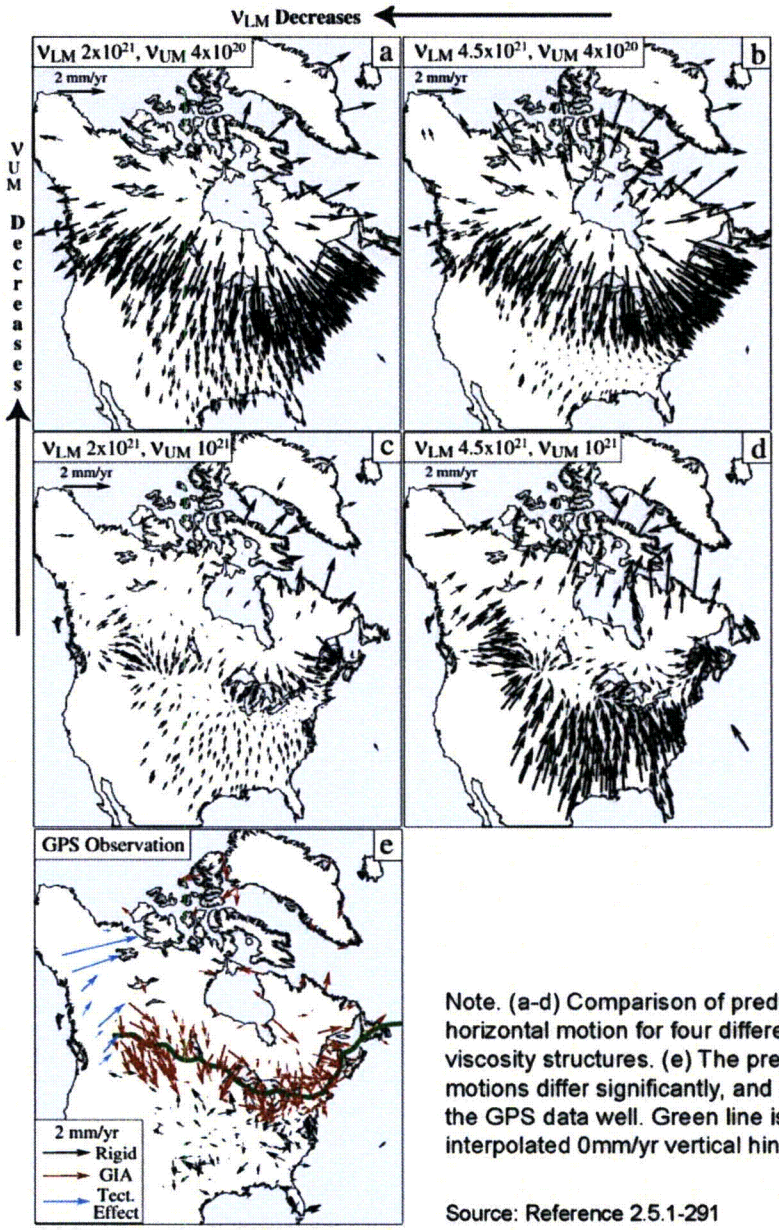

Note. (a-d) Comparison of predicted horizontal motion for four different viscosity structures. (e) The predicted motions differ significantly, and none fit the GPS data well. Green line is interpolated 0mm/yr vertical hinge line.

Source: Reference 2.5.1-291

Figure 2. Vertical Velocity Based on Water Level 1 Changes

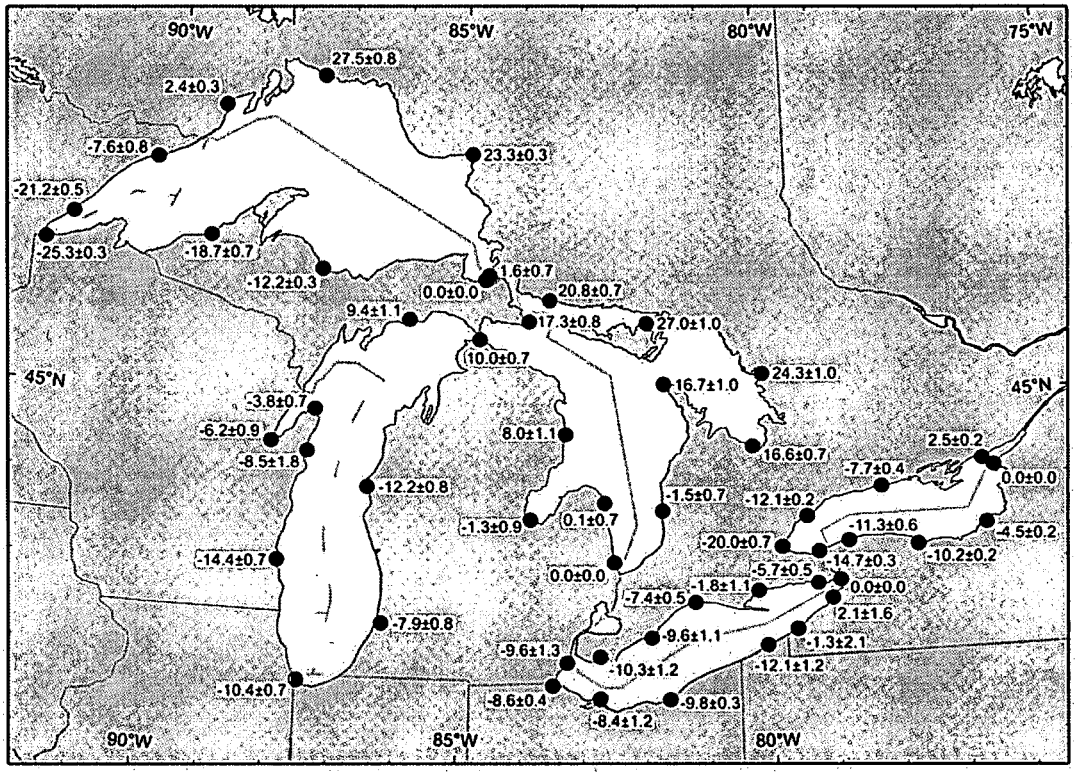

Note. Vertical velocity and standard error relative to each outlet: Cape Vincent for Lake Ontario, Buffalo for Lake Erie, Lakeport for Lakes Michigan-Huron, Point Iroquois for Lake Superior, in centimeters per century.

Source: Reference 2.5.1-298

Figure 3. Glacial Lake Inundation and Outlet Controls.

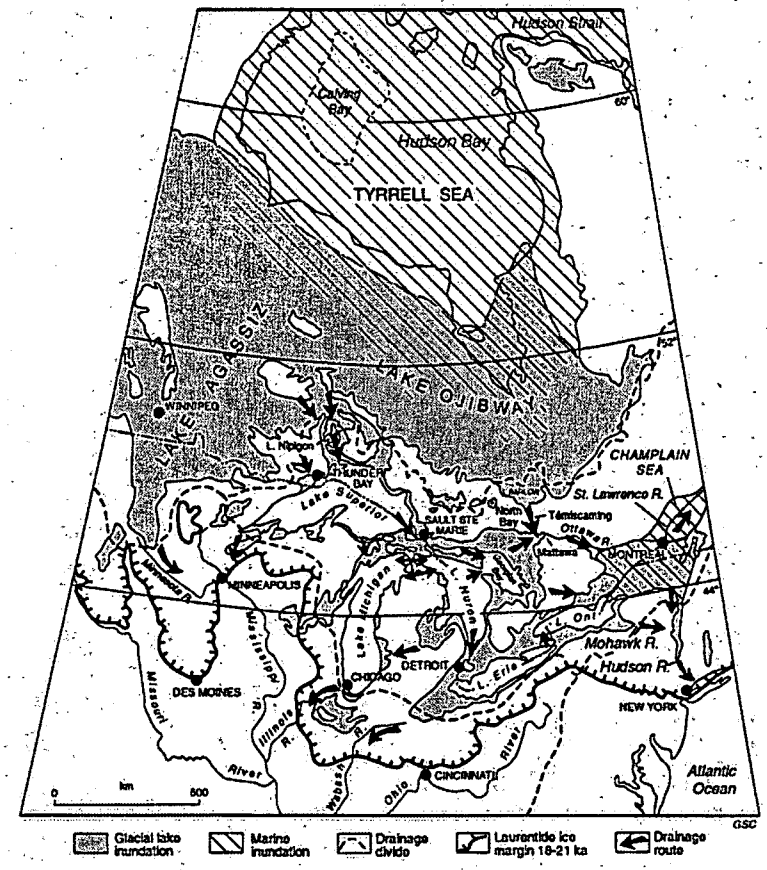

Map showing location of the Lake Huron basin in relation to drainage divides in central North America, the 18–21 ka BP glacial maximum, and glacial lakes Agassiz, Ojibway and Barlow. The cumulative areas of inundation by glacial lake and marine waters are shown together with routes (arrows) of principal lake outlets (adapted from Teller, 1987;

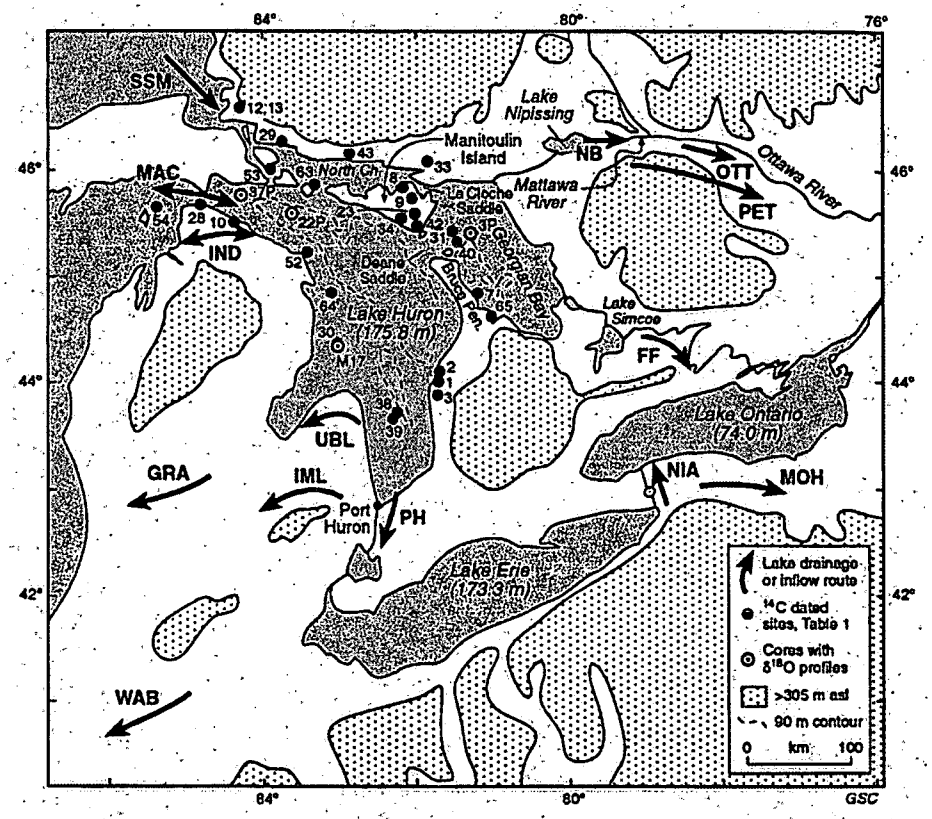

Map showing regional relief above the 305 m contour, the 90 m isobath in Lake Huron and Georgian Bay, and flow direction through lake outlets of the Huron basin including Georgian Bay and the Nipissing–Mattawa lowland. Numerals refer to positions of radiocarbon-dated sites listed in Table 1, and cores with $\delta^{18}O$ profiles. The arrows represent drainage routes and lake outlets as follows: FF — Fenelon Falls; GRA — Grand River valley; IML — Imlay channel; IND — Indian River lowland; MAC — Straits of Mackinac; MOH — Mohawk River valley; NIA — Niagara River; NB — North Bay outlet; OTT — Ottawa River valley; PET — Petawawa; PH — Port Huron; SSM — Sault Ste. Marie; UBL — Ubly; WAB — Wabash River valley.

Source: Reference 2.5.1-272

Markup of Detroit Edison COLA
(following 13 pages)

The following markup represents how Detroit Edison intends to reflect this RAI response in a future submittal of the Fermi 3 COLA. However, the same COLA content may be impacted by revisions to the ESBWR DCD, responses to other COLA RAIs, other COLA changes, plant design changes, editorial or typographical corrections, etc. As a result, the final COLA content that appears in a future submittal may be different than presented here.

Illinoian and prior to the late Wisconsinan (MIS 5-3), a period of approximately 130,000 years.

In Illinois the Farmdale and Sangamon geosols developed during this time and are dated by the accumulation of cosmogenic ^{10}Be in the soil horizon (Reference 2.5.1-261).

2.5.1.1.2.3.4.3 Late Pleistocene Events (MIS 2)

The ice sheet had a major expansion between 25,000 and 15,000 years ago (BP), as indicated by the low sea-level stand and magnitude of the oxygen isotopic excursion of MIS 2 (Reference 2.5.1-267). The many glacial advances of the late Wisconsinan, also known as the Woodfordian Substage, are referred to as stades or stadials (assumed to be cold periods). Periods of ice retreat are referred to as interstadials and are assumed to be warmer (Reference 2.5.1-256) (Figure 2.5.1-215, Reference 2.5.1-256). However, ice lobes advance in response to dynamics of the ice sheet, which have large time lags, and do not respond concurrently to local climate (Reference 2.5.1-254).

The first late Wisconsinan advance of the Michigan lobe is dated at approximately 24,000 radiocarbon years BP (Reference 2.5.1-256). In Ontario (Reference 2.5.1-268) and in Ohio, the Ontario and Huron-Erie lobes reached their maximum extent between 23,000 and 21,000 years BP, respectively, during the Late Wisconsinan. The first advance into Ohio occurred shortly after 24,600 radiocarbon years BP (Reference 2.5.1-269, as cited in Reference 2.5.1-270). The outer moraines of the Scioto lobe are overlapping and suggest some oscillation in the ice front when it was in Ohio, approximately 21,400 years BP (Reference 2.5.1-270). This was followed in Ohio by a withdrawal of ice referred to as the Erie Interstade, which occurred approximately 16,000 radiocarbon years BP. This period is documented by a lake that formed in the Erie basin as the ice retreated into Ontario. No forests developed on the deglaciated landscape during this time and there is no good radiocarbon control to document this interval. (Reference 2.5.1-268)

Post-Erie Interstade tills are silty and clayey (Reference 2.5.1-271). The fine-grained till matrix (Reference 2.5.1-268) as well as areas of preserved lake sediment in the subsurface are used to infer the former presence of a lake that was completely overridden by the subsequent ice advances. In Michigan all but the Saginaw lobe readvanced to near their former positions. This allowed the Huron/Erie and Michigan lobes to

expand into the area vacated by the Saginaw lobe during Post-Erie Interstade events.

Add "Insert 1" Here

Lewis et al. (Reference 2.5.1-272) provide a summary time-distance diagram of lake levels for the Late Wisconsinan through the Holocene (Figure 2.5.1-216, Reference 2.5.1-272).

2.5.1.1.2.3.4.4 Latest Pleistocene to Holocene Lake History and the Final Glacial Advances

During the next withdrawal of ice, referred to as the Mackinaw Interstade, most of the lower peninsula of Michigan was ice free (Reference 2.5.1-263). This was followed by another advance during the Port Huron Stade at about 13,000 years BP. Lakes that had formed during the Mackinaw Interstade in the regional basins were forced to higher levels. Collectively referred to as Lake Whittlesey, these lakes occupied part of the Huron, Erie, and Saginaw basins. The tills of the Port Huron Stade are fine grained, and the lobes appeared to have fluctuated to create two closely spaced moraines. (Reference 2.5.1-263)

As ice retreated, a series of lower lakes formed in the Great Lakes basins with continuous and discernable shorelines and outlets. Retreat was far enough north to allow waters of Lake Superior, containing red clays, to spill into the waters of the more southerly Great Lakes. All subsequent advances through the Huron and Michigan basins were therefore tinted red with the clays of Lake Superior. (Reference 2.5.1-263)

The next to last advance occurred approximately 11,700 years BP and is called the Greatlakean Substage (Reference 2.5.1-273). This advance is well dated in eastern Wisconsin where the Two Creeks Forest Bed was sheared off by the advancing ice. The ice lobe responsible for this shearing occupied the northern half of the Lake Michigan basin, raised lake levels once more, deposited red clayey till in western Michigan, and shaped the drumlin fields of northwestern Michigan. (Reference 2.5.1-256)

An unnamed interstade followed and the lakes within the site region reached the Algonquin high stand (lake water level). Water was confluent across the Lower Peninsula of Michigan and through the Straits of Mackinac (Reference 2.5.1-274). This was followed by declining lake levels as waters found new, lower outlets to the north with continued ice retreat. Most drainage eventually found its way to the Ottawa River Valley, a marine estuary. When the area now occupied by North Bay,

for Fermi 3. The following sections describe the region in terms of (1) the contemporary tectonic stress environment (Subsection 2.5.1.1.4.1); (2) regional geophysical data sets that have been used to evaluate basement geology and structures (Subsection 2.5.1.1.4.2); (3) primary structural provinces and tectonic features within the 320-km (200-mi) radius of the site (Subsection 2.5.1.1.4.3); and (4) significant seismic sources at distances greater than 320 km (200 mi) (Subsection 2.5.1.1.4.4). Historical seismicity is shown on Figure 2.5.1-207 described in Subsection 2.5.1.1.4 and discussed in more detail in Subsection 2.5.2.1.

2.5.1.1.4.1 Contemporary Tectonic Stress Environment

Fermi 3 lies within a compressive midplate stress province, characterized by a relatively uniform east-northeast compressive stress field that extends from the midcontinent east toward the Atlantic continental margin and possibly into the western Atlantic basin (Reference 2.5.1-287). Zoback and Zoback (Reference 2.5.1-287) note that although localized stresses may be important in places, the overall uniformity in the midplate stress pattern suggests a far-field source, and the range in orientations coincides with both absolute plate motion and ridge push directions for North America. Modeling of various tectonic processes using an elastic finite-element analysis has indicated that distributed ridge forces are capable of accounting for the dominant east-northeast trend of maximum compression throughout much of the North American plate east of the Rocky Mountains (Reference 2.5.1-288).

Based on analysis of well-constrained focal mechanisms of North American midplate earthquakes, Zoback (Reference 2.5.1-289) concludes that earthquakes in the CEUS occur primarily on strike-slip faults that dip between 43 and 80 degrees, primarily in the range of 60 to 75 degrees and primarily in response to a strike-slip stress regime. This is indicated by a more recent compilation of worldwide stress information that shows east-northeast-oriented maximum horizontal compression and strike-slip events within the study region (Reference 2.5.1-290) (Figure 2.5.1-219).

2.5.1.1.4.1.1 Glacial Isostatic Adjustments

Post-glacial rebound or glacial isostatic adjustment (GIA) is the response of the solid earth to changing surface loads brought on by the waxing and

waning of large-scale ice sheets and glaciers. Tilting of relic lake shorelines, changes to modern lake levels, and secular (persisting for a long time) changes to surface gravity observations are manifestations of land uplift and subsidence brought about by GIA (Reference 2.5.1-291). ~~GIA is also suspected to be a cause of deformation within continental plates and may be a trigger of seismicity in eastern North America and other formerly glaciated regions (Reference 2.5.1-292; Reference 2.5.1-293).~~

Add "Insert 2" Here

~~The Port Huron shoreline (approximately 13,000 years BP) was uplifted approximately 60 m (197 ft) between 11,000 and 7,000 years BP (Reference 2.5.1-272), and shorelines dated between 10,500 and 4,700 years BP were upwarped, with more uplift occurring in the north (Reference 2.5.1-294). Early rebound concepts of immediate rebound north of a "hinge line" were eventually replaced, and it is now recognized that there was continued uplift and rebound over the entire region through the Holocene (Reference 2.5.1-295). Rebound information is most easily conveyed in plots of the elevation of a given shoreline across a distance (Reference 2.5.1-296).~~

Larsen (Reference 2.5.1-274) reviewed various historical measurements and concluded that uplift continues to the present. In Lake Erie the directional trend in uplift does not strictly correlate with those of proposed isostatic rebound, but is very small (less than 64 mm/century) (Reference 2.5.1-297). ~~Minor climate fluctuations during the Holocene may have affected lake levels on the order of 1 to 2 m (3.3 to 6.6 ft), although this is difficult to prove (Reference 2.5.1-274).~~ The main control on the level of Lake Erie now is the elevation of the Onondaga Limestone at Buffalo, New York (Reference 2.5.1-297), which is 25 km (~~8200 ft~~) upriver from Niagara Falls and has experienced some uplift ~~(Reference 2.5.1-296).~~ The outflow through the Niagara appears to have been variable; retreat of the falls is estimated to have been 1.6 m (5.25 ft) per year since its inception 12,400 years ago and 1.1 m/yr (3.6 ft/yr) between 1670 and 1969 (Reference 2.5.1-297). ~~The complexity of lake-level history is not adequately accounted for in previous models, suggesting that neotectonics may influence lake-level history (Reference 2.5.1-296).~~

15.5 mi

Add "Insert 3" Here

~~Recent observations of Glacial Isostatic Adjustment (GIA) from Global Positioning System (GPS) velocity field data indicate that the~~ hinge line marking the approximate boundary between regions of vertical rebound

to the north and subsidence to the south lies close to the northern margin of the site region. The site lies at the southern margin of the region affected by GIA. The residual velocity field indicates subsidence (1 ~~+~~ 2 mm/yr) throughout most of the site region with possible minor uplift near the western end of Lake Erie (Reference 2.5.1-291). ~~Data from water level gauges along the Great Lakes show subsidence along the southern shores of the Great Lakes (Reference 2.5.1-298).~~

to

Add "Insert 4" Here

2.5.1.1.4.2 **Regional Geophysical Data**

Regional gravity and magnetic survey maps are important data sets that in conjunction with borehole data and regional seismic profile surveys have been used to decipher major structural and rheological boundaries within the basement underlying the site region.

2.5.1.1.4.2.1 **Gravity and Magnetic Survey Data and Maps**

Regional gravity and magnetic survey data and derivative maps are used to study the basement geology of the midcontinent region, including the lithology and depth of basement rocks and the location and origin of basement structures. Patterns and lineaments on gravity maps are used to infer faults, structure boundaries, and the boundaries between basement provinces. Strong magnetic anomalies are used to infer basalt and related mafic igneous rock which are often associated with basement rifts.

Portions of the Gravity Anomaly Map of North America (Reference 2.5.1-299) and the Magnetic Anomaly Map of North America (Reference 2.5.1-300) covering the site region are reproduced as Figure 2.5.1-220 and Figure 2.5.1-221, respectively. Several prominent gravity anomalies are shown on Figure 2.5.1-220, including the Mid-Michigan Gravity Anomaly (MGA), the East Continent Gravity High (ECGH), the Anorthosite Complex Anomaly (ACA), the Seneca anomaly, and the Butler anomaly (Reference 2.5.1-301; Reference 2.5.1-302; Reference 2.5.1-227; Reference 2.5.1-303).

The MGA, located in the southern peninsula of Michigan, is associated with the midcontinent gravity anomaly, which extends southwestward from Lake Superior. Both anomalies are associated with the midcontinent rift system (MRS) and are characterized by a strong, curvilinear gravity high flanked by gravity lows, and both are associated with magnetic highs (Reference 2.5.1-301).

Insert 1 located at end of section 2.5.1.1.2.3.4.3

Following the retreat of Late Woodfordian ice from the Lake Erie basin about 14,500 years ago, a series of lakes formed at high levels. These lakes, commonly referred to as glacial or deglacial lakes, were direct ancestors of present Lake Erie. The lakes, which can be grouped into proglacial (ice-dammed) and nonglacial low lake phases, resulted from repeated ice-marginal readvances, crustal warping due to glacial unloading and reloading, and downcutting of lake outlets during the overall ice-sheet dissipation. (Reference 2.5.1-297) Strandline features and deposits associated with these deglacial lake levels in the Fermi 3 site vicinity are discussed in Section 2.5.1.2.3.2.1. The early lakes first resided in Lake Erie and later expanded into the Lake Huron basin when ice retreated north of Port Huron. The retreat of ice was oscillatory with major recessions during the Lake Erie Interstade (about 15.5 ka), the Mackinaw Interstade (about 13.2 ka), and the Two Creeks Interstade (about 11.9 ka). (Reference 2.5.1-272) Lewis et al. (Reference 2.5.1-272) provide a summary time-distance diagram of lake levels for the Late Wisconsinan through the Holocene (Figure 2.5.1-216, Reference 2.5.1-272).

Insert 2 located at end of first paragraph in section 2.5.1.1.4.1.1

GIA is suspected to be a cause of deformation within continental plates and may be a trigger of seismicity in eastern North America and other formerly glaciated regions (Reference 2.5.1-292). The spatial distribution of Holocene high seismicity areas in eastern North America is commonly explained by the isostatic stress perturbation in the lithosphere associated with the melting of the Laurentide ice sheet about 19,000 – 8,000 years ago (Reference 2.5.1-484; Reference 2.5.1-485; Reference 2.5.1-292; Reference 2.5.1-460; Reference 2.5.1-480). Mazzotti and Adams (Reference 2.5.1-293), however, provide a discussion of this hypothesis and conclude that it is likely that only a very small percentage of the elastic postglacial rebound deformation translates into plastic deformation to produce earthquakes. Modeling of the strain and resulting changes in seismic stress caused by GIA in other areas (e.g., New Madrid seismic zone [Reference 2.5.1-460] and eastern Canada [Reference 2.5.1-293]) indicates that the effects on seismicity rates are expected to remain essentially unchanged over a few hundred to thousands of years. Therefore, it is not expected that seismicity rates in the site region will vary significantly in the future due to GIA.

Glacial and postglacial GIA in the study region is evidenced by deformation (tilting or warping) of glacial lake strandlines. Long-term average rebound information is most easily conveyed in plots of the elevation of a given shoreline across a distance (Reference 2.5.1-296). Figure 2.5.1-251 shows a summary plot of elevation versus distance of raised and uplifted shorelines of Lake Whittlesey and subsequent lake phases, as well as elevations of submerged features in the Lake Erie basin as compiled by Coakley and Lewis (Reference 2.5.1-296). Data for Lake Whittlesey in the Lake Erie basin yields a direction of maximum differential uplift of N24°E (Figure 2.5.1-251) and suggests that the post-Whittlesey change in elevation has been 52 m (171 ft) from Cleveland, Ohio to Buffalo, New York. Similarily, change in elevation since the lowest Lake Warren time has been about 43 m (141 ft) from Conneaut, Ohio to Buffalo and 66 m (217 ft) at its most northern point, 13 km (8.1 mi) north of Batavia, New York. (Reference 2.5.1-297)

Detailed mapping of strandlines and shoreline features related to glacial lakes provides information on the location of the 'zero isobase' (also referred to as the 'hinge line') for several individual relict lake strandlines (Reference 2.5.1-274; Reference 2.5.1-294; Reference 2.5.1-296). The zero isobase or hinge line as defined in early studies represents the general location of the boundary between a 'zone of horizontality' and zones of warping or relative uplift. Early rebound concepts of immediate rebound north of a "hinge-line" were eventually replaced, and it is now recognized that there was continued uplift and rebound over much of the region in the Holocene (Reference 2.5.1-295 and Reference 2.5.1-297). Geodynamical models that predict how the viscous mantle of the earth moves under surface loads show that the glacioisostatic recovery with a northward migration of a collapsing forebulge for the Great Lakes is a more appropriate model (Reference 2.5.1-486).

In Michigan, the Lake Whittlesey, Lake Maumee, and Lake Arkona beaches were observed to rise northward from within an area located north of Detroit. The hinge line of the younger Lake Warren and Lake Wayne strands and of Lakes Grassmere and Lunday were recognized in the Lake Huron basin about 20 km (12.4 mi) and 117 km (72.7 mi) north of the Lake Whittlesey hinge line. (Reference 2.5.1-297).

Holcombe et al. (Reference 2.5.1-487) provide a revised Lake Erie postglacial lake level history based on new detailed bathymetry. Previous reconstructions (e.g., Reference 2.5.1-296; Reference 2.5.1-297) varied in detail and water levels, but shared the following salient features: (1) high lake level stages of proglacial lakes and Lake Algonquin followed by very low lake levels in early Holocene time; (2) isostatic rebound and concomitant gradual rise in lake levels in the early Holocene; (3) stable or slowly rising lake levels in Middle Lake Erie time; (4) rise in lake levels accompanying the Nipissing rise to slightly higher than at present; and (5) lowering of lake levels to just below present level following the Nipissing rise event. The reconstructions recognize that lake level has been controlled since deglaciation by isostatically rebounding outlet sills of the Niagara River, and that the Nipissing rise accompanied a shift in upper Great Lakes drainage from the North Bay outlet to the Port Huron outlet. In the new model, Holcombe et al. (Reference 2.5.1-487) note that in an isostatically rebounding lake, lake level histories vary with location, especially as a function of distance from the outlet sill. A new feature of the model is a proposed extended period of low lake level in the middle Holocene (9 – 6 ka), when lake level was controlled not by the level of the outlet sill, but by climate and water budget. Also contributing to a low water level during this time was flooding of the central basin of Lake Erie as isostatic rebound continued, greatly increasing lake surface area and concomitantly increasing surface evaporation. At the time of the Nipissing rise (5,400 – 3,600 years ago), water level in eastern Lake Erie was 4 – 5 m (13 – 16.4 ft) higher than present. The western subbasin was flooded, but water level was about 3 m (10 ft) below present lake level.

Insert 3 is located towards bottom of section 2.5.1.1.4.1.1

Lake level was lowered several meters during the interval 3,600 – 3,000 years ago by headward erosion of the Niagara gorge. In the western basin, water level did not fall significantly because lower water level at the sill was partially compensated by differential isostatic rebound in the west. (Reference 2.5.1-487)

Motions from 360 Global Positioning System (GPS) sites in Canada and the United States yield a detailed image of present-day vertical and horizontal velocity fields within the nominally stable interior of the North American Plate (Reference 2.5.1-291) (Figures 2.5.1-253 and 2.5.1-254). Sella et al. (Reference 2.5.1-291) note that by far the strongest signal is the effect of GIA due to ice mass unloading during deglaciation. Vertical velocities show present-day uplift (approximately 10 mm/yr) near Hudson Bay, the site of thickest ice at the last glacial maximum. The uplift rates generally decrease with distance from Hudson Bay and change to subsidence (1 to 2 mm/yr) south of the Great Lakes. The

Insert 4 located above section 2.5.1.1.4.2

Monitoring of present-day tilting of the Great Lakes region based on water level gauges illustrates uplift in the northeast and subsidence in the south, indicating a pattern of land tilting upward to the northeast consistent with expected GIA (Reference 2.5.1-298). The data are consistent with the geodetic data that show the Fermi 3 site and surrounding region is not characterized by strong vertical gradients or anomalies.

Add the following References:

Reference 2.5.1-484 Stein, S., Sleep, N., Geller, R., Wang, S., and Kroeger, G., 1979, "Earthquakes Along the Passive Margin of Eastern Canada," *Geophysical Research Letters,* Vol. 6, pp. 537-540, 1979.

Reference 2.5.1-485 James, T.S., and Bent, A.L., "A Comparison of Eastern North American Seismic Strain Rates to Glacial Rebound Strain Rates," *Geophysical Research Letters,* Vol. 21, pp. 2127-2130, 1994.

Reference 2.5.1-486 Clark, J.A., Hendricks, M., Timmermans, T.J., Struck, C., and Hilverda, K.J., "Glacial Isostatic Deformation of the Great Lakes Region," *Geological Society of America Bulletin,* Vol. 106, pp. 19-31, 1994.

Reference 2.5.1-460 Grollimund, B., and Zoback, M.D., "Did Deglaciation Trigger Intraplate Seismicity in the New Madrid Seismic Zone?" *Geology*, Vol. 29, No.2, pp. 175 – 178, 2001.

Reference 2.5.1-480 Calais, E., Han, J.Y., DeMets, C., and Nocquet, J.M., "Deformation of the North American Plate Interior from a Decade of Continuous GPS Measurements," *Journal of Geophysical Research*, Vol. 111, B06402, doi:10.1029/2005JB004253, 2006.

Reference 2.5.1-487 Holcombe, T.L., Taylor, L.A., Reid, D.F., Warren, J.S., Vincent, P.A., and Herdendorf, C.E., "Revised Lake Erie Postglacial Lake Level History Based on New Detailed Bathymetry," *Journal of Great Lakes Research*, Vol. 29, No. 4, pp. 681-704, 2003.

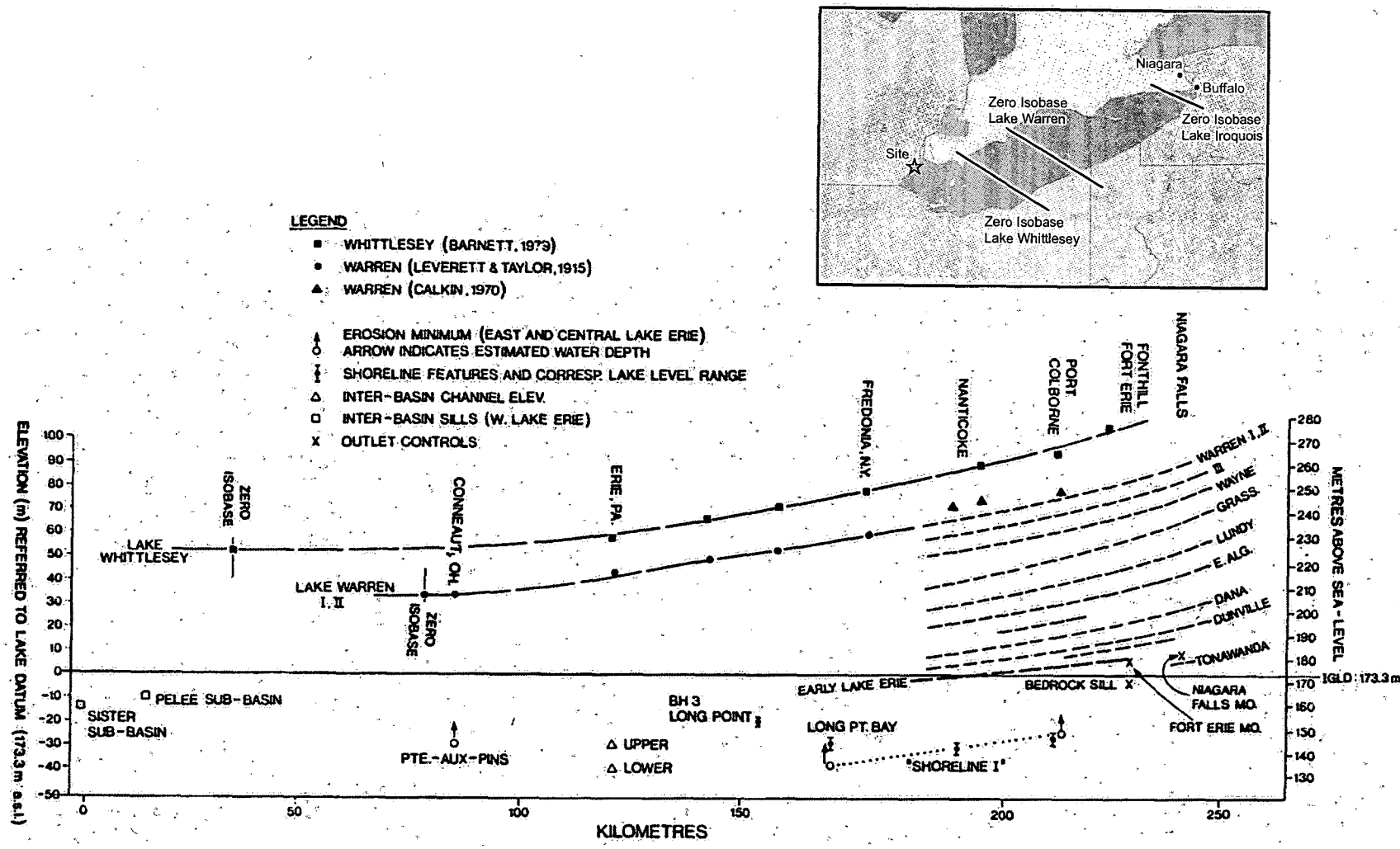

Note. Profile is oriented N 24° E, the direction of maximum tilting. Also plotted are submerged geomorphological features noted on or below the lake bottom, and their relationship to possible outlet controls at the Niagara River.

Source: Reference 2.5.1-296

Figure 2.5.1-251. Plot of Elevation Versus Distance of Raised and Uptilted Shorelines of the Whittlesey and Subsequent Lake Phases.

File path: S:\13300\\13356_001\Figures\RAI Figures\.RAI 02.05.01-03 Figure 5.ai; Date: [01/12/2010]

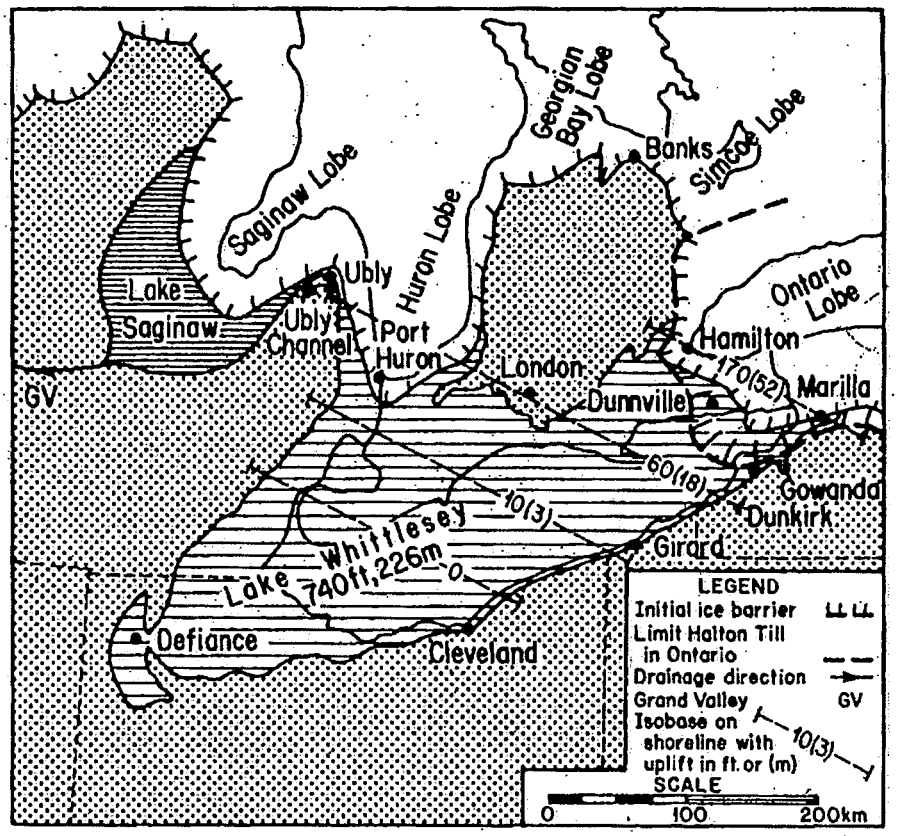

Note. Isobases on Whittlesey shoreline features tilted in N27°E direction. The true isobases may bow southwestward more nearly parallel to former ice margins as they cross the basin.

Source: Reference 2.5.1-297

Figure 2.5.1-252. Lakes Whittlesey and Saginaw, and the Port Huron Stade Ice Barriers.

File path: S:\13300\\13356_001\Figures\RAI Figures\.RAI 02.05.01-03 Figure 6.ai; Date: [01/12/2010]

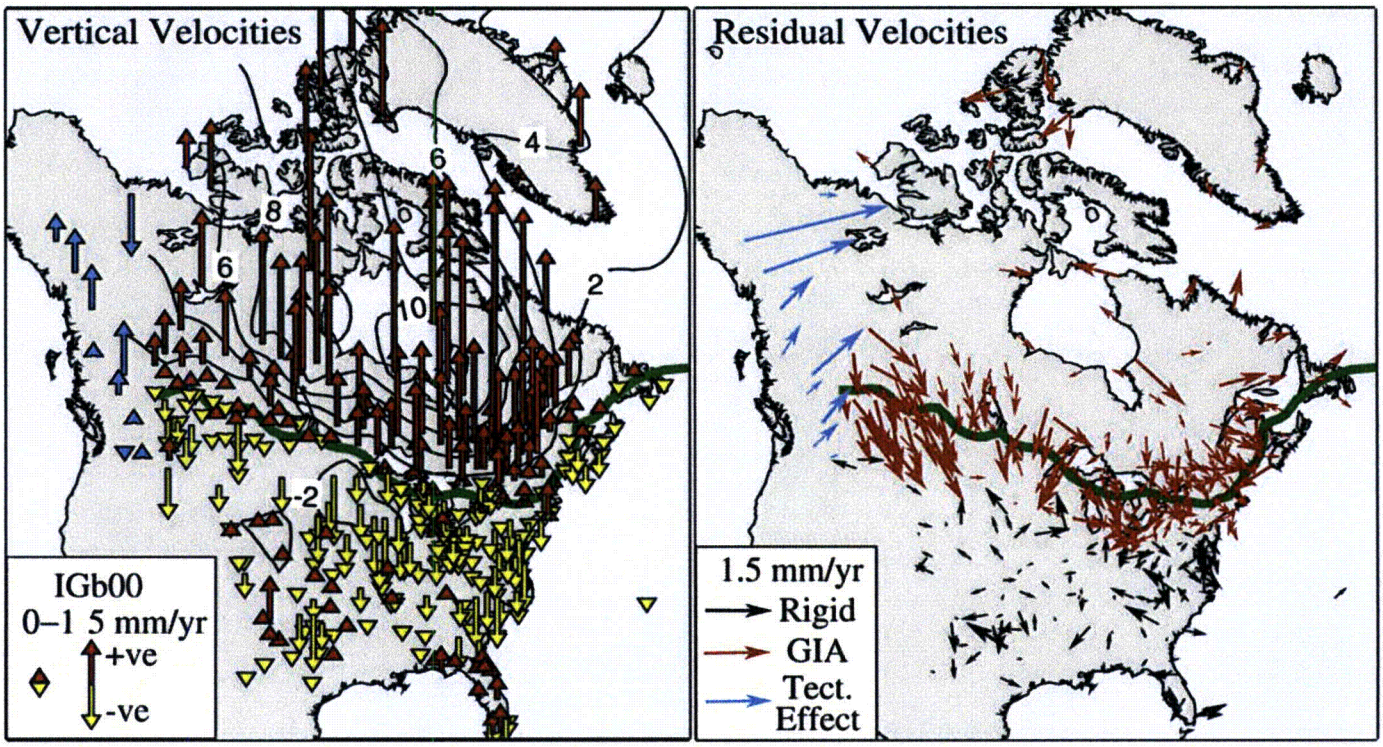

Note. (left) Vertical GPS site motions with respect to IGb00. Note large uplift rates around Hudson Bay, and subsidence to the south. Green line shows interpolated 0 mm/yr vertical "hinge line" separating uplift from subsidence. (right) Horizontal motion site residuals after substracting best fit rigid plate rotation model defined by sites shown with black arrows. Red vectors represent sites primarily affected by GIA. Blue vectors represent sites that include effects of tectonics.

Source: Reference 2.5.1-291

Figure 2.5.1-253. GPS Motions

File path: S:\13300\\13356_001\Figures\RAI Figures\.RAI 02.05.01-03 Figure 1.ai; Date: [01/12/2010]

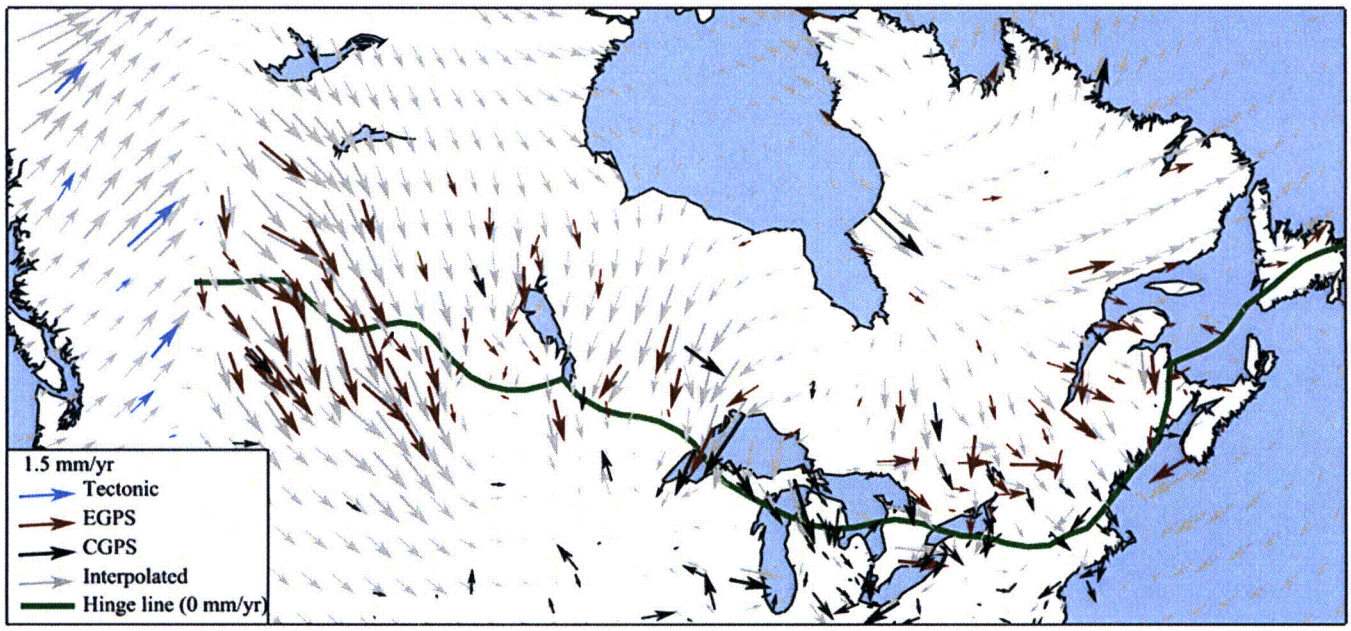

Notes.
CGPS = Continuosly Recorded GPS
EGPS = Episodic GPS

Source: Reference 2.5.1-291

Figure 2.5.1-254. GPS Horizontal Velocities with Motion of Rigid North America Removed.

File path: S:\13300\\13356_001\Figures\RAI Figures\.RAI 02.05.01-03 Figure 1.ai; Date: [01/12/2010]

Attachment 2
NRC3-10-0006

Response to RAI Letter No. 16
(eRAI Tracking No. 3913)

RAI Question No. 02.05.01-4

RAI 02.05.01-04

FSAR Section 2.5.1.1.4.1.1 describes (1) substantial deformation of the Port Huron shoreline (60 meters of uplift between 11,000 and 7,000 years BP), (2) upwarping of shorelines as young as 4,700 years, and (3) recognition of widespread uplift and rebound through the Holocene.

a. As noted in FSAR Section 2.5.1.1.4.1.1, "rebound information is most easily conveyed in plots of the elevation of a given shoreline across a distance." Therefore, please provide maps and/or profiles to illustrate the extent of this deformation and its relation to the Fermi site. In addition, discuss the implications of regional deformation data for assessing potential uplift or subsidence at the Fermi site.

b. FSAR Section 2.5.1.1.4.1.1 also describes regions of recent uplift and subsidence in relation to the site, as indicated by the GPS velocity field. Please include one or more figures illustrating this deformation.

Response

a. *As noted in FSAR Section 2.5.1.1.4.1.1, "rebound information is most easily conveyed in plots of the elevation of a given shoreline across a distance." Therefore, please provide maps and/or profiles to illustrate the extent of this deformation and its relation to the Fermi site. In addition, discuss the implications of regional deformation data for assessing potential uplift or subsidence at the Fermi site.*

Deformation of glacial lake strandlines (relict shorelines) in the site region is addressed in the Response to RAI 02.05.01-3 (Attachment 1). The Fermi 3 site lies within the "zone of horizontality" west of the mapped "zero isobase" lines (or 0 mm/yr hinge lines) for Glacial Lake Whittlesley (13 ka) and younger lakes (Reference 2.5.1-296; Reference 2.5.1-297) (see RAI 02.05.01-3 Figure 2 and proposed FSAR Figure 2.5.1-251). The location of the site with respect to the zero isobases marking the boundary of relative glacioisostatic uplift suggests that significant warping of glacial strandlines within the site vicinity would not be expected. Evaluation of mapped shorelines (Reference 2.5.1-451) using the USGS 10-meter digital elevation model (DEM) shows no apparent warping of the shorelines of these glacial lakes in the site vicinity as discussed in the response to RAI 02.05.03-6 Attachment 29).

b. *FSAR Section 2.5.1.1.4.1.1 also describes regions of recent uplift and subsidence in relation to the site, as indicated by the GPS velocity field. Please include one or more figures illustrating this deformation.*

Present-day uplift and subsidence in the site region as inferred from geodetic data is addressed in the response to RAI 02.05.01-3 and is illustrated in proposed Figures 2.5.1-253 and 2.5.1-254. The Fermi 3 site lies south of the "zero isobase" line in a region where measurements suggests subsidence of between 0 and 2 mm/yr (Reference 2.5.1-291). Measurements of relative lake-level change based on water-level gauge data also suggest that the relatively flat velocity

gradient in the southern part of Lake Erie is on or approaching the subsiding forebulge of the postglacial rebound, but results are not significant enough to actually support this claim (Reference 2.5.1-298).

Proposed COLA Revision

Proposed markup to revise FSAR Section 2.5.1.1.4.1.1, including clarification of the statements regarding possible deformation of the Port Huron shoreline, is provided in the response to RAI 02.05.01-3 .

Attachment 3
NRC3-10-0006

Response to RAI Letter No. 16
(eRAI Tracking No. 3913)

RAI Question No. 02.05.01-6

RAI 02.05.01-06

FSAR Section 2.5.1.1.4.3 systematically discusses significant structures in the site region (320-km radius). For many structures, the FSAR describes the observations and relations that establish limits on the times of most recent deformation on specific structures. This important information is not included for all structures. Please summarize the observations that define limits on the times of the most recent deformation for the following structures in the Fermi site region:

a. *Peck fault (FSAR Section 2.5.1.1.4.3.2.11)*

b. *Sharpsville fault (FSAR Section 2.5.1.1.4.3.2.13)*

c. *Transylvania fault extension (FSAR Section 2.5.1.1.4.3.2.14)*

Response

a. Detailed studies of the Peck fault are based on subsurface data in Precambrian through Middle Devonian units. Based on subsidence patterns and deformation in the Michigan Basin and adjacent basins, Fisher (Reference 2.5.1-329) states that it is reasonable to assume that deformation on the Peck fault occurred through the end of Paleozoic time. The early Mississippian Sunbury Shale is offset by the Peck fault; however, it is unclear whether the overlying early Mississippian Coldwater Shale is offset by the fault. FSAR Section 2.5.1.1.4.3.2.11 has been revised to clarify the age of the youngest deformed unit based on personal communication with John Esch of the Michigan Department of Environmental Quality. The Peck fault is overlain by glacial and postglacial deposits of late Wisconsinan to Holocene age (Reference 2.5.1-207). There is no known evidence of Quaternary faulting in Michigan.

b. The Sharpesville fault juxtaposes Devonian Muscatatuck Group limestone and dolomite against Silurian Wabash Formation limestone, dolomite, and shale (Reference 2.5.1-339). Based on the above relationship, the youngest deformation on the fault is Devonian. FSAR Section 2.5.1.1.4.3.2.13 will be revised to clarify the age of the youngest deformed unit based on a more detailed literature search. The fault is overlain by glacial till of Wisconsinan to possible Holocene age (Reference 2.5.1-207).

c. The Transylvania fault extension (TFE) comprises the Pittsburgh-Washington cross-strike structural discontinuity, the Highlandtown fault, the Smith Township fault, the Suffield fault system, the Akron fault, and the Middleburg fault (Reference 2.5.1-237). The TFE is an extension of the Transylvania fault zone, a zone of steeply-dipping basement faults that extends from the early Mesozoic Gettysburg Basin in Pennsylvania to Ohio. Mesozoic faulting has been documented in the early Mesozoic Gettysburg Basin, which lies along the projection of the TFE; however, no Mesozoic rocks are present in the area of the TFE. Based on discussions with Mark Baranoski of the Ohio Division of Geological Survey and a more in-depth literature search, there is no evidence for Mesozoic reactivation on the TFE in Ohio. The TFE is overlain by alluvium and

colluvium of middle Pleistocene to Holocene age (Reference 2.5.1-207). There is no known evidence of Quaternary tectonic faulting in Ohio.

Ages of deformation on the Peck and Sharpesville faults, and Transylvania fault extension will be added to FSAR Table 2.5.1-201, which will be provided in response to RAI 02.05.01-07 (Attachment 4).

Proposed COLA Revision

Proposed markups to revise FSAR Sections 2.5.1.1.4.3.2.11, 2.5.1.1.4.3.2.13, and 2.5.1.1.4.3.2.14 are attached and proposed markups to revise FSAR Table 2.5.1-201 will be provided with the response to RAI 02.05.01-07.

Markup of Detroit Edison COLA
(following 7 pages)

The following markup represents how Detroit Edison intends to reflect this RAI response in a future submittal of the Fermi 3 COLA. However, the same COLA content may be impacted by revisions to the ESBWR DCD, responses to other COLA RAIs, other COLA changes, plant design changes, editorial or typographical corrections, etc. As a result, the final COLA content that appears in a future submittal may be different than presented here.

deformation associated with the Howell anticline after Early Mississippian. The Howell anticline is approximately coincident with the axis of the MRS (MMGA) in southeast Michigan (Figure 2.5.1-203 and Figure 2.5.1-220). The Howell structure may extend southwest to the Detroit River as a series of folds expressed on the structure contour map on the top of the Trenton Formation (Reference 2.5.1-341), one of which may be the Stony Island Anticline (Reference 2.5.1-341). These folds are discussed in more detail in Subsection 2.5.1.2.4.1.

2.5.1.1.4.3.2.10 **Maumee Fault**

The Maumee fault is a northeast-southwest trending normal fault in the subsurface of Henry, Lucas, and Wood Counties in Ohio, and is about 56 km (35 mi) long on the structural contour map on the Precambrian unconformity surface (Figure 2.5.1-203) (Reference 2.5.1-237). At its closest, the Maumee fault is approximately 34 km (21 mi) south of Fermi 3 (Figure 2.5.1-203). The fault is offset about 2 km (1.2 mi) in an apparent left-lateral sense by the Bowling Green fault. The fault trace is coincident with a moderate lineament formed by the Maumee River (Reference 2.5.1-237).

(Reference 2.5.1-325)

group

2.5.1.1.4.3.2.11 **Peck Fault**

The Peck Fault, also known as the Sanilac Fault, is a north-south trending fault present in the subsurface of St. Clair and Sanilac Counties (Reference 2.5.1-325; Reference 2.5.1-329; Reference 2.5.1-333). Brigham characterized the Peck fault as a north-south trending, west-side-down, vertical normal fault based on structure contour maps on the top of the Trenton Limestone, Clinton group, Guelph formation, Bass Islands formation, and Dundee formation. Fisher (Reference 2.5.1-329) described the Peck fault as a N10° to 20°W trending faulted monocline, the fault being an east-dipping thrust. The total length of the Peck Fault is approximately 61 km (38 mi) long (Figure 2.5.1-203). At its closest, the Peck fault is approximately 133 km (82 mi) north of the site (Figure 2.5.1-203). The Peck fault has a maximum displacement on the Middle Ordovician Trenton group (approximately 91 m [300 ft]) and is present on the structure contour map on the through lowest Middle Devonian Dundee Formation (Reference 2.5.1-325). The Peck fault offsets the contact between early late-Silurian Salina group A-1 Evaporite and overlying A-1 Carbonate units (Reference 2.5.1-329).

point

Add Insert #1 here

Insert 1

Noting anomalous patterns on isopach maps of Paleozoic units, Fisher (Reference 2.5.1-329) concludes that movement on the fault occurred through the end of Paleozoic time. Geologic maps of Michigan (Reference 2.5.1-205 and Reference 2.5.1-442) show early Mississippian Coldwater and Sunbury Shale in the area where the Peck fault has been mapped. The early Mississippian Sunbury Shale is offset by the Peck fault; however, it is unclear whether the overlying early Mississippian Coldwater Shale is offset by the fault. Late Wisconsinan – Holocene glacial and postglacial deposits, including till and lacustrine clay and silt, overlie the Peck fault (Reference 2.5.1-207 and Reference 2.5.1-451). There is no known evidence of Quaternary faulting in Michigan.

2.5.1.1.4.3.2.12 **Royal Center Fault**

The Royal Center fault is a northeast-southwest trending fault in the subsurface of Cass, Fulton, and Kosciusko Counties in Indiana, and is about 77 km (48 mi) long. At its closest, the Royal Center fault is approximately 223 km (138 mi) southwest of Fermi 3 (Figure 2.5.1-203). The fault is a steeply southeast-dipping, down-to-the-southwest normal fault on the north flank of the Kankakee arch. The fault offsets the top of the Precambrian surface and the top of the Middle Silurian Salamonie Dolomite, but not the top of the Middle Devonian Muscatatuck group. (Reference 2.5.1-338)

2.5.1.1.4.3.2.13 **Sharpsville Fault**

Add Insert #2 here

The Sharpsville fault is a northeast-southwest-trending, vertical normal fault in the subsurface of Tipton and Howard Counties of central Indiana. The fault is approximately 21 km (13 mi) long and offsets the top of the Middle Ordovician ~~Trenton~~ Formation down-to-the-southeast on the crest of the Kankakee arch. (Reference 2.5.1-339)

Add Insert #3 here

2.5.1.1.4.3.2.14 **Transylvania Fault Extension**

~~The Transylvania fault extension is the extension of faulting identified in Pennsylvania into Ohio. The Transylvania fault is a major zone of east-west trending, near-vertical faults in the subsurface in Pennsylvania recognized from boring and geophysical data. The westernmost of these faults, the Middleburg fault, is approximately 186 km (115 mi) southeast of Fermi 3 at its closest distance (Figure 2.5.1-203). The fault originated in the Precambrian and was reactivated during the Middle Ordovician Taconic orogeny, during the terminal Paleozoic Alleghenian orogeny, and during the Early Jurassic faulting of the rift basins along the margin of the continent (Reference 2.5.1-342). Transylvania fault zone has been extended northwest from the Ohio-Pennsylvania border to Cuyahoga County near Lake Erie in northeast Ohio. The zone is defined by six high-angle (>80 degrees), normal, southwest-dipping, down-to-the-southwest faults: the Pittsburg-Washington cross-strike structural discontinuity, the Highlandtown fault, the Smith Township fault, the Suffield fault system, the Akron fault, and the Middleburg fault (Figure 2.5.1-203). These faults are mapped on the structure contour map of the Precambrian unconformity surface (Reference 2.5.1-237), and on structure maps on the top of the latest Early Mississippian Berea~~

Insert 2

The fault juxtaposes the Devonian Muscatatuck Group limestone and dolomite against Silurian Wabash Formation limestone, dolomite, and shale (Reference 2.5.1-339). Based on the above relationship, the youngest deformation on the fault is Devonian. The fault is overlain by glacial till of Wisconsinan to possible Holocene age (Reference 2.5.1-207).

Insert 3

The Transylvania fault extension is a zone of en-echelon steeply dipping basement faults that extends across northeastern Ohio nearly to the shore of Lake Erie. The zone is defined by six high-angle (>80 degrees), normal, southwest-dipping, down-to-the-southwest faults: the Pittsburgh-Washington cross-strike structural discontinuity, the Highlandtown fault, the Smith Township fault, the Suffield fault system, the Akron fault, and the Middleburg fault (Reference 2.5.1-237). These faults are mapped on the structure contour map of the Precambrian unconformity surface (Reference 2.5.1-237), and on structure maps on the top of the latest Early Mississippian Berea Sandstone, Devonian Onondaga Limestone, and Silurian Packer Shell horizon (Reference 2.5.1-342). The westernmost of these faults, the Middleburg fault, is approximately 186 km (115 mi) southeast of Fermi 3 at its closest distance (Figure 2.5.1-203).

The Transylvania fault extension is an extension of the Transylvania fault zone, a zone of steeply dipping basement faults that extends from the early Mesozoic Gettysburg Basin in Pennsylvania to Ohio. In Pennsylvania, the Transylvania fault zone is mapped as a series of large, subvertical, east-west-trending faults in the Blue Ridge Mountains, the Great Valley region, and theValley and Ridge province. Westward on the Appalachian Plateau, the fault zone is recognized from subsurface mapping and geophysical studies. The Transylvania fault zone in Pennsylvania originated in the Precambrian and was reactivated during the Middle Ordovician Taconic orogeny, during the terminal Paleozoic Alleghenian orogeny, and during the Early Jurassic faulting of the rift basins along the margin of the continent (Reference 2.5.1-342). Mesozoic faulting has been documented in the early Mesozoic Gettysburg Basin, which lies along the projection of the Transylvania fault extension; however, no Mesozoic rocks are present in the area of the Transylvania fault extension (Reference 2.5.1-442). Pennsylvanian-Permian age faulting related to Alleghanian deformation is recognized on faults within the Transylvania fault extension (Reference 2.5.1-213; Reference 2.5.1-342; Reference 2.5.1-343).

~~Sandstone, Devonian Onondaga Limestone, and top of the Silurian Packer Shell horizon (Reference 2.5.1-342).~~

The geometry of the Akron-Suffield-Smith Township faults suggest that they originated as en-echelon, synthetic faults produced by right-lateral wrenching, with inferred minimum displacement of 21 km (13 mi) and subsequent normal displacements on the faults (Reference 2.5.1-342). Displacement on the Precambrian unconformity surface is 60 – 120 m (200 – 400 ft), while maximum vertical displacement of the Devonian Onondaga Limestone across the Akron-Suffield faults is 60 m (200 ft) and across the Highlandtown fault it is 72 m (240 ft) (Reference 2.5.1-342). Hook and Ferm (Reference 2.5.1-343) postulate that deposition of the Linton channel deposits below the Middle Pennsylvanian (Westphalian D) Upper Freeport coal may have been controlled by movement on the Transylvania fault extension (Pittsburgh-Washington cross-strike ~~structural discontinuity~~). Post-Lower Pennsylvanian faulting cannot be assessed because of the absence of younger units. The northeast-southwest-trending Akron magnetic boundary crosses between the Middleburg and Akron faults.

ı Cambrian through
ower Carboniferous
trata

Add Insert #4
here

2.5.1.1.4.3.3 **Seismic Zones**

Earthquakes in the site region are generally shallow events associated with reactivated Precambrian faults favorably oriented in the modern northeast-southwest compressive stress regime (Reference 2.5.1-344). None of these events has associated surface rupture, and no faults in the site region exhibit evidence of movement since the Paleozoic (Reference 2.5.1-344). Two seismic zones in the study region, the Anna seismic zone and the northeast Ohio seismic are designated as Class C features in the USGS Quaternary fault and fold database (Reference 2.5.1-316).

2.5.1.1.4.3.3.1 **Northeast Ohio Seismic Zone**

The Northeast Ohio seismic zone, also called the Ohio-Pennsylvania seismic zone, defines an approximately 50-km (30.5-mi) long, northeast-southwest-trending zone of earthquakes south of Lake Erie on the Ohio-Pennsylvania border (Reference 2.5.1-328). The largest historic event in this zone was the January 31, 1986, magnitude (m_b) 5.0 event located about 40 km (24.4 mi) east of Cleveland in southern Lake County, Ohio, and about 17 km (10.4 mi) south of the Perry Nuclear Power Plant (Reference 2.5.1-345). The earthquake produced Modified Mercalli

Insert 4

The Transylvania fault extension is overlain by alluvium and colluvium of Middle Pleistocene to Holocene age (Reference 2.5.1-207). There is no known evidence of Quaternary tectonic faulting in Ohio.

Attachment 4
NRC3-10-0006

Response to RAI Letter No. 16
(eRAI Tracking No. 3913)

RAI Question No. 02.05.01-7

RAI 02.05.01-07

FSAR Table 2.5.1–201 summarizes information about faults and folds in the Fermi site region. The table includes a column entitled "Unit/Age/Amount of Youngest Deformation/Offset" that lists the youngest faulted or deformed unit for most structures. However, the table (and the FSAR in general) does not provide explicit discussion of the oldest unfaulted unit associated with each fault or fold. For the faults and folds in Table 2.5.1–201, please summarize observations that place limits on the cessation of faulting (i.e., describe the oldest unfaulted or undeformed units for the structures included in the table).

Response

FSAR Table 2.5.1-201 provided a summary of information on the timing of the most recent faulting and related deformation from available publications, oil and gas reports, and discussions with researchers and geologists from the Michigan and Ohio geological surveys. The previous review of available information had not identified any known Quaternary tectonic faulting in the site region. In response to the request to further document the ages of the oldest unfaulted units associated with each fault or fold, the following researchers were contacted to determine whether there was additional information on the age of faulting within the 320 km (200 mi.) radius of the Fermi 3 site that could be used to supplement the existing information in FSAR Table 2.5.1-201:

- John Esch, Michigan Department of Environmental Quality.
- Bill Harrison, Western Michigan University.
- Mark Baranoski, Ohio Division of Geological Survey.
- John Rupp, Indiana Geological Survey.

Information obtained from the above researchers is summarized in this RAI response.

In most of the site region, Paleozoic bedrock is overlain by Quaternary sediments of glacial, fluvial, or lacustrine origin. In general, the age of faulting in the site region is constrained between faulted Paleozoic rocks and the overlying Quaternary sediments. Based on a thorough literature search and discussions with the above researchers, there is no known evidence of Quaternary tectonic faulting in the site region. There are, however, several faults in Quaternary sediments associated with glacial processes. Many of the references that describe faulting in the site region are based on subsurface investigations, largely related to oil and gas exploration. The data is presented as contour maps on the top surfaces of stratigraphic units. The top of the youngest Paleozoic units are eroded and, therefore, based on structural contour maps, it is uncertain whether the youngest Paleozoic units are faulted (e.g., Peck fault).

Based on discussions with the above researchers, in most cases the youngest Paleozoic unit shown on the geologic map would indicate the youngest age of faulting on most of the structures included in FSAR Table 2.5.1-201. The age of the oldest unfaulted unit over most of these structures is uncertain but is likely the oldest mapped Quaternary unit. Table 2.5.1-201 has been revised to indicate the age of the oldest unfaulted Quaternary unit based on Reference 2.5.1-207,

unless there is evidence for an older unfaulted unit. Because there are not extensive field investigations to determine the presence or absence of faulting in Quaternary sediments over the faults, the age of the oldest unfaulted unit in most cases is not well documented.

Minor structures included in Table 2.5.1-201 are described in oil and gas reports (Reference 2.5.1-325; Reference 2.5.1-341; References 2.5.1-429 through 2.5.1-439). Ninety (90) percent of the minor structures included in Table 2.5.1-201 in Michigan are likely to be folds that may be associated with faults.

Table 2.5.1-201 has been revised to include a column describing the "Age of Oldest Unfaulted Unit" and to clarify the age of the youngest faulting, where appropriate. The Colchester fault will be added to the table in response to RAI 02.05.01-24. A comment will be added to Table 2.5.1-201 to indicate the uncertainty in age of faulting on the minor structures.

Proposed COLA Revision

Markups to Table 2.5.1-201 are attached.

Markup of Detroit Edison COLA
(following 20 pages)

The following markup represents how Detroit Edison intends to reflect this RAI response in a future submittal of the Fermi 3 COLA. However, the same COLA content may be impacted by revisions to the ESBWR DCD, responses to other COLA RAIs, other COLA changes, plant design changes, editorial or typographical corrections, etc. As a result, the final COLA content that appears in a future submittal may be different than presented here.

Table 2.5.1-201 Regional Tectonic Structures Within 320 km (200 mi) (Sheet 1 of 13) [EF3 COL 2.0-26-A]

Name	Location	Closest Distance to Site	Structure Trend, Plunge and Any Associated Fault	Trend, Type of Fault, Dip, Sense of Displacement	Unit/Age/Amount of Maximum Deformation/Offset	Unit/Age/Amount of Youngest Deformation/Offset	Associated Oil and Gas Field	Means of Identification[a]	Source
MAJOR STRUCTURES									
Akron Magnetic Boundary (AMB)	NE Ohio	176 km (106 mi)	NE-SW trending magnetic anomaly (low) associated with possible pre-existing basement structure			Possible lake-loading-induced seismicity		G	Reference 2.5.1-237; Reference 2.5.1-327
Albion-Scipio Fault (ASF)	Hillsdale and Calhoun counties, Michigan	108 km (67 mi)	NW-SE trending anticline associated with en-echelon wrench faults			Offsets the Middle Ordovician Trenton Formation[1]	Albion-Pulaski-Scipio-Trend oil and gas field	B, G	Reference 2.5.1-331
Northern Segment Bowling Green Fault (BGF), also known as the Lucas-Monroe Monocline (LMM) in Michigan	Lenawee/ Monroe counties northwest to Livingston County, Michigan	48 km (28 mi)	NW-SE trending asymmetrical anticline(s) with steeply dipping SW flank (faulted); merges with Howell anticline at north end	Several NW-SE trending, normal, steeply dipping to vertical, right- and left-stepping, southwest-side-down faults; includes Deerfield anticline, a N-S trending, north-plunging anticline with normal, steeply dipping to vertical, down-to-the-west fault on west	Top of Middle Ordovician Trenton Formation is offset 61 m (200 ft) down-to-the-west	Offsets top of Early Mississippian Sunbury Shale on structure contour map	Deerfield oil field	B, G	Reference 2.5.1-333; Reference 2.5.1-335

Replace with Table 2.5.1-201 in Insert 1

Table 2.5.1-201 Regional Tectonic Structures Within 320 km (200 mi) (Sheet 2 of 13) [EF3 COL 2.0-26-A]

Name	Location	Closest Distance to Site	Structure Trend, Plunge and Any Associated Fault	Trend, Type of Fault, Dip, Sense of Displacement	Unit/Age/Amount of Maximum Deformation/Offset	Unit/Age/Amount of Youngest Deformation/Offset	Associated Oil and Gas Field	Means of Identification[a]	Source
Central Segment Bowling Green Fault, also known as the Lucas-Monroe Monocline	Hancock County, Ohio north to Lenawee/ Monroe counties, Michigan	40 km (24 mi)		N10 – 20°W trending, normal, vertical fault, down-to-the-west with recurrent, variable displacements (see Figure 2.5.1-223). Waterville Quarry exposures suggest thrusts are interformational ramp faults (see Episode VI on Figure 2.5.1-223)	Offsets top of Middle Silurian Lockport Dolomite approximately 122 m (400 ft)	Slickensides and offset bedding in uppermost Late Silurian Bass Islands Group; <5 m (16 ft) thrusting in Cenozoic is highly speculative		S, B, G	Reference 2.5.1-332; Reference 2.5.1-237
Southern Segment Bowling Green Fault (BGF)	Wood County north to Marion County, Ohio	101 km (62 mi)		SE tre… steepl… vertica… down-… splays (Outlet and Marion faults) and down-to-the-west fault splays (see Figure 2.5.1-203)				B, G	Reference 2.5.1-237

Replace with Table 2.5.1-201 in Insert 1

Table 2.5.1-201 Regional Tectonic Structures Within 320 km (200 mi) (Sheet 3 of 13) [EF3 COL 2.0-26-A]

Name	Location	Closest Distance to Site	Structure Trend, Plunge and Any Associated Fault	Trend, Type of Fault, Dip, Sense of Displacement	Unit/Age/Amount of Maximum Deformation/Offset	Unit/Age/Amount of Youngest Deformation/Offset	Associated Oil and Gas Field	Means of Identification[a]	Source
Burning Springs Anticline (BSA) (50 – 150 km long)	West Virginia	327 km (203 mi)	N-S trending anticline faulted in core; splays into several right-stepping traces at Ohio River; may extend south to include Mann Mountain anticline	N-S trending, normal, steeply east-dipping fault, down-to-the-east with recurrent displacements, including: a. Offsets Precambrian unconformity surface south of the Ohio River b. Reactivation during Silurian restricting salt deposition to a c. R d. [illegible] deposition of Devonian through Permian strata d. NW directed Alleghanian age thrusting on decollements in Late Silurian Salina Group salts at the salt edge and development of imbricate ramp thrusts coring anticline in Salina Group and younger strata	300 m (980 ft) down-to-the-east on base of Cambrian	Only folding in Late Silurian Salina Group and younger strata		B, G	Reference 2.5.1-237; Reference 2.5.1-336; Reference 2.5.1-337

Replace with Table 2.5.1-201 in Insert 1

Table 2.5.1-201 Regional Tectonic Structures Within 320 km (200 mi) (Sheet 4 of 13)

[EF3 COL 2.0-26-A]

Name	Location	Closest Distance to Site	Structure Trend, Plunge and Any Associated Fault	Trend, Type of Fault, Dip, Sense of Displacement	Unit/Age/Amount of Maximum Deformation/Offset	Unit/Age/Amount of Youngest Deformation/Offset	Associated Oil and Gas Field	Means of Identification[a]	Source
Cambridge Arch (CA) (100 km long)	Eastern Ohio	118 km (73 mi)	N20°W trending fault-bounded arch (horst) with half graben (Parkersburg-Lorain syncline) on west; splays into three arches at Ohio River	N20°W trending normal faults, dipping >80°, bounding 1.5 km (0.9 mi) wide uplifted block (horst) with some right-lateral slip at north end	≈80 m (262 ft) structural relief on Devonian Onondaga Limestone			S (north end), B, G	Reference 2.5.1-237; Reference 2.5.1-336
Chatham Sag and Electric Fault	SW Ontario, Canada	81 km (50 mi)	E-W trending sag defined by mutual plunges of Findlay and Algonquin arches and bound on the north by EW trending Electric fault	E-W trending, normal, vertical, south-side-down	Precambrian surface displaced about 93 m (305 ft) [illegible]	Present on the structure contour map on the uppermost Late Silurian Bass Islands Group but probably does not displace the base of the Middle Devonian Dundee Formation		B, G	Reference 2.5.1-325
Fort Wayne Rift	Western Ohio and eastern Indiana	173 km (107 mi)	NW-SE trending fault-bounded graben with central high	NW-SE trending, normal, vertical, northeast-side-down Anna-Champaign fault and southwest-side-down Logan fault forming central high; unnamed northeast and southwest side-down fault bounding graben		Truncated by GFTZ (1.25 Ga to 980 Ma); seismically active		B, G	Reference 2.5.1-237

Replace with Table 2.5.1-201 in Insert 1

Table 2.5.1-201 Regional Tectonic Structures Within 320 km (200 mi) (Sheet 5 of 13) [EF3 COL 2.0-26-A]

Name	Location	Closest Distance to Site	Structure Trend, Plunge and Any Associated Fault	Trend, Type of Fault, Dip, Sense of Displacement	Unit/Age/Amount of Maximum Deformation/Offset	Unit/Age/Amount of Youngest Deformation/Offset	Associated Oil and Gas Field	Means of Identification[a]	Source
Name	Location	Closest Distance to Site	Structure Trend, Plunge and Any Associated Fault	Trend, Type of Fault, Dip, Sense of Displacement	Unit/Age/Amount of Maximum Deformation/Offset	Unit/Age/Amount of Youngest Deformation/Offset	Associated Oil and Gas Field	Means of Identification[a]	Source
Fortville Fault (FF)	Marion, Hancock, and Madison counties, Indiana	271 km (168 mi)	N-NE to S-SW trending, normal fault, steeply southeast dipping, down-to-the-southeast; on west flank of Cincinnati arch	Offsets top of Precambrian surface	Offsets top of Middle Silurian Salamonie Dolomite but not top of Middle Devonian Muscatatuck Group			B, G	Reference 2.5.1-338
Grenville Front Tectonic Zone (GFTZ)	Mississippi north and north through Ohio and NE Canada	0 km (0 mi)	NE to N to NE trending zone of faults 10 – 100 km (6 – 60 mi) wide	NE to thrust east. associated with Grenville orogeny	Grenville orogeny (1.25 Ga to 980 Ma)	Movement along the Bowling Green fault is attributed to reactivation of GFTZ. Uppermost Late Silurian Bass Islands Group offset by central segment of Bowling Green fault		B, G	Reference 2.5.1-237; Reference 2.5.1-234

Replace with Table 2.5.1-201 in Insert 1

Table 2.5.1-201 Regional Tectonic Structures Within 320 km (200 mi) (Sheet 6 of 13) [EF3 COL 2.0-26-A]

Name	Location	Closest Distance to Site	Structure Trend, Plunge and Any Associated Fault	Trend, Type of Fault, Dip, Sense of Displacement	Unit/Age/Amount of Maximum Deformation/Offset	Unit/Age/Amount of Youngest Deformation/Offset	Associated Oil and Gas Field	Means of Identification[a]	Source
Hoosier Thrust Belt - Louisville Uplift (south portion of Mount Carmel fault/Leesville anticline)	SW Indiana	393 km (244 mi)		Series of N-NW trending thrust faults, west-dipping (Hoosier thrust fault) bound on east by N-NW trending, foreland-style thrust fault (Louisville uplift)	Hoosier thrust belt is developed within the Precambrian (Mesoproterozoic) Centralia Group and truncated by overlying unconformity; Louisville uplift has ≈8 km (5 mi) of vertical uplift dated at 600 Ma, reactivated in Seismic Zone)	Mount Carmel fault offsets base of Upper Devonian[1] New Albany Shale		B, G	Reference 2.5.1-338; Reference 2.5.1-229

Replace with Table 2.5.1-201 in Insert 1

Table 2.5.1-201 Regional Tectonic Structures Within 320 km (200 mi) (Sheet 7 of 13) [EF3 COL 2.0-26-A]

Name	Location	Closest Distance to Site	Structure Trend, Plunge and Any Associated Fault	Trend, Type of Fault, Dip, Sense of Displacement	Unit/Age/Amount of Maximum Deformation/Offset	Unit/Age/Amount of Youngest Deformation/Offset	Associated Oil and Gas Field	Means of Identification[a]	Source
Howell Anticline/Fault (HA) (100 km long; 145 km if folds near Detroit River included)	Wayne northwest to Shiawassee counties, Michigan. May extend southeast to Detroit River to Stony Island Anticline and associated folds (see Minor Structures)	45 km (27 mi) / 5-15 km (3.1-9.3 mi) if folds near Detroit River included	NW-SE trending, NW plunging anticline, faulted on NW flank	Fault is NW-SE trending, normal, near-vertical, NE dipping, down-to-the-southwest	Anticline is expressed in the Precambrian unconformity surface; offsets top of Middle Ordovician Trenton Formation >300 m (1000 ft)	Influences deposition of Early Mississippian Sunbury Shale; does not offset top of lower Middle Devonian[1] Detroit River Group in cross section	Northville oil and gas field (southeast) and Fowlerville gas field (northwest). New Boston and Sumpter oil and gas fields associated with folds near Detroit River	B, G	Reference 2.5.1-340; Reference 2.5.1-237
Maumee Fault (MF)	Henry, Lucas, and Wood counties, Ohio	34 km (21 mi)	NE-SW trending fault	NE-SW trending, normal, vertical	Offset by central segment of Bowling Green fault; coincident with Maumee River lineament			G	Reference 2.5.1-237

Replace with Table 2.5.1-201 in Insert 1

Table 2.5.1-201 Regional Tectonic Structures Within 320 km (200 mi) (Sheet 8 of 13) [EF3 COL 2.0-26-A]

Name	Location	Closest Distance to Site	Structure Trend, Plunge and Any Associated Fault	Trend, Type of Fault, Dip, Sense of Displacement	Unit/Age/Amount of Maximum Deformation/Offset	Unit/Age/Amount of Youngest Deformation/Offset	Associated Oil and Gas Field	Means of Identification[a]	Source
Mount Carmel Fault / Leesville Anticline	Monroe, Lawrence, and Washington counties, Indiana	397 km (246 mi)	N-NW trending anticlines over graben along southwest side of antithetic normal fault associated with east-dipping thrust fault along NE margin of Illinois basin	N-SW trending, normal, southwest-dipping, down-to-the-southwest	Associated with paleoliquefaction centers (see discussion of Wabash Valley Seismic Zone)	Anticlines Devonian; fault offsets base of Upper Devonian New Albany Shale		B, G	Reference 2.5.1-338; Reference 2.5.1-229
Peck Fault (PF) (also known as Sanilac Fault)	St. Clair and Sanilac counties, Michigan	133 km (82 mi.)	N-S trending fault (Figure 2.5.1-203). N10° – 20°W trending faulted monocline (Reference 2.5.1-329)	N-S trending, normal, vertical [illegible] (Refer N10° [illegible] east d (Reference 2.5.1-329)	91 m (300 ft.) on [illegible] repeats early Late Silurian Salina Group A-1 Evaporite unit with approximately 29 m (95 ft.) of net slip (Reference 2.5.1-329)	Present on structure contour map on top of lowest Middle Devonian[1] Dundee Formation (Reference 2.5.1-325). Fault offsets contact between early Late Silurian Salina Group A-1 Evaporite and A-1 Carbonate units (Reference 2.5.1-329)		B, G	Reference 2.5.1-325; Reference 2.5.1-329; Reference 2.5.1-333
Royal Center Fault (RCF)	Cass, Fulton, and Kosciusko counties, Indiana	223 km (138 mi.)	NE-SW trending, normal, steeply southeast dipping, down-to-the-southwest	NE-SW trending, normal, steeply southeast dipping, down-to-the-southwest	Approximately 100 on the top of the Cambrian Mount Simon sandstone	Offsets top of Middle Silurian Salamonie Dolomite but not top of Middle Devonian[1] Muscatatuck Group		B, G	Reference 2.5.1-338

Replace with Table 2.5.1-201 in Insert 1

Table 2.5.1-201 Regional Tectonic Structures Within 320 km (200 mi) (Sheet 9 of 13) [EF3 COL 2.0-26-A]

Name	Location	Closest Distance to Site	Structure Trend, Plunge and Any Associated Fault	Trend, Type of Fault, Dip, Sense of Displacement	Unit/Age/Amount of Maximum Deformation/Offset	Unit/Age/Amount of Youngest Deformation/Offset	Associated Oil and Gas Field	Means of Identification[a]	Source
Sharpsville Fault (SF)	Tipton and Howard counties, Indiana	286 km (177 mi.)	NE-SW trending fault	NE-SW trending, normal, vertical, down-to-the-southeast		Offsets top of Middle Ordovician Trenton Formation		B	Reference 2.5.1-339
Transylvania Fault Extension (TFE)	NE Ohio	186 km (115 mi.)	Zone of NW to S-SE trending faults including the Pittsburg-Washington cross-strike structural discontinuity, Highland Town, Smith Township, Suffield, Akron, and Middleburg faults	NW-SE trending, early right-lateral-wrench faults with minimum of 21 km (13 mi.) of lateral displacement, reactivated normal, steeply (80°) southwest-dipping down faults	60 – 120 m (200 – 400 ft.), vertical, down-to-the-southwest, on Precambrian unconformity surface	72 m (240 ft.) vertical, down-to-the-southwest on Devonian Onondaga Limestone; controls deposition of strata as young as Pennsylvanian[1]		B, G	Reference 2.5.1-237; Reference 2.5.1-342
MINOR STRUCTURES									
Akron Anticline	Tuscola County, Michigan	180 km (110 mi.)	E-W trending anticline			Lower Middle Ordovician St. Peter Sandstone	Akron deep oil and gas field	B, G	Reference 2.5.1-429
Burdell Anticline	Osceola County, Michigan	130 km (90 mi)	Faulted dome	Two intersecting N-NW and N-NE trending faults, normal, vertical	Faults top of Early to Middle Ordovician Foster Formation with vertical closure of about 46 m (150 ft)	Overlying St. Peter Sandstone not faulted but domed; deformation extends up into the Late Silurian Salina Group A-2 Carbonate	Burdell oil and gas field	B, G	Reference 2.5.1-430

Replace with Table 2.5.1-201 in Insert 1

Table 2.5.1-201 Regional Tectonic Structures Within 320 km (200 mi) (Sheet 10 of 13) [EF3 COL 2.0-26-A]

Name	Location	Closest Distance to Site	Structure Trend, Plunge and Any Associated Fault	Trend, Type of Fault, Dip, Sense of Displacement	Unit/Age/Amount of Maximum Deformation/Offset	Unit/Age/Amount of Youngest Deformation/Offset	Associated Oil and Gas Field	Means of Identification[1]	Source
Clayton Anticline	Arenac and Ogemaw counties, Michigan	250 km (155 mi)	NW-SE trending anticline faulted on NE flank	NW-SE trending fault, down-to-the-northeast	Top of Middle Ordovician Glenwood Formation faulted	Deformation extends up into the latest Late Devonian Berea Sandstone	Cayton gas field	B, G	Reference 2.5.1-431
Clearville Fault	SW Ontario, Canada	138 km (85 mi)	N-NW trending fault	N-NW trending, normal, vertical west-side-down	Present on the Precambrian surface; 52 m (170 ft) on top of Middle Silurian Clinton Group	Probably present on structure contour map on top of Lower Devonian Detroit Group	Clearville oil field	B, G	Reference 2.5.1-325
Dawn Fault	SW Ontario, Canada	99 km (61 mi)	E-W trending fault	E-W t… vertica…	Replace with Table 2.5.1-201 in Insert 1 … uppermost Silurian Bass Islands Group	Displaces base but not top of lower Devonian Detroit River Group	Dawn gas field	B, G	Reference 2.5.1-325
Dover Syncline/Fault	SE Ontario, Canada	85 km (52 mi)	E-W fault	E-W, normal, vertical, down-to-the-south	Present on the structure contour map on the top of the Middle Ordovician Trenton Group with ≈45 m (≈150 ft) of relief		Dover oil and gas field	B, G	Reference 2.5.1-325
Falmouth Anticline	Missaukee County, Michigan	300 km (186 mi)	NW-SE trending anticline (dome) with Paleozoic units draped over recurrently active basement faults			Earliest Middle Devonian[1] Dundee Limestone faulted	Falmouth gas field	B, G	Reference 2.5.1-432

Table 2.5.1-201 Regional Tectonic Structures Within 320 km (200 mi) (Sheet 11 of 13) [EF3 COL 2.0-26-A]

Name	Location	Closest Distance to Site	Structure Trend, Plunge and Any Associated Fault	Trend, Type of Fault, Dip, Sense of Displacement	Unit/Age/Amount of Maximum Deformation/Offset	Unit/Age/Amount of Youngest Deformation/Offset	Associated Oil and Gas Field	Means of Identification(a)	Source
Kawkawlin Anticline	Bay County, Michigan	190 km (120 mi)	NW-SE trending asymmetrical anticline with steeply dipping SW flank			Earliest Middle Devonian[1] Dundee Limestone deformed	Kawkawlin gas field	B, G	Reference 2.5.1-433
Kimball-Colinville Monocline/Fault	crosses St. Clair River, Michigan/ Ontario	123 km (76 mi)	NW-SE trending fault	NW-SE trending, steeply SW dipping faulted monocline	64 m (210 ft) on uppermost Silurian Bass Islands Group; possibly more on lower Middle Devonian[1] Detroit River Group	Probably present on structure contour map on top of Middle Devonian[1] Dundee Formation	Kimball-Colinville oil and gas field	B, G	Reference 2.5.1-325
New Lothrop Anticline	Shiawassee County, Michigan	140 km (87 mi)	N-NW to S-SE trending, NW plunging anticline		Replace with Table 2.5.1-201 in Insert 1	Uppermost Late Devonian[1] Berea Sandstone (production formation)	New Lothrop oil field	B	Reference 2.5.1-434
Rose City Anticline	Ogemaw County, Michigan	280 km (170 mi)	NW-SE trending asymmetrical anticline with steeply dipping northeast flank			Earliest Middle Devonian[1] Dundee Limestone deformed	Rose City gas field	B, G	Reference 2.5.1-435
Shaver Anticline	Gratiot and Montcalm counties, Michigan	190 km (118 mi)	NW-SE trending anticline			Deforms Early Mississippian Brown Limestone unit of Michigan Formation but not overlying Triple Gypsum unit	Shaver gas field	B, G	Reference 2.5.1-436

Table 2.5.1-201 Regional Tectonic Structures Within 320 km (200 mi) (Sheet 12 of 13) [EF3 COL 2.0-26-A]

Name	Location	Closest Distance to Site	Structure Trend, Plunge and Any Associated Fault	Trend, Type of Fault, Dip, Sense of Displacement	Unit/Age/Amount of Maximum Deformation/Offset	Unit/Age/Amount of Youngest Deformation/Offset	Associated Oil and Gas Field	Means of Identification[a]	Source
South Buckeye Anticline	Gladwin County, Michigan	234 km (145 mi)	NW-SE trending asymmetrical anticline with steeply dipping southwest flank			Earliest Middle Devonian[1] Dundee Limestone deformed	South Buckeye oil and gas field	B, G	Reference 2.5.1-431
Stony Island Anticline (SIA)	Wayne County, Michigan	18 km (11 mi)	N30°W trending anticline with steeply dipping (50°SW) southwest flank; may be southeast extension of Howell anticline (see Major Structures)			Lower Middle Devonian[1] Sylvania Sandstone deformed		S, B	Reference 2.5.1-341
West Branch Anticline	Ogemaw County, Michigan	270 km (168 mi)	NW-SE trending faulted anticline	NW-SE trending, normal, steeply dipping, down-to-the southwest (1 SW dipping, southeast of axis), down-to the northeast (1 NE dipping, northeast of axis and 1 main, NE dipping, on NE flank); 2-3 N-NE trending, normal, steeply east-dipping, down-to-the-east on SE nose		Earliest Middle Devonian[1] Dundee Limestone deformed/faulted; about 53.3 m (175 ft) of closure on top of Early Ordovician Prairie du Chien Group[1]	West Branch gas field	B, G	Reference 2.5.1-437

Replace with Table 2.5.1-201 in Insert 1

Table 2.5.1-201 Regional Tectonic Structures Within 320 km (200 mi) (Sheet 13 of 13) [EF3 COL 2.0-26-A]

Name	Location	Closest Distance to Site	Structure Trend, Plunge and Any Associated Fault	Trend, Type of Fault, Dip, Sense of Displacement	Unit/Age/Amount of Maximum Deformation/Offset	Unit/Age/Amount of Youngest Deformation/Offset	Associated Oil and Gas Field	Means of Identification[a]	Source
Williams-Larkin Anticline	Bay County, Michigan	200 km (120 mi)	NW-SE trending, NW plunging anticline (Larkin may be a dome)			Latest Late Devonian[1] Berea Sandstone (production formation)	Larkin-Williams oil and gas field	B	Reference 2.5.1-438
Winterfield Anticline	Clare County, Michigan	280 km (174 mi)	NW-SE trending anticline (dome)			Deforms top of lower Middle Devonian[1] Detroit River Group massive anhydrite unit with vertical relief of about 21 m (70 ft)	Winterfield oil and gas field	B, G	Reference 2.5.1-439

Replace with Table 2.5.1-201 in Insert 1

a) B = Borings; G = Geophysical; S = Surface

Includes revisions from RAI 02.05.01-6, RAI 02.05.01-7, and RAI 02.05.01-8

Insert 1

Table 2.5.1-201 Regional Tectonic Structures Within 320 km (200 mi) (Sheet 1 of 7)

Name	Location	Closest Distance to Site	Structure Trend, Plunge and Any Associated Fault	Trend, Type of Fault, Dip, Sense of Displacement	Unit/Age/Amount of Maximum Deformation/Offset	Unit/Age/Amount of Youngest Deformation/Offset	Age of Oldest Unfaulted Unit	Associated Oil and Gas Field	Means of Identification[a]	Source
MAJOR STRUCTURES										
Akron Magnetic Boundary (AMB)	NE Ohio	170 km (106 mi)	NE-SW trending magnetic anomaly (low) associated with possible pre-existing basement structure			Possible lake-loading-induced seismicity	n/a		G	Reference 2.5.1-237; Reference 2.5.1-327; Reference 2.5.1-207
Albion-Scipio Fault (ASF)	Hillsdale and Calhoun counties, Michigan	108 km (67 mi)	NW-SE trending anticline associated with en-echelon wrench faults			Offsets the Middle Ordovician Trenton Formation and the Mississippian Coldwater Shale	Late Wisconsinan to Holocene till and glaciofluvial deposits	Albion-Pulaski-Scipio-Trend oil and gas field	B, G	Reference 2.5.1-331; Reference 2.5.1-207
Northern Segment Bowling Green Fault (BGF), also known as the Lucas-Monroe Monocline (LMM) in Michigan	Lenawee/ Monroe counties northwest to Livingston County, Michigan	48 km (28 mi)	NW-SE trending asymmetrical anticline(s) with steeply dipping SW flank (faulted); merges with Howell anticline at north end	Several NW-SE trending, normal, steeply dipping to vertical, right- and left-stepping, southwest-side-down faults; includes Deerfield anticline, a N-S trending, north-plunging anticline with normal, steeply dipping to vertical, down-to-the-west fault on west	Top of Middle Ordovician Trenton Formation is offset 61 m (200 ft) down-to-the-west	Offsets top of Early Mississippian Sunbury Shale on structure contour map	Late Wisconsinan to Holocene till and glaciofluvial deposits	Deerfield oil field	B, G	Reference 2.5.1-333; Reference 2.5.1-335; Reference 2.5.1-207
Central Segment Bowling Green Fault, also known as the Lucas-Monroe Monocline	Hancock County, Ohio south to Lenawee/ Monroe counties, Michigan	40 km (24 mi)		N10 – 20°W trending, normal, vertical fault, down-to-the-west with recurrent, variable displacements (see Figure 2.5.1-223). Waterville Quarry exposures suggest thrusts are interformational ramp faults (see Episode VI on Figure 2.5.1-223)	Offsets top of Middle Silurian Lockport Dolomite approximately 122 m (400 ft)	Slickensides and offset bedding in uppermost Late Silurian Bass Islands Group; <5 m (16 ft) thrusting in Cenozoic is highly speculative	Late Silurian to Early Devonian. Late Wisconsinan to Holocene till and lacustrine deposits		S, B, G	Reference 2.5.1-332; Reference 2.5.1-237; Reference 2.5.1-207
Southern Segment Bowling Green Fault (BGF)	Wood County south to Marion County, Ohio	101 km (62 mi)		SE trending, normal, steeply dipping to vertical, down-to-the-northeast splays (Outlet and Marion faults) and down-to-the-west fault splays (see Figure 2.5.1-203)	Offsets Precambrian unconformity surface		Late Silurian to Early Devonian. Late Wisconsinan to Holocene till and lacustrine deposits		B, G	Reference 2.5.1-237; Reference 2.5.1-207

Table 2.5.1-201 Regional Tectonic Structures Within 320 km (200 mi) (Sheet 2 of 7)

Name	Location	Closest Distance to Site	Structure Trend, Plunge and Any Associated Fault	Trend, Type of Fault, Dip, Sense of Displacement	Unit/Age/Amount of Maximum Deformation/Offset	Unit/Age/Amount of Youngest Deformation/Offset	Age of Oldest Unfaulted Unit	Associated Oil and Gas Field	Means of Identification[a]	Source
Burning Springs Anticline (BSA) (50 – 150 km long)	West Virginia	327 km (203 mi)	N-S trending anticline faulted in core; splays into several right-stepping traces at Ohio River; may extend south to include Mann Mountain anticline	N-S trending, normal, steeply east-dipping fault, down-to-the-east with recurrent displacements, including: a. Offsets Precambrian unconformity surface south of the Ohio River b. Reactivation during Silurian restricting salt deposition to a basin east of the fault c. Recurrent movement during deposition of Devonian through Permian strata d. NW directed Alleghanian age thrusting on decollements in Late Silurian Salina Group salts at the salt edge and development of imbricate ramp thrusts coring anticline in Salina Group and younger strata	300 m (980 ft) down-to-the-east on base of Cambrian	Only folding in Late Silurian Salina Group through Pennsylvanian-Permian units	Middle Pleistocene to Holocene colluvium, and Late Wisconsinan to Holocene alluvium		B, G	Reference 2.5.1-237; Reference 2.5.1-336; Reference 2.5.1-337; Reference 2.5.1-207
Cambridge Arch (CA) (100 km long)	Eastern Ohio	118 km (73 mi)	N20°W trending fault-bounded arch (horst) with half graben (Parkersburg-Lorain syncline) on west; splays into three arches at Ohio River	N20°W trending normal faults, dipping >80°, bounding 1.5 km (0.9 mi) wide uplifted block (horst) with some right-lateral slip at north end	≈80 m (262 ft) structural relief on Devonian Onondaga Limestone	Late Permian	Late Wisconsinan to Holocene till and glaciofluvial deposits		S (north end), B, G	Reference 2.5.1-237; Reference 2.5.1-336; Reference 2.5.1-207
Chatham Sag and Electric Fault	SW Ontario, Canada	81 km (50 mi)	E-W trending sag defined by mutual plunges of Findlay and Algonquin arches and bound on the north by EW trending Electric fault	E-W trending, normal, vertical, south-side-down	Precambrian surface displaced about 93 m (305 ft) vertically	Present on the structure contour map on the uppermost Late Silurian Bass Islands Group but probably does not displace the base of the Middle Devonian Dundee Formation	Middle Devonian Dundee Formation. Pleistocene glaciolacustrine deposits		B, G	Reference 2.5.1-325; Reference 2.5.1-207

Table 2.5.1-201 Regional Tectonic Structures Within 320 km (200 mi) (Sheet 3 of 7)

Name	Location	Closest Distance to Site	Structure Trend, Plunge and Any Associated Fault	Trend, Type of Fault, Dip, Sense of Displacement	Unit/Age/Amount of Maximum Deformation/Offset	Unit/Age/Amount of Youngest Deformation/Offset	Age of Oldest Unfaulted Unit	Associated Oil and Gas Field	Means of Identification[a]	Source
Colchester Fault	Essex County, southeast Ontario	52 km (32 mi)	North-northwest-trending faults or syncline	Two subparallel, northwest-trending down-to-the-east faults. Zone of dolomitization along a fracture zone in the Middle Ordovician Trenton Formation	Interpreted 12.2 m (40 ft) of relief on syncline in Middle Ordovician and Lower to Middle Silurian rocks	Middle Ordovician through Middle Silurian	Pleistocene glaciolacustrine deposits	Colchester Oil Pool	B, G	Reference 2.5.1-406; Reference 2.5.1-409; Reference 2.5.1-412; Reference 2.5.1-413; Reference 2.5.1-207
Fort Wayne Rift	Western Ohio and eastern Indiana	173 km (107 mi)	NW-SE trending fault-bounded graben with central high	NW-SE trending, normal, vertical, northeast-side-down Anna-Champaign fault and southwest-side-down Logan fault forming central high; unnamed northeast and southwest side-down fault bounding graben		Truncated by GFTZ (1.25 Ga to 980 Ma); seismically active	Paleozoic sediments		B, G	Reference 2.5.1-237; Reference 2.5.1-207
Fortville Fault (FF)	Marion, Hancock, and Madison counties, Indiana	271 km (168 mi)	N-NE to S-SW trending, normal fault, steeply southeast dipping, down-to-the-southeast; on west flank of Cincinnati arch	Offsets top of Precambrian surface	Offsets top of Middle Silurian Salamonie Dolomite but not top of Middle Devonian Muscatatuck Group	Lower Mississippian	Late Wisconsinan to Holocene till and glacial outwash deposits		B, G	Reference 2.5.1-338; Reference 2.5.1-207
Grenville Front Tectonic Zone (GFTZ)	Mississippi north and north through Ohio and NE Canada	0 km (0 mi)	NE to N to NE trending zone of faults 10 – 100 km (6 – 60 mi) wide	NE to N-NE trending thrust faults, dipping east. Suture zone associated with Grenville orogeny	Probably tens of km of E-W crustal shortening during Grenville orogeny (1.25 Ga to 980 Ma)	Movement along the Bowling Green fault is attributed to reactivation of GFTZ. Uppermost Late Silurian Bass Islands Group offset by central segment of Bowling Green fault	Movement along the Bowling Green fault is attributed to reactivation of GFTZ. Uppermost Late Silurian Bass Islands Group offset by central segment of Bowling Green fault		B, G	Reference 2.5.1-237; Reference 2.5.1-234
Hoosier Thrust Belt - Louisville Uplift	SW Indiana	393 km (244 mi)		Series of N-NW trending thrust faults, west-dipping (Hoosier thrust fault) bound on east by N-NW trending, foreland-style thrust fault (Louisville uplift)	Hoosier thrust belt is developed within the Precambrian (Mesoproterozoic) Centralia Group and truncated by overlying unconformity; Louisville uplift has ≈8 km (5 mi) of vertical uplift dated at 600 Ma (see discussion of Wabash Valley Seismic Zone)	Precambrian	Paleozoic units		B, G	Reference 2.5.1-338; Reference 2.5.1-229

Table 2.5.1-201 Regional Tectonic Structures Within 320 km (200 mi) (Sheet 4 of 7)

Name	Location	Closest Distance to Site	Structure Trend, Plunge and Any Associated Fault	Trend, Type of Fault, Dip, Sense of Displacement	Unit/Age/Amount of Maximum Deformation/Offset	Unit/Age/Amount of Youngest Deformation/Offset	Age of Oldest Unfaulted Unit	Associated Oil and Gas Field	Means of Identification[a]	Source
Howell Anticline/Fault (HA) (100 km long; 145 km if folds near Detroit River included)	Wayne northwest to Shiawassee counties, Michigan. May extend southeast to Detroit River to Stony Island Anticline and associated folds (see Minor Structures)	45 km (27 mi) / 5-15 km (3.1-9.3 mi) if folds near Detroit River included	NW-SE trending, NW plunging anticline, faulted on NW flank	Fault is NW-SE trending, normal, near-vertical, NE dipping, down-to-the-southwest	Anticline is expressed in the Precambrian unconformity surface; offsets top of Middle Ordovician Trenton Formation >300 m (1000 ft)	Influences deposition of Early Mississippian Sunbury Shale	Lower Middle Devonian Detroit River Group. Late Wisconsinan and Holocene till, glaciofluvial and lacustrine deposits	Northville oil and gas field (southeast) and Fowlerville gas field (northwest). New Boston and Sumpter oil and gas fields associated with folds near Detroit River	B, G	Reference 2.5.1-340; Reference 2.5.1-237
Maumee Fault (MF)	Henry, Lucas, and Wood counties, Ohio	34 km (21 mi)	NE-SW trending fault	NE-SW trending, normal, vertical	Offset by central segment of Bowling Green fault; coincident with Maumee River lineament	Unknown	Unknown		G	Reference 2.5.1-237
Mount Carmel Fault / Leesville Anticline	Monroe, Lawrence, and Washington counties, Indiana	397 km (246 mi)	N-NW trending anticlines over graben along southwest side of antithetic normal fault associated with east-dipping thrust fault along NE margin of Illinois basin	N-SW trending, normal, southwest-dipping, down-to-the-southwest	Associated with paleoliquefaction centers (see discussion of Wabash Valley Seismic Zone)	Middle Mississippian	Pleistocene and Holocene alluvium and colluvium		B, G	Reference 2.5.1-338; Reference 2.5.1-229
Peck Fault (PF) (also known as Sanilac Fault)	St. Clair and Sanilac counties, Michigan	133 km (82 mi.)	N-S trending fault (Figure 2.5.1-203). N10° – 20°W trending faulted monocline (Reference 2.5.1-329)	N-S trending, normal, vertical, west-side-down (Reference 2.5.1-325). N10° – 20°W trending, east dipping thrust fault (Reference 2.5.1-329)	91 m (300 ft.) on Middle Ordovician Trenton Group (Reference 2.5.1-325). Sanilac fault repeats early Late Silurian Salina Group A-1 Evaporite unit with approximately 29 m (95 ft.) of net slip (Reference 2.5.1-329)	Present on structure contour map on top of lowest Middle Devonian Dundee Formation (Reference 2.5.1-325). Fault offsets contact between early Late Silurian Salina Group A-1 Evaporite and A-1 Carbonate units (Reference 2.5.1-329). Early Mississippian Sunbury Shale	Late Wisconsinan and Holocene till and glacial and postglacial lacustrine deposits		B, G	Reference 2.5.1-325; Reference 2.5.1-329; Reference 2.5.1-333; Reference 2.5.1-207
Royal Center Fault (RCF)	Cass, Fulton, and Kosciusko counties, Indiana	223 km (138 mi.)	NE-SW trending, normal, steeply southeast dipping, down-to-the-southeast	NE-SW trending, normal, steeply southeast dipping, down-to-the-southeast	Approximately 100 on the top of the Cambrian Mount Simon sandstone	Offsets top of Middle Silurian Salamonie Dolomite and the Mississippian Black Shale	Late Wisconsinan and Holocene till, glacial outwash and ice contact deposits		B, G	Reference 2.5.1-338; Reference 2.5.1-207
Sharpsville Fault (SF)	Tipton and Howard counties, Indiana	286 km (177 mi.)	NE-SW trending fault	NE-SW trending, normal, vertical, down-to-the-southeast		Offsets top of Middle Ordovician Trenton Formation and Devonian rocks	Late Wisconsinan and Holocene till		B	Reference 2.5.1-339; Reference 2.5.1-207

Table 2.5.1-201 Regional Tectonic Structures Within 320 km (200 mi) (Sheet 5 of 7)

Name	Location	Closest Distance to Site	Structure Trend, Plunge and Any Associated Fault	Trend, Type of Fault, Dip, Sense of Displacement	Unit/Age/Amount of Maximum Deformation/Offset	Unit/Age/Amount of Youngest Deformation/Offset	Age of Oldest Unfaulted Unit	Associated Oil and Gas Field	Means of Identification[a]	Source
Transylvania Fault Extension (TFE)	NE Ohio	186 km (115 mi.)	Zone of NW to S-SE trending faults including the Pittsburg-Washington cross-strike structural discontinuity, Highland Town, Smith Township, Suffield, Akron, and Middleburg faults	NW-SE trending, early right-lateral-wrench faults with minimum of 21 km (13 mi.) of lateral displacement, reactivated normal, steeply (80°) southwest-dipping, down-to-the-southwest faults	60 – 120 m (200 – 400 ft.), vertical, down-to-the-southwest, on Precambrian unconformity surface	72 m (240 ft.) vertical, down-to-the-southwest on Devonian Onondaga Limestone; controls deposition of strata as young as Pennsylvanian	Mid-Pleistocene to Holocene alluvium and colluvium		B, G	Reference 2.5.1-237; Reference 2.5.1-342; Reference 2.5.1-207
MINOR STRUCTURES (Note: Minor structures are identified from oil and gas explorations reports that focus on the producing horizons; only limited information cited below is available to evaluate the age of youngest deformation or the oldest unfaulted unit.)										
Akron Anticline	Tuscola County, Michigan	180 km (110 mi.)	E-W trending anticline			Lower Middle Ordovician St. Peter Sandstone	Late Wisconsinan and Holocene glacial and postglacial lacustrine deposits	Akron deep oil and gas field	B, G	Reference 2.5.1-429; Reference 2.5.1-207
Burdell Anticline	Osceola County, Michigan	130 km (190 mi)	Faulted dome	Two intersecting N-NW and N-NE trending faults, normal, vertical	Faults top of Early to Middle Ordovician Foster Formation with vertical closure of about 46 m (150 ft)	Overlying St. Peter Sandstone not faulted but domed; deformation extends up into the Late Silurian Salina Group A-2 Carbonate	Late Wisconsinan and Holocene till	Burdell oil and gas field	B, G	Reference 2.5.1-430; Reference 2.5.1-207
Clayton Anticline	Arenac and Ogemaw counties, Michigan	250 km (155 mi)	NW-SE trending anticline faulted on NE flank	NW-SE trending fault, down-to-the-northeast	Top of Middle Ordovician Glenwood Formation faulted	Deformation extends up into the latest Late Devonian Berea Sandstone	Late Wisconsinan and Holocene glacial and postglacial lacustrine deposits	Cayton gas field	B, G	Reference 2.5.1-431; Reference 2.5.1-207
Clearville Fault	SW Ontario, Canada	138 km (85 mi)	N-NW trending fault	N-NW trending, normal, vertical west-side-down	Present on the Precambrian surface; 52 m (170 ft) on top of Middle Silurian Clinton Group	Probably present on structure contour map on top of Lower Devonian Detroit Group	Pleistocene till and glaciolacustrine deposits	Clearville oil field	B, G	Reference 2.5.1-325; Reference 2.5.1-207
Dawn Fault	SW Ontario, Canada	99 km (61 mi)	E-W trending fault	E-W trending, normal, vertical, south-side-down	Probably 47 m (155 ft) on top of Middle Silurian Clinton Group; 60 m (≈200 ft) trough on uppermost Silurian Bass Islands Group	Displaces base but not top of lower Devonian Detroit River Group	Pleistocene till and glaciolacustrine deposits	Dawn gas field	B, G	Reference 2.5.1-325; Reference 2.5.1-207
Dover Syncline/Fault	SE Ontario, Canada	85 km (52 mi)	E-W fault	E-W, normal, vertical, down-to-the-south	Present on the structure contour map on the top of the Middle Ordovician Trenton Group with ≈45 m (≈150 ft) of relief		Pleistocene glaciolacustrine deposits	Dover oil and gas field	B, G	Reference 2.5.1-325; Reference 2.5.1-207
Falmouth Anticline	Missaukee County, Michigan	300 km (186 mi)	NW-SE trending anticline (dome) with Paleozoic units draped over recurrently active basement faults			Earliest Middle Devonian Dundee Limestone faulted	Late Wisconsinan and Holocene glaciofluvial and ice contact deposits	Falmouth gas field	B, G	Reference 2.5.1-432; Reference 2.5.1-207

Table 2.5.1-201 Regional Tectonic Structures Within 320 km (200 mi) (Sheet 6 of 7)

Name	Location	Closest Distance to Site	Structure Trend, Plunge and Any Associated Fault	Trend, Type of Fault, Dip, Sense of Displacement	Unit/Age/Amount of Maximum Deformation/Offset	Unit/Age/Amount of Youngest Deformation/Offset	Age of Oldest Unfaulted Unit	Associated Oil and Gas Field	Means of Identification[a]	Source
Kawkawlin Anticline	Bay County, Michigan	190 km (120 mi)	NW-SE trending asymmetrical anticline with steeply dipping SW flank			Earliest Middle Devonian Dundee Limestone deformed	Late Wisconsinan and Holocene glacial and postglacial lacustrine deposits and till	Kawkawlin gas field	B, G	Reference 2.5.1-433; Reference 2.5.1-207
Kimball-Colinville Monocline/Fault	crosses St. Clair River, Michigan/ Ontario	123 km (76 mi)	NW-SE trending fault	NW-SE trending, steeply SW dipping faulted monocline	64 m (210 ft) on uppermost Silurian Bass Islands Group; possibly more on lower Middle Devonian Detroit River Group	Probably present on structure contour map on top of Middle Devonian Dundee Formation	Pleistocene till and glaciolacustrine deposits	Kimball-Colinville oil and gas field	B, G	Reference 2.5.1-325; Reference 2.5.1-207
New Lothrop Anticline	Shiawassee County, Michigan	140 km (87 mi)	N-NW to S-SE trending, NW plunging anticline		18.3 m (60 ft) relief on top of lowermost Middle Devonian Dundee Limestone	Uppermost Late Devonian Berea Sandstone (production formation)	Late Wisconsinan and Holocene glacial and postglacial lacustrine deposits	New Lothrop oil field	B	Reference 2.5.1-434; Reference 2.5.1-207
Rose City Anticline	Ogemaw County, Michigan	280 km (170 mi)	NW-SE trending asymmetrical anticline with steeply dipping northeast flank			Earliest Middle Devonian Dundee Limestone deformed	Late Wisconsinan and Holocene glacial and postglacial outwash and till	Rose City gas field	B, G	Reference 2.5.1-435; Reference 2.5.1-207
Shaver Anticline	Gratiot and Montcalm counties, Michigan	190 km (118 mi)	NW-SE trending anticline			Deforms Early Mississippian Brown Limestone unit of Michigan Formation	Late Mississippian Triple Gypsum	Shaver gas field	B, G	Reference 2.5.1-436; Reference 2.5.1-207
South Buckeye Anticline	Gladwin County, Michigan	234 km (145 mi)	NW-SE trending asymmetrical anticline with steeply dipping southwest flank			Earliest Middle Devonian Dundee Limestone deformed	Late Wisconsinan and Holocene glacial and postglacial lacustrine deposits	South Buckeye oil and gas field	B, G	Reference 2.5.1-431; Reference 2.5.1-207
Stony Island Anticline (SIA)	Wayne County, Michigan	18 km (11 mi)	N30°W trending anticline with steeply dipping (50°SW) southwest flank; may be southeast extension of Howell anticline (see Major Structures)			Lower Middle Devonian Sylvania Sandstone deformed	Late Wisconsinan and Holocene glacial and postglacial lacustrine deposits		S, B	Reference 2.5.1-341; Reference 2.5.1-207
West Branch Anticline	Ogemaw County, Michigan	270 km (168 mi)	NW-SE trending faulted anticline	NW-SE trending, normal, steeply dipping, down-to-the southwest (1 SW dipping, southeast of axis), down-to the northeast (1 NE dipping, northeast of axis and 1 main, NE dipping, on NE flank); 2-3 N-NE trending, normal, steeply east-dipping, down-to-the-east on SE nose		Earliest Middle Devonian Dundee Limestone deformed/faulted; about 53.3 m (175 ft) of closure on top of Early Ordovician Prairie du Chien Group	Late Wisconsinan and Holocene till, glaciofluvial and ice contact deposits	West Branch gas field	B, G	Reference 2.5.1-437; Reference 2.5.1-207

Table 2.5.1-201 Regional Tectonic Structures Within 320 km (200 mi) (Sheet 7 of 7)

Name	Location	Closest Distance to Site	Structure Trend, Plunge and Any Associated Fault	Trend, Type of Fault, Dip, Sense of Displacement	Unit/Age/Amount of Maximum Deformation/Offset	Unit/Age/Amount of Youngest Deformation/Offset	Age of Oldest Unfaulted Unit	Associated Oil and Gas Field	Means of Identification[a]	Source
Williams-Larkin Anticline	Bay County, Michigan	200 km (120 mi)	NW-SE trending, NW plunging anticline (Larkin may be a dome)			Latest Late Devonian Berea Sandstone (production formation)	Late Wisconsinan and Holocene glacial and postglacial lacustrine deposits	Larkin-Williams oil and gas field	B	Reference 2.5.1-438; Reference 2.5.1-207
Winterfield Anticline	Clare County, Michigan	280 km (174 mi)	NW-SE trending anticline (dome)			Deforms top of lower Middle Devonian Detroit River Group massive anhydrite unit with vertical relief of about 21 m (70 ft)	Late Wisconsinan and Holocene till, glaciofluvial outwash	Winterfield oil and gas field	B, G	Reference 2.5.1-439; Reference 2.5.1-207

a) B = Borings; G = Geophysical; S = Surface

Attachment 5
NRC3-10-0006

Response to RAI Letter No. 16
(eRAI Tracking No. 3913)

RAI Question No. 02.05.01-9

RAI 02.05.01-09

FSAR Section 2.5.1.1.4.3.3 states that "no faults in the site region exhibit evidence of movement since the Paleozoic (Reference 2.5.1–344)." Similarly, FSAR Section 2.5.1.1.4.3 states, "There is no evidence to indicate that reactivation of structures in the Mesozoic ... occurred in the region." However, FSAR Section 2.5.1.1.4.3.2.14, which discusses the Transylvania fault extension, states that the Middleburg fault was reactivated "during the Early Jurassic faulting of the rift basins along the margin of the continent (Reference 2.5.1–342)." Please resolve these statements.

Response

Based on discussions with Mark Baranoski, of the Ohio Division of Geological Survey, and further review of the published literature, there is no evidence for Mesozoic reactivation of the Middleburg fault or other Transylvania fault extension structures in Ohio. A modification to the FSAR text has been made to clarify the evidence for timing of faulting on the Transylvanian fault extension in Ohio *is* contained in the response to RAI 02.05.01-6 (Attachment 3). The statements in FSAR Section 2.5.1.1.4.3.3 and 2.5.1.1.4.3 regarding no evidence of movement since the Paleozoic and the lack of evidence for Mesozoic reactivation, respectively, are correct.

Proposed COLA Revision

Revisions to FSAR Section 2.5.1.1.4.3.2.14 are provided in response to RAI 02.05.01-06.

Attachment 6
NRC3-10-0006

Response to RAI Letter No. 16
(eRAI Tracking No. 3913)

RAI Question No. 02.05.01-10

RAI 02.05.01-10

FSAR Section 2.5.1.1.4.3.3.1 does not discuss liquefaction studies within the Northeast Ohio seismic zone. However, Crone and Wheeler (FSAR Reference 2.5.1–316) cite Obermeier for his examination of streambanks for liquefaction features in the Northeast Ohio seismic zone. Paleoliquefaction investigations are relevant to evaluating the potential for magnitude 6 or larger earthquakes that may have occurred within the Northeast Ohio seismic zone. Given the proximity of the Northeast Ohio seismic zone to the Fermi site, an earthquake of magnitude 6 or larger may impact the seismic hazard at the Fermi site. Therefore, please include a description of any paleoseismic investigations conducted in the Northeast Ohio seismic zone including the locations investigated and the level of detail of the investigations.

Response

In a 1995 National Earthquake Hazards Reduction Program (NEHRP) annual summary report, Obermeier (Reference 2.5.1-482) discussed the results of a paleoseismic liquefaction field study along two of the larger drainages in northeast Ohio: the Grand River and the Cuyahoga River. Approximately 25 km (15.5 mi.) of stream banks along each river were searched and no evidence of liquefaction was observed along either transect. Conditions and ages of the sediment encountered along each of these rivers as noted by Obermeier (Reference 2.5.1-482) were summarized in the report, as follows:

- Radiocarbon data from along the Grand River show that many of the exposures searched are at least 2,000 years old. Many others are probably mid-Holocene in age, based on depth and severity of weathering. A few scattered sites are earliest Holocene in age. Liquefaction susceptibility at many of the sites examined is at least moderate.
- Numerous exposures along the Cuyahoga River are at least a few thousand years in age, and scattered exposures are up to 8,000 years old, based on radiocarbon data. Conditions are very good for forming liquefaction effects at many places.

Additional documentation of the 1995 paleoliquefaction field search in northeast Ohio, which focused on the vicinity of the nuclear power plant near Perry, Ohio, was provided to the NRC in a letter report submitted to Dr. Andrew Murphy by Dr. Obermeier on May 23, 1996 (Reference 2.5.1-483). A copy of this letter report and additional notes on communications with Dr. Obermeier were made available to this project by Dr. Russell Wheeler, U.S. Geological Survey, on November 17, 2009. Figure 1 shows the locations of the rivers searched as described in the letter report to the NRC. Table 1 summarizes the conditions (liquefaction susceptibility and estimated ages of sediments) and observations at various localities within the study area.

Based on these observations, Dr. Obermeier made the following conclusions:

- The lack of suitable exposures within 20 km of the nuclear power plant at Perry, Ohio, precludes definitive statements as to whether there has been strong seismic shaking for most of Holocene time.

- The lack of exposures with liquefiable sediment more than a few thousand years old, within 20 (12.4) to 25 km (15.5 mi.) of the plant, precludes any statement concerning whether there could have been strong shaking at the plant locale from even moderate-sized earthquakes (M ~ 6) occurring more than a few thousand years ago.
- The lack of liquefaction features in latest Pleistocene sediment (moderate to high liquefaction susceptibility through time) in the Pit-CL locality does not provide sufficient data to make a statement on seismic shaking at a distance of 32 km (19.8 mi.) from the Perry nuclear power plant.

Dr. Obermeier noted in the letter report that perennial streams flowing subparallel and through a beach ridge/sand dune complex within 2 (1.2) to 6 km (37 mi.) inland from the shore (identified from examination of the Soil Survey Report of Lake County) might offer the possibility of a field setting where liquefaction features could have developed for much of Holocene time. These streams were not searched during the 1995 study or in any subsequent studies by Obermeier.

Erik Venteris with the Ohio Geological Survey, a graduate student who participated with Dr. Obermeier on the paleoliquefaction studies in northeast Ohio, was contacted to determine whether additional work had been done since the studies in 1995. Mr. Venteris indicated that he has not done any additional paleoliquefaction reconnaissance in the area since the 1995 study. Based on a thorough literature search, no additional paleoliquefaction studies have been done in the area since the 1995 studies.

References

2.5.1-482 Obermeier, S., "Paleoseismic Liquefaction Studies—Central and Eastern US," USGS Annual Report, Volume 37, 1995, accessed in 1998 at http://erp-web.er.usgs.gov/reports/VOL37/CU/obermeier.htm, paper copy provided by Russ Wheeler on November 17, 2009.

2.5.1-483 Obermeier, S., "Summary of 1995 Paleoliquefaction Field Search in the Vicinity of Perry, Ohio," Letter submitted to Dr. Andrew Murphy, U.S. Nuclear Regulatory Commission, 10 pp., May 23, 1996.

Table 1. Summary of paleoliquefaction study areas of Obermeier (1995) in northeast Ohio

Stream	Reconaissance Area	Approx. Stream Length	Location Along Stream	Geology	Liquefaction Susceptibility	Age of Deposits	Conclusions Regarding Strong Ground Shaking
Grand River	GR-A	4 km	Swine Creek at intersection with SR 87 beyond confluence with Grand River	Clean liquefiable sand (inferred from augering) capped by clay-rich sediments	High	Base of clay-rich cap at two localities 4,690 and 13,780 radiocarbon yr before present (BP)	Unlikely that area has experienced strong ground shaking during the past 4,000 years
Grand River	GR-B	3 km	From Montgomery Road to Johnson Road	Not specified	Uncertain	Not provided	
Grand River	GR-C	3 km	Shaffer Road to Footville-Richmond Road	3-5 m (9.8 to 16.4 ft.)thick clay-rich cap over thick, clean sand	High	Base of clay-rich cap 2,080 to 2,230 radiocarbon yr BP	Unlikely that area has experienced strong ground shaking during the past 2,000 years
Grand River	GR-D	3 km	Sweitzer Road to Cork-Cold Springs Road	Clay-rich cap over local clean sands (no sand identified by augering)	High in places	Base of clay-rich cap 1,000 to 3,000 yr BP based on degree of weathering	
Grand River	GR-E	3 km	Lampson Road to Sexton Road	Clay-rich deposits to at least 8 ft depth, shallow bedrock	Low	Clay-rich cap 1,000 to 2,000 yr BP based on degree of weathering	
Grand River	GR-F	4 km	Blair Road to Madison Avenue	Clay-rich cap over clean sand, shallow depth to bedrock	Low	Clay-rich cap less than 1,000 yr BP based on degree of weathering	
Grand River	GR-G	3.5 km	"V" in "River" on topographic map to bridge at SR 535	Upstream area: clay-rich cap over clean sand downstream area: clay-rich cap with some local sand	Low within past several thousand years based on water table	Upstream area: clay-rich cap more than several thousand yr BP based on degree of weathering downstream area: clay-rich cap less than 1,000 yr BP based on degree of weathering	Unlikely that area has experienced strong ground shaking during the past few thousand years

Trumbull Creek	TR-A	1.5 km	Riverdale to confluence with Grand River	Clay-rich cap over local sand	High to low	Clay-rich cap more than several thousand years BP based on degree of weathering	Unlikely that area has experienced strong ground shaking during the past few thousand years
Cuyahoga River	CUY-A	16 km	Boston Mills to Rockside Road	Clay-rich cap over liquefiable sand	High	Oldest clay-rich cap 4,000 radiocarbon yr BP to 710 yr BP	Area has not experienced strong ground shaking during the past 500-1,000 years and probably not during the past 4,000 years
Cuyahoga River	CUY-B	5 km	Bridge at SR 87 to 5 km downstream	Not specified—exposure only at bridge	Uncertain	Not provided	
Near Tributary to Phelps Creek	PIT-CL	400 m	Sand pit on SR 534 just north of Ashtabula-Trumbull county line	Glaciofluvial sand with low-permeability cap	High to moderate—lack of weathering suggests a shallow groundwater table through Holocene time	Uncertain	Unlikely that area has experienced strong ground shaking through all or most of Holocene time
Streams unsuitable for paleoliquefaction studies							
Chagrin River							
East Branch Chagrin River							
Most of the east-west portion of the Grand River downstream from Mechanicsville							
Big Creek							
Paine Creek							

Mill Creek
Rock Creek
Lake Erie shoreline exposures between Ashtabula and the mouth of the Chagrin River were examined and found to be too clay-rich to be susceptible to liquefaction.
Abandoned sand pits in beach sands and dune deposits formed during high levels of ancient Lake Erie were examined. The water table was very deep in all pits, and no suitable exposures were found that contained liquefiable deposits.
Note: The field survey was conducted from a canoe at a time when the seasonal water table was extraordinarily low because of a prolonged drought; therefore, any paleoliquefaction features should have been conspicuous.

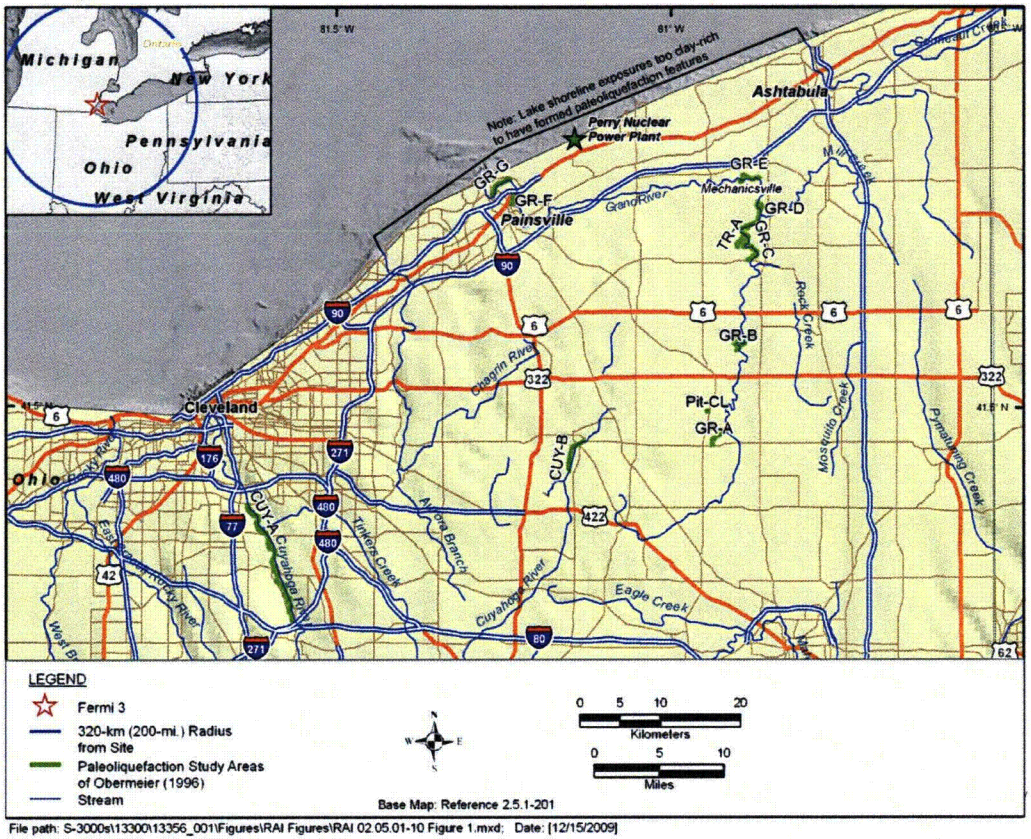

Figure 1. Paleoliquefaction study areas of Obermeier (1995) in northeast Ohio.

Proposed COLA Revision

Revisions to Section 2.5.1.1.4.3.3.1 to discuss the results of paleoliquefaction studies conducted in the Northeast Ohio seismic zone region are provided with the Response to RAI 02.05.01-28.

Attachment 7
NRC3-10-0006

Response to RAI Letter No. 16
(eRAI Tracking No. 3913)

RAI Question No. 02.05.01-11

RAI 02.05.01-11

FSAR Section 2.5.1.1.4.3.3.1 makes the point that the "sequence of earthquakes near Ashtabula ... is likely due to fluid injection causing failure along favorably oriented, pre-existing fractures....". Because artificial changes in subsurface hydrology can alter the mechanical conditions of the upper crust and trigger seismicity, it is important to know whether there are any other locations within the site region where large volumes of fluid are being injected or withdrawn. Please provide this information.

Response

FSAR Section 2.5.1.1.4.3.3.1 on the Northeast Ohio Seismic Zone states the following:

> "In 1987, the first in a series of earthquakes continuing to 2001 occurred within the Northeast Ohio seismic zone near Ashtabula in Ashtabula County Ohio, northeast of the 1986 earthquakes (Reference 2.5.1-347). The initial magnitude 3.8 event occurred on July 13, 1987, followed by a magnitude 2.6 event on January 19, 2001, a foreshock to a magnitude 4.5 event on January 25, 2001, which had a MMI of VI, followed by a magnitude 3.2 event on June 3, 2001, and a magnitude 2.3 event on June 5, 2001 (Reference 2.5.1-347). The July 13, 1987, main shock was close to a deep Class I injection well pumping fluids into the Mount Simon Sandstone, the basal Paleozoic unit overlying Precambrian crystalline basement, at a depth of about 1.8 km (1.1 mi), and a number of portable seismographs were deployed to study the aftershocks (Reference 2.5.1-347). The 1987 aftershocks (36) were all within 1 km (0.6 mi) of the injection well, and defined a 1.5-km (1-mi) long by 0.25-km (0.15-mi) wide area at a depth of about 2 km (1.2 mi), with left-lateral strike-slip movement on an east-west-striking fault (Reference 2.5.1-345). The Ohio Seismic Network was installed in 1999 and precisely recorded the 2001 earthquakes (Reference 2.5.1-347). The sequence of earthquakes near Ashtabula beginning in 1987 is likely due to fluid injection causing failure along favorably oriented, pre-existing fractures (Reference 2.5.1-347; Reference 2.5.1-346)."

Active waste disposal wells located within the site region are listed in Table 1 (Reference 1). Injection activity has stopped in many wells, including the well (Reserve Environmental Services, Inc.) associated with the seismicity in northeastern Ohio. Inactive disposal wells are tabulated in Table 2 (Reference 1). The depth of the well and formations into which waste was injected are included in Tables 1 and 2.

Reference:

1) U.S. Environmental Protection Agency, "Class 1 Injection wells in Region 5", Website http://www.epa.gov/R5water/uic/cl1sites.htm, 2010

Table 1 – Active Class I Injection Wells

Facility	State	County	USEPA Permit or Application #	H or NH	Well Name	Depth (ft)	Year Drilled	Injection Formation
BioLabs, Inc.	MI	Lenawee	MI-091-1I-0001	NH	Adrian #1	4856	1989	Franconia, Galesville, Eau Claire, Mt. Simon
			MI-091-1I-0002	NH	Well #2	4850	1997	
Cooper-Standard Products	MI	Otsego	MI-137-1I-0001	NH	StdPrd 1-21	2654	1989	Dundee
Dow Chemical Co.	MI	Mason	MI-105-1I-0003	NH	Dow #25	2350	2005	Traverse & Dundee Limestones and Reed City Dolomite
Env. Geo-Technologies (EGT) (formerly Env. Disposal Systems (EDS)	MI	Wayne	MI-163-1W-0006 [1]	H	Well #1-20	4490	1993	Mt. Simon
			MI-163-1W-C007	H	Well #1-12	4535	2002	
			MI-163-1W-C008	H	Well #2-12	4550	2002	
			MI-163-1W-0009 [2]	H	Well #2-20		NA	
Heinz	MI	Ottawa	MI-139-1I-0001	NH	Well #1	5910	1972	Franconia, Galesville, Eau Claire, Mt. Simon
			MI-139-1I-0002	NH	Well #2	6194	1972	
			MI-139-1I-0003	NH	Well #3	5905	1973	
Mosaic Potash Hersey LLC (formerly IMC Kalium)	MI	Osceola	MI-133-1I-0001	NH	Woodward #1-26	4247 (8140)	1983	Reed City Dolomite
			MI-133-1I-0002	NH	Thomas #1-26	4391 (8085)	1984	
Leelanau Fruit Co.	MI	Wexford	MI-165-1I-0001	NH	Fee #1	3700	1974	Traverse Limestone, Bell Shale, Dundee
Liquid Mgmt.	MI	Montcalm	MI-017-1I-C003	NH	PCDW #1	5100	1993	Sylvania
Martin Marietta	MI	Manistee	MI-101-1I-0001 [3]	NH	S-14	2100[4]	NA	Traverse Limestone, Bell Shale, Dundee, Detroit River Group
		Mason	MI-105-1I-0002	NH	S-35	1929	1998	Traverse Group
Michigan Ethanol	MI	Tuscola	MI-157-1I-0001	NH	Disposal Well #1	3380	2003	Berea & Sylvania
Mirant Zeeland	MI	Ottawa	MI-139-1I-0004	NH	IW-1	6675	2001	Franconia through Mt. Simon
			MI-139-1I-0005	NH	IW-2	6630	2001	
Morton Int'l	MI	Manistee	MI-101-1I-0002	NH	Well #2-36	1890	2000	Traverse Limestone, Bell Shale, Dundee
Northeastern	MI	Montmorency	MI-119-1I-C002	NH	Davis #1-19	3950	1983	Dundee
Pfizer (Parke-Davis)	MI	Ottawa	MI-139-1W-0003	H	Well #3	5945	1975	Mt. Simon
			MI-139-1W-0004	H	Well #4	5946	1975	

Facility	State	County	USEPA Permit or Application #	H or NH	Well Name	Depth (ft)	Year Drilled	Injection Formation
			MI-139-1W-0005	H	Well #5	6027	1990	
Sun Pipeline Co.	MI	Wayne	MI-163-1I-0001 [3]	NH	Well #1A	4452[4]	NA	Eau Claire, Mt. Simon
Pharmacia & Upjohn (Pfizer)	MI	Kalamazoo	MI-077-1W-0001	H	Well #3	5615	1975	Eau Claire, Mt. Simon
			MI-077-1W-0002	H	Well #4	5600	1980	
AK Steel Corp. (formerly Armco Steel)	OH	Butler		H	Well #1	3288	1967	Eau Claire, Mt. Simon
				H	Well #2	3281	1968	
BP Amoco (formerly BP Chemical Co.; Vistron; Sohio)	OH	Allen		H	Well #1	3125	1968	Eau Claire, Mt. Simon
				H	Well #2	3158	1969	
				H	Well #3	3157	1972	
				H	Well #4	3150		
Vickery Environmental, Inc. (formerly Waste Management of Ohio; Chemcial Waste Management Inc.) (Commercial)	OH	Sandusky		H	Well #2	2952	1975-1980	Mt. Simon
				H	Well #4	2902	1975-1980	
				H	Well #5	2938	1975-1980	
				H	Well #6	2922	1975-1980	
ArcelorMittal Burns Harbor, LLC (formerly Bethlehem Steel Corp.)	IN	Porter	IN-127-1W-0001	H	WPL #1	4048	1963	Mt. Simon
			IN-127-1W-0003	H	WAL #1	4298	1968	
			IN-127-1W-0004	H	WAL #2	4301	1968	
			IN-127-1W-0007 [2]	H	WAL/ SPL-1	4400[5]	NA	
Criterion Catalyst	IN	LaPorte	IN-091-1I-0001	NH	Well #1	4300	1991	Mt. Simon
			IN-091-1I-0002	NH	Well #2	4200	1991	
			IN-091-1I-0004	NH	Well #3	4200[5]	NA	
Indiana Dept. of Transportation	IN	Porter	IN-127-1I-0009	NH	Well #1	4558	1999	Eau Claire, Mt. Simon
Cathay Deep Well Disposal, LLC (fka ISK Magnetics Indiana General; Pfizer, Inc.; Harcros Pigments)	IN	Porter	IN-127-1I-C007	NH	Well #1	4538	1969	Mt. Simon
			IN-127-1I-C008	NH	Well #2	4526	1981	
Midco Remedial Corp.	IN	Lake	IN-089-1I-0014	NH	WDW #1	4426	1993	Mt. Simon

Facility	State	County	USEPA Permit or Application #	H or NH	Well Name	Depth (ft)	Year Drilled	Injection Formation
Duke Energy Indiana, Inc.	IN	Gibson	IN-051-1I-0001	NH	WDW #1	8480	2006	Trenton Limestone, Black River Group, Ancell Group, Knox Group, Eau Claire Formation and Mount Simon Sandstone
			IN-051-1I-0002	NH	WDW #2	11734	2007	
			IN-051-1I-0003	NH	WDW #3	8501	2008	
		Knox	IN-083-1I-0001	NH	WDW #1	appr. 10000	2008	St. Peter Sandstone, Eau Claire Formation, Trenton Limestone, Plattin Formation, Pecatonica Formation, Joachim Dolomite, Dutchtown Formation, Oneata Dolomite, Potosi Dolomite, Mt Simon
U.S. Steel (formerly Midwest Steel)	IN	Porter	IN-127-1W-0006	H	WPL #2	4235	1965	Mt. Simon

Footnotes
[1] Temporarily Abandoned
[2] Application In House
[3] Final Permit Issued
[4] Intended Depth
[5] Proposed Depth

Abbreviations
H = Hazardous
NH = Non-Hazardous

Table 2 – Inactive Class I Injection Wells

Facility	State	County	USEPA Permit or Application #	H or NH	Well Name	Depth (ft)	Year Drilled	Year Plugged	Injection Formation
BASF	MI	Ottawa	Note #1		#1	5894	1965	1975	Mt. Simon
			MI-139-1W-0001	H	D-2	5910	1969	1992	
			MI-139-1W-0002	H	D-3	5900	1977	1966	
Blunk Laundromat	MI	Oakland	Note #1	NH	#1-23	1840	1967	1993	Sylvania
Honeywell (Detroit Coke)	MI	Wayne	MI-163-1W-0003	H	Well #1	4231	1969		Eau Claire, Mt. Simon
			MI-163-1W-0004	H	Well #2	4112	1976	2008	Black River, Glenwood, Trempealeau, Eau Claire, Mt. Simon
			MI-163-1W-0005	H	Well #3	4127	1978	2004	
Dow Chemical Co.	MI	Bay	Note #1	NH		4710	1954	1967	Sylvania
						4605	1959		
		Midland	Note #1	NH	Well #2	3978	1952		Dundee
			Note #1	NH	Well #4	5153	1969		Sylvania
			Note #1	NH	Well #5	4269	1974		Dundee
			Note #1	NH	Well #8	5150	1950		Sylvania
E.I. Dupont	MI	Muskegon	Note #1		Well #1	6482			Franconia, Galesville
Fluid Securities Inc. (Beckman)	MI	Roscommon	MI-143-1I-C001	NH	Dalrymple #1-16	12288 (5700)[a]	1981	2002	Sylvania
Gelman	MI	Washtenaw	MI-161-1I-0001	NH	Well #1	5804	1981	1995	Mt. Simon
Hoskins	MI	Oscoda	MI-135-1I-0001	NH	WDW #1	2903	1972	2003	Dundee
Hooker ElectroChemical	MI	Muskegon	Note #1			2066	1956	1969	Traverse
						2083	1956	1968	
Marathon	MI	Muskegon	Note #1			2346	1948		Traverse, Detroit River
Parke-Davis	MI	Ottawa	Note #1	H	Well #1	1635	1951		Traverse
			Note #1	H	Well #2	1946	1956		Detroit River
TPI Inc.	MI	Gratiot	Note #1	NH	Well #1	1244	1957		Marshall
			MI-057-1I-0002	NH	Well #2	3622	1974	1999	Dundee
Reichhold Chemical	MI	Oakland	Note #1			1053	1953	1957	Detroit River, Sylvania
Rouge Steel (Ford Motor Co.)	MI	Wayne	Note #1		D-1	563	1956		Sylvania
			MI-163-1W-0002	H	D-2	4300	1976	1988	Eau Claire, Mt. Simon

Facility	State	County	USEPA Permit or Application #	H or NH	Well Name	Depth (ft)	Year Drilled	Year Plugged	Injection Formation
			MI-163-1W-0001	H	D-3	4308		1988	Eau Claire, Mt. Simon
The Upjohn Co.	MI	Kalamazoo	Note #1	H	Well #1	1532	1954		Traverse, Detroit River
					Well #2	1475	1954		
Velsicol	MI	Gratiot	MI-057-1W-0001	H	Well #2	3750	1967	2002	Dundee
Wyandotte	MI	Wayne	Note #1			850	1966	1968	Salina
						1400	1966		
AK Steel (Empire Reeves Steel)	OH	Richland		H		5085	1968	1971	Mt. Simon
Aristech (formerly United States Steel Corp.; Sunoco Chemicals)	OH	Lawrence		H	Well #1	5617	1969		Mt. Simon
				H	Well #2	5568	1978		
				H	Well #3***				
Arvesta Corp. (formerly Toman Agro; Calhio Chemical Inc.; ICI Americas; Zeneca)	OH	Lake		NH	Well #1	6072	1971	2004	Knox, Kerbel, Conasauga, Rome,
				NH	Well #2	6110	1979	2004	Mt. Simon
Cargill Inc., Salt Division (Int'l. Salt)	OH	Cuyahoga		NH		1435	1971		Oriskany
Chemical Waste Management, Inc.	OH	Sandusky		H	Well #1A	2965	1975-1980		Mt. Simon
				H	Well #1				
				H	Well #3	2960	1975-1980		
Reserve Environmental Services, Inc.	OH	Ashtabula		NH		> 5496			Conasauga, Rome, Mt. Simon
USS Chemical, Div. of US Steel	OH	Scioto		H		5617	1968		Mt. Simon
Criterion Catalyst	IN	LaPorte	Note #1	NH		650	1951		Devonian/Silurian Unit

Facility	State	County	USEPA Permit or Application #	H or NH	Well Name	Depth (ft)	Year Drilled	Year Plugged	Injection Formation
(American Cyanamid)			Note #1	NH		295	1952		Devonian Unit
General Electric	IN	Posey	Note #1	H	Well #1	2805	1967		Bethel
			Note #1	H	Well #2	2878	1971		Bethel, Cypress
Hoskins	IN	Elkhart	IN-039-1I-0001	NH	WDW #1	4132	1984		Mt. Simon
Indiana Farm Bureau Cooperative	IN	Posey	Note #1	H	IN3	2427	1955		Tar Springs
Inland Steel Co.	IN	Lake	IN-089-1W-0012	H	Well #1	4333	1968		Mt. Simon
			IN-089-1W-0013	H	Well #2	4385	1984		
Turris Coal	IN	Vanderburgh	IN-163-1I-0001	NH	D50-1-13	2500		1998	
Uniroyal Inc. (EMC Corp.)	IN	Vermillion	Note #1	H	Newport Army Munitions Plant Well #1	6160	1960	1980s	Mt. Simon
United States Steel Corp.	IN	Lake	IN-089-1W-0011	H	IN9	4291	1964		Mt. Simon

Notes
1. These wells predate the UIC program and were not assigned permit numbers

Footnote
[a] The meaning of the number in brackets was not defined in the Reference 1.

Blank cell: Information not available.

Abbreviations
H = Hazardous
NH = Non-Hazardous

Proposed COLA Revision

None.

Attachment 8
NRC3-10-0006

Response to RAI Letter No. 16
(eRAI Tracking No. 3913)

RAI Question No. 02.05.01-12

RAI 02.05.01-12

FSAR Section 2.5.1.1.4.3.3.1 indicates that "Seeber and Armbruster (FSAR Reference 2.5.1-346) speculate that a single-event rupture of a 5 to 10 km (3 to 6 mi) long fault could generate a magnitude 5 to 6 earthquake." As stated, however, the relationship of such a fault to the Ashtabula seismicity is unclear. In FSAR Reference 2.5.1-346, Seeber and Armbruster indicate that a single active fault of this length is consistent with the combined Ashtabula seismicity (through 1992). Please clarify this point.

Response

Seeber and Armbruster (Reference 2.5.1-346) evaluated the hypothesis that the July 13, 1987, M_{bLg} 3.8 Ashtabula earthquake and the 36 aftershocks of the Ashtabula sequence were triggered by injection of waste into a well penetrating the basal Mt. Simon Sandstone, which commenced in July 1986. Accurately-located earthquakes of the Ashtabula sequence cluster in a narrow, east-trending vertical zone about 1.5 km long and between 1.7 and 3.5 km (1.1 and 2.2 mi) in depth. This observation led Seeber and Armbruster to interpret this narrow zone, which is located as close as 0.7 km (1.4 mi) from the injection well, as an active fault, referred to as the Ashtabula fault. The depth to basement in this area is approximately 1.8 km (1.1 mi) , indicating that this cluster of seismicity is concentrated below the Mt. Simon – Grenville unconformity. Subsequent seismicity from 1987 to 1992 suggested a westward migration by 5 – 10 km (3 - 6 mi), possibly along the same fault. However, because the temporary seismic network used to locate the aftershocks of the 1987 main shock was no longer in operation, the location of the 1992 events are not as well constrained as the aftershocks of the main 1987 event.

Based on the assumption that the 1992 seismicity and the 1987 earthquakes defined a single rupture plane, Seeber and Armbruster (Reference 2.5.1-346) estimated that the postulated Ashtabula fault could produce a magnitude 5 to 6 earthquake. However, in a more recent paper, Seeber et al. (Reference 2.5.1-455) revised their interpretation, concluding that the linear patch of 1987 earthquakes represents a portion of the fault activated by high pore pressure. The new interpretation does not support the previous concept of a single rupture segment extending 5 – 10 km (3 - 6 mi) to the west. Additional discussion of the Seeber et al. paper is provided in the response to RAI 02.05.01-28. Due to poor location constraints for the earthquakes that occurred from August 1987 to 2001, the location of the M 2.9 earthquake on March 28, 1992, cannot be definitely associated with the Ashtabula fault (Reference 2.5.1-455).

Proposed COLA Revision

Proposed markups to revise Section 2.5.1.1.4.3.3.1 to discuss the Ashtabula aftershock sequence are provided in the Response to RAI 02.05.01-28.

Attachment 9
NRC3-10-0006

Response to RAI Letter No. 16
(eRAI Tracking No. 3913)

RAI Question No. 02.05.01-13

RAI 02.05.01-13

FSAR Section 2.5.1.1.4.3.3.2 cites Hansen (1993) (FSAR Reference 2.5.1–344) which suggests that the Anna seismic zone is capable of producing a magnitude 6.0 to 7.0 event. Given the proximity of the Anna seismic zone to the Fermi site, please provide a more complete discussion of the basis for this interpretation.

Response

Mike Hansen of the Ohio Department of Natural Resources Division of Geological Survey indicates that his statement that western Ohio could produce a M 6.0 – 7.0 earthquake was made in reference to the EPRI-SOG (Reference 2.5.1-286) maximum magnitude assessments. The full range of estimated maximum magnitude (body-wave magnitude [m_b] 5.2 – 7.6 or moment magnitude [**M**] 4.7 – 8.2) assigned by the EPRI-SOG teams (Table 1) was incorporated into the hazard analysis for Fermi 3. The conversion from body-wave to moment magnitude listed in Table 1 was performed by taking the average of the three relationships from Atkinson and Boore (Reference 2.5.2-262), Johnston (Reference 2.5.2-268), and EPRI (Reference 2.5.2-269) as discussed in FSAR Section 2.5.2.2.4.3. This composite distribution of maximum moment magnitude used as inputs to the PSHA for Fermi 3 captures the statement made by Hansen (1993) (FSAR Reference 2.5.1–344) that the Anna, Ohio seismic zone could produce a **M** 6.0 to 7.0 earthquake.

Table 1 – EPRI-SOG Mmax inputs for the Anna, Ohio, seismic zone

Source	**P***	**Closest Distance to Fermi 3 Site (km)**	**EPRI (1989) Maximum Magnitude Distribution for Fermi 3 Site (m_b)**	**Equivalent Maximum Magnitude Distribution for Fermi 3 Site (M)**
Anna, Ohio, Area (BEC-N1)	0.6	98.1	5.4 (0.10), 5.7 (0.40), 6.0 (0.40), 6.6 (0.10)	5.0 (0.10), 5.3 (0.40), 5.7 (0.40), 6.5 (0.10)
Anna, Ohio (DAM-12)	1	127.7	6.8 (0.75), 7.2 (0.25)	6.9 (0.75), 7.5 (0.25)
Indiana Block (LAW-115)	1	17.4	5.2 (0.5), 5.5 (0.5)	4.8 (0.5), 5.1 (0.5)
Anna, Ohio (RND-8)	1	116.8	5.8 (0.15), 6.5 (0.60), 6.8 (0.25)	5.5 (0.15), 6.4 (0.60), 6.9 (0.25)
Anna, Ohio (WGC-29)	0.93	107.5	5.4 (0.19), 6.0 (0.68), 6.6 (0.13)	5.0 (0.19), 5.7 (0.68), 6.5 (0.13)
Bowling Green–Auglaize Fault System (WCC-37)	0.072	43.3	5.6 (0.33), 6.5 (0.34), 7.2 (0.33)	5.2 (0.33), 6.4 (0.34), 7.5 (0.33)
Champaign-Anna Fault System (WCC-38)	0.065	169.5	5.7 (0.33), 6.8 (0.34), 7.6 (0.33)	5.3 (0.33), 6.9 (0.34), 8.2 (0.33)
Anna, Ohio, Geophysical Intersection (WCC-39) and NOTA	0.773	138.5	5.5 (0.33), 6.5 (0.34), 7.3 (0.33)	5.1 (0.33), 6.4 (0.34), 7.7 (0.33)

Notes:

P* = the probability that the source is included in the hazard model.
M = moment magnitude
(Weight) = relative contribution of the source

Proposed COLA Revision

None.

Attachment 10
NRC3-10-0006

Response to RAI Letter No. 16
(eRAI Tracking No. 3913)

RAI Question No. 02.05.01-14

RAI 02.05.01-14

FSAR Section 2.5.1.1.4.3.3.2 indicates that Obermeier (FSAR Reference 2.5.1–350) investigated streambanks in the vicinity of the Anna seismic zone and found no evidence of paleoliquefaction features. Given the proximity of the Anna seismic zone to the Fermi site, please provide additional discussion regarding the extent of the Obermeier investigations, including the locations investigated, and the basis for his conclusion that no evidence for paleoliquefaction features exist in the Anna seismic zone vicinity.

Response

Obermeier (Reference 2.5.1-350) investigated more than 100 km of stream banks in western Ohio in the vicinity of the Anna seismic zone. The search was conducted by canoe on portions of the Auglaize, Great Miami, Stillwater, and St. Mary's rivers and Loramie Creek (Figure 1). Additionally, portions of the Scioto and Little Sciotto rivers in north-central Ohio and scattered sand and gravel pits that contained thick glaciofluvial deposits and had high water tables were searched for paleoliquefaction features. Obermeier (Reference 2.5.1-350) concluded that although the amount and quality of outcrop was not generally very good, there was adequate outcrop to have some confidence that the region has not experienced and earthquake greater than M 7 in the last several thousand years. He states however that the scarcity of outcrops did not exclude the possibility of earthquakes of lower magnitudes.

Dr. Obermeierand and Dr. Russell Wheeler and Dr. Richard Harrison of the U.S. Geological Survey (USGS) were contacted to determine if field maps or other written documentation of the field reconnaissance were available. Maps or supporting documentation from these studies are not available and ,therefore, additional details on the exact portions of the rivers observed by Dr. Obermeier cannot be provided.

In addition to Dr. Obermeier, we also communicated with Mr. Erik Venteris, of the Ohio Geological Survey. As a graduate student, Erik Venteris worked with Dr. Obermeier in the mid 1990's performing a general survey of rivers in northern Ohio, including the Ashtabula, and Grand Rivers in northeastern Ohio, and from Dayton north in western Ohio. Mr. Venteris stated that they had performed an exhaustive search in Wisconsinan deposits and did not observe evidence of strong motion since the retreat of glaciers and that, if these features exist, they would have seen them. Mr. Venteris does not have field maps or electronic GIS shapefiles as this study predates Geographic Information System (GIS) mapping. Mr. Venteris has not performed subsequent work since these investigations. We also contacted Dr. Pat Munson with the University of Indiana, who participated in the reconnaissance investigations in northeastern Ohio, but was not involved in the reconnaissance investigations in western Ohio.

Figure 1. Locations of Rivers Searched in the Vicinity of the Anna, Ohio Seismic Zone

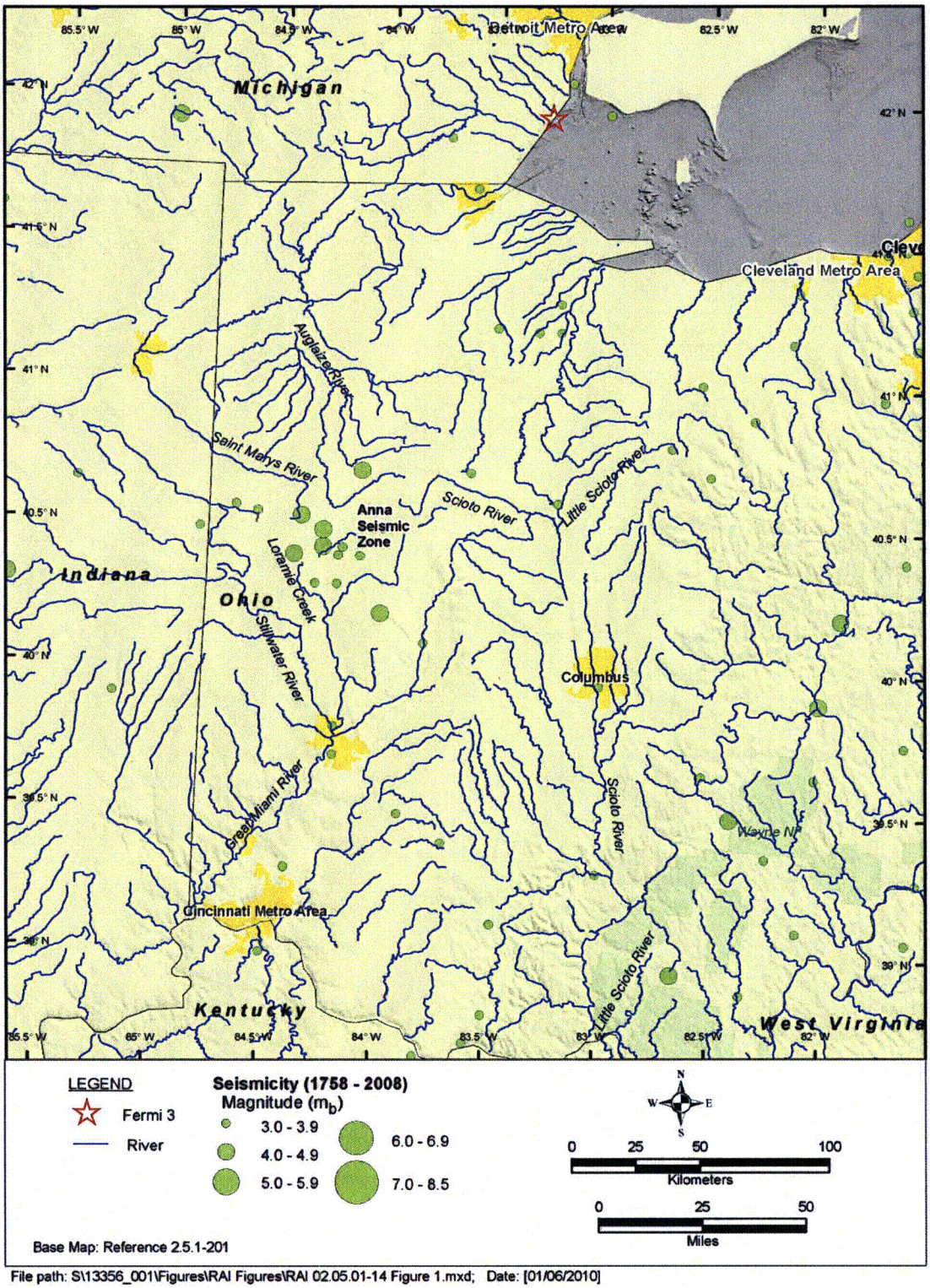

Proposed COLA Revision

None

Attachment 11
NRC3-10-0006

Response to RAI Letter No. 16
(eRAI Tracking No. 3913)

RAI Question No. 02.05.01-16

RAI 02.05.01-16

FSAR Section 2.5.1.2.1 describes the physiographic subdivisions in the site vicinity. The St. Clair clay plain and the Maumee Lake plains are not shown on the regional physiographic map (FSAR Figure 2.5.1–202). Please include these subdivisions in the context of the overall physiographic framework, either on this map or on a larger-scale map showing the physiography of the site vicinity. Also, the term "section" is used within the FSAR text, but "subprovince" is used on the map. Please clarify the appropriate terminology.

Response

Physiographic subdivisions in the site region are discussed in FSAR Section 2.5.1.1.1 and in the site vicinity in FSAR Section 2.5.1.2.1.

a) FSAR Section 2.5.1.2.1 makes reference to the St. Clair clay plain and the Maumee Lake plains that are not shown in the Rev. 1 FSAR figures. A new figure (FSAR Figure 2.5.1-250) will be added showing the extent of these two regions in the site vicinity along with other physiographic regions outside the 40 km (25 mile) radius site vicinity. The Maumee Lake plains region is a subdivision of the Eastern Lake section developed by the Division of Geological Survey for the State of Ohio (FSAR Reference 2.5.1-219) and is labeled on Figure 2.5.1-250 as "Eastern Lake Section – Maumee Lake Plains". Since the State of Michigan has not subdivided the Eastern Lake section, the area of the Figure 2.5.1-250 in Michigan is labeled as "Eastern Lake Section – undifferentiated". A modification of FSAR Section 2.5.1.2.1 citing this figure has been made.

b) Fenneman and Johnson (FSAR Reference 2.5.1-203) use the following hierarchy for the Physiography of the United States: Divisions, Provinces, and Sections. The U. S. Geological Survey continues to use the same hierarchy. A revision to FSAR Figure 2.5.1-202 is provided with "Subprovince" replaced with "Section".

Reference

U. S. Geological Survey, "A Tapestry of Time and Terrain: Physiographic Regions," http://tapestry.usgs.gov/physiogr/physio.html, accessed on December 22, 2009

Proposed COLA Revision

Markups to revise FSAR Section 2.5.1.2.1, FSAR Figure 2.5.1-202, and new FSAR Figure 2.5.1-250 are attached.

Markup of Detroit Edison COLA
(following 4 pages)

The following markup represents how Detroit Edison intends to reflect this RAI response in a future submittal of the Fermi 3 COLA. However, the same COLA content may be impacted by revisions to the ESBWR DCD, responses to other COLA RAIs, other COLA changes, plant design changes, editorial or typographical corrections, etc. As a result, the final COLA content that appears in a future submittal may be different than presented here.

the site vicinity applies to the site area and the site location unless specifically discussed. Where information is presented for the site area, it applies to the site location unless specifically discussed.

2.5.1.2.1 Site Physiography and Geomorphology

Fermi 3 is located in the Eastern Lake section of the Central Lowlands physiographic province, and the (40-km [25-mi] radius) site vicinity includes the St. Lawrence Lowlands physiographic province in Canada (Figure 2.5.1-202). Subsection 2.5.1.1.1.1 and Subsection 2.5.1.1.1.3 cover the overall details of the Central Lowlands and the St. Lawrence Lowlands physiographic provinces, respectively. The St. Clair clay plain is the subdivision of the St. Lawrence Lowlands physiographic province that is in the site vicinity. The St. Clair clay plain is described as a region of low relief with elevations ranging from 175 to 213 m (575 to 700 ft) and is developed on clay tills that are thinly covered with lacustrine deposits. (Reference 2.5.1-222) In adjacent Ohio, the subdivision of the Eastern Lake section is called the Maumee Lake plains and is described by Brockman (Reference 2.5.1-219) as a "flat-lying Ice-Age lake basin...slightly dissected by modern streams; elevation 174 to 243 m (570 to 800 ft); very low relief (1.5 m[5 ft])." The surface materials In the Maumee Lake plains include silt, clay and clayey glacial till that overlie Silurian carbonate rocks and shales (Reference 2.5.1-220). The 8-km (5-mi) radius site area is entirely within the Eastern Lake section of the Central Lowlands physiographic province (Reference 2.5.1-218). The 1:24,000 scale U.S. Geological Survey topographic maps for Monroe County show the site area is relatively flat with minor incision (< 15 ft) by east-flowing streams and elevations range from 174 to 185 m (570 ft to 605 ft). Within the 1-km (0.6-mi) radius site location, data from the Fermi 3 subsurface investigation encountered lacustrine deposits over glacial till and the U.S. Geological Survey topographic maps indicate an elevation range from 173 to 180 m (570 to 590 ft) (Figure 2.5.1-229).

(Figure 2.5.1-250)

(Figure 2.5.1-250)

2.5.1.2.2 Site Geologic History

The (40-km [25-mi] radius) site vicinity for Fermi 3 is located within the North America Craton. The site vicinity is located on the west flank of the Findlay arch at the margin of the Michigan basin (Figure 2.5.1-208 and Figure 2.5.1-218). The regional geologic history of the Precambrian is covered in Subsection 2.5.1.1.2.1 and Subsection 2.5.1.1.2.2. No surface exposures of Precambrian rocks exist in the site vicinity (Figure

Figure 2.5.1-202 Fermi 3 Site RegionalPhysiographic Map [EF3 COL 2.0-26-A]

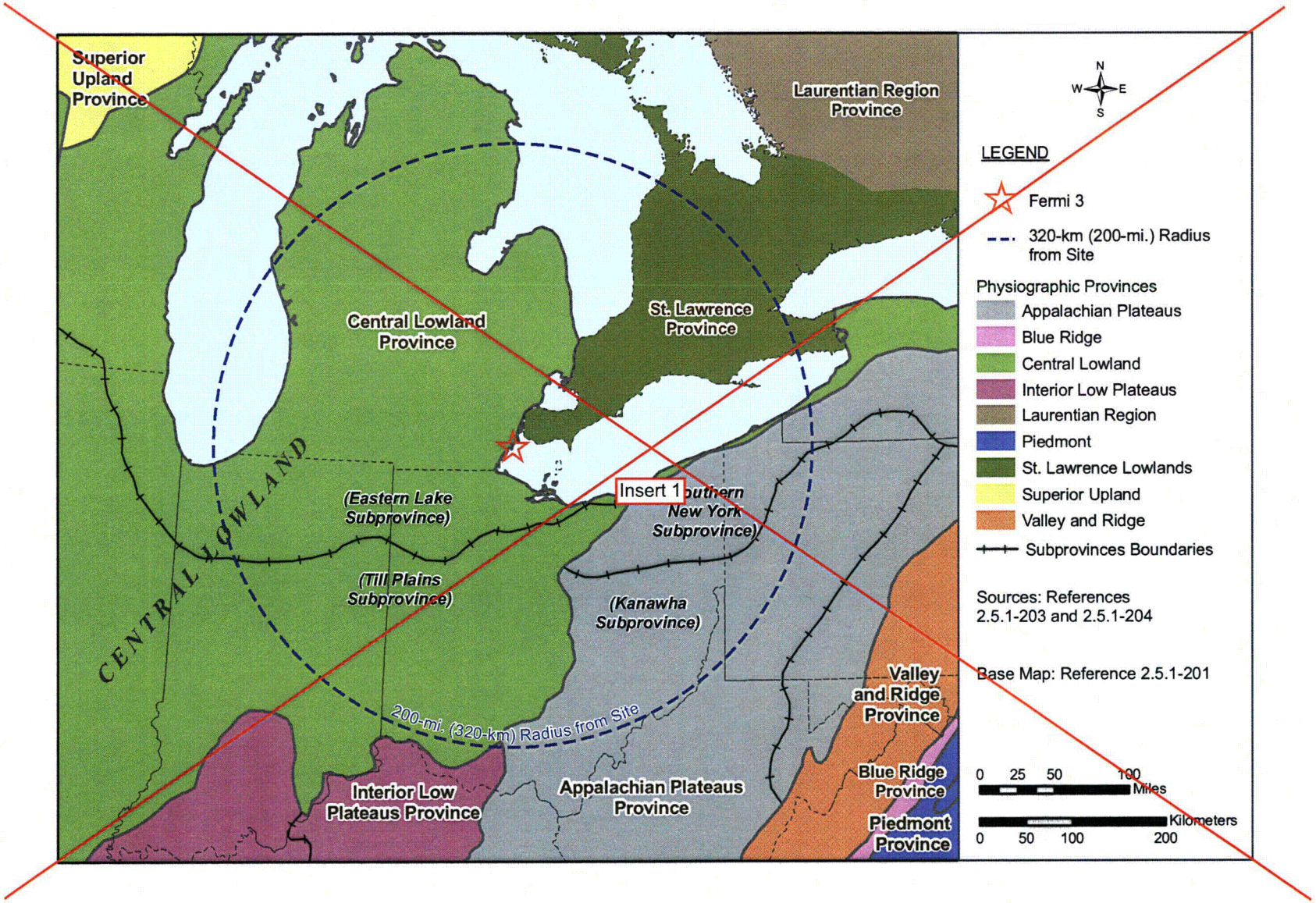

Insert 1

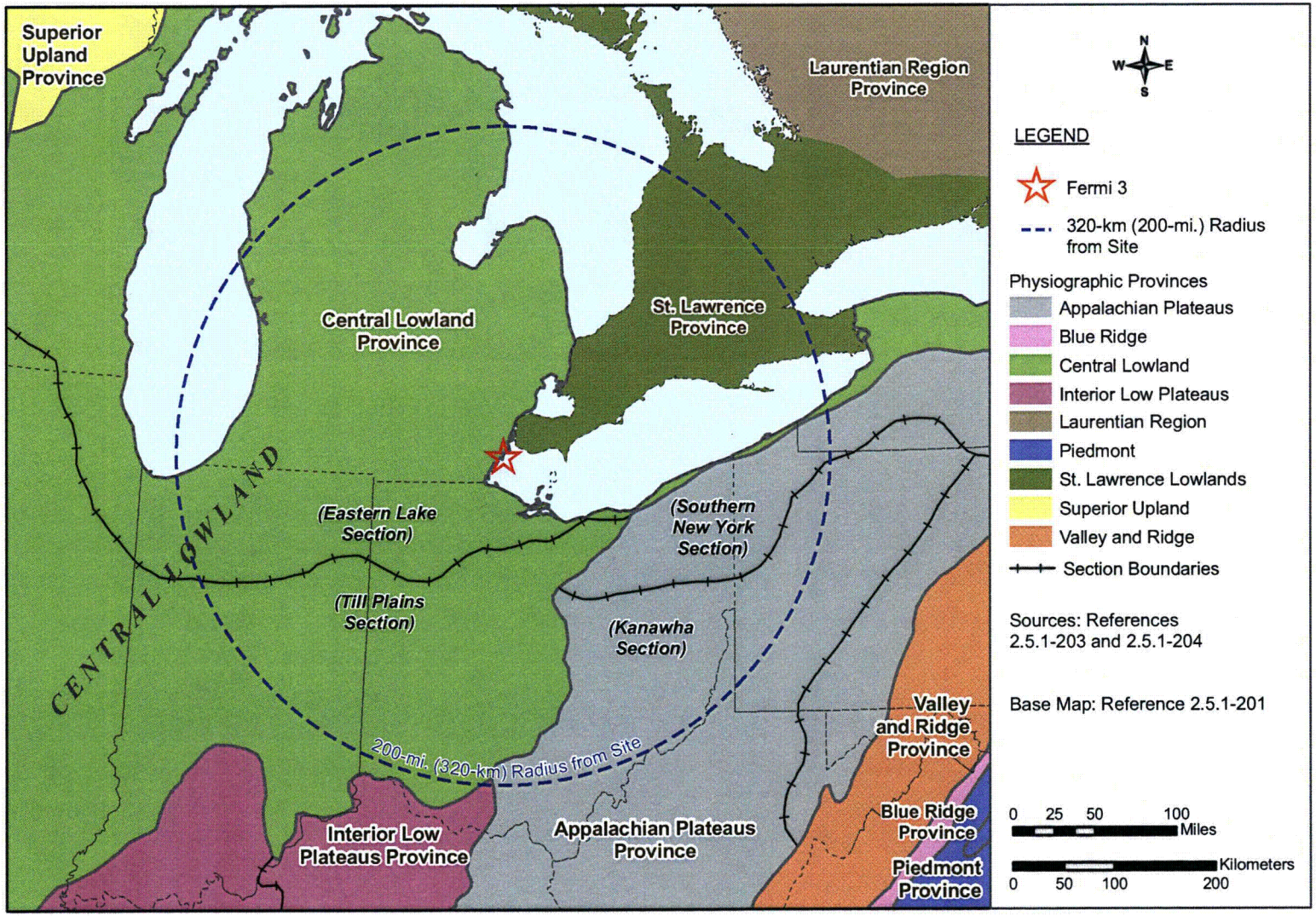

File path: S\13300\13356_001\Figures\Revised FSAR Figures\DTE_FSAR_FIG02_05_01_202.mxd; Date: [12/22/2009]

Insert after Figure 2.5.1-249

Figure 2.5.1-250 Fermi 3 Site Vicinity Physiographic Map

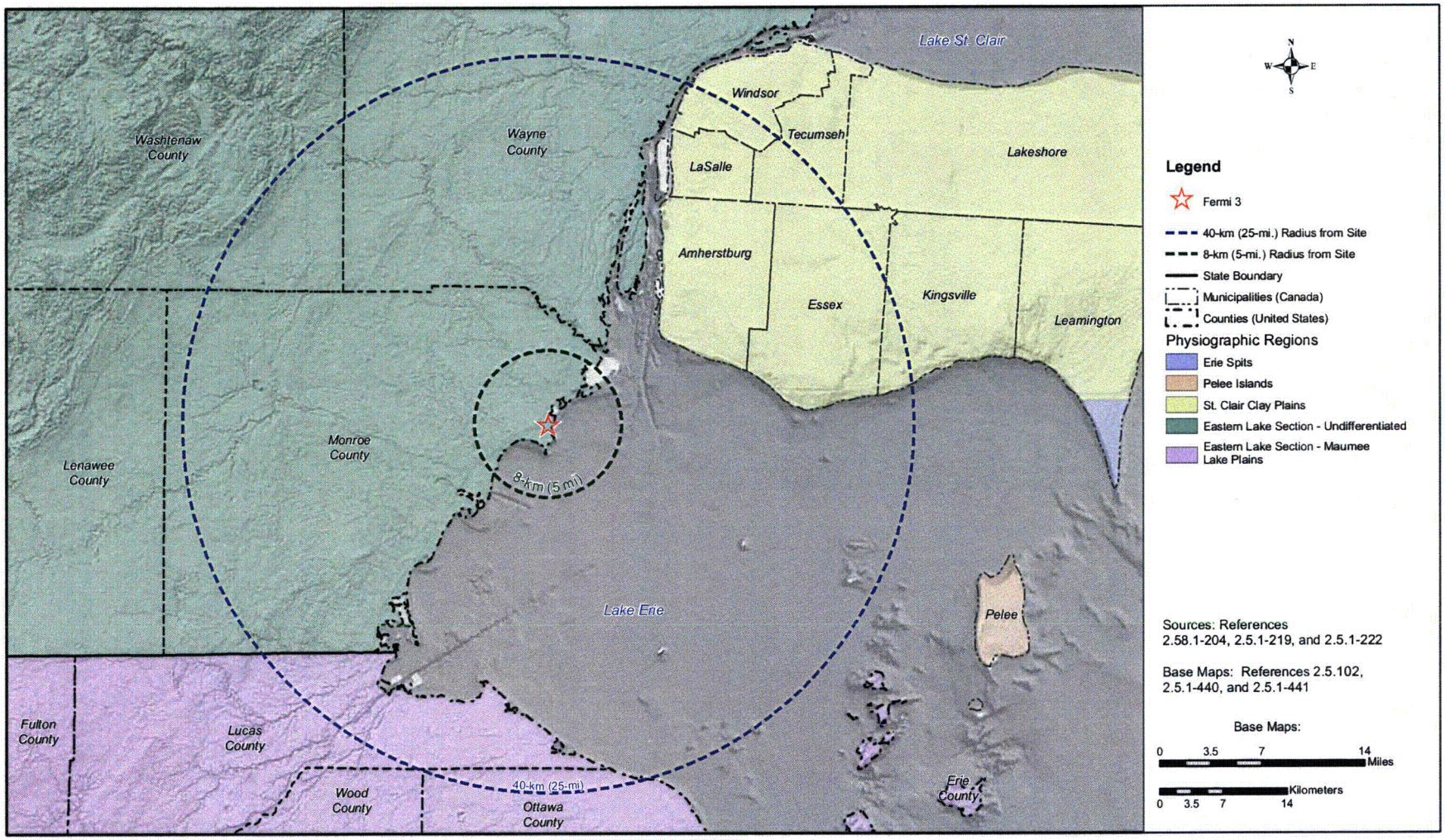

Path: \\na\data\Corp\Water\GIS2\Projects\Fermi_RAI_Physiography\MapDoc\Fig_2.5.1-230_Physiography.mxd Date Printed: January 8, 2010 Map By: K Robinson

Attachment 12
NRC3-10-0006

Response to RAI Letter No. 16
(eRAI Tracking No. 3913)

RAI Question No. 02.05.01-17

RAI 02.05.01-17

FSAR Section 2.5.1.2.2.2 mentions that the shoreline of Glacial Lake Leverett "would have been in or near the site study vicinity..." Please indicate whether shorelines mapped within the site vicinity may be correlated to this (or other previously mapped) shorelines.

Response

As stated in FSAR Section 2.5.1.2.2.2, Glacial Lake Leverett, which was nearly coincident with modern Lake Erie (Figure 2.5.1-234b), existed during the Erie Interstade between the ice advances of the last glacial maximum (Nissouri Stade) and the Port Bruce Stade (Reference 2.5.1-272). Dreimanis (Reference 1) reports that the lake level dropped to an elevation of 178 m above sea level (5 m above the present Lake Erie level) during the Lake Leverett phase of Lake Erie. References reviewed did not identify Lake Leverett shoreline features. Any shoreline features associated with Lake Leverett would have been overridden by ice during the advance of the Port Huron Stade (Reference 2.5.1-272), and also impacted by subsequent glacial lake transgressions and regressions across the site vicinity, which explains the lack of information available. Shoreline features mapped in the Fermi 3 site vicinity (Figure 2.5.1-231) have been correlated with glacial lake strandlines that postdate the Port Huron Stade. These shoreline features are discussed in the response to RAI 02.05.03-6 (Attachment 29) and are shown on new FSAR Figure 2.5.1-256.

Reference

Dreimanis, A., 1977, "Late Wisonsin Glacial Retreat in the Great Lakes Region, North America," *New York Academy of Science, Annals*, Vol. 288, pp. 70-89.

Proposed COLA Revision

There is no markup associated with Lake Leverett. A markup to revise FSAR Section 2.5.1.2.3.2 to discuss the correlation of mapped shorelines to glacial lake strandlines and new FSAR Figure 2.5.1-256 illustrating these shorelines, is provided in the markup for RAI 02.05.03-6.

Attachment 13
NRC3-10-0006

Response to RAI Letter No. 16
(eRAI Tracking No. 3913)

RAI Question No. 02.05.01-18

RAI 02.05.01-18

FSAR Section 2.5.1.2.2.2 states that "Lakes of the Mackinaw Interstade (Glacial Lakes Maumee and Arkona in the site vicinity).... and younger lakes have surface expression continuity and preserved landforms that document the rebound history of the area." Please describe this rebound history and cite any pertinent references. This appears to be important information bearing on the latest Pleistocene to Holocene history of vertical movement in the site vicinity.

Response

The Response to RAI 02.05.01-3 provides a discussion of the evidence for vertical deformation of glacial and postglacial lake shoreline features that record glacial isostatic adjustment (GIA) in the site region. The relict shorelines in the vicinity of the Fermi 3 site lie west and southwest of the mapped hinge lines marking the boundary between the warped and uplifted strandlines to the northeast and the zone of horizontality to the southwest (Figures 2.5.1-251 and 2.5.1-252 included in the response to RAI 02.05.01-3). The elevations of specific features along strandlines and related geomorphic features formed by these lakes in the site vicinity, suggest that the site vicinity has experienced relatively uniform glacial isostatic adjustments in latest Pleistocene to Holocene time. Further discussion and documentation of the elevations of paleoshorelines (relict strandlines and associated geomorphic features) in the site vicinity (40-km [25-mi.] wide radius) is provided in the Response to RAI 02.05.03-6.

Holocene lake level history and paleogeography of Lake Erie reinterpreted using the latest bathymetry, water budget data, and published information are described by Holcombe et al. (Reference 2.5.1-487). This publication describes the various factors that influenced Holocene lake history, including blocking and unblocking of outlet sills, erosion of outlet sills, distance from outlet sills, differential isostatic rebound, upper Great Lakes drainage flowing into or bypassing the lake, and climate-driven water budget of the Lake Erie drainage basin. Differential rebound did impact the formation and history of Holocene shoreline features in the central basin, and particularly the eastern basin and eastern outlet of Lake Erie and had lesser influence in the western basin, which includes the site vicinity. The rate and amount of differential isostatic rebound are modeled as decreasing non-linearly with increasing distance from the outlet sill. The western basin was the site of dry land or small marsh/lake basins until it was finally flooded about 5,400 years ago. Holcombe et al. (Reference 2.5.1-487) concludes that after 3,600-3,000 years ago when erosion of the outlet sill at the Lyell-Johnson outlet returned Lake Erie to the level of the Niagara River at Fort Erie, the water level fell in eastern Lake Erie fell, but did no tfall significantly in the western basin of the lake because water level was partially compensated by differential rebound in the west,

Reference

2.5.1-48 Holcombe, T.L., Taylor, L.A., Reid, D.F., Warren, J.S., Vincent, P.A., and Herdendorf, C.E., "Revised Lake Erie Postglacial Lake Level History Based on New Detailed Bathymetry," *Journal of Great Lakes Research*, Vol. 29, No. 4, pp. 681-704, 2003.

Proposed COLA Revision

Markup to revise Section 2.5.1.2.2.2 is attached. A markup of Section 2.5.1.2.3.2.1 that is referenced in the revised text is included in the Response to RAI 02.05.03-6 (Attachment 29).

Markup of Detroit Edison COLA
(following 4 pages)

The following markup represents how Detroit Edison intends to reflect this RAI response in a future submittal of the Fermi 3 COLA. However, the same COLA content may be impacted by revisions to the ESBWR DCD, responses to other COLA RAIs, other COLA changes, plant design changes, editorial or typographical corrections, etc. As a result, the final COLA content that appears in a future submittal may be different than presented here.

2.5.1-230). The site vicinity Phanerozoic geologic history is essentially the same as the (320-km [200-mi] radius) site region presented in Subsection 2.5.1.1.2. All of the major Phanerozoic tectonic events of North America take place outside the (320-km [200-mi] radius) site region (see Subsection 2.5.1.1.3) and are outside the site vicinity, site area, and site location. Some minor reactivation of basement faults has occurred in the site vicinity during the Paleozoic (see Subsection 2.5.1.2.4). Bedrock units exposed in the site vicinity are Silurian and Devonian in age (Figure 2.5.1-230). These bedrock units are overlain by Quaternary sediments ().

2.5.1.2.2.1 Paleozoic Depositional History

The Paleozoic depositional history of the (40-km [25-mi] radius) site vicinity extends from the Cambrian into the Devonian. Deposition during the Paleozoic was controlled by repeated transgressions (inundations) and regressions of epeiric seas (Subsection 2.5.1.1.3.2) over the North American Craton. A cratonic sequence is a depositional sequence related to a pair of transgressions and regressions and is bounded by interregional unconformities. Interregional unconformities are time intervals when most of the craton is exposed to erosion. (Reference 2.5.1-275) Of the six cratonic sequences identified for the North American Craton (Reference 2.5.1-275), three sequences exist in the subsurface of the site vicinity: Sauk, Tippecanoe, and Kaskaskia sequences. Because of the relatively uniform geology of the site vicinity featuring nearly horizontal sedimentary rocks (Reference 2.5.1-389), no significant changes in the geologic history are anticipated for the site area and site location. Further details of the cratonic sequences are discussed in Subsection 2.5.1.1.3.2 and Subsection 2.5.1.2.3.

2.5.1.2.2.2 Quaternary History of the Site Area

The Quaternary history of the (320-km [200-mi] radius) site region is covered in Subsection 2.5.1.1.4.1.1. Three ice lobes coalesced on the lower peninsula of Michigan beginning about 24,000 years BP. The area was ice free immediately prior to this (Reference 2.5.1-263). The ice lobes are, from west to east, the Michigan, Saginaw (equivalent to the Huron-Erie lobe on Figure 2.5.1-214), and Erie lobes (Reference 2.5.1-390). The positions of the lobes fluctuated with time and their deposits overlap.

Calkin and Feenstra (Reference 2.5.1-297) and Lewis et al. (Reference 2.5.1-272) provide overviews of the history of development of

latest

~~late~~ Wisconsinan lakes with respect to ice barriers that affected the 40-km (25-mi) [radius site vicinity and 8-km [5-mi] radius site area. A map showing features of the Erie basin and the relationships and ages of lake phases versus ice margin positions in the study vicinity are shown on Figure 2.5.1-232 and Figure 2.5.1-233, respectively. Maps showing the positions of ice margins and proglacial lake shorelines at different times during the Late Wisconsinan are presented on Figure 2.5.1-234. The sequence of events that affected the site vicinity is summarized below.

but slightly lower than

At the last glacial maximum (Nissouri Stade) about 18 to 21 ka, the Laurentide ~~ice~~ margin lay south of the Huron and Erie basins (Figure 2.5.1-234a). Ice retreated ~~north~~ of Port Huron, Ontario (out of the site region), during the Erie Interstade and ~~exposed~~ all of Saginaw Bay and southern Lake Huron (Reference 2.5.1-272) (Figure 2.5.1-234b). The shoreline of Glacial Lake Leverett, which was nearly coincident ~~with~~ modern Lake Erie, would have been in or near the site study vicinity at this time, with water draining into Glacial Lake Leverett from the north through Lake St. Clair.

After the Erie Interstade, all but the Saginaw lobe advanced to nearly the same position as the Nissouri Stade (Reference 2.5.1-263) during what is known as the Port Bruce Stade (Reference 2.5.1-272) (Figure 2.5.1-234c). The Michigan and Erie lobes encroached on the area formerly occupied by the Saginaw (Huron-Erie) lobe with Michigan lobe deposits overlapping Saginaw (Huron-Erie) lobe deposits as far east as St. Joseph County, Indiana, and Erie lobe deposits overlapping Saginaw (Huron-Erie) lobe deposits as far west as Lenawee County, Michigan (Reference 2.5.1-390). The Michigan and Erie lobes continued to discharge water to the southwest across the area vacated by the Saginaw lobe and into Indiana. The Wabash Fort Wayne and Defiance moraines formed at the confluence of the Ontario-Erie and Huron-Erie lobes (Reference 2.5.1-297). The first two of these lie southwest of the site vicinity; the Defiance moraine passes through Ann Arbor, Michigan, and Adrian, Ohio (Figure 2.5.1-232).

The correlation of lake levels and outlets are useful relative stratigraphic tools where they are preserved and not destroyed by later ice advances. The lake plain boundary passes through Ypsilanti and Adrian, Michigan, and trends southwest toward Fort Wayne, Indiana (Reference 2.5.1-297) (Figure 2.5.1-232). Lakes of the Mackinaw Interstade (Glacial Lakes Maumee and Arkona in the site vicinity) (Figure 2.5.1-234d through

reflect

cumulative response of the site vicinity to glacial isostatic adjustments (see Subsections 2.5.1.1.4.1.1 and 2.5.1.2.3.2.1)

Figure 2.5.1-234f) and younger lakes have surface expression continuity and preserved landforms that ~~document~~ the ~~rebound history of the area~~. The Michigan Peninsula has valleys that were lake outlets (Imlay Channel and Grand River Valley in Michigan and the Glacial Grand Valley that allowed the waters of Glacial Lake Arkona, which extended east from the Saginaw lowland into the Lake Erie basin, to drain west to the Michigan basin) (Reference 2.5.1-263) (Figure 2.5.1-234e and Figure 2.5.1-234f).

Advance of ice during the Port Huron Stade, which did not enter the site vicinity, still affected the site region. It created higher lake levels (Subsection 2.5.1.1.2.3.4.4), and proglacial lakes transgressed the site area. Deposits of Glacial Lakes Whittlesey and Warren, dated as 13,000 and 12,800 years BP, form the bulk of the glacial-age sediments deposited in the site vicinity (Reference 2.5.1-297) (Figure 2.5.1-234h and Figure 2.5.1-234i). ~~Minor fluctuations of lake level as recently as 7,500 years BP could have reworked older sediments (Reference 2.5.1-272) (Figure 2.5.1-235)~~. Glacial Lake Whittlesey's beaches, with 3 to 5 m (10 to 16 ft) of relief in western Ohio, are nearly continuous and include gravels as well as sand (Reference 2.5.1-297). The younger beaches are sandy, may have multiple ridges, and have been windblown (Reference 2.5.1-297) and are difficult to trace through southeastern Michigan (Reference 2.5.1-391). A lower Lake Warren level, sometimes called Lake Wayne, is named for the broad, flat-topped sandy ridge that may be a modified beach that passes through Wayne, Michigan, 28 km (17.4 mi) west of Detroit (Reference 2.5.1-391).

Add "Insert 1" Here

2.5.1.2.3 Site Stratigraphy

The stratigraphy of the (40-km [25-mi] radius) site vicinity, the 8-km (5-mi radius) site area and the 1-km (0.6-mi radius) site location is roughly equivalent to the stratigraphy of the (320-km [200-mi] radius) site region (Subsection 2.5.1.1.3.2) except for the effects on deposition caused by the proximity of the site to the Findlay arch. For a portion of the Paleozoic, the Findlay arch was a positive topographic feature (higher than the surrounding surfaces). The top of the arch was one of the last areas flooded during a transgression and the first area exposed during a regression. Because the depositional interval on the arch was shorter, the geologic units deposited on the arch were thinner than those in the center of the basin, and the duration of the period of erosion on the arch will be longer (Reference 2.5.1-325; Reference 2.5.1-276). Exposure of

Insert 1 located before Section 2.5.1.2.3

Holocene lake level history and paleogeography of Lake Erie reinterpreted using the latest bathymetry, water budget data, and published information are described by Holcombe et al. (Reference 2.5.1-487). This publication describes the various factors that influenced Holocene lake history, including blocking and unblocking of outlet sills, erosion of outlet sills, distance from outlet sills, differential isostatic rebound, upper Great Lakes drainage flowing into or bypassing the lake, and climate-driven water budget of the Lake Erie drainage basin. The western basin of Lake Erie as illustrated in a series of postulated paleogeographic maps was not flooded throughout much of the Holocene; flooding of the western basin occurred after about 4,000 years ago during the Nipissing II phase when the final introduction of large volumes of upper Great Lakes water flowed into Lake Erie. Water level in the western basin at that time was several meters lower than at present. The water level of the western basin has risen since this time due to subsidence (glacial isostatic adjustment) and changes in the climate and water budget (Reference 2.5.1-487).

Attachment 14
NRC3-10-0006

Response to RAI Letter No. 16
(eRAI Tracking No. 3913)

RAI Question No. 02.05.01-21

RAI 02.05.01-21

FSAR Figure 2.5.1-227 shows a high incidence landslide area less than 50 km southwest of the proposed Fermi 3 site, and possibly within the 40 km site vicinity. Please discuss the relevance of such high landslide susceptibility within the site vicinity.

Response

The "high incidence" landslide area mapped on FSAR Figure 2.5.1-227 by Radbruch-Hall et al. (Reference 2.5.1-387) is within 50 km (31 mi.) of the proposed Fermi 3 site, but outside the 40 km (25mi.) site vicinity. FSAR Figure 2.5.1-227 indicates that in the Fermi 3 site vicinity, the landslide hazard is characterized as "low incidence, moderate susceptibility."

The RAI referenced "high incidence" landslide hazard shown southwest of Fermi 3 on FSAR Figure 2.5.1-227 is associated with the Maumee River. Detailed studies of landslides along the Maumee River by Lounsbury and Melhorn (Reference 1) and Dimit (Reference 2) are both outside but close to the 40 km site vicinity.

Lounsbury and Melhorn (Reference 1) report slumps along the banks of the Maumee River in glacio-lacustrine Erie clay at Maumee, Ohio, about 14 km (8.6 mi) southwest of Toledo. In Lounsbury and Melhorn's study area, the Erie clay is 24 to 30 m (80 to 100 ft) thick, which is thicker than the lacustrine deposits encountered at the Fermi 3 site.

Dimit studied landslides along the Maumee River from Grand Rapids, Ohio to Toledo, Ohio. The landslides are confined to the steeper topography including the banks and bluffs along the Maumee River, especially on the cut banks (outside of the meander bends). Both lacustrine deposits and glacial till were involved in the landslides. The glacial till layers had been softened by groundwater percolating through the lacustrine deposits. The local relief along the Maumee River is about 15 m (50 ft), and the local relief along streams near the Fermi 3 site is less that 3 m (10 ft). The lower relief will decrease the probability of landslides. The landslide map included in Dimit shows that the landslides are confined to the river banks and bluffs.

The response to NRC RAI 02.04.09-01 on channel diversions states:

> "The increase of strength with depth of the subsurface soil and bedrock minimizes the possibility of a block-type failure of a stronger layer on a shallow failure plane in a weaker underlying layer; therefore, shallow large area landslides into Swan Creek are not envisioned as a plausible scenario. The shallow slope of the land surface toward the creek combined with the lack of a weak soil layer at depth also reduces the potential for the occurrence of a large area landslide into the creek. Along the incised banks of Swan Creek, local slope failures of the creek bank are part of the natural creek erosion process. However, the size of these slope failures will be limited to near bank events that will not result in diversion of Swan Creek."

Swan Creek is north of the Fermi 3 site (FSAR Figure 2.5.1-244). The results published in Lounsbury and Melhorn and Dimit support these statements.

The landslide area southwest of Fermi 3 referenced in the RAI is associated with the Maumee River, and the landslides are confined to the Maumee River banks and bluffs. The site vicinity of Fermi 3, the landslide hazard on FSAR Figure 2.5.1-227 is characterized as "low incidence, moderate susceptibility."

References

1) Lounsbury, R.W. and W.N. Melhorn, "Slumps in the Maumee River Valley, Maumee, Ohio," Abstracts with Programs, Geological Society of America, v. 3, p. 270, 1971
2) Dimit, G., "An investigation of slope failure along the Maumee River from Grand Rapids, Ohio, to Toledo, Ohio," Unpublished Masters Thesis, University of Toledo, pp. 128, 1 map, 1988.

Proposed COLA Revision

None

Attachment 15
NRC3-10-0006

Response to RAI Letter No. 1
(eRAI Tracking No. 3913)

RAI Question No. 02.05.01-24

RAI 02.05.01-24

FSAR Figure 2.5.1–203 shows numerous faults within the 320 km site radius, including: the Outlet fault, the Marian fault, and the Colchester fault. These three structures are not discussed in the FSAR text even though they are located well within the 320 km site radius. Please provide a discussion of these faults similar to those presented for other regional structures described in the FSAR.

Response

Information about the Colchester fault will be added to FSAR Table 2.5.1-201.

The Outlet and Marion faults are part of the southern segment of the Bowling Green fault zone, and are discussed in FSAR Section 2.5.1.1.4.3.2.3. These faults are also included in FSAR Table 2.5.1-201 under the southern segment of the Bowling Green fault. More detailed information regarding these two faults will be added to FSAR Section 2.5.1.1.4.3.2.3.

Proposed COLA Revision

Additional information on the Outlet and Marion faults will be dded to Section 2.5.1.1.4.3.2.3 as shown in the attached markup. The proposed markup of FSAR Table 2.5.1-201 is provided in response to RAI 02.05.01-07 (Attachment 4).

Markup of Detroit Edison COLA
(following 12pages)

The following markup represents how Detroit Edison intends to reflect this RAI response in a future submittal of the Fermi 3 COLA. However, the same COLA content may be impacted by revisions to the ESBWR DCD, responses to other COLA RAIs, other COLA changes, plant design changes, editorial or typographical corrections, etc. As a result, the final COLA content that appears in a future submittal may be different than presented here.

(Figure 2.5.1-203). Fisher (Reference 2.5.1-329) postulates that the Albion-Scipio anticline and associated en-echelon wrench faults control the Albion-Pulaski-Scipio-trend oil and gas field. The mapped length of the fault is approximately 48 km (30 mi) and the structure is subparallel to the Howell anticline and portions of the northern segment of the Bowling Green fault (Reference 2.5.1-329). The sense of displacement is uncertain; Fisher (Reference 2.5.1-329) shows a southwest-side-down fault, whereas Fisher (Reference 2.5.1-330) postulates mainly strike-slip displacement due to the lack of vertical displacement. The youngest unit affected by the structure is the Middle Ordovician Trenton Formation (Reference 2.5.1-331).

2.5.1.1.4.3.2.3 Bowling Green (Lucas-Monroe) Fault/Monocline

The Bowling Green fault, known locally as the Lucas-Monroe monocline or fault, in the subsurface of Ohio and Michigan, consists of three segments: (1) a central north-south-trending, generally linear segment; (2) a southern, southeast-trending splay of faults; and (3) a northern, northwest-trending segment of stepped faults (Table 2.5.1-201 and Figure 2.5.1-203, Figure 2.5.1-223, and Figure 2.5.1-224). The total length of the three segments is approximately 190 km (118 mi) (Figure 2.5.1-203). At its closest distance, the Bowling Green fault is approximately 40 km (24 mi) west of the site.

The central segment, known as the Bowling Green fault, extends from approximately the southeastern corner of Hancock County, Ohio, north to the middle of the boundary between Lenawee and Monroe Counties, Michigan, and is well studied because of quarry exposures. The fault displaces the Precambrian unconformity surface west-side-down (Reference 2.5.1-237), and has had at least six episodes of displacement through the Middle Silurian~~(Reference 2.5.1-332; Figure 2.5.1-223).~~

(Reference 2.5.1-332) (Figure 2.5.1-223).

As exposed in the Waterville quarry in southern Lucas County, the fault is a 10-m (33-ft) wide near-vertical zone of highly sheared rock striking N10° to 20°W, with secondary faulting extending out 10 to 90 m (33 to 300 ft) on either side (Reference 2.5.1-332). The fault juxtaposes the uppermost Silurian Bass Islands Group on the west against the Tymochtee Dolomite, which stratigraphically underlies the Bass Islands Group on the east. The contact between the two units is offset approximately 70 m (230 ft), west-side-down (Reference 2.5.1-332) (Figure 2.5.1-224). Maximum displacement appears to be approximately

122 m (400 ft), west-side-down, on the top of the Middle Silurian Lockport Dolomite (Reference 2.5.1-332). The latest Silurian Bass Islands Group is the youngest unit displaced by the Bowling Green fault; no younger units except for unfaulted Pleistocene glacial deposits occur along the fault (Reference 2.5.1-332). Onasch and Kahle (Reference 2.5.1-332) speculate fault-parallel, east-dipping thrust faults with maximum displacements of less than 5 m (16 ft)~~,~~ (Episode VI on Figure 2.5.1-223) generally on the east side of the fault, are consistent with the contemporary stress field~~,~~ and if related to contemporary stresses, the Bowling Green fault is Late Cretaceous or younger. The central segment of the fault is essentially coincident with the GFTZ and the Findlay arch (Figure 2.5.1-203). Onasch and Kahle (Reference 2.5.1-332) suggest that the location of the fault and recurrent displacement through latest Silurian on the fault are controlled by the Grenville Front and Paleozoic orogenic activity to the east, including the Middle to Late Ordovician Taconic event (ca. 470 – 440 Ma), the Late Silurian Acadian or Caledonian event, the Devonian[1] A~~r~~cadian event, and possibly the Carboniferous – Permian Alleghenian event. ~~Onash~~ and Kahle (Reference 2.5.1-332) speculate that the recurrent displacement may have been due to stresses related to migration of the Findlay arch (as a forebulge) during the Acadian and/or ~~Allegenian~~ events.

The southern segment consists of several steeply dipping to vertical, southeast-trending fault splays in Ohio that extend from approximately the southern boundary of Wood County to the southern portion of Marion County. These faults roughly define a northwest-southeast-trending high and low on the map of the Precambrian unconformity surface in Ohio, and include the Outlet (northeast-side-down) and Marion (also northeast-side-down) faults and several unnamed faults (Reference 2.5.1-237).

The northern segment, also known as the Lucas-Monroe monocline/fault, consists of short, steeply dipping to vertical, southwest-side-down, northwest-southeast- to north-trending, right- and left-stepping faults that extend from the middle of the boundary between Lenawee and Monroe Counties to the northwestern corner of Livingston County, where the segment appears to merge with the Howell anticline (Figure 2.5.1-203). The youngest unit affected by the structure is the early Carboniferous Sunbury Shale (Reference 2.5.1-333). A magnitude 3.4 earthquake occurred September 2, 1994, on a N70°W, left-lateral, strike-slip fault at a

Onasch

Alleghenian

Add Insert #1 here

Insert 1

The Outlet fault zone trends northwest and extends from Wyandot County to Wood County. Based on the sense of folding and nature of displacement between the Outlet and Bowling Green faults, the Outlet fault is interpreted as a large synthetic shear zone to the Bowling Green fault (Reference 2.5.1-453). Based on boreholes along the fault zone, the Ordovician Trenton limestone has been extensively fractured and brecciated in a zone that is a few hundred to a few thousand feet wide. Vertical displacement on the Outlet fault zone ranges from approximately 6 to 30 m (20 to 100 ft). The amount of lateral displacement cannot be determined (Reference 2.5.1-453). Deposition of the Late Ordovician Cincinnati Group and possibly the Point Pleasant Formation also were affected by the Outlet fault zone (Reference 2.5.1-454). The Marion fault is one of several small faults that have been recognized based on well data. The structural trends of the Marion and other faults are supported by subsurface data on the top of the Trenton limestone, unpublished lineament analyses by the Ohio Geological Survey, analysis of proprietary seismic data, and anomalies in gravity and magnetic maps (Reference 2.5.1-454).

depth of 10 – 15 km (6 – 9 mi) in Precambrian basement rocks near Potterville, approximately 21 km (12.6 m) southwest of Lansing, Michigan and approximately 130 km (90 mi) northwest of Fermi 3 (Reference 2.5.1-334). Faust et al. (Reference 2.5.1-334) suggest that this earthquake was on a hypothetical fault associated with a northwest extension of the Lucas-Monroe fault, or possibly on a shallow dipping feature associated with the ~~MRS /MMGH.~~ Structure contour maps of Paleozoic units (e.g., see Figure 2.5.1-225) do not support the Lucas-Monroe fault extension hypothesis. Because the epicenter and zone of intense shaking of this earthquake are approximately 25 km (15.5 mi) southwest of and not coincident with the southwest margin of the MRS /MMGH (Reference 2.5.1-334), it is unlikely that the earthquake is associated with this structure.

2.5.1.1.4.3.2.4 Burning Springs Anticline/Fault – Cambridge Arch/Fault

The Burning Springs anticline/fault and Cambridge arch/fault comprise a narrow zone of recurrent Paleozoic faults in the cores of anticlinal structures embedded in the Precambrian Grenville province about 100 km (60 mi) east of the Grenville Front (Reference 2.5.1-336) (Figure 2.5.1-203). The zone trends north to south in northern West Virginia and extends N20°W across Ohio to Lake Erie, a total distance of approximately 350 km (213 mi).

The southern segment of the zone in northern West Virginia is termed the Burning Springs anticline and has a length of approximately 50 km (30 mi) up to about 150 km (91 mi) if the Mann Mountain anticline south of the Burning Springs anticline is included. Near the Ohio River the structure loses definition and appears to step en-echelon to the left toward splays of the southeast end of the Cambridge arch (Reference 2.5.1-336). Between the structures at the Ohio River is an approximately 16-km (10-mi) break. The structure is present in the Precambrian unconformity surface as an east-side-down normal fault. (Reference 2.5.1-237) Paleozoic displacement on the structure included: (1) reactivation of older basement faults during the Silurian which created an evaporite basin east of the structure, (2) displacement during deposition of Devonian through Permian units, and (3) northwest-directed Alleghanian orogeny thrusting on decollements in the Salina salt units, which created ramp faults and a system of imbricate thrusts in the cores of anticlines (Reference 2.5.1-336). Seismic data

The following discussion of structures within the site vicinity was based on a review of published literature, discussions with geologists from the Ohio Geological Survey and Michigan Geological Survey, interpretation of high-altitude imagery and aerial photographs, and field and helicopter reconnaissance conducted during August 2007. Identification and characterization of structures at the site is based on subsurface information developed as part of previous studies conducted for Fermi 2 and results of more recent drilling completed as part of the Fermi 3 subsurface investigations.

2.5.1.2.4.1 Structures Within the Site Vicinity

Major Precambrian structures in the site vicinity include the GFTZ and the MRS, which intersect in the site vicinity (Figure 2.5.1-203). These structures, which are buried beneath a thick (approximately 1100-m [3600-ft] section of Paleozoic sediments, are interpreted from potential field and seismic data as discussed in detail in Subsection 2.5.1.1.2.2.4.

The structure of Paleozoic rocks in the subsurface in the site vicinity has been interpreted from boring and geophysical data obtained primarily from oil and gas exploration (Reference 2.5.1-406; Reference 2.5.1-407; Reference 2.5.1-408; Reference 2.5.1-333).

The surface of the Precambrian basement unconformity is regular with a gentle gradient ranging from about 0.3 degree (5.9 m/km [31 ft/mi]) to locally about 1 degree [Chatham Sag] (16 m/km [85 ft/mi]) on the northwest flank of the Findlay arch northwest into the Michigan basin and about 1 degree (6 m/km [32 ft/mi]) southeast into the Appalachian basin (Reference 2.5.1-325). Dips on Paleozoic units through the lower Middle Devonian Detroit River Group are similar (Reference 2.5.1-325) and define the pattern of Paleozoic rocks in the site vicinity (Reference 2.5.1-325) (Figure 2.5.1-241). The youngest Paleozoic rocks at Fermi 3 are the Upper Silurian Bass Islands Group. Younger Paleozoic rocks were either deposited and eroded or not deposited on the crest of the positive Findlay arch.

No Quaternary faults are known within the site vicinity. The Bowling Green fault and the Maumee fault are bedrock faults mapped within 40 km (25 mi) of the site (Figure 2.5.1-246). The Howell anticline and associated fault, which is mapped to within 45 km (28 mi) of the site, are discussed in Subsection 2.5.1.1.4.3.2. A series of folds are recognized in subsurface bedrock units along the southeastern projected trend of the

Howell anticline/fault structure (Reference 2.5.1-341). Two possible fault trends associated with the small New Boston and Sumpter oil and gas pools in Huron Township and Sumpter Township, Wayne County, Michigan, respectively, are mapped along the southwestern flank of this series of folds (Reference 2.5.1-406). Additional shorter faults are mapped in southwestern Ontario, including two subparallel unnamed faults, one of which is associated with the Colchester oil and gas field (Reference 2.5.1-409). Structures within the site vicinity (40-km [25-mi] radius) are described in more detail below.

The central and northern segments of the Bowling Green fault are located approximately 40 km (25 mi) from the site (Figure 2.5.1-231; Subsection 2.5.1.1.4.3.2). The Bowling Green fault displaces the Precambrian unconformity surface down to the west (Reference 2.5.1-237) and has approximately 122 m (400 ft), down to the west displacement on the top of the Middle Silurian Lockport Dolomite (Reference 2.5.1-332). The Bowling Green fault has had at least six episodes of displacement through the Middle Silurian (Reference 2.5.1-332; Figure 2.5.1-234). Onasch and Kahle (Reference 2.5.1-332) speculate that fault-parallel, east-dipping thrust faults with maximum displacements of less than 5 m (16 ft), generally on the east side of the fault, may represent younger deformation (post-Middle Silurian to Cenozoic). The youngest unit displaced by the Bowling Green fault is the latest Silurian Bass Islands Group; no younger units except for unfaulted Pleistocene glacial deposits occur along the fault (Reference 2.5.1-332).

The northeast-southwest-trending Maumee fault is coincident with the Maumee River in northwest Ohio, and extends to the shore of Lake Erie (Figure 2.5.1-203; Subsection 2.5.1.1.4.3.2). The Maumee fault is a normal fault that trends northeast-southwest and is expressed on the Precambrian unconformity surface (Figure 2.5.1-203) (Reference 2.5.1-237). The Maumee fault is offset in an apparent left-lateral sense about 2 km (1.2 mi) by the Bowling Green fault. No geomorphic expression of the Maumee fault was identified in aerial photographs or during the helicopter reconnaissance (August 2007) along the mapped trace of the fault where it is overlain by late Pleistocene glacial lacustrine deposits.

The southeast end of the Howell anticline/fault extends into the northwest corner of Wayne County, 45 km (28 mi) north of the site (Figure 2.5.1-234

and Figure 2.5.1-230). As discussed in Subsection 2.5.1.1.4.3.2 the Howell anticline is interpreted as a steep, asymmetrical, northwest-southeast trending, northwest-plunging, faulted anticline, having maximum relief of approximately 300 m (1000 ft) on the top of the Middle Ordovician Trenton Formation (Reference 2.5.1-325). The Howell fault offsets the base but not the top of the lower Middle Devonian Detroit River Group (Reference 2.5.1-340). In detail, this second order structure, which is superimposed on the flanks of the first order Findley arch, is probably more complex, consisting of several en-echelon folds and associated faults, as expressed in the structure contour maps on the top of lower Middle Devonian Dundee Formation, Middle Devonian Traverse Formation, and Early Mississippian Sunbury Shale (Figure 2.5.1-225). Overall, the Howell fault trends northwest-southeast and is normal, steeply dipping to vertical, and down-to-the-southwest.

To gain an understanding of the bedrock structure in the site vicinity, available structure contour maps were reviewed. No available structure contour map covered the entire site vicinity sufficiently to provide a complete interpretation; therefore, structure contour maps for the following have been combined on Figure 2.5.1-247:

- Structure contours of the top of the Devonian Dundee Limestone (Reference 2.5.1-333),
- Structure contours of the top of the Devonian Sylvania Sandstone (Reference 2.5.1-341), and
- Structure contours of the top of the Ordovician Trenton Formation (Reference 2.5.1-341).

The structure contours on the top of the Trenton Formation in Figure 2.5.1-247 define a number of folds in the site vicinity. A subsequent map of structure contours on the top of the Trenton Formation covering the site vicinity (Reference 2.5.1-352) (Figure 2.5.1-248a) does not show these folds. The discussion presented below uses a conservative approach that assumes the folds defined by the structure contours from Reference 2.5.1-341 presented in Figure 2.5.1-247 exist.

A series of north to northwest-southeast trending, southeast plunging synclines and intervening anticlines are expressed in structure contour maps on the top of the Ordovician Trenton Formation along the southeastern projected trend of the Howell anticline in Wayne and northeast Monroe Counties (Reference 2.5.1-341) (Figure 2.5.1-247).

Newcombe (Reference 2.5.1-341) also discusses a structure exposed in the Livingston Channel of the Detroit River, the Stony Island anticline. Based on a contour map of the top of the Lower Devonian Sylvania Sandstone, the anticline trends approximately N30°W and lies slightly to the southwest of the anticlinal axis as expressed in the older (lower) Trenton Limestone (Figure 2.5.1-247). This structure is also defined by rock exposures in the Anderdon quarry in Ontario, the Patrick quarry near the south end of Grosse Isle, Michigan, and the Sibley quarry near Sibley Michigan. Newcombe (Reference 2.5.1-341) observes that the Stony Island anticline is almost directly in line with the Howell anticline/fault structure to the northwest.

In a publication that focuses on the Albion-Scipio oil field in southern Michigan, Ells (Reference 2.5.1-406) shows in the site vicinity two possible northwest-southeast-trending faults associated with the small New Boston and Sumpter oil pools. These pools were previously identified by Cohee (Reference 2.5.1-410). Uncertain locations of the possible faults are illustrated on Figure 2.5.1-230. The southwestern possible fault associated with the Sumpter oil pool possibly extends into the site area (8-km [5-mi] radius). The Ells (Reference 2.5.1-406) figure showing these possible faults is scaled at approximately one inch equals 96 km (60 mi), and a note on the map states "Fault Trends Not To Scale",: therefore, the exact location of these faults is uncertain. In fact, Ells (Reference 2.5.1-406) mislabeled the oil pools from Cohee (Reference 2.5.1-410), associating the southwestern possible fault with the New Boston oil pool and the northeastern possible fault with the Sumpter oil pool. The Ells (Reference 2.5.1-406) report is based on well data, maps, and unpublished studies by the Michigan Department of Natural Resources. However, these possible faults are not discussed by Ells (Reference 2.5.1-406) in the report, nor were they identified by Cohee or other reports reviewed for this study. The inferred locations of the possible faults lie along the southwestern flank of an anticline expressed in the top of Ordovician Trenton Formation as mapped by Cohee (Figure 2.5.1-247). There is nothing in the character of the contours on the southwest flank of the anticline (e.g., offset contours or very steep contours) that provides evidence for the possible faults. No evidence for the possible faults is present on the structure contour map on the top of the Trenton Formation as illustrated in Reference 2.5.1-325 (Figure 2.5.1-248a). In summary, there is little evidence for these two

possible faults and, if present, their exact locations, extent, and association with any oil pools are unclear.

The Ordovician Trenton Formation is the source zone for the New Boston and Sumpter oil pools (Figure 2.5.1-247). Two wells were drilled in 1942 in the New Boston field in Sec. 18, Huron Township, Wayne County, Michigan, with the producing zone at a depth of 36.6 m (120 ft) below the top of the Trenton Formation (Reference 2.5.1-410). One well was drilled in 1941 in Sec. 22, Sumpter Township, Wayne County, Michigan, with production zones at depths of 3-5.2 m (10-17 ft) and 13 -22.6 m (43-74 ft) below the top of the Trenton Formation. As discussed above, there is no discussion in any of the reports reviewed for this study about the nature of structures associated with the New Boston and Sumpter fields. In southeastern Michigan, oil in the Trenton Formation is generally found along folds in zones of dolomitization associated with fracture zones that are sometimes related to pre-existing faults (Reference 2.5.1-411); so the New Boston and Sumpter fields may be associated with pre-existing faults. However, the fields, which occur along the northwestern ends of the postulated faults, are small, and any associated folds/faults, if present, are likely minor structures. There is no evidence of any dolomitization, deformation, or displacement in rocks younger than about Upper Silurian. The lack of dolomitization and deformation indicates that if these possible faults do exist, they became inactive at the end of the Silurian.

Minor broad, shallow, north and northwest-southeast- trending folds superimposed on the Findley arch are also expressed in the structural contours on the top of the Upper Silurian Bass Islands Group in southern Ontario (Reference 2.5.1-325) (Figure 2.5.1-248b). Minor fold structures identified at Fermi 3 have a similar northwest-southeast trend as discussed below in Subsection 2.5.1.2.4.2. These minor folds may be third order structures that are structurally related to the distal end of the Howell anticline/fault structure as it dies out to the southeast. By association with the Howell anticline/fault structure, these minor folds and postulated faults are assumed to be comparable in age to the Howell anticline/fault structure that is older than late Mississippian.

Ells (Reference 2.5.1-406) also shows in the site vicinity a probable north-northwest/south-southeast-trending fault associated with the Colchester oil pool in Essex County, southeastern Ontario, Canada. Burges and Hadley (Reference 2.5.1-413) show the Colchester oil field

coincident with a northwest-southeast trending syncline with about 12.2 m (40 ft) of relief. The oil pool is interpreted to be associated with a zone of dolomitization along a fracture zone in the Middle Ordovician Trenton Formation. The syncline in the uppermost ~~Orodivician~~ and middle and lower Silurian rock overlying the Trenton Formation resulted from shrinkage accompanying dolomitization of the Trenton ~~Fromation.~~ Bailey Geological Services and R.G. Cochrane subsequently interpreted the Colchester oil pool as two subparallel north-northwest/south-southeast trending normal, ~~down-to-east~~ faults (Reference 2.5.1-412). These ~~structures~~ are shown on Figure 2.5.1-230.

Ordovician

Formation

down-to-the-east

2.5.1.2.4.2 **Structures Within the Site Location**

Previous investigations, including borings and mapping of excavations for Fermi 2, and recent borings for Fermi 3 provide site-specific data to evaluate deformation at Fermi 3.

Previous and recent borings at the site indicate that the Silurian Salina Group and Bass Islands Group rocks underlying the site are folded into a broad, shallow syncline (Figure 2.5.1-237). Structural contours on the oolitic dolomite within the Bass Islands Group (Figure 2.5.1-249) are slightly irregular in shape. This is possibly indicating that these surfaces had some relief prior to folding. The axis of the syncline trends approximately N50°W. The flanks of the syncline dip less than 4°. The plunge of the syncline could not be determined because the surface of the marker horizons is irregular.

2.5.1.2.4.3 **Discontinuities**

Two joint sets have been mapped at the site in a quarry less than 1.6 km (1 mi) from the site and in excavations for Fermi 2 site structures (Reference 2.5.1-221). These joint sets trend N21° to 60°W and N54° to 72°E. Several trends of joint sets have been observed at quarries and outcrops in Michigan, Ohio, and Ontario, Canada. The most prominent trends are N40° to 60°W and N45° to 60°E. A primary joint set trending approximately N24°E is present in the Ottawa Lake quarry in Monroe County, Michigan (Reference 2.5.1-414) (Figure 2.5.1-230). Four primary joint sets are present in the Waterville quarry in northwest Ohio, trending approximately N45°W, N45° to 50°E, N5°E, and N80° to 90°W (Reference 2.5.1-414). Observed joint orientations along the northeast-southwest-trending Middle Devonian Columbus Limestone cuesta in northwest Ohio range from N50° to 70°E to N35°W near the

2.5.1-444 National Geophysical Data Center, National Oceanic and Atmospheric Administration (NOAA), "2-Minute Gridded Global Relief Data (ETOPO2v2) June, 2006," Bathymetric Data, http://www.ngdc.noaa.gov/mgg/fliers/01mgg04.html, accessed 1 January 2007.

2.5.1-445 Tennessee Valley Authority, "Application for a Combined License (COL) for Two Westinghouse Advance Passive 1000 (AP1000) Pressurized Water Reactors (PWRs) Designated as Bellefonte Nuclear Station Units 3 & 4," date of application submittal October 30, 2007.

2.5.1-446 Indiana Geological Survey, "Structural Features of Indiana (Indiana Geological Survey, Line Shapefile," 2002. http://129.79.145.7/arcims/statewide_mxd/dload_page/geology.html, accessed 2 June 2008.

2.5.1-447 Taylor, K.B., R.B. Herrmann, M.W. Hamburger, G.L. Pavlis, A. Johnston, C. Langer, and C. Lam, "The Southeastern Illinois Earthquake of 10 June 1987," *Seismological Research Letters*, Volume 60, No. 3, pp. 101-110, July – September 1989.

2.5.1-448 Slucher, E.R., E.M. Swinford, G.E. Larson, and D.M. Powers, "Bedrock Geologic Map of Ohio," Ohio Geological Survey, Map BG-1, version 6.0, scale 1:500,000, 2006.

2.5.1-449 Armstrong, D.K., and J.E.P. Dodge, "Paleozoic Geology of Southern Ontario," Ontario Geological Survey, Miscellaneous Release — Data 219, 2007.

2.5.1-450 Pavey, R.R., R.P. Goldthwait, C.S. Brockman, D.N. Hull, E.M. Swinford, and R.G. Van Horn, "Quaternary Geology of Ohio," Ohio Geological Survey, Map M-2, 1:500,000-scale map and 1:250,000-scale GIS files, 1999.

2.5.1-451 Michigan Department of Natural Resources, "Quaternary Geology of Michigan," Edition 2.0, digital map, 1998.

2.5.1-452 Ontario Geological Survey, "Quaternary Geology, Seamless Coverage of the Province of Ontario," Data Set 14, 1997.

Add Insert #2 Here

Insert 2

2.5.1-453 Wickstrom, L.H., "A New Look at Trenton (Ordovician) Structure in Northwestern Ohio," *Northeastern Geology*, Vol. 12, No. 3, pp. 103-113, 1990.

2.5.1-454 Wickstrom, L.H., J.D. Gray, and R.D. Stieglitz, "Stratigraphy, Structure, and Production History of the Trenton Limestone (Ordovician) and Adjacent Strata in Northwestern Ohio," Ohio Department of Natural Resources, Division of Geological Survey, Report of Investigations No. 143, 78 pp., 1992.

Attachment 16
NRC3-10-0006

Response to RAI Letter No. 16
(eRAI Tracking No. 3935)

RAI Question No. 02.05.01-28

RAI 02.05.01-28

FSAR Section 2.5.1.1.4.3.3.1 states that a series of earthquakes occurred between 1987 and 2001 near Ashtabula County, Ohio and that a July 1987 mainshock was followed by a January 2001 event making it seem that there were no earthquakes between these events. The FSAR goes on to state that the 1987 event, and its aftershocks, were within 1 km of an injection well. The FSAR states that the series of earthquakes in 2001 were precisely recorded by the Ohio seismic network but the FSAR does not provide any additional details of the larger 2001 event (or associated smaller events) including their location or the basis for linking the 1987 and 2001 events. In addition, FSAR Figure 2.5.1-207 does not differentiate the 1987 from the 2001 events. Please provide additional information regarding the 2001 series of earthquakes in the Northeast Ohio seismic zone including how they are clearly linked to the 1987 event and if they are related to fluid injection or the regional tectonics. In addition, please update FSAR Figure 2.5.1-207 to distinguish between the 1987 and 2001 events.

Response

Seeber et al. (Reference 2.5.1-455) discuss these fore-main-aftershock sequences and interpretations of these events based on information obtained from three short-term deployments of portable seismographs (in 1987, 2001, and 2003) and from regional broadband seismograms. The main observations and conclusions from this analysis are as follows:

- A persistent earthquake sequence in northeast Ohio includes multiple distinct fore-main-aftershock sequences that illuminate two faults approximately 4 km (2.5 mi) apart.
- The seismicity is closely associated with the injection of waste fluid from 1986 to 1994 into the basal Paleozoic formation.
- All the earthquakes originated from a relatively small area (~ 10 km [6 mi] wide) and are assumed to form a single sequence of causally related earthquakes.
- Felt earthquakes started in 1987, a year after the onset of injection. At that time earthquakes were located 0.7 – 2.0 km (0.4 - 1.2 mi)from the injection site. Seismicity continued and in 2001, 5.5 years after the end of injection, hypocenters were then 5 – 9 km (3 - 6 mi) from the injection site. The only known episode of seismicity in Ashtabula is closely associated with the 1986 – 1994 Class 1 injection, and the pattern of accurate hypocenters is consistent with the one expected for a high pore-pressure anomaly spreading from the injection site.
- This correlation is strong evidence that the seismicity was triggered by the injection.

The Ashtabula, Ohio, area has experienced eight distinct episodes of felt earthquakes since 1987 (Figure 2.5.1-266 and Figure 1). The largest events in the sequence include an initial M_{bLg} [1] 3.8 event on July 13, 1987; a M_{bLg} 2.6 foreshock event on January 19, 2001; a M_{bLg} 4.3 event on January 26, 2001, which had a MMI of VI, followed by a M_{bLg} 3.0 event on June 3, 2001; and a M_{bLg} 2.4 event on June 5, 2001 (Reference 2.5.1-347). The latest subsequence started in July 2003 with a M_{bLg} 2.5 event (Reference 2.5.1-455).

Accurately located aftershocks of the June 3, 2001, M_{bLg} 3.0 and the July 17, 2003, M_{bLg} 2.5 earthquakes define a 5 – 7 km long planar zone striking 96 degrees and dipping 65 degrees south (Figure 2.5.1-266). Seeber et al. (Reference 2.5.1-455) interpret this planar zone as the source fault for the 2001 seismicity. The 2001 zone of aftershocks subparallel a previously postulated east-west-striking fault with left-lateral slip defined by the July 1987 main shock and aftershock sequence. These subparallel faults are, respectively, 4.5 and 0.7 km (2.8 and 0.4 mi) southwest of the injection well. Seeber et al. revised their previous interpretation (Reference 2.5.1-346) of the tectonic implications of the earthquake sequence in 1987 and events in 1992 that they initially interpreted to be associated with the same fault to conclude that the linear patch of 1987 earthquakes is a portion of a basement fault activated by high pore pressure rather than a single rupture. Their conclusion was based in part on the observation that the aftershock events are scattered over the main shock patch as opposed to clustered at the edges.

Seeber et al. observe quiescence from 1995 to 2000, which they attribute to a lack of favorably oriented structures that could produce earthquakes between the two subparallel strike-slip faults. They speculate that seismicity initiates when and where pore pressure rises significantly along an existing fault that is stressed close to failure, and turns off when pressure starts dropping back. This hypothesis implies that in the absence of existing favorably oriented faults, the outward propagating zone of increased pore pressure induced from the injection well will not trigger seismicity. Seeber et al. conclude that the seismicity is occurring along existing faults located in the uppermost portion of the Grenville basement reactivated by a region of high pore pressure spreading from the injection site.

---

[1] Currently, in an effort to reduce confusion about earthquake magnitudes and apply the most reliable measure of earthquake size, the U.S. Geological Survey (http://earthquake.usgs.gov) reports most magnitudes with the label "magnitude" or "**M**," which refer to moment magnitude (sometimes denoted as M_w) determinations (when available). However, traditional magnitude determinations such as body wave magnitude (m_b), surface wave magnitude (M_S) and Lg wave magnitude (m_{bLg}) are also reported in USGS earthquake catalogs. Unless specified otherwise, the magnitudes reported for the Ashtabula events are the estimated body wave magnitudes (m_b*) for the earthquakes in the project catalog.

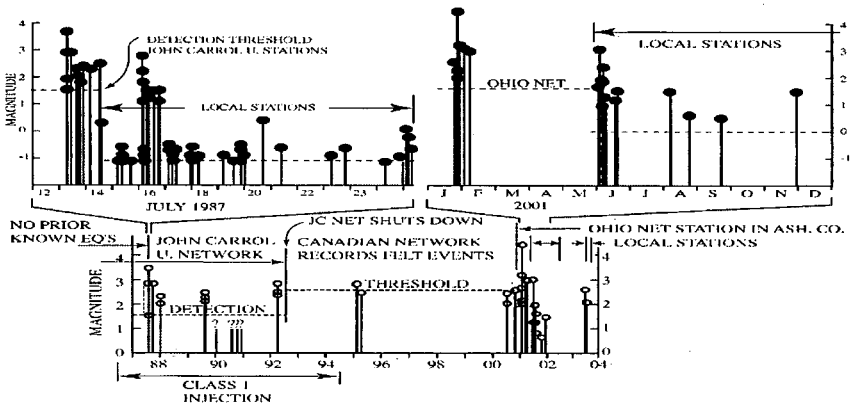

Temporal distribution of known seismicity in Ashtabula. The closest epicenter prior to 1987 is about 30 km from Ashtabula. The detection threshold drops about 2 orders of magnitude when local networks are in place. Monitoring continued until May 2002 without detecting other local events. The magnitudes of small earthquakes recorded only by the local analog recorders in 1987 are probably underestimated.

Source: Reference 2.5.1-455

Figure 1
Temporal Distribution of Known Seismicity in the Vicinity of Ashtabula, Ohio

Proposed COLA Revision

Revisions to FSAR Section 2.5.1.1.4.3.3.1 and FSAR Figures 2.5.1-207 (Sheet 2 of 3) and 2.5.1-266 are provided in the attached markup.

Markup of Detroit Edison COLA
(following 10 pages)

The following markup represents how Detroit Edison intends to reflect this RAI response in a future submittal of the Fermi 3 COLA. However, the same COLA content may be impacted by revisions to the ESBWR DCD, responses to other COLA RAIs, other COLA changes, plant design changes, editorial or typographical corrections, etc. As a result, the final COLA content that appears in a future submittal may be different than presented here.

Sandstone, Devonian Onondaga Limestone, and top of the Silurian Packer Shell horizon (Reference 2.5.1-342).

The geometry of the Akron-Suffield-Smith Township faults suggest that they originated as en-echelon, synthetic faults produced by right-lateral wrenching, with inferred minimum displacement of 21 km (13 mi) and subsequent normal displacements on the faults (Reference 2.5.1-342). Displacement on the Precambrian unconformity surface is 60 – 120 m (200 – 400 ft), while maximum vertical displacement of the Devonian Onondaga Limestone across the Akron-Suffield faults is 60 m (200 ft) and across the Highlandtown fault it is 72 m (240 ft) (Reference 2.5.1-342). Hook and Ferm (Reference 2.5.1-343) postulate that deposition of the Linton channel deposits below the Middle Pennsylvanian (Westphalian D) Upper Freeport coal may have been controlled by movement on the Transylvania fault extension (Pittsburgh-Washington cross-strike structural discontinuity). Post-Lower Pennsylvanian faulting cannot be assessed because of the absence of younger units. The northeast-southwest-trending Akron magnetic boundary crosses between the Middleburg and Akron faults.

2.5.1.1.4.3.3 Seismic Zones

Earthquakes in the site region are generally shallow events associated with reactivated Precambrian faults favorably oriented in the modern northeast-southwest compressive stress regime (Reference 2.5.1-344). None of these events has associated surface rupture, and no faults in the site region exhibit evidence of movement since the Paleozoic (Reference 2.5.1-344). Two seismic zones in the study region, the Anna seismic zone and the northeast Ohio seismic are designated as Class C features in the USGS Quaternary fault and fold database (Reference 2.5.1-316).

2.5.1.1.4.3.3.1 Northeast Ohio Seismic Zone

The Northeast Ohio seismic zone, also called the Ohio-Pennsylvania seismic zone, defines an approximately 50-km (30.5-mi) long, northeast-southwest-trending zone of earthquakes south of Lake Erie on the Ohio-Pennsylvania border (Reference 2.5.1-328). The largest historic event in this zone was the January 31, 1986, magnitude (m_b) 5.0 event located about 40 km (24.4 mi) east of Cleveland in southern Lake County, Ohio, and about 17 km (10.4 mi) south of the Perry Nuclear Power Plant (Reference 2.5.1-345). The earthquake produced Modified Mercalli

intensity (MMI) VI to VII at distances of 15 km (9 mi) from the epicenter and short-duration high accelerations of 0.18 g at the Perry Plant (Reference 2.5.1-345). Thirteen aftershocks were detected by April 15, 1986, with magnitudes ranging from 0.5 to 2.5 and focal depths ranging from 2 to 6 km (1.2 to 3.7 mi) (Reference 2.5.1-345). The aftershocks occurred in a tight cluster about 1 km wide and oriented north-northeast, and focal mechanisms of the aftershocks represent predominantly oblique, right-slip motion on nearly vertical planes oriented N15° to 45°E, with a nearly horizontal *P* (maximum compressive stress) axis (Reference 2.5.1-345), consistent with the modern stress regime. This earthquake and the aftershocks were within 12 km (7.3 mi) of deep waste disposal injection wells, and ~~this~~ earthquake sequence ~~may be~~ due to injection activities at the ~~well-reactivating~~ favorably oriented, pre-existing fractures (Reference 2.5.1-346; Reference 2.5.1-345). However, the relative distance ~~to~~ the earthquake cluster (12 km [7.3 mi]), as well as the lack of large numbers of earthquakes typical of induced sequences, a history of small to moderate earthquakes in the region prior to well activities, and the attenuation of the pressure field with distance from the wells all argue for a natural origin for the earthquakes (Reference 2.5.1-345).

is possibly

the

¶

wells that reactivated

of the wells from

that are

2003

, Reference 2.5.1-455

Add Insert "1" Here

In 1987, the first in a series of earthquakes continuing to ~~2001~~ occurred within the Northeast Ohio seismic zone near Ashtabula in Ashtabula County, Ohio, northeast of the 1986 earthquakes (Reference 2.5.1-347). ~~The initial magnitude 3.8 event occurred on July 13, 1987, followed by a magnitude 2.6 event on January 19, 2001, a foreshock to a magnitude 4.5 event on January 25, 2001, which had a MMI of VI, followed by a magnitude 3.2 event on June 3, 2001, and a magnitude 2.3 event on June 5, 2001 (Reference 2.5.1-347).~~ The July 13, 1987, main shock was close to a deep Class I injection well pumping fluids into the Mount Simon Sandstone, the basal Paleozoic unit overlying Precambrian crystalline basement, at a depth of about 1.8 km (1.1 mi), and a number of portable seismographs were deployed to study the aftershocks (Reference 2.5.1-347). ~~The 1987 aftershocks (36) were all within 1 km (0.6 mi) of the injection well, and defined a 1.5-km (1-mi) long by 0.25-km (0.15-mi) wide area at a depth of about 2 km (1.2 mi), with left-lateral strike-slip movement on an east-west-striking fault (Reference 2.5.1-345). The Ohio Seismic Network was installed in 1999 and precisely recorded the 2001 earthquakes (Reference 2.5.1-347). The sequence of earthquakes near Ashtabula beginning in 1987 is likely due~~

,

Add Insert "2" Here

¶

that was

Add Insert "3" Here

~~to fluid injection causing failure along favorably oriented, pre-existing fractures (Reference 2.5.1-347; Reference 2.5.1-346). Seeber and Armbruster (Reference 2.5.1-346) speculate that a single event rupture of a 5 to 10 km (3 to 6 mi) long fault could generate a magnitude 5 to 6 earthquake~~.

~~Nicholson et al. (Reference 2.5.1-345) observe that the 1986 cluster is coincident with a N40°E trending gravity and magnetic anomaly (Akron magnetic boundary). Seeber and Armbruster (Reference 2.5.1-346) and Dineva et al. (Reference 2.5.1-328) also associate the Northeast Ohio seismic zone with the Akron magnetic boundary, which is also called the Akron magnetic anomaly or lineament. Seeber and Armbruster (Reference 2.5.1-346) speculate that the Akron magnetic boundary may be associated with the Niagara-Pickering magnetic lineament/Central Metasedimentary Belt boundary zone as a continental-scale Grenville-age structure~~.

The Northeast Ohio seismic zone was included in alternative smaller seismic source zones by two of the EPRI-SOG earth science teams (EST), the Rondout and Woodward-Clyde Consultants teams, and was partly incorporated into a smaller zone by a third team (Bechtel team) (see Subsection 2.5.2).

2.5.1.1.4.3.3.2 Anna Seismic Zone

The Anna seismic zone, also called the Western Ohio seismic zone, coincides with northwest-southeast-trending basement faults associated with the Fort Wayne rift in Shelby, Auglaize, and nearby counties (Reference 2.5.1-344). Ruff et al. (Reference 2.5.1-348) attribute seismicity to the Anna-Champaign, Logan, and Auglaize faults. This zone has produced at least 40 felt earthquakes since 1875, including events in 1875, 1930, 1931, 1937, 1977, and 1986 that caused minor to moderate damage (Reference 2.5.1-344). The July 12, 1986, event near the town of St. Marys in Auglaize County was the largest earthquake to occur in the zone since 1937 (Reference 2.5.1-344). Schwartz and Christensen (Reference 2.5.1-349) determined a hypocenter of 5 km (3 mi) for the magnitude (m_b) 4.5 event and a focal mechanism (strike = 25°, dip = 90°, rake = 175°) representing mostly strike-slip with a small oblique component approximately parallel to the Anna-Champaign fault and a nearly horizontal *P* axis oriented east-northeast. The earthquake produced an MMI V1 event (Reference 2.5.1-349). Hansen

2.5.1-444 National Geophysical Data Center, National Oceanic and Atmospheric Administration (NOAA), "2-Minute Gridded Global Relief Data (ETOPO2v2) June, 2006," Bathymetric Data, http://www.ngdc.noaa.gov/mgg/fliers/01mgg04.html, accessed 1 January 2007.

2.5.1-445 Tennessee Valley Authority, "Application for a Combined License (COL) for Two Westinghouse Advance Passive 1000 (AP1000) Pressurized Water Reactors (PWRs) Designated as Bellefonte Nuclear Station Units 3 & 4," date of application submittal October 30, 2007.

2.5.1-446 Indiana Geological Survey, "Structural Features of Indiana (Indiana Geological Survey, Line Shapefile," 2002. http://129.79.145.7/arcims/statewide_mxd/dload_page/geology.html, accessed 2 June 2008.

2.5.1-447 Taylor, K.B., R.B. Herrmann, M.W. Hamburger, G.L. Pavlis, A. Johnston, C. Langer, and C. Lam, "The Southeastern Illinois Earthquake of 10 June 1987," *Seismological Research Letters*, Volume 60, No. 3, pp. 101-110, July – September 1989.

2.5.1-448 Slucher, E.R., E.M. Swinford, G.E. Larson, and D.M. Powers, "Bedrock Geologic Map of Ohio," Ohio Geological Survey, Map BG-1, version 6.0, scale 1:500,000, 2006.

2.5.1-449 Armstrong, D.K., and J.E.P. Dodge, "Paleozoic Geology of Southern Ontario," Ontario Geological Survey, Miscellaneous Release — Data 219, 2007.

2.5.1-450 Pavey, R.R., R.P. Goldthwait, C.S. Brockman, D.N. Hull, E.M. Swinford, and R.G. Van Horn, "Quaternary Geology of Ohio," Ohio Geological Survey, Map M-2, 1:500,000-scale map and 1:250,000-scale GIS files, 1999.

2.5.1-451 Michigan Department of Natural Resources, "Quaternary Geology of Michigan," Edition 2.0, digital map, 1998.

2.5.1-452 Ontario Geological Survey, "Quaternary Geology, Seamless Coverage of the Province of Ontario," Data Set 14, 1997.

2.5.1-455 Seeber, L., Armbruster, J.G., and Kim, W.-Y., "A Fluid-Injection-Triggered Earthquake Sequence in Ashtabula, Ohio: Implications for Seismogenesis in Stable Continental Regions," Bulletin of the Seismological Society of America, Vol. 94, No. 1, pp. 76-87, 2004.

Insert 1

Nicholson et al. (Reference 2.5.1-345) observe that the 1986 cluster (Figure 2.5.1-207 (Sheet 2 of 3)) is coincident with a N40°E trending gravity and magnetic anomaly, the Akron Magnetic Boundary. Seeber and Armbruster (Reference 2.5.1-346) and Dineva et al. (Reference 2.5.1-328) also associate the Northeast Ohio seismic zone with the Akron Magnetic Boundary, which is also called the Akron magnetic anomaly or lineament. Seeber and Armbruster (Reference 2.5.1-346) speculate that the Akron Magnetic Boundary may be associated with the Niagara-Pickering magnetic lineament/Central Metasedimentary Belt boundary zone as a continental-scale Grenville-age structure. Since the Akron lineament is imaged as ductile shear zones on regional seismic lines and no structures are observed in the overlying Paleozoic sediments, Seeber and Armbruster (Reference 2.5.1-346) acknowledge that the geometry of brittle faulting within or near this ductile deformation may have a complex relationship with the geometry of these shear zones.

Insert 2

The largest events in the sequence include an initial Lg wave magnitude (M_{bLg}) 3.8 event on July 13, 1987; a M_{bLg} 2.6 foreshock event on January 19, 2001; a M_{bLg} 4.3 event on January 26, 2001, which had a MMI of VI, followed by a M_{bLg} 3.0 event on June 3, 2001; and a M_{bLg} 2.4 event on June 5, 2001 (Reference 2.5.1-347). The latest subsequence started in July 2003 with a M_{bLg} 2.5 event (Reference 2.5.1-455)

Seeber et al. (Reference 2.5.1-455) discuss these fore-main-aftershock sequences and interpretations of these events based on information obtained from three short-term deployments of portable seismographs (in 1987, 2001, 2003) and from regional broadband seismograms. The main observations and conclusions from this analysis are as follows:

- A persistent earthquake sequence in northeast Ohio includes multiple distinct fore-main-aftershock sequences that illuminate two faults approximately 4 km (2.5 mi) apart (Figure 2.5.1-266).
- The seismicity is closely associated with injection of waste fluid in the basal Paleozoic formation from 1986 to 1994.
- All the earthquakes originated from a relatively small area (~ 10 km [6 mi] wide) and are assumed to form a single sequence of casually related earthquakes.
- Felt earthquakes started in 1987, a year after the onset of injection. At that time earthquakes were located 0.7 – 2.0 km from the injection site. Seismicity continued and in 2001, 5.5 years after the end of injection, hypocenters were then 5 – 9 km from the injection site. The only known episode of seismicity in Ashtabula is closely associated with the 1986 – 1994 Class 1 injection, and the pattern of accurate hypocenters is consistent with the one expected for the high pore-pressure anomaly spreading from the injection site.
- This correlation is strong evidence that the seismicity was triggered by the injection.

Insert 3

RAI 2.5.1-12
Start

The first 13 well-recorded aftershocks defined a nearly vertical fault with a north-northeast orientation (Reference 2.5.1-245). Analysis of a larger set of well-located aftershocks (36) indicates a cluster in a narrow (0.25 km [0.15 mi] wide), east-striking vertical zone about 1.5 km (1 mi) long, extending from a depth of 1.7 km (1 mi) to 3.5 km (2.1 mi) (Reference 2.5.1-346, Figure 2.5.1-266). The first motions are consistent with left-lateral strike-slip movement on an east-west-striking fault, referred to as the Ashtabula fault (Reference 2.5.1-346). The temporal and spatial proximity between injection and earthquake generation suggested that the injection of

waste fluids, which commenced in 1986, triggered the seismicity (Reference 2.5.1-345; Reference 2.5.1-346). Seeber and Armbruster concluded that the zone of seismicity represented a pre-existing basement fault brought to failure by the fluid flow and/or increased pore pressure induced by fluid injection. Seeber and Armbruster noted that from 1987 to 1992, the seismicity appeared to migrate westward out to a distance of 5 to 10 km, possibly along the Ashtabula fault. However, in a more recent paper, Seeber et al. (Reference 2.5.1-455) revised their interpretation to conclude that the linear patch of 1987 earthquakes is a portion of the fault activated by high pore pressure rather than a single rupture. Due to poor location constraints on earthquakes from August 1987 to 2001, the location of the M 2.9 earthquake on March, 28, 1992, cannot be definitely associated with the Ashtabula fault (Reference 2.5.1-455).

RAI 2.5.1-12
End

The Ohio Seismic Network was installed in 1999 and precisely recorded the 2001 earthquakes (Reference 2.5.1-347). After a felt M_{bLg} 2.6 foreshock on January 20, 2001, an M_{bLg} 4.3 main shock caused slight damage (MMI VI) on January 26. A focal mechanism obtained by modeling regional waveforms of this earthquake is consistent with composite focal mechanisms from locally recorded earthquakes. Well-located aftershocks of the June 3, 2001, M_{bLg} 3.0 and July 17, 2003, M_{bLg} 2.5 earthquakes define a 5 – 7 km long plane striking 96 degrees and dipping 65 degrees south. (Reference 2.5.1-455, Figure 2.5.1-266) Seeber et al. (Reference 2.5.1-455) interpret this plane as the source fault for the 2001 seismicity, which resembles the postulated 1.5 km long, east-west-striking basement fault having left-lateral slip defined by the 1987 seismicity.

The two subparallel faults are 4.5 (2.8 mi) and 0.7 km (0.4 mi) south of the injection well, respectively, and are 4 km (2.5 mi) apart (Figure 2.5.1-266). Seeber et al. (Reference 2.5.1-455) observed quiescence from 1995 to 2000, which they attribute to a lack of favorably oriented structures between these two fault planes. They speculate that seismicity initiates when and where a significant pore-pressure rise intersects pre-existing faults close to failure, turning off when pressure starts dropping back. Seeber et al. (Reference 2.5.1-455) conclude that these faults are pre-existing faults located in the uppermost portion of the Grenville basement and are reactivated by a high pore-pressure anomaly spreading from the injection site.

RAI 2.5.1-10
Start

In the CEUS, the most common types of surficial evidence of large, prehistoric earthquakes are liquefaction features and faults that offset young strata. A paleoseismic liquefaction field study along two of the larger drainages in northeast Ohio, the Grand River and the Cuyahoga River, was conducted by Obermeier (Reference 2.5.1-482) and involved reconnaissance along approximately 25 km (7.6 mi) of stream bank. No evidence of liquefaction was observed along either river. Although the scarcity of suitable exposures precludes definitive statements about prehistoric earthquakes, this led Crone and Wheeler (Reference 2.5.1-316) to classify the Northeast Ohio seismic zone as a Class C feature. Conditions and ages of the sediment encountered along each of these rivers as noted by Obermeier (Reference 2.5.1-482) were summarized in the report, as follows:

- Radiocarbon data from along the Grand River show that many of the exposures searched are at least 2,000 years old. Many others are probably mid-Holocene in age, based on depth and severity of weathering. A few scattered sites are earliest Holocene in age. Liquefaction susceptibility at many of the sites examined is at least moderate.
- Numerous exposures along the Cuyahoga River are at least a few thousand years old, and scattered exposures are up to 8,000 years old, based on radiocarbon data. Conditions are very good for forming liquefaction effects at many places.
- It is unlikely that sediments exposed in a sand pit near the Ashtabula-Trumbull County line experienced strong ground shaking through most or all of Holocene time.

Additional documentation of the 1995 paleoliquefaction field search in northeastern Ohio, which focused on the vicinity of the nuclear power plant near Perry, Ohio, was provided to the U.S. Nuclear Regulatory Commission (NRC) in a letter report submitted by Dr. Obermeier to Dr. Andrew Murphy on May 23, 1996 (Reference 2.5.1-483). From the ages and liquefaction

susceptibility of the sediments observed during the reconnaissance, Dr. Obermeier made the following conclusions specific to the Perry nuclear plant:

> "...within 20 km of the plant, the lack of suitable exposures precludes definitive statements concerning whether or not there has been strong seismic shaking for most of Holocene time."
>
> "The lack of exposures with liquefiable sediment more than a few thousand years old, within 20 to 25 km of the plant, precludes any statement concerning whether there could have been strong shaking at the plant locale from even moderate-sized earthquakes (say, M ~ 6) occurring more than a few thousand years ago."

"...one large sand and gravel pit (Pit-CL) of latest Pleistocene sediment, probably with a moderate to high liquefaction susceptibility, is located within 32 km of the plant...The lack of liquefaction features indicates a lack of strong seismic shaking through most or all Holocene time."

RAI 2.5.1-10
End

Figure 2.5.1-207 Regional Seismicity and tectonic Features in the Fermi 3 Site Region (Sheet 2 of 3)[EF3 COL 2.0-26-A]

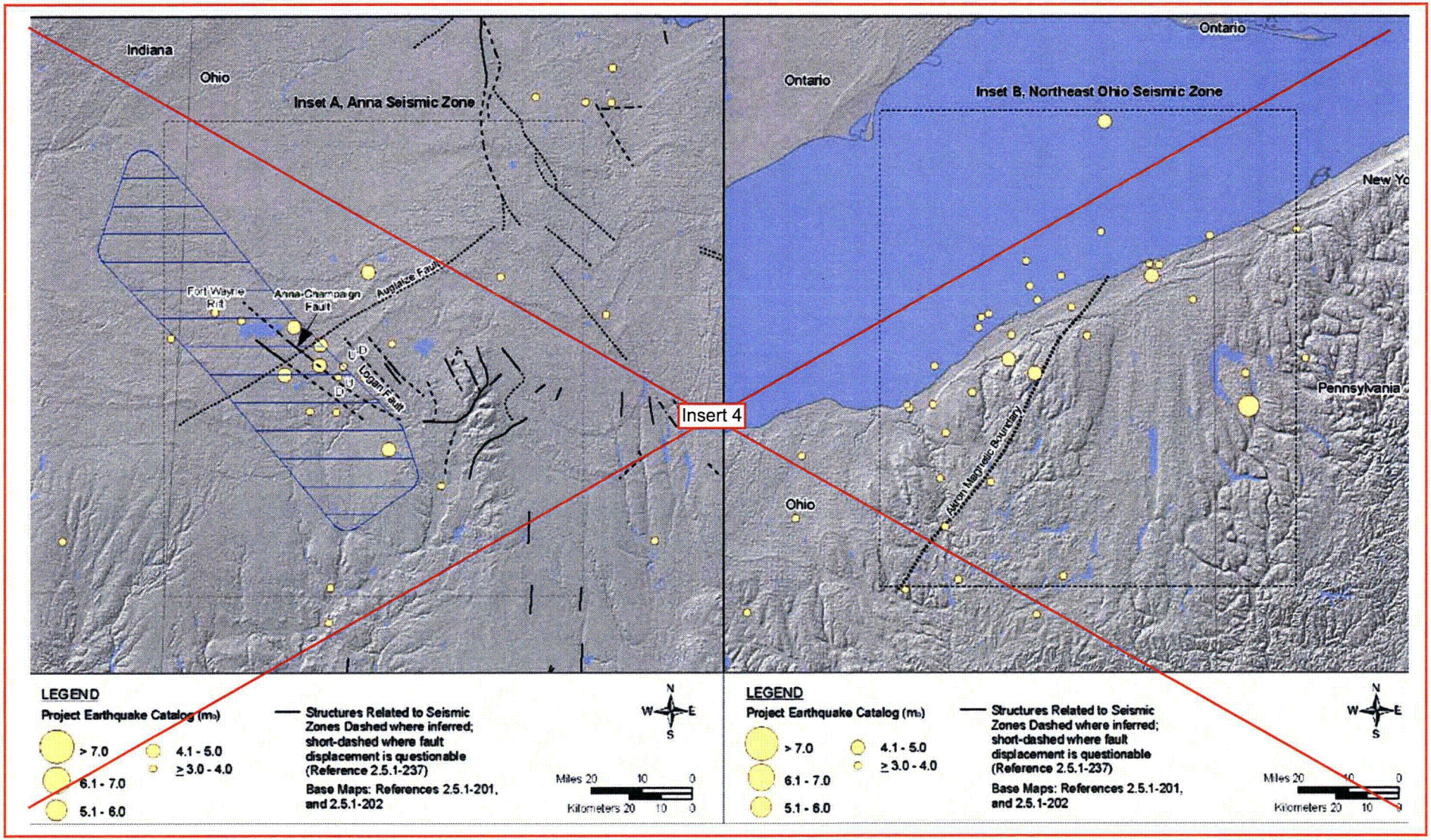

Insert 4

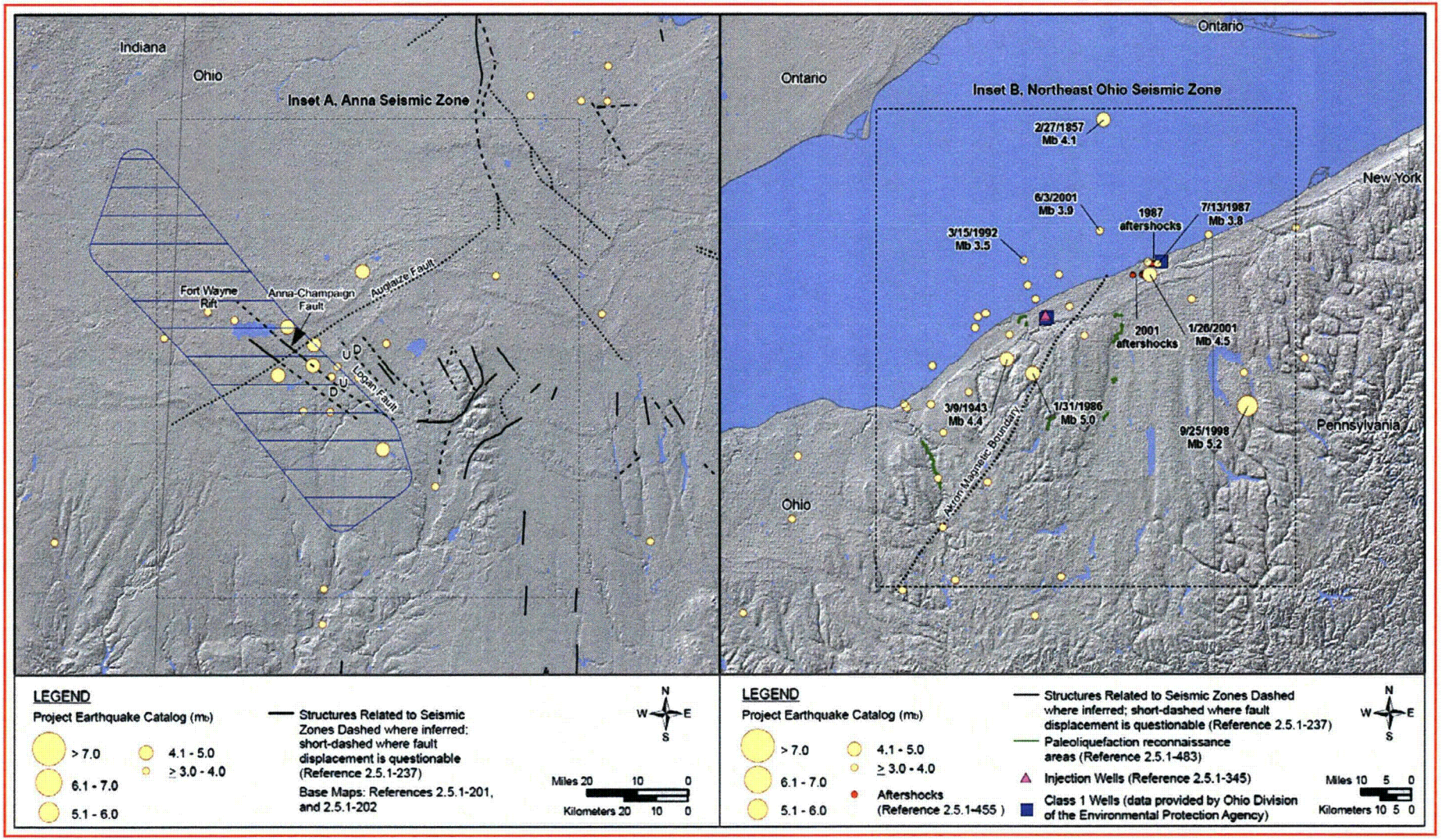
Indiana
Ohio
Inset A. Anna Seismic Zone
Fort Wayne Rift
Anna-Champaign Fault
Auglaize Fault
Logan Fault
U
D
U
D
Ontario
Ontario
Inset B. Northeast Ohio Seismic Zone
2/27/1857 Mb 4.1
6/3/2001 Mb 3.9
1987 aftershocks
7/13/1987 Mb 3.8
3/15/1992 Mb 3.5
New York
2001 aftershocks
1/26/2001 Mb 4.5
3/9/1943 Mb 4.4
1/31/1986 Mb 5.0
9/25/1998 Mb 5.2
Pennsylvania
Akron Magnetic Boundary
Ohio
LEGEND
Project Earthquake Catalog (mb)
> 7.0
6.1 - 7.0
5.1 - 6.0
4.1 - 5.0
≥ 3.0 - 4.0
Structures Related to Seismic Zones Dashed where inferred; short-dashed where fault displacement is questionable (Reference 2.5.1-237)
Base Maps: References 2.5.1-201, and 2.5.1-202
N
W
E
S
Miles 20 10 0
Kilometers 20 10 0
LEGEND
Project Earthquake Catalog (mb)
> 7.0
6.1 - 7.0
5.1 - 6.0
4.1 - 5.0
≥ 3.0 - 4.0
Aftershocks (Reference 2.5.1-455)
Structures Related to Seismic Zones Dashed where inferred; short-dashed where fault displacement is questionable (Reference 2.5.1-237)
Paleoliquefaction reconnaissance areas (Reference 2.5.1-483)
Injection Wells (Reference 2.5.1-345)
Class 1 Wells (data provided by Ohio Division of the Environmental Protection Agency)
N
W
E
S
Miles 10 5 0
Kilometers 10 5 0

Figure 2.5.1-266 Earthquakes and Inferred Fault Planes in the Ashtabula, Ohio, Area

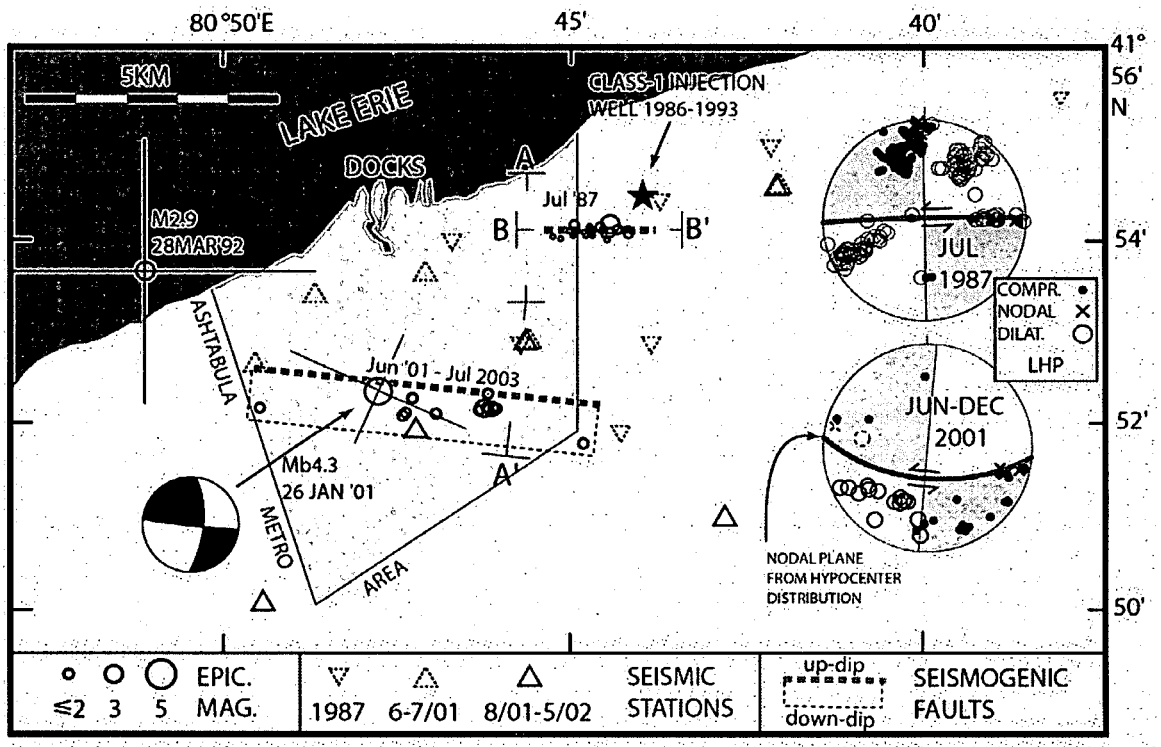

Reference 2.5.1-455

Accurate hypocenters and first motions in Ashtabula, Ohio, from two short-term deployments of portable seismographs. Data from 1987 illuminated a vertical east–west–striking left-lateral fault in the basement (Seeber and Armbruster, 1993). This activity was 0.7–2.0 km from a waste-disposal well (star) and started 1 year after the onset of injection. Several episodes of felt earthquakes during the following years were not monitored by local instruments. An M_{blg} 4.3 mainshock on 26 January 2001 caused light damage (MMI VI). The focal mechanism (Du *et al.*, 2003) and epicenter of this event were obtained from regional waveforms. Another fore– main–aftershock subsequence during June 2001 was captured with a local network. These data illuminate another fault (thick line is fault trace at unconformity) similar to the one in 1987, but 4 km south. The January mainshock is probably also from this source. The two dotted first motions are from the latest and westernmost hypocenter and are inconsistent with the composite focal mechanism.

Attachment 17
NRC3-10-0006

Response to RAI Letter No. 17
(eRAI Tracking No. 4007)

RAI Question No. 02.05.01-29

02.05.01-29

During the visit to the Denniston Quarry as part of a November 2009, Fermi 3 COL site audit, the staff noted at least three zones of disrupted bedding exposed in the quarry walls. These disrupted zones suggest possible faulting of the Bass Islands Group that should be fully documented because they may affect the younger overlying Quaternary deposits at the quarry site. In one location, disrupted bedding exists beneath an interpreted karst feature (located near the top of the geologic section) suggesting that the karst development may be associated with faulting at depth. In a second quarry location, a zone of disrupted bedding exists with mostly undisturbed bedding on either side. This second zone appears to be at least seven to ten meters wide; contains disrupted bedding from the top to the bottom of the exposed wall; and is flanked by relatively undisturbed bedding on both sides. The third zone of possible disturbed bedding was visible in a distant wall and could be related to vertical offsets within the Bass Islands Group. In each of these zones, disturbed bedding within the Bass Islands Group could be associated with faulting, and this potential faulting may or may not affect the overlying Quaternary deposits. Please provide further evaluation of disturbed zones and apparent offset beds at the Denniston quarry including a determination of whether or not the disturbed bedding and apparent offsets are fault related. In addition, evaluate the overlying Quaternary units to determine if these younger deposits are deformed by the underlying structures. Document all evaluations including photographs and maps of the exposures and include information that establishes the ages of deformation, including a description of the oldest and youngest deformed strata.

Response

The results of the investigation conducted at Denniston Quarry are provided in the attached Technical Memorandum from Glen Goodson, Black & Veatch Corporation to Detroit Edison Company on February 4, 2010.

A proposed markup to revise FSAR Section 2.5.1.2.4.1 presents a description and timing of two faults (locality 3) recognized at Denniston Quarry. A proposed markup to revise FSAR Section 2.5.1.2.5 presents the description and timing of two paleokarst features (localities 1 and 2) recognized at Denniston Quarry.

Proposed COLA Revision

A proposed revision to FSAR Sections 2.5.1.2.4.1 and 2.5.1.2.5 is attached.

Markup of Detroit Edison COLA
(following 10 pages)

The following markup represents how Detroit Edison intends to reflect this RAI response in a future submittal of the Fermi 3 COLA. However, the same COLA content may be impacted by revisions to the ESBWR DCD, responses to other COLA RAIs, other COLA changes, plant design changes, editorial or typographical corrections, etc. As a result, the final COLA content that appears in a future submittal may be different than presented here.

The following discussion of structures within the site vicinity was based on a review of published literature, discussions with geologists from the Ohio Geological Survey and Michigan Geological Survey, interpretation of high-altitude imagery and aerial photographs, and field and helicopter reconnaissance conducted during August 2007. Identification and characterization of structures at the site is based on subsurface information developed as part of previous studies conducted for Fermi 2 and results of more recent drilling completed as part of the Fermi 3 subsurface investigations.

2.5.1.2.4.1 Structures Within the Site Vicinity

Major Precambrian structures in the site vicinity include the GFTZ and the MRS, which intersect in the site vicinity (Figure 2.5.1-203). These structures, which are buried beneath a thick (approximately 1100-m [3600-ft] section of Paleozoic sediments, are interpreted from potential field and seismic data as discussed in detail in Subsection 2.5.1.1.2.2.4.

The structure of Paleozoic rocks in the subsurface in the site vicinity has been interpreted from boring and geophysical data obtained primarily from oil and gas exploration (Reference 2.5.1-406; Reference 2.5.1-407; Reference 2.5.1-408; Reference 2.5.1-333).

The surface of the Precambrian basement unconformity is regular with a gentle gradient ranging from about 0.3 degree (5.9 m/km [31 ft/mi]) to locally about 1 degree [Chatham Sag] (16 m/km [85 ft/mi]) on the northwest flank of the Findlay arch northwest into the Michigan basin and about 1 degree (6 m/km [32 ft/mi]) southeast into the Appalachian basin (Reference 2.5.1-325). Dips on Paleozoic units through the lower Middle Devonian Detroit River Group are similar (Reference 2.5.1-325) and define the pattern of Paleozoic rocks in the site vicinity (Reference 2.5.1-325) (Figure 2.5.1-241). The youngest Paleozoic rocks at Fermi 3 are the Upper Silurian Bass Islands Group. Younger Paleozoic rocks were either deposited and eroded or not deposited on the crest of the positive Findlay arch.

No Quaternary faults are known within the site vicinity. The Bowling Green fault and the Maumee fault are bedrock faults mapped within 40 km (25 mi) of the site (Figure 2.5.1-246). The Howell anticline and associated fault, which is mapped to within 45 km (28 mi) of the site, are discussed in Subsection 2.5.1.1.4.3.2. A series of folds are recognized in subsurface bedrock units along the southeastern projected trend of the

Howell anticline/fault structure (Reference 2.5.1-341). Two possible fault trends associated with the small New Boston and Sumpter oil and gas pools in Huron Township and Sumpter Township, Wayne County, Michigan, respectively, are mapped along the southwestern flank of this series of folds (Reference 2.5.1-406). Additional shorter faults are mapped in southwestern Ontario, including two subparallel unnamed faults, one of which is associated with the Colchester oil and gas field (Reference 2.5.1-409). Structures within the site vicinity (40-km [25-mi] radius) are described in more detail below.

The central and northern segments of the Bowling Green fault are located approximately 40 km (25 mi) from the site (Figure 2.5.1-231; Subsection 2.5.1.1.4.3.2). The Bowling Green fault displaces the Precambrian unconformity surface down to the west (Reference 2.5.1-237) and has approximately 122 m (400 ft), down to the west displacement on the top of the Middle Silurian Lockport Dolomite (Reference 2.5.1-332). The Bowling Green fault has had at least six episodes of displacement through the Middle Silurian (Reference 2.5.1-332; Figure 2.5.1-234). Onasch and Kahle (Reference 2.5.1-332) speculate that fault-parallel, east-dipping thrust faults with maximum displacements of less than 5 m (16 ft), generally on the east side of the fault, may represent younger deformation (post-Middle Silurian to Cenozoic). The youngest unit displaced by the Bowling Green fault is the latest Silurian Bass Islands Group; no younger units except for unfaulted Pleistocene glacial deposits occur along the fault (Reference 2.5.1-332).

The northeast-southwest-trending Maumee fault is coincident with the Maumee River in northwest Ohio, and extends to the shore of Lake Erie (Figure 2.5.1-203; Subsection 2.5.1.1.4.3.2). The Maumee fault is a normal fault that trends northeast-southwest and is expressed on the Precambrian unconformity surface (Figure 2.5.1-203) (Reference 2.5.1-237). The Maumee fault is offset in an apparent left-lateral sense about 2 km (1.2 mi) by the Bowling Green fault. No geomorphic expression of the Maumee fault was identified in aerial photographs or during the helicopter reconnaissance (August 2007) along the mapped trace of the fault where it is overlain by late Pleistocene glacial lacustrine deposits.

The southeast end of the Howell anticline/fault extends into the northwest corner of Wayne County, 45 km (28 mi) north of the site (Figure 2.5.1-234

and Figure 2.5.1-230). As discussed in Subsection 2.5.1.1.4.3.2 the Howell anticline is interpreted as a steep, asymmetrical, northwest-southeast trending, northwest-plunging, faulted anticline, having maximum relief of approximately 300 m (1000 ft) on the top of the Middle Ordovician Trenton Formation (Reference 2.5.1-325). The Howell fault offsets the base but not the top of the lower Middle Devonian Detroit River Group (Reference 2.5.1-340). In detail, this second order structure, which is superimposed on the flanks of the first order Findley arch, is probably more complex, consisting of several en-echelon folds and associated faults, as expressed in the structure contour maps on the top of lower Middle Devonian Dundee Formation, Middle Devonian Traverse Formation, and Early Mississippian Sunbury Shale (Figure 2.5.1-225). Overall, the Howell fault trends northwest-southeast and is normal, steeply dipping to vertical, and down-to-the-southwest.

To gain an understanding of the bedrock structure in the site vicinity, available structure contour maps were reviewed. No available structure contour map covered the entire site vicinity sufficiently to provide a complete interpretation; therefore, structure contour maps for the following have been combined on Figure 2.5.1-247:

- Structure contours of the top of the Devonian Dundee Limestone (Reference 2.5.1-333),
- Structure contours of the top of the Devonian Sylvania Sandstone (Reference 2.5.1-341), and
- Structure contours of the top of the Ordovician Trenton Formation (Reference 2.5.1-341).

The structure contours on the top of the Trenton Formation in Figure 2.5.1-247 define a number of folds in the site vicinity. A subsequent map of structure contours on the top of the Trenton Formation covering the site vicinity (Reference 2.5.1-352) (Figure 2.5.1-248a) does not show these folds. The discussion presented below uses a conservative approach that assumes the folds defined by the structure contours from Reference 2.5.1-341 presented in Figure 2.5.1-247 exist.

A series of north to northwest-southeast trending, southeast plunging synclines and intervening anticlines are expressed in structure contour maps on the top of the Ordovician Trenton Formation along the southeastern projected trend of the Howell anticline in Wayne and northeast Monroe Counties (Reference 2.5.1-341) (Figure 2.5.1-247).

Newcombe (Reference 2.5.1-341) also discusses a structure exposed in the Livingston Channel of the Detroit River, the Stony Island anticline. Based on a contour map of the top of the Lower Devonian Sylvania Sandstone, the anticline trends approximately N30°W and lies slightly to the southwest of the anticlinal axis as expressed in the older (lower) Trenton Limestone (Figure 2.5.1-247). This structure is also defined by rock exposures in the Anderdon quarry in Ontario, the Patrick quarry near the south end of Grosse Isle, Michigan, and the Sibley quarry near Sibley Michigan. Newcombe (Reference 2.5.1-341) observes that the Stony Island anticline is almost directly in line with the Howell anticline/fault structure to the northwest.

In a publication that focuses on the Albion-Scipio oil field in southern Michigan, Ells (Reference 2.5.1-406) shows in the site vicinity two possible northwest-southeast-trending faults associated with the small New Boston and Sumpter oil pools. These pools were previously identified by Cohee (Reference 2.5.1-410). Uncertain locations of the possible faults are illustrated on Figure 2.5.1-230. The southwestern possible fault associated with the Sumpter oil pool possibly extends into the site area (8-km [5-mi] radius). The Ells (Reference 2.5.1-406) figure showing these possible faults is scaled at approximately one inch equals 96 km (60 mi), and a note on the map states "Fault Trends Not To Scale",: therefore, the exact location of these faults is uncertain. In fact, Ells (Reference 2.5.1-406) mislabeled the oil pools from Cohee (Reference 2.5.1-410), associating the southwestern possible fault with the New Boston oil pool and the northeastern possible fault with the Sumpter oil pool. The Ells (Reference 2.5.1-406) report is based on well data, maps, and unpublished studies by the Michigan Department of Natural Resources. However, these possible faults are not discussed by Ells (Reference 2.5.1-406) in the report, nor were they identified by Cohee or other reports reviewed for this study. The inferred locations of the possible faults lie along the southwestern flank of an anticline expressed in the top of Ordovician Trenton Formation as mapped by Cohee (Figure 2.5.1-247). There is nothing in the character of the contours on the southwest flank of the anticline (e.g., offset contours or very steep contours) that provides evidence for the possible faults. No evidence for the possible faults is present on the structure contour map on the top of the Trenton Formation as illustrated in Reference 2.5.1-325 (Figure 2.5.1-248a). In summary, there is little evidence for these two

possible faults and, if present, their exact locations, extent, and association with any oil pools are unclear.

The Ordovician Trenton Formation is the source zone for the New Boston and Sumpter oil pools (Figure 2.5.1-247). Two wells were drilled in 1942 in the New Boston field in Sec. 18, Huron Township, Wayne County, Michigan, with the producing zone at a depth of 36.6 m (120 ft) below the top of the Trenton Formation (Reference 2.5.1-410). One well was drilled in 1941 in Sec. 22, Sumpter Township, Wayne County, Michigan, with production zones at depths of 3-5.2 m (10-17 ft) and 13 -22.6 m (43-74 ft) below the top of the Trenton Formation. As discussed above, there is no discussion in any of the reports reviewed for this study about the nature of structures associated with the New Boston and Sumpter fields. In southeastern Michigan, oil in the Trenton Formation is generally found along folds in zones of dolomitization associated with fracture zones that are sometimes related to pre-existing faults (Reference 2.5.1-411); so the New Boston and Sumpter fields may be associated with pre-existing faults. However, the fields, which occur along the northwestern ends of the postulated faults, are small, and any associated folds/faults, if present, are likely minor structures. There is no evidence of any dolomitization, deformation, or displacement in rocks younger than about Upper Silurian. The lack of dolomitization and deformation indicates that if these possible faults do exist, they became inactive at the end of the Silurian.

Add Insert 1 here →

Minor broad, shallow, north and northwest-southeast- trending folds superimposed on the Findley arch are also expressed in the structural contours on the top of the Upper Silurian Bass Islands Group in southern Ontario (Reference 2.5.1-325) (Figure 2.5.1-248b). Minor fold structures identified at Fermi 3 have a similar northwest-southeast trend as discussed below in Subsection 2.5.1.2.4.2. These minor folds may be third order structures that are structurally related to the distal end of the Howell anticline/fault structure as it dies out to the southeast. By association with the Howell anticline/fault structure, these minor folds and postulated faults are assumed to be comparable in age to the Howell anticline/fault structure that is older than late Mississippian.

Ells (Reference 2.5.1-406) also shows in the site vicinity a probable north-northwest/south-southeast-trending fault associated with the Colchester oil pool in Essex County, southeastern Ontario, Canada. Burges and Hadley (Reference 2.5.1-413) show the Colchester oil field

Insert 1

Two faults were identified within the Silurian Bass Islands Group Dolomite along a south-southwest-facing wall on the north side of the Denniston Quarry in Monroe County, Michigan. The two faults offset two approximately 1 m (3 ft)-thick light gray dolomite beds in a reverse sense. The faults dip to the west-southwest and are spaced approximately 10 m (33 ft) apart. The average orientation of the western fault is N15°W 58°SW and of the eastern fault is N2°W 60°SW. The relative offsets across the west and east fault are 1.4 m (4.6 ft) and 1.3 m (4.4 ft), respectively. The two faults cross-cut sub-horizontal bedding that dips slightly to the east up to 5 degrees. The western fault terminates approximately 2 m (6.6 ft) from the top of the outcrop and is therefore an intraformational structure, whereas the eastern fault is traceable to the top of bedrock. An investigation of the latest Pleistocene till and lacustrine deposits along the projection of the two faults provided evidence for no faulting in the overlying Quaternary deposits that are about 12,000 ka. (Reference 2.5.1-498)

coincident with a northwest-southeast trending syncline with about 12.2 m (40 ft) of relief. The oil pool is interpreted to be associated with a zone of dolomitization along a fracture zone in the Middle Ordovician Trenton Formation. The syncline in the uppermost Orodivician and middle and lower Silurian rock overlying the Trenton Formation resulted from shrinkage accompanying dolomitization of the Trenton Fromation. Bailey Geological Services and R.G. Cochrane subsequently interpreted the Colchester oil pool as two subparallel north-northwest/south-southeast trending normal, down-to-east faults (Reference 2.5.1-412). These structures are shown on Figure 2.5.1-230.

2.5.1.2.4.2 Structures Within the Site Location

Previous investigations, including borings and mapping of excavations for Fermi 2, and recent borings for Fermi 3 provide site-specific data to evaluate deformation at Fermi 3.

Previous and recent borings at the site indicate that the Silurian Salina Group and Bass Islands Group rocks underlying the site are folded into a broad, shallow syncline (Figure 2.5.1-237). Structural contours on the oolitic dolomite within the Bass Islands Group (Figure 2.5.1-249) are slightly irregular in shape. This is possibly indicating that these surfaces had some relief prior to folding. The axis of the syncline trends approximately N50°W. The flanks of the syncline dip less than 4°. The plunge of the syncline could not be determined because the surface of the marker horizons is irregular.

2.5.1.2.4.3 Discontinuities

Two joint sets have been mapped at the site in a quarry less than 1.6 km (1 mi) from the site and in excavations for Fermi 2 site structures (Reference 2.5.1-221). These joint sets trend N21° to 60°W and N54° to 72°E. Several trends of joint sets have been observed at quarries and outcrops in Michigan, Ohio, and Ontario, Canada. The most prominent trends are N40° to 60°W and N45° to 60°E. A primary joint set trending approximately N24°E is present in the Ottawa Lake quarry in Monroe County, Michigan (Reference 2.5.1-414) (Figure 2.5.1-230). Four primary joint sets are present in the Waterville quarry in northwest Ohio, trending approximately N45°W, N45° to 50°E, N5°E, and N80° to 90°W (Reference 2.5.1-414). Observed joint orientations along the northeast-southwest-trending Middle Devonian Columbus Limestone cuesta in northwest Ohio range from N50° to 70°E to N35°W near the

is from 1.2 to 6 m (2 to 10 ft). A minor set of joints trend from N54° to 72° E and dips from 30° to 60° to the northwest. Generally, these joints vary in length from 0.6 to 3.0 m (1 to 5 ft) but some are as much as 9.1 m (30 ft) long. Joints of the minor set are more irregular than the major set. Some minor joints terminate against major joints. Bedding plane joints, which undulate but are essentially horizontal, are spaced from 15 cm (6 in) to 1.2 m (2 ft) apart. These joints are generally tight but occasionally have minor openings which are often clay filled. (Reference 2.5.1-417)

During the Fermi 3 subsurface investigation jointing was observed throughout the Bass Islands Group and Salina Group Unit F. The joints encountered are opening-mode fractures. The joint density in the Bass Islands Group and Salina Group Unit F varies from isolated joints to groups of closely spaced joints referred to on the logs as highly fractured zones. The existence of joints and fracture zones is confirmed on the optical televiewer logs; however, the field boring logs have more joints and fracture zones possibly indicating mechanical breaking of the core during the drilling process. The orientations vary from horizontal to vertical with near horizontal and near vertical fractures dominating. The joint apertures were from tight or hairline up to several inches. Some joints were filled with anhydrite, calcite, or clay while others had no filling. A small percentage of joints have weathering along the joint walls or display minor dissolution (solutioning). Below Salina Group Unit F, the joint density decreases, and joints are rare in Salina Group Units C and B, but mineral (anhydrite) filled joints are present even in the deepest formations.

Joint orientations vary from horizontal to vertical, with near horizontal and near vertical joints dominating. Optical televiewer logging completed for the Fermi 3 project determined the presence of low angle (< 45°) bedding planes, low angle fractures (< 45°), and high angle fractures (> 45°). The dominant strike orientations of the bedding planes are north-northeast and west-northwest. The dominant strike orientations of all fracture planes are north-northwest and west-northwest. (Reference 2.5.1-418)

2.5.1.2.5 Site Geologic Hazard Evaluation

This section covers the non-seismic geologic hazards in the 40-km (25-mi) radius site vicinity including landslides and karst. The Landslide Overview Map of the conterminous United States (Figure 2.5.1-227) indicates the site vicinity, site area, and site location are in a region of

moderate landslide susceptibility. The susceptibility is based on the presence of lacustrine deposits (lake beds). The (8-km [5-mi] radius) site area has a maximum relief of 10.7 m (35 ft) (Subsection 2.5.1.2.1) and is best described as relatively flat with no steep slopes. The lacustrine deposits in the (1-km [0.6-mi] radius) site location are up to 3-m (9-ft) thick. The natural slopes are probably not landslide prone; however, the stability of the lacustrine deposits should be considered in excavation design (Reference 2.5.1-387).

The National Atlas Map showing the Engineering Aspects of Karst indicates the site vicinity, site area, and site location are in an area that can have fissures, tubes, and caves up to 300-m (1,000-ft) long below at least 3 m (10 ft) of noncarbonate overburden (Figure 2.5.1-228) (Reference 2.5.1-388). Davies et al. (Reference 2.5.1-388) emphasize that active karst in adjacent areas of northwestern Ohio occurs in areas where the noncarbonate overburden is less than 6-m (20-ft) thick. In the 1-km (0.6-mi) radius site location, the combined thickness of the till and lacustrine deposits is over 6 m (20 ft), indicating that the probability for karst is low.

Several sinkholes have been mapped in southwestern and southern Monroe County (Bedford, Whiteford, and Ida Townships). At least seven sinkholes are located in Devonian-age Detroit River group, which is outside the 8-km (5-mi) radius site area. Two sinkholes are in the Bass Islands Group. No sinkholes are in the (8-km [5-mi] radius) site area. (Reference 2.5.1-419; Reference 2.5.1-389; Reference 2.5.1-420)

Add Insert 2 here →

Subsection 2.5.1.2.3.1.2.1 discussed breccias and soft zones and potential explanations for their presence at the site. The formation of paleokarst was indicated as a possible reason for breccias and soft zones, with paleokarst episodes related to the dissolution of evaporite minerals, primarily halite and gypsum (Reference 2.5.1-392; Reference 2.5.1-397). Since no halite exists at the site and only minor amounts (nodule fillings and beds less than 3 cm [0.1 ft]) of gypsum and anhydrite exist in the Bass Islands Group and in Salina Group Unit F, the potential for modern evaporite karst is small.

The presence of voids was evaluated and discussed in Subsection 2.5.1.2.3 for applicable stratigraphic units.

Insert 2

In the Denniston Quarry located near Monroe, Michigan, disrupted zones interpreted as filled caves or paleokarst features related to Silurian/Devonian karst development were observed. The disrupted zones have the following features:

- Breccias composed of gravel- to boulder-sized dolomite fragments in either a fine-grained sediment matrix or carbonate cement.
- The host Bass Islands dolomite bedrock bedding is deflected downward adjacent to the disrupted zone. At some locations, tilted blocks of Bass Islands dolomite adjacent to the disrupted zone extend into the disrupted zone from their original layer.
- Discordant layers that appear to drape over the host rock along the margins of the disrupted zone.
- Horizontal bedded sediments within the disrupted zone that do not match the materials in the surrounding host rock.
- Near the top of the disrupted zones some porosity exists between the larger fragments.

No open caves or modern karst features were identified in Denniston Quarry. An investigation of the latest Pleistocene till and lacustrine deposits in the vicinity of two paleokarst features revealed that the overlying Quaternary deposits, which are about 12,000 ka, were undeformed indicating no recent karst activity. (Reference 2.5.1-498)

Attachment 17
NRC3-10-0006

Black & Veatch to Detroit Edison Memo Dated February 4, 2010
Denniston Quarry Investigation

Enclosure 1
(following 56 pages)

BLACK & VEATCH
Building a world of difference.

TECHNICAL MEMORANDUM

Detroit Edison Company
Fermi 3 COL Application Phase II

B&V Project: 163696
B&V File: 15.1000/18.2700
B&V Record No. BVDE2-2010-0037
February 4, 2010

Response to Fermi 3 FSAR RAI 02.05.01-29
Denniston Quarry Investigation

To: File

From Gregory C. Ohlmacher, Black & Veatch Corporation
Kathryn Hanson, AMEC Geomatrix, Inc.
Ryan Coppersmith, AMEC Geomatrix, Inc.

This memorandum presents the results of the Denniston Quarry investigation in Monroe, Michigan, which was conducted to fulfill the Nuclear Regulatory Commission (NRC) Request for Additional Information (RAI) 02.05.01-29 associated with the Fermi 3 Final Safety Analysis Report (FSAR), Revision 1 (Reference 1). The RAI requested a description and genesis of geologic structures related to disrupted bedding in bedrock and possible deformation of the overlying Quaternary deposits.

INTRODUCTION

Denniston Quarry is a limestone aggregate mine near Monroe, Michigan, approximately 16 km (10 mi.) southwest of the Fermi site within the (40 km [25 mi.] radius) site vicinity (Figure 1). On the Fermi 3 COLA audit field trip (November 4, 2009), three localities of disrupted bedding were observed in the quarry walls. NRC RAI 02.05.01-29 requested additional information on the three localities with disrupted bedding. This memorandum presents the findings of the additional study that was performed, the scope of which includes the following:

- Conducting detailed geologic mapping of the quarry walls at the three localities with disrupted bedding to evaluate the nature of the disruption and relationships to fracturing.
- Conducting detailed geologic mapping of the Quaternary deposits in the vicinity of the three localities of disrupted bedding to evaluate whether the disruption extends into the Quaternary deposits, which would indicate possible Quaternary deformation in the Fermi site vicinity
- Preparing a report with maps and photographs and information that estimates the age of deformation for features in the three localities of disrupted bedding.

The Denniston Quarry exposure provides an opportunity to evaluate the spatial and temporal relationships of stratigraphic and structural features in the same geologic unit that underlies the Fermi 3 site. Geologists from AMEC Geomatrix and Black & Veatch performed this study using conventional geologic mapping supplemented with Light Detection and Ranging (LiDAR) data collection to assist in the interpretation of bedrock exposures and trenching of Quaternary deposits as described herein.

Denniston Quarry is laid out in a series of rectangular areas (Figure 2). The quarry walls are up to 30 m (100 ft) high and are oriented either west-northwest/east-southeast or north-northeast/south-southwest. The footprint of the quarry is approximately 745 m (2,444 ft) by 820 m (2,690 ft). The length of the quarry walls that are mappable is approximately 3.2 km (2 mi.). Accessibility to the remaining quarry walls is limited by ponds and spoil piles that cover the quarry walls. There are limited exposures of bedrock in the quarry floor as most of the floor is covered with gravel The rectangular geometry of the quarry allows a

3-Dimensional perspective that allows for projecting structures and stratigraphy across the quarry floor to outcrops across the quarry (Figure 2).

Safety regulations imposed by the quarry did not allow for conventional mapping techniques at the three localities described by the NRC (herein referred to as Localities 1, 2, and 3 (Figure 2)). The safety standard required workers to stay back approximately 6 m (20 ft) from the quarry wall. Mapping from beyond the prescribed setback distance sufficed to document the presence of continuous subhorizontal bedding for a large portion of the quarry due to the lack of jointing and faulting. Localities 1, 2, and 3 described herein, however, required detailed documentation and structural analysis that was not possible from such a distance.

In order to provide documentation requested by the NRC at Localities 1, 2, and 3, ground-based LiDAR was used to characterize the disrupted bedding. A Leica ScanStation 2 high-definition scanner was used for this task (Figure 3). The instrument scanned the quarry walls at centimeter-scale resolution, creating a three-dimensional point cloud of the rock surface. The 3-Dimensional point cloud provides detailed information about the rock surface that would be impossible to obtain while meeting the safety regulations imposed by the quarry. Control points were established with a survey-grade Topcon HiPer GA/GPS unit. This allowed the LiDAR scans to be tied to the Michigan South state plane coordinate system and the North American Vertical Datum 1988 (NAVD88). The LiDAR data provided a means to characterize and accurately map the upward extent of deformation in bedrock.

A triangulated irregular network (TIN) is constructed from the 3-Dimensional point cloud. The Leica LiDAR instrument takes a digital photograph that can be draped on the TIN, allowing for easier interpretation of bedrock features. The TIN was used to better visualize geologic features in the quarry wall, to trace planes through the outcrop, and to measure dimensions of the disrupted zones and other features in the exposures. The 3-Dimensional point cloud was used to estimate orientations along bedding, joint, and fault planes, with orientations estimated where planes on the exposed rock face protrude from the quarry wall.

BEDROCK STRATIGRAPHY

Based on the proximity of Denniston Quarry to the Fermi 3 site, the same stratigraphic sequence is used at both locations (Reference 1 (Subsection 2.5.1.2.3; Figure 2.5.1-242)). A nearly complete section of Silurian Bass Islands Group dolomite is exposed at Denniston Quarry. Figure 4 provides a photograph depicting the bedrock stratigraphy. A broad anticline identified in the center of the quarry results in the exposure of about 2.4 m (8 ft) of dark gray dolomitic shale at the base of the quarry wall, which is the top of Salina Group Unit F. The Bass Islands Group exposed in the quarry is composed of well-bedded dolomite varying in thickness from several centimeters up to two meters with local thin interbedded shale units. The basal Bass Islands exposure is a light gray, bedded to massive dolomite (lower light gray dolomite on Figure 4) overlain by a medium gray, bedded to massive dolomite. Approximately 6 m (20 ft) above the contact with Salina Group Unit F is a black/gray shale layer less than 0.3 m (1 ft) thick. This layer is equivalent to the black shale marker horizon identified at the Fermi 3 site.

Above the black/gray shale is approximately 9 m (30 ft) of medium gray dolomite that is massive. Above this is the middle gray dolomite shown on Figure 4. The middle gray dolomite is roughly horizontal; however, the internal bedding planes are slightly undulating and two gray to black shale layers are observed within this layer. At the Fermi 3 site, gray to black shale layers were observed above and below an oolitic dolomite marker horizon at about the same distance above the black shale. Because of the safety restrictions, the presence of oolitic dolomite in the middle gray dolomite could not be investigated; however, fragments of oolitic dolomite were discovered on the quarry floor. Above the middle light gray

dolomite is a layer of medium gray dolomite that is massive. This is overlain by the upper light gray dolomite shown in Figure 4. Above the upper light gray dolomite is another medium gray dolomite that is bedded. This last medium gray dolomite is the youngest part of the Bass Islands Group exposed in the quarry. No younger bedrock formations are exposed at Denniston quarry. The light gray dolomites are the best layers to use to correlate the geology in different areas of the quarry walls. The lower light gray dolomite is only exposed at Locality 1 (Figure 2), whereas the middle and upper light gray dolomites are exposed at all three localities. Zones of disrupted bedding occur at all levels in the Bass Islands Group.

The LiDAR scans did not provide insight regarding deformation of or within the Quaternary deposits because the Quaternary deposits directly overlying the vertical bedrock quarry faces were either disturbed by excavation/erosion or removed during the quarry operations. However, structural trend information obtained from the LiDAR surveying was used to site trenches that were excavated to expose the Quaternary stratigraphy along/above the projected trends of the structural features observed in the quarry walls.

BEDROCK STRUCTURAL GEOLOGY

The bedding attitudes of the bedrock in the quarry walls are subhorizontal. At a few locations erosional contacts create undulated bedding surfaces that are structurally flat lying. Local folding is limited to monoclines with apparent dip changes of 5 to 10 degrees from horizontal (Figure 5). Bedding on either side of these local folds is subhorizontal. In addition to local folding, the subhorizontal bedding is disrupted by irregularly shaped zones that contain the following:

- Breccias composed of gravel- to boulder-sized dolomite fragments in either a fine-grained sediment matrix or carbonate cement (Figure 6).
- Downward tilted blocks/bedding of host Bass Islands Group dolomite adjacent to the disrupted zone, some of which extend into the disrupted zone from their original layer (Figure 6).
- Discordant layers that appear to drape over the host rock layering along the margins of the disrupted zone (Figure 6).
- Small zones of horizontal bedded sediments that are younger and do not correlate with the surrounding host rock.

The disrupted zones are filled with coarse-grained sediments that are infilled and cemented to partially cemented within the feature. Near the top of the features some porosity exists between the larger fragments. These disrupted zones are interpreted as filled caves or paleokarst related to Silurian/Devonian karst development. Regionally, paleokarst features in Silurian rocks are filled with Devonian sediments indicating that the karst activity was younger than the Silurian rocks, but no younger than the Devonian (Reference 1 (Section 2.5.1.2.3.1.2.1)). No open caves or modern karst features were identified in Denniston Quarry. Paleokarst was mentioned in Reference 1 (Section 2.5.1.2.3.1.2.1) as a possible cause of the breccias and poorly indurated rock encountered during the subsurface investigation at the Fermi 3 site.

The paleokarst zones observed in Denniston Quarry are up to 20 m (66 ft) in width and are bounded by subhorizontal beds on both sides. No surface expression of ongoing karst deformation exists in the Quaternary deposits overlying the paleokarst features as discussed below, indicating that these paleokarst features are older than the Quaternary. The paleokarst features are bounded by joints and are

also crosscut by younger joints. The joints that bound the paleokarst features are commonly covered due to filling with cemented collapse debris. The lack of vertical displacement of beds across the paleokarst features, along with the presence of joints along the feature boundaries, supports the finding that the features are related to Silurian/Devonian karst development localized along joints.

Joint sets are present throughout the exposure of the Bass Islands Group in Denniston Quarry. Two prominent joint sets were observed oriented north-northwest, dipping southwest, and oriented north-northeast, dipping northwest. These joint sets were observed crosscutting the paleokarst features. A less prominent third joint set strikes to the north-northwest and dips to the east-northeast. Most joint sets have dips that range from 60 to 80 degrees with a few joints dipping from 35 to 60 degrees.

North-northwest-striking, southwest-dipping reverse faults are observed at Localities 1 and 3 and west-northwest of Locality 2 (Figure 2). The two reverse faults west-northwest of Locality 2 were identified based on minor offsets less than 0.25 m (10 in.) of a shale bed associated with the middle light gray dolomite. The displacement cannot be traced throughout the exposed quarry wall, and these reverse faults do not offset beds at the top of the quarry wall. Because these two reverse faults did not penetrate the top of the bedrock, no additional studies were deemed necessary. Other reverse faults in the Denniston Quarry will be discussed as part of the discussions of the detailed mapping at Localities 1, 2, and 3. A summary of bedding, joint, and fault attitudes extracted from the analysis of the LiDAR 3-Dimensional point cloud data is presented on stereonets in Figure 7.

Detailed Locality Mapping

This section describes the structural features associated with disrupted bedding observed in bedrock at Localities 1, 2, and 3.

Locality 1 is located in the western portion of Denniston Quarry along a north-northeast-facing quarry wall (Figures 2). Figure 8 provides the following for Locality 1:

- A photograph of the bedrock draped on the LiDAR TIN
- Mapped contacts of the Quaternary deposits exposed in Quaternary Excavation QE-1 that was partially excavated over the top of Locality 1. The plan area of QE-1 is shown on Figure 2.

The disrupted zone (Figure 9) is interpreted to be a paleokarst feature, because of the presence of collapse breccia filling and the geometry of the disrupted zone. The irregularly shaped zone at Locality 1 extends from the top to the base of the 24 m (80 ft) high outcrop. The LiDAR scan produced a centimeter-scale 3-D point cloud that was processed into a TIN that represents an area 51 m (166 ft) wide horizontally along the outcrop face. The paleokarst zone is 12 m (40 ft) wide and is located in the center of the scan (Figure 9). Estimation of joint planes from the point cloud revealed a prominent set of northwest-striking, southwest-dipping joints with a crosscutting set that strikes to the northeast and dips to the northwest (Figure 10). The northwest-striking joints crosscut the paleokarst feature and, therefore, record a deformation event that postdates the Silurian/Devonian karst development. Two north-northwest-striking, southwest-dipping faults were observed adjacent to the paleokarst feature (Figure 9 Sheet 1). The fault west of the paleokarst feature offsets a pair of shale beds approximately 0.25 m (10 in.) in an apparent reverse sense. No displacement of beds is observed in the upper portion of the exposure, suggesting this fault is restricted to the Bass Islands group. Bedding is subhorizontal with a dip of up to 5 degrees to the south. The bedding is in the same orientation and at the same elevation on either side of the paleokarst feature, recording no vertical displacement across the zone (Figure 9 Sheet 2). A lowering in the elevation of individual beds is observed as the beds approach the paleokarst feature from either side. This is consistent with collapse of bedding near a paleokarst feature. There is no evidence of faulting within or across the paleokarst feature (Figure 9).

Locality 2 is located west of Locality 1 on a north-northeast-facing wall in Denniston Quarry (Figures 2). Figure 11 provides the following for Locality 2:

- The LiDAR TIN with a photo of the bedrock draped over the TIN.
- Mapped contacts of the Quaternary deposits exposed in QE-2 that was excavated over the top of Locality 2. The plan area of QE-2 is shown on Figure 2.

The disrupted zone is interpreted as a paleokarst feature based on the presence of collapse breccia and the geometry of the adjacent bedding (Figure 12, Sheet 1). The disrupted zone at Locality 2 extends throughout the 14 m (46 ft) high outcrop. The LiDAR scan had a horizontal measurement of 62 m (203 ft). The paleokarst feature is 21 m (69 ft) wide and is located in the center of the scan (Figure 12 Sheet 1). Field observations found that the paleokarst feature is bounded by a N 36° W 75° SW joint on the west side and a N 76° E 86° NW joint on the east side. These joints are located along the yellow lines that mark the boundary of the paleokarst feature in the bottom half of the quarry wall (Figure 12, Sheet 1). The attitudes of five joint planes estimated using the LiDAR 3-Dimensional point cloud reveal a prominent set of northwest-striking, southwest-dipping joints, along with one joint dipping to the northeast (Figure 13). One additional joint strikes to the northeast and dips to the northwest. The apparent northeast-striking joint bounding the east side of the paleokarst feature could not be estimated using the 3-Dimensional point cloud due to the lack of an exposed plane. The northwest-striking joints cut the paleokarst feature similar to Locality 1; thereby, indicating this joint set postdates Silurian/Devonian karst development and subsequent karst collapse. Three bedding plane orientations were extracted from the scan data that record subhorizontal planes dipping very gently (less than 8 degrees) to the south. Bedding near the top of bedrock is deflected downward along both the east and west margins of the paleokarst feature, indicating collapse of the beds into the paleokarst feature (Figure 12 Sheet 2). Individual beds are 0.3 – 0.6 m (1 – 2 ft) higher on the west (right) side of the disrupted bedding zone. This change in elevation of the beds along the quarry face could result from either the intersection of the southerly dipping bedding and the west-northwest trend of the quarry wall or minor faulting within the paleokarst feature (Figure 12, Sheet 2). No fault planes were identified in the field or in the LiDAR data analysis at Locality 2; however, a down-to-the-east displacement of up to 1 m (3 ft) would be consistent with other faults observed at the quarry indicating that the disrupted zone may be masking a fault. Since the change in elevation across the disrupted zone exists outside of the zone of bedding deflected downward near the margins of the disrupted zone, this change in bedding is probably not directly related to the collapse associated with the paleokarst feature.

Locality 3 is located along a south-southwest-facing wall on the north side of Denniston quarry where two minor faults are observed in the Bass Islands Group dolomite (Figures 2). Figure 14 provides an overview photo of the quarry wall where the faults were identified. Figure 15 provides an image of the LiDAR TIN for Locality 3 with a photo of the bedrock draped over the TIN without interpretation. Figure 16, Sheet 1 delineates the two faults, which offset the middle and upper light gray dolomite beds in a reverse sense. Two LiDAR scans were performed at Locality 3. One scan was taken from the southeast, toward the northwest; the second scan was taken from the southwest, toward the northeast. The two scans were stitched together to densify the point cloud and to maximize the resolution of the rock surface to make one TIN. The combined scans resulted in a TIN that represents an area 46 m (150 ft) wide and 18 m (60 ft) high (Figure 15). Bedding is near horizontal with dip angles of 5 and 6 degrees to the east, based on two orientations estimated using the 3-Dimensional point cloud data (Figure 17). Three joint plane orientations were estimated using the LiDAR data, with two north-northwest striking planes that dip 73 and 84 degrees to the east-southeast and one north-northeast striking plane that dips 50 degrees to the west-northwest.

Two faults highlight the deformation at Locality 3 (Figure 16, Sheet 1). These faults dip to the west-southwest and are spaced approximately 10 m (33 ft) apart along the quarry wall. LiDAR data indicates that the western fault offsets two light gray dolomite beds as much as 1.4 m (4.6 ft) in an apparent

reverse sense. The eastern fault offsets the same light gray dolomite bed up to 1.3 m (4.4 ft). Bedding horizons from west to east across the two faults record a 4.1m (13.5 ft) elevation drop in the upper light gray dolomite across the scanned outcrop (Figure 16 Sheet 2). The total change in elevation across the outcrop is accommodated by offsets along the two faults and by the eastward dip of the beds. The western fault terminates approximately 2 m (6.6 ft) from the top of the outcrop, whereas the eastern fault is traceable to the top of the bedrock outcrop. A detailed analysis of the fault planes in 3-Dimensional space revealed slight variability in the strike of the plane, and therefore, multiple orientations were taken from both planes in order to create an average orientation. Eleven strikes were estimated for the two planes, seven from the western fault, and four from the eastern fault (Figure 17). The average orientation of the western fault is N15°W 58°SW and the average orientation of the eastern fault is N2°W 60°SW. The average orientation of all of the attitudes is N7°W 58°SW. On either side of the western fault between the two light gray dolomite beds a zone of breccia exists with rounded to subangular clasts (Figure 18). The western fault is clearly visible within the breccia. The coarse-grained fragments are cemented. The area is high on the quarry face and could not be accessed while meeting the safety regulations imposed by the quarry. The breccia appears to be similar to the paleokarst breccias at Localities 1 and 2, and the relationships indicate that the faulting may be younger than karst activity.

QUATERNARY STRATIGRAPHY

Quaternary surficial geologic units exposed in the Fermi 3 site vicinity (40 km [25 mi.] radius) consist primarily of till of Wisconsinan age overlain by a thin mantle of lacustrine and eolian sands or locally thicker beach–dune ridge deposits formed along late glacial lake shorelines (Figure 19). The ground surface around the perimeter of Denniston Quarry, which varies between approximately 183 and 186 m (600 and 610 ft), is eroded into the lacustrine/till plain below the mapped strandline of Lake Lundy (189 to 192 m [620 to 630 ft]) (Reference 1 (References 2.5.1-391 and 2.5.1-392)) (Figure 20). Lake Lundy appears to have been relatively short-lived, coming to an end about 12,400 years before present (BP) (Reference 1; Reference 2.5.1-391). Beaches that are projected to the Lake Lundy level are generally sandy, have a relief of 1 to 2 m (3.3 to 6.6 ft), and are discontinuous (Reference 1 (Reference 2.5.1-297)). Some of the beaches probably are offshore bars formed in earlier lakes and some may be windblown sand (Reference 1 (Reference 2.5.1-297)).

Surficial soil units mapped in the vicinity of Denniston Quarry show the areas generally underlain by thicker sand (Figure 2). On Figure 2, the areas mapped as Selfridge loamy sand (Unit 19A) correlate with the thicker sand associated with slightly higher topography identified in the QE-1 and QE-2 above Localities 1 and 2. The sand in these areas is observed to be as much as 1.5 m (5 ft) thick. The Pewamo clay loam unit (Unit 22) is mapped on the nearly level, poorly drained till/lacustrine plain where the thickness of sediment mantling till or very firm clay loam is about 30 cm (1 ft). Areas where units are too small or intricately mixed to differentiate between these two soil units are mapped as the Selfridge-Pewamo complex (Unit 20A).

A major objective of the study was to document evidence for the presence or absence of deformation in the Quaternary deposits overlying deformation features identified in bedrock. In the vicinity of Localities 1 and 2, the Quaternary deposits were partially exposed in upper bench quarry cuts. However, these exposures were degraded and obscured by slope wash and colluvium. In these areas the existing upper quarry walls were re-excavated using a backhoe to provide better-quality, more-continuous exposures (QE-1 and QE-2, Figure 2).

Quaternary deposits immediately above the faults at Locality 3 were covered by berms associated with the water removal canal from the quarry and were not accessible for detailed study. In this area, a backhoe trench was excavated to provide exposures of the Quaternary deposits across the projected

trends of the faults (QE-3, Figure 2). The location and depth of the backhoe excavation that could be excavated at this location was restricted to an area of property between the berms and the property line. The presence of overhead electrical lines further limited backhoe operations (Figure 21). A benched trench was excavated in the area available at Locality 3 (Figure 21). Heavy rainfall the night after the trench was excavated resulted in ponding in the bottom of the trench and destabilization of the spoil pile, both of which resulted in unsafe conditions that precluded detailed mapping of the till in the bottom of the trench. However, the benches on the side of the trench away from the berm and spoil piles were available for detailed mapping, which allowed critical observations regarding the contact between the till and overlying lacustrine sediments and the general character of the till units in the trench.

Key contacts in these excavations were flagged, and locations were surveyed using a survey-grade Topcon HiPer GA/GPS unit. All survey points of the contacts were tied into the Michigan South state coordinate system and the NAVD 88. Photographs showing the deposits exposed in the excavations and specific surveyed points are shown on Figures 22 through 27. The Quaternary deposits exposed in the excavations are described below. Soil profiles measured at three locations and additional samples described for units in the QE-2 excavation are provided in Tables 1 through 4.

Glacial Deposits

The oldest Quaternary material identified in the site vicinity is till that directly overlies Paleozoic bedrock. The re-excavated upper quarry bench walls at QE-1 and QE-2 above Localities 1 and 2 and QE-3 above Locality 3 provided good exposures of the till. Two till units, an upper brown till and a lower gray till, were well exposed in these excavations. Both till units, which are very compact and hard, are silt and clay rich. The tills are sparsely pebbly, and except for the basal clast pavements observed in QE-1 and QE-2, cobbles and boulders are rare. The brown till is sandier, especially in the upper parts of the unit, and locally exhibits a fissile or subhorizontal blocky structural fabric. The underlying gray till generally has fewer gravel clasts, with the exception of some cobble and boulders that are present in the basal part of the unit. The compacted character of the till units indicates that both the gray till and the brown till were deposited subglacially.

In the upper quarry bench wall excavations QE-1 and QE-2 (above Localities 1 and 2, respectively), the two till units are separated by a discontinuous clast pavement and locally by possible glaciofluvial sediments in poorly defined channels at the base of the brown till. A lower clast pavement also was present at the base of the gray till unit. Clast pavements are common at the base of fine-grained diamictons (glacial deposits consisting of poorly-sorted, inhomogeneous, nonstratified sediments of which till is a member) associated with the late Pleistocene Laurentide ice sheet (References 2 and 3). The clast pavement at the contact between the brown and gray till units observed at Denniston Quarry is typical of clast pavements described in literature in that it consists of a layer of rounded-to-subrounded cobbles and small boulders, generally one clast thick, with individual clasts separated from each other by enclosing sediment. Settling of clasts through low-strength, fine-grained deforming subglacial sediment, followed by clast abrasion by overriding deforming sediment analogous to a debris flow, is suggested by Clark (Reference 2) as a formative mechanism for explaining the observed characteristics of such clast pavements. Hicock (Reference 3) notes that subglacial processes including lodgment, deformation, meltout, and erosion are probably all end-members in a continuum of pavement-forming processes.

Due to the flooding of the lower part of QE-3 before detailed observations could be made, it is not known if there was a distinct clast pavement marking the contact between the brown till and underlying gray till exposed in the QE-3 excavation. The presence of cobbles and boulders in the lower part of the trench was noted in preliminary observations (Table 2).

The overall color and appearance of the brown till was similar in all excavations, but there was some variability in apparent sand content within the till unit both vertically and laterally within exposures within a given excavation and between the exposures in the three excavations. The upper part of the brown till is noticeably sandier and exhibits a blocky structure relative to the lower part of the unit in QE-3 (Figure 28). A similar blocky structure was observed in the brown till unit in QE-1 (near GPS points 262 and 263 Figure 23) and in QE-2 (below GPS point 284 Figure 25).

The underlying gray till, which has a very similar appearance in both QE-2 and QE-3, generally has fewer gravel clasts than the overlying brown till. The lower till in the QE-1 exposure, however, locally includes more rubble and larger blocks of the underlying Bass Islands Group bedrock. The more abundant, larger blocks appear to be localized in the vicinity of the paleokarst feature in the quarry wall at Locality 1 and are likely due to the plucking of more easily eroded bedrock in these zones by the overriding glacier. Larger blocks of bedrock would tend to be deposited close to their source.

The contact between till and bedrock was exposed along the western end of QE-1 and throughout most of QE-2. In QE-1 the gray till is not observed in the western end of the excavation, and the brown till with possible glaciofluvial sediments in the basal part of the unit sits directly on bedrock. In QE-2 the gray till directly overlies the bedrock, and throughout most of the exposure the top of bedrock is a smooth, planar surface. At the western end of QE-2, the contact between the gray till and bedrock was not clearly exposed. Larger blocks of bedrock appeared to be present in the lower part of the till just above the till-bedrock contact. It is uncertain whether these larger blocks are part of basal gray till or a glaciofluvial channel fill unit. In either case, the larger blocks at Locality 2 may derive from the more easily eroded paleokarst zone exposed in the top of bedrock in the underlying quarry wall at Locality 2 and, like the coarser blocks in QE-1 at the base of the gray till, the blocks may be due to differential erosion or plucking by the glacier. Larger blocks of bedrock would tend to be deposited close to their source.

Possible Glaciofluvial Sediments

Evidence for subglacial channels and associated glaciofluvial sediments were observed locally at the contact between the brown till and gray till (or bedrock) in QE-1. The postulated glaciofluvial sediments are poorly sorted mixtures containing subrounded cobbles and small boulders in a sandy clay loam matrix. The channel morphology in each case is not well expressed but is defined primarily by the concentrations of cobble clasts. The glaciofluvial deposits, which are compacted, likely were deposited in subglacial meltwater channels.

Sand Units

Except for a thin unit of laminated, thinly bedded sand observed at the base of the sand unit exposed in QE-1 (Figure 29, Soil Unit 2C Table 2), the sand unit overlying till in most of the exposures was massive, moderately well-sorted medium-to-fine grained sand. The thicker sand units were observed in QE-1 and QE-2, which are associated with topographically higher areas. It is not known whether these represent submerged sandbars or beach ridges formed near a late glacial lake strandline.

A younger, possible channel fill unit was observed at the east-southeast end of the QE-2 exposure to the left of GPS point 277 in Figure 25 Sheet 1. The channel fill from bottom to top includes a basal, poorly sorted sandy clay loam, and gray to grayish brown lens of loamy sand with possible detrital charcoal or manganese-oxide staining, and an upper, very pale brown to dark gray loamy sand. This channel fill unit appears to truncate the massive sand unit that can be traced along most of QE-2, suggesting that the upper channel fill unit postdates the deposition of the main sand ridge unit.

The thin mantle of loamy, fine-to-medium grained sand observed overlying the till in the QE-3 excavation is interpreted to be a thin deposit of lacustrine sediments laid down as the lake receded across the area. A description of the soil formed in these deposits (SP-3) and underlying till (SP-2) is given in Tables 2 and 3). The unit maintains a relatively uniform thickness of between 0.3 and 0.5 m (1 and 1.5 ft) throughout most of the QE-3 excavation, except for a zone in the middle of the trench (approximately 100 ft) from the southern end where the unit is slightly thicker (0.76 m [2.5 ft]) (Figures 26 and 27, GPS points 24 to 32/110 to 102). Evidence of possible bioturbation (mixing of sediments by burrowing animals or possible disruption by a former tree throw [a depression formed when a tree falls exposing its roots and surrounding soil]) includes large clasts of underlying till material in the thickened zone of sediment. Krotovina (filled burrows) and smaller clasts of brown till-like material were observed elsewhere in the unit. Subvertical zones of manganese staining observed in the lacustrine and underlying till units are associated with roots or former root canals. There are no anomalies or disruptions in the underlying till to suggest that the thickening of the lacustrine unit is due to tectonic deformation (Figure 30).

Ages of Quaternary Deposits

The exact ages of the till units observed at Denniston Quarry are unknown. Both till units are assumed to be Woodfordian in age (Marine Isotope Stage [MIS] 2 see Reference 1 (Section 2.5.1.1.2.3.4)), based on the location and geomorphic position of the till units relative to late Wisconsinan end and ground moraines (Reference 1 (Figure 2.5.1-205)), the presence of calcareous material in the unweathered parent material of both units, and the lack of buried soils between the two units to indicate significant periods of subaerial exposure. It is uncertain whether the two units are significantly different in age or whether the brown color of the upper till unit is primarily due to oxidation of the upper part of a till related to a single glacial advance, as has been noted in Ohio till units (Reference 5). The available data do not permit a conclusive correlation of the till units to substages within the Woodfordian. The clayey texture of the lower gray till unit suggests that it may have formed as the glacier advanced across lacustrine sediments (possibly sediments deposited in Lake Everett formed during the Erie Interstadial between about 16 and 15.5 ka) (Reference 4). The clay-rich character of the till, however, is similar to that of the Hiram Till, a local till mapped throughout northeastern Ohio, which was deposited prior to 14,050 years ago, probably 17,000 years ago (Reference 5). Slightly older tills recognized locally in northeastern Ohio, such as the Lavery Till, which is assumed to be about 19,000 years old, also have a similar color and texture. The differing texture and color of the two till units exposed in the Denniston Quarry excavations, as well as the clast pavement between the two till units, suggests a change in the provenance of the overriding ice sheet lobe or a change in the subglacial dynamics, but does not provide proof of an interval of deglaciation.

The overlying sand deposits are interpreted to have been deposited as the lake receded in earliest postglacial time from the Lundy Lake level after about 12,400 years BP to no later than 12,000 years BP.

ORIGIN AND TIMING OF DEFORMATION

Disturbed zones and deformation features observed in the Bass Islands Group bedrock exposed in Denniston Quarry include nontectonic paleokarst collapse features, tectonic joints, minor folds, and small displacement tectonic faults. Till of probable late Wisconsinan age and overlying sand deposits that cross the projected trends of minor faults and paleokarst features observed in the Bass Islands Group at the Denniston Quarry are not deformed. Key observations related to the timing and origins of deformation features observed in Denniston Quarry are as follows:

- Paleokarst features formed subsequent to the deposition of the Silurian Bass Islands Group sediments. Paleokarst deposits are cemented and there are no voids indicative of active

karst formation. The paleokarst features likely are related to Silurian/Devonian karst development.

- Southeast-striking joints crosscut the paleokarst feature and, therefore, record a younger set of joints that postdate the joints that controlled Silurian/Devonian karst development. The two prominent joint sets observed in Denniston Quarry are consistent with the two major joint set trends observed in the Fermi 2 excavation (N21°W to N38°W dipping 60 to 80 degrees southwest and N54°E to N72°E dipping 30 to 60 degrees northwest).

- The faults observed in the quarry at Locality 3 are interpreted to be tectonic in origin. One of the two faults observed in the scan of the quarry wall at Locality 3 appears to die out within the Silurian Bass Islands Group rocks and cannot be traced to the surface. A second fault at that locality extends to the top of the exposed rock imaged by the LiDAR scan.

- Stratigraphic relationships exposed in the excavations into Quaternary deposits across the projected trend of the zones of disruption and faulting observed at Localities 1, 2, and 3 clearly document the absence of tectonic deformation over the past approximately 12,000 years. The excavations were located to extend beyond the projected locations of the deformation structures, based on the structural orientations measured from conventional mapping and the LiDAR scans. The sand/till and till/top of bedrock contacts exposed in the QE-2 and QE-3 excavations are sharp, clear contacts that demonstrate the absence of deformation with a high degree of resolution. The sand/till contact exposed in the QE-3 trench is subhorizontal across the trench except in local areas where the deposit thickens slightly. There is no indication of tectonic deformation within the lacustrine sand or underlying till to indicate that the thickening is tectonic.

- Coarser clasts within the basal till unit in QE-1 and the western end of QE-2 may be due to differential erosion and plucking of material from the paleokarst features observed at Localities 1 and 2, respectively. However, there is no evidence of ongoing karst development or deformation of the upper till or sand/till contacts anywhere in the QE-1 or QE-2 exposures.

- No anomalous zones of increased weathering or fracturing of the till units were observed in any of the QE excavations. It would be expected that if the till units had been displaced by a recent faulting event, there would be localization of groundwater flow along the fault or fracture zone that might lead to increased weathering.

REFERENCES

1. DTE Energy, "Fermi 3 Final Safety Analysis Report," Revision 1, March 2008.

2. Clark, P.U., "Striated Clast Pavements: Products of Deforming Subglacial Sediment?", *Geology*, Vol. 19, pp. 530-533, 1991.

3. Hicock, S.R., "On Subglacial Stone Pavements in Till," *The Journal of Geology,* Vol. 99, No. 4, pp. 607-619, 1991.

4. Lewis, C.F., T.C. Moore, D.K. Rea, D.L. Dettman, A.M. Smith, and L.A. Mayer, "Lakes of the Huron Basin: Their Record of Runoff from the Laurentide Ice Sheet," *Quaternary Science Reviews*, Vol. 13, pp. 891-992, 1995.

5. White, G.W., "Glacial Geology of Northeastern Ohio," Ohio Geological Survey, Bulletin 68, 1982.

Table 1: Soil Profile SP-1 Description

Denniston Quarry in Quaternary Excavation QE-1 at Locality 1 Vertical exposure cut into sand ridge on the side of access road near west-southwest end of QE-1 . (Location indicated on Figure 22. Figure 29 provides a photo of location SP-1)		
Soil Horizon	**Depth (cm)**	**Description**
Disturbed	+55 from top of B1 horizon	Quarry FILL, possible Ap (plow layer) in lower 15 cm.
B11	0 to 31 cm	MASSIVE SAND UNIT- Brownish yellow (10 YR 6/6, dry) (Mussell Color Chart designation), dark yellowish brown (10YR 4/6, moist); faint brown (10YR 5/3, dry) mottles are most prominent in lower 10 cm of horizon; fine to medium grained SAND; single grain, soft; very friable; nonplastic, nonsticky, dark gray mottles along roots up to 1 cm diameter; largest roots are densest at base of B1 and into B2t; clear smooth lower boundary
B2t	31 to 55 cm	MASSIVE SAND UNIT- Yellowish brown (10YR 5/6, dry to slightly damp), dark yellowish brown (10YR 4/6, moist) SANDY LOAM; slightly plastic, nonsticky to slightly sticky; very friable; soft; slightly grayer in lower 7 cm with more manganese oxide staining around roots; clear, smooth lower boundary.
B3	55 to 70 cm	MASSIVE SAND UNIT- Yellowish brown (10YR 5/7, dry), dark yellowish brown (10YR 4/4, moist); mottles on ped (discrete soil element formed by fracturing) faces (7.5 YR 4.5/6, dry) and yellowish red (5YR 4/6, dry) SANDY LOAM to LOAMY SAND; massive; nonsticky, slightly plastic; loose to very friable; clear to gradual smooth lower boundary.
C11	70 to 98 cm	MASSIVE SAND UNIT- Light yellowish brown to yellowish brown (10 YR 5.5/4, damp); strong brown (7.5YR 4/6, moist) mottles (5 to 15 percent); well sorted, fine grained SAND, angular to subrounded grains; nonsticky, nonplastic; clear to gradual, smooth lower boundary marked by more abundant mottles, iron concretions (cementation); few small roots.
C12	98 to 120 cm	MASSIVE SAND UNIT- Mottled yellowish brown (10 YR 5/6, damp), light yellowish brown to yellowish brown (10YR 5.5/4, damp), and yellowish red (5YR 4/6, damp) fine grained SAND, moderately well sorted, (approximately 10 percent heavy minerals), subangular to subrounded grains.
C13	120 to 130 cm	MASSIVE SAND UNIT- Similar to above, less yellowish red mottles; manganese oxide staining on small mottles; manganese oxide staining on small roots (less than 2 to 3 mm in diameter); subangular to subrounded grains.
C14	130 to 137 cm	MASSIVE SAND UNIT- Yellowish brown (10YR 5/6, damp and moist) SANDY LOAM; slightly sticky, slightly plastic; very friable.

Table 1: Soil Profile SP-1 Description (Continued)

Soil Horizon	Depth (cm)	Description
2C	137 to 150 cm	BEDDED SAND UNIT- Light yellowish brown (10YR 6/4, dry), dark yellowish brown (10YR 4/4, moist); well bedded, fine to medium grained, poorly sorted SAND; subangular to subrounded grains; alternating light to dark beds (approximately 2 mm to 3 mm thick); some manganese staining along fine roots; abrupt, smooth lower boundary.
3C	150 cm	TILL (sandy loam); pale brown (10YR 6/3, dry), (10YR 4/3, moist) with faint light yellowish brown (10YR 6/4, dry) (10YR 4/4, moist) mottles; massive; effervesces; less than 10 cm thickness exposed, lower boundary not exposed.

Table 2: Soil Profile SP-2 Description

Denniston Quarry, Quaternary Excavation QE-3 at Locality 3 Profile described along ramp at eastern end of QE-3 (Figure 21 provides a photo of location SP-2)		
Soil Horizon	**Depth (cm)**	**Description**
Road fill	0 -13 cm	
A/B	13-18 cm	LACUSTRINE SAND- Dark grayish brown (10YR 4/2, dry), very dark grayish brown (10YR 3/2, moist) LOAMY SAND, slightly sticky, plastic, sorted fine-to medium sand, clay bridges, weak, subangular blocky structure, few fine roots, noneffervescent; abrupt, wavy lower boundary (clear to irregular where bioturbated).
2B21tg	18 to 25 cm	BROWN TILL-Pale brown (10YR 6/3, dry), dark yellowish brown (10YR 4/4, moist), faint mottles of dark brown (7.5YR 4/2, moist), yellowish brown (10YR 5/6, moist), pinkish gray (7.5YR 6/2, dry), and reddish yellow (7.5 YR 6/2, dry), prominent dark grayish brown mottles along decayed roots; CLAY LOAM, slightly sticky, plastic, hard, firm; thin clay films on ped faces and clay bridges between grains; medium coarse subangular blocky structure; abrupt, wavy lower boundary.
2B22tg	25 to 39 cm	BROWN TILL-Pale brown (10YR 6/3, dry), brown (10YR 4/3, moist) CLAY LOAM; faint mottles of brown (7.5YR 5/4,dry) (7.5 YR 4/4, moist) and light yellowish brown (10YR 6/3.5, dry) (10YR 4/5, moist); slightly sticky, plastic; hard; firm; moderately thick clay films on ped faces, clay bridges; clear to gradual wavy boundary,
2B23tg	39-103 cm	BROWN TILL- Light gray (10YR 7/2, dry), grayish brown (10YR 5/2, moist), SANDY CLAY LOAM; poorly sorted, fine to coarse grained sand; 3 to 5 percent gravel , rounded to subangular clasts, gravel content is variable throughout excavation exposures; faint pale brown (10YR 6/3 and 6/4, dry) and a few strong brown (7.5YR 5/8, dry) mottles; subvertical gleyed zone up to 5 mm wide (associated with roots and decayed organic material); massive, clay bridges, effervescence variable from slight to strong.
Ground surface: Flat lacustrine/till plain surface, grasses. Note: Preliminary observations made of till units in the lower part of the trench made on December 8, 2009 prior to overnight rain that caused slope instabilities and flooding in the lower part of the trench (precluding access to the lower part of the trench) were: (1) Sandy, gravelly diamicton (till) overlies brown clay-rich till that transitions into a lower gray till at the base of the trench; (2) the lower gray till (~ 30 cm thick) is hard, and contains scattered cobble to small boulder clasts; and (3) the upper part of the brown till has a moderate medium (to coarse) subangular blocky structure, subhorizontal partings or structure.		

Table 3: Soil Profile SP-3 Description

Denniston Quarry, Quaternary Excavation QE-3 at Locality 3 Profile near eastern end of QE-3 (Figure 21 provides a photo of location SP-3 Located between GPS points 7 and 8)		
Soil Horizon	**Depth (cm)**	**Description**
A11	0-15 cm	LACUSTRINE UNIT: Light brownish gray (10YR 5/2, dry), very dark gray (10YR 3/1, moist) SANDY LOAM; slightly sticky, slightly plastic; very friable; soft; massive; few fine roots; root mat down to approximately 10 cm
A12	15-30 cm	LACUSTRINE UNIT: Light brownish gray (10YR 5/2, dry), very dark gray (10YR 3/1, moist) LOAMY SAND; slightly sticky, plastic; fine subangular blocky structure; friable; plentiful fine roots, clear, wavy lower boundary.
A13 to A/B	30-50 cm	LACUSTRINE UNIT: Dark grayish brown to gray brown (10YR 4.5/2, dry), very dark grayish brown (10YR 3/2, moist) LOAMY SAND; medium to fine grained sand; slightly sticky, slightly plastic; few clay bridges between grains; very friable; noneffervescent; irregular clasts of underlying unit incorporated into this unit (possible bioturbation or rip up clasts in the parent material), contact to sandy brown till is a clear, wavy contact.
Ground surface: Flat lacustrine/till plain surface, grasses.		

Table 4: Quaternary Excavation QE-2 Sample Descriptions

Sample	Description
Sample 1	(Unit above upper brown till) SANDY CLAY LOAM, distinct yellowish brown (10 YR 5/6, moist) mottles; sticky, slightly plastic; firm; coarse subangular blocky structure, thin clay films on ped faces; clay bridges.
Sample 2	Upper brown till Similar to Soil Profile SP-2 (25-39 cm depth), but slightly sandier.
Sample 3	Lower gray till Similar to gray till from QE-3 Trench. Gray (10YR 6/1, dry), dark gray (10YR 4/1, moist) CLAY LOAM, faint (light gray to gray 10YR 6/3, dry, brown to dark brown 10YR 4/3, moist) mottles; sticky, plastic; hard; very firm; 1 to 2 percent small, subrounded to subangular pebbles.
Sample 4	Very pale brown (10YR 7/3.5, dry), yellowish brown (10YR 5/4, moist) LOAMY SAND; fine to medium grained sand; poorly sorted; massive; nonsticky, slightly plastic.
Sample 5	Dark gray (10YR 4/1, dry), very dark gray (10YR 3/1, moist) LOAMY SAND; faint dark grayish brown (10YR 4/2, dry), dark gray (10YR 4/1, moist); nonsticky, nonplastic; massive to weak fine to medium granule structure; very friable, few fine roots.
Sample 6	Organic-rich horizon Gray to grayish brown (10YR 5/1.2, dry) LOAMY SAND, poorly sorted, fine to medium (some coarse) grained sand, subangular to subrounded grains; few distinct fine strong brown (7.5YR 5/6, dry) mottles, faint light yellowish brown (10YR 6/4, dry) mottles; nonsticky, slightly plastic; hard; few thin clay films and clay bridges; fine subangular blocky structure; possible detrital (transported to this location rather than formed insitu) charcoal or alternatively decomposed roots (with manganese staining)

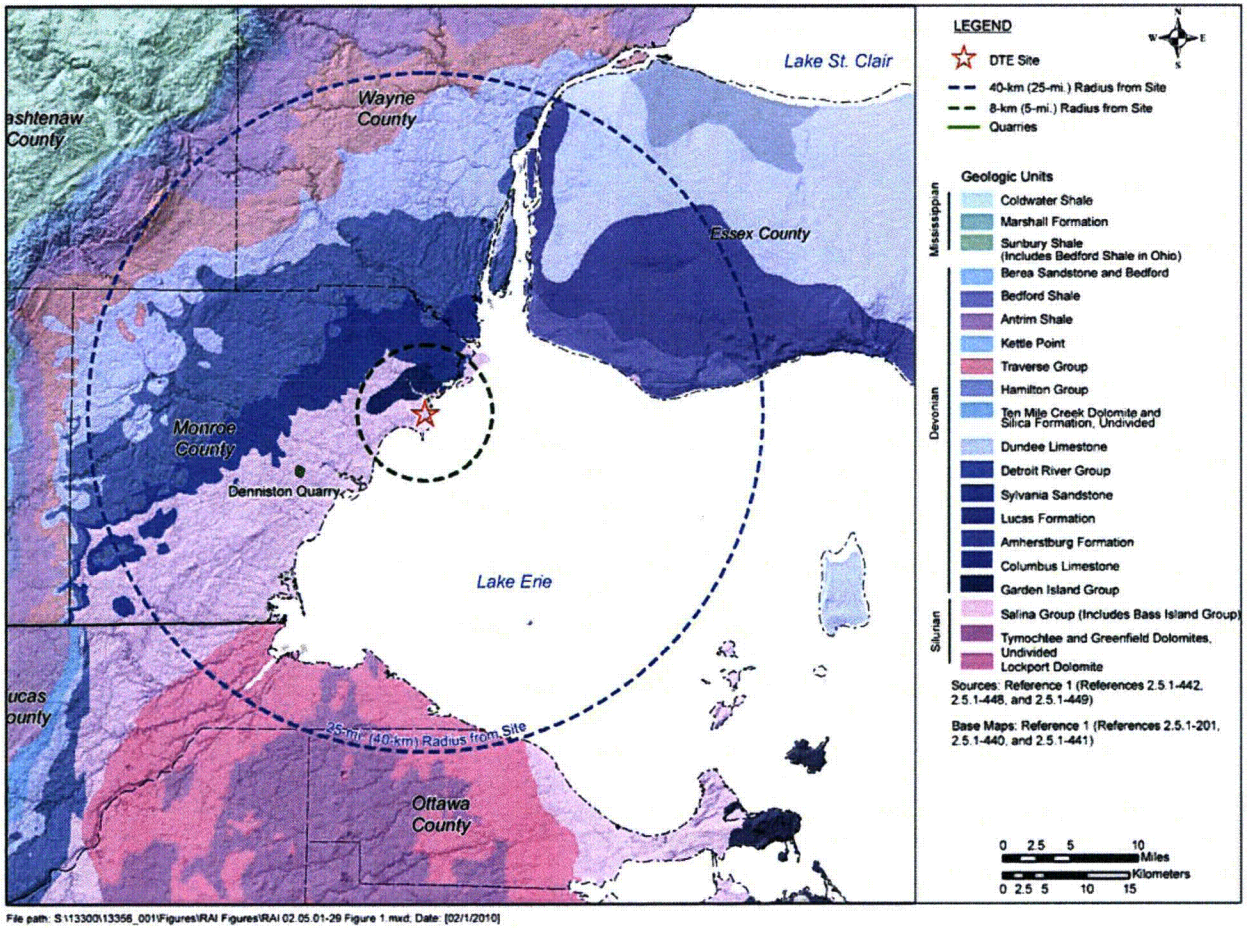

Figure 1. Geologic Map Showing Location of Denniston Quarry

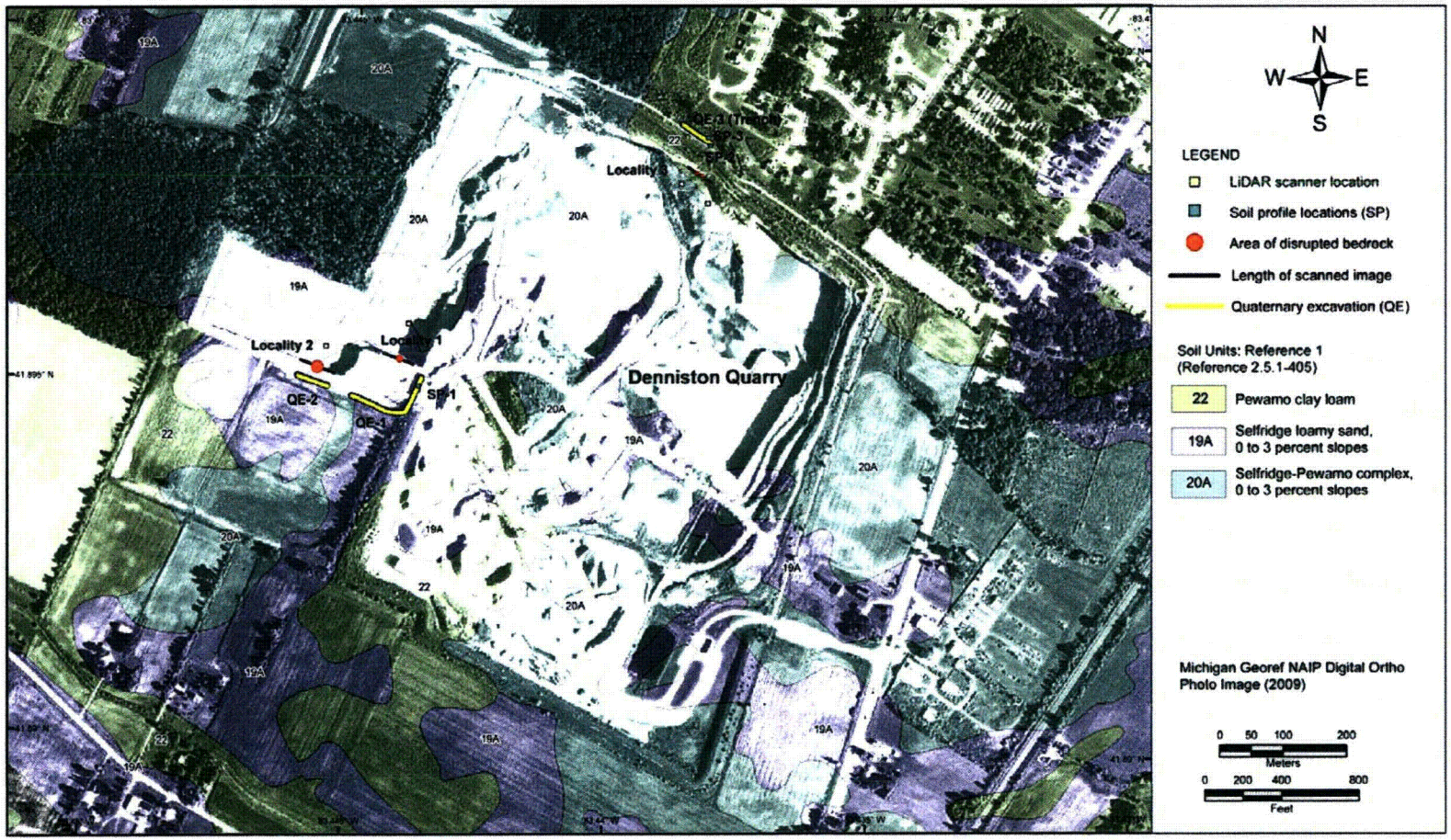

S:\13300\13356_001\Figures\working_figures\RAI 02.05.01-29 Figure 2.mxd

Figure 2. Aerial Photography Showing Mapped Soil Units and Localities Investigated at Denniston Quarry

Figure 3. Photograph Showing Setup of the Leica ScanStation 2 LiDAR Instrument

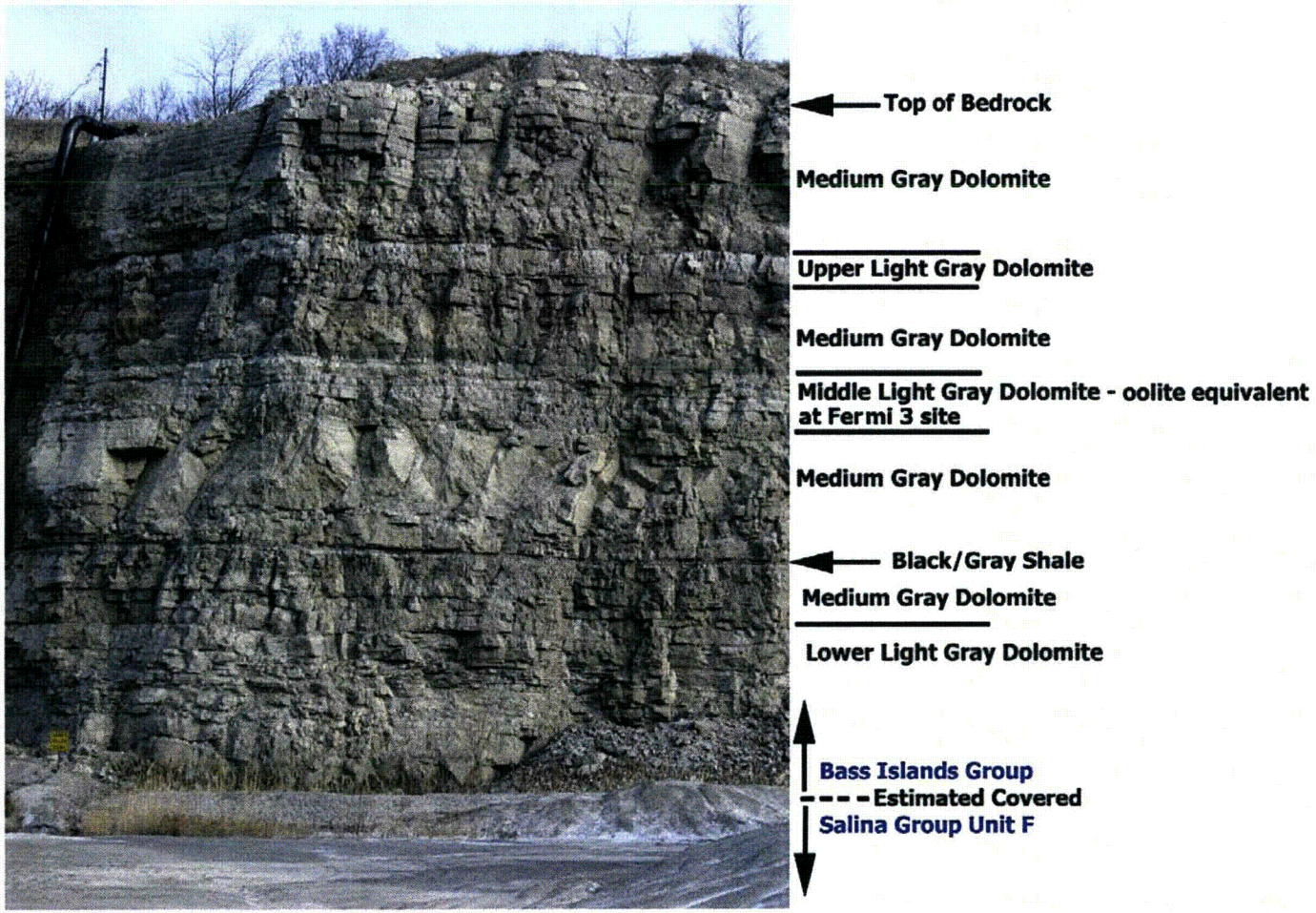

Figure 4. Photograph Showing the Bedrock Stratigraphy at Denniston Quarry

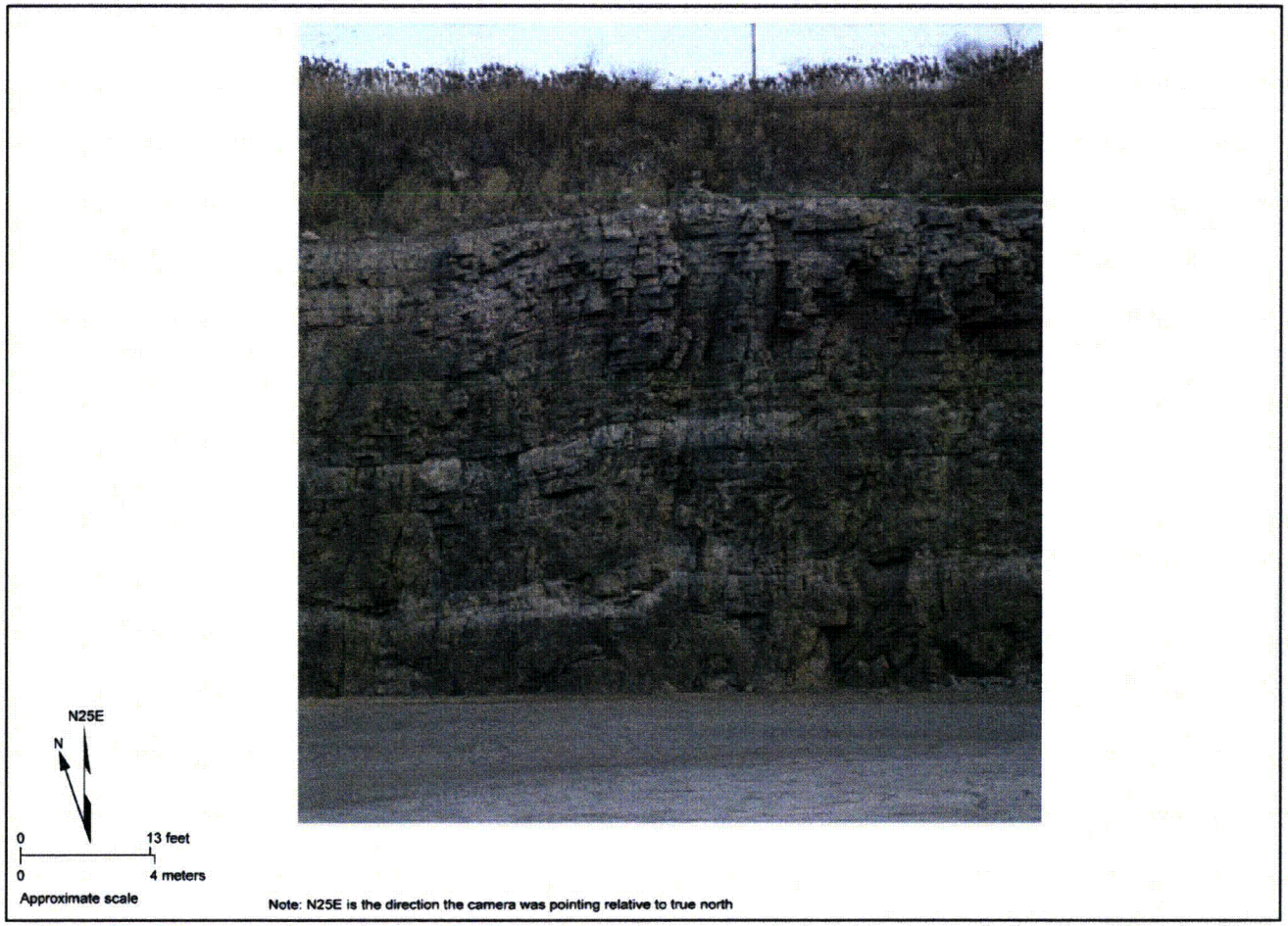

Figure 5. Denniston Quarry Northern Wall Showing Monocline fold in Bass Islands Group Bedrock

Figure 6. Photograph Showing Features Associated with Disrupted Zones Interpreted as Paleokarst

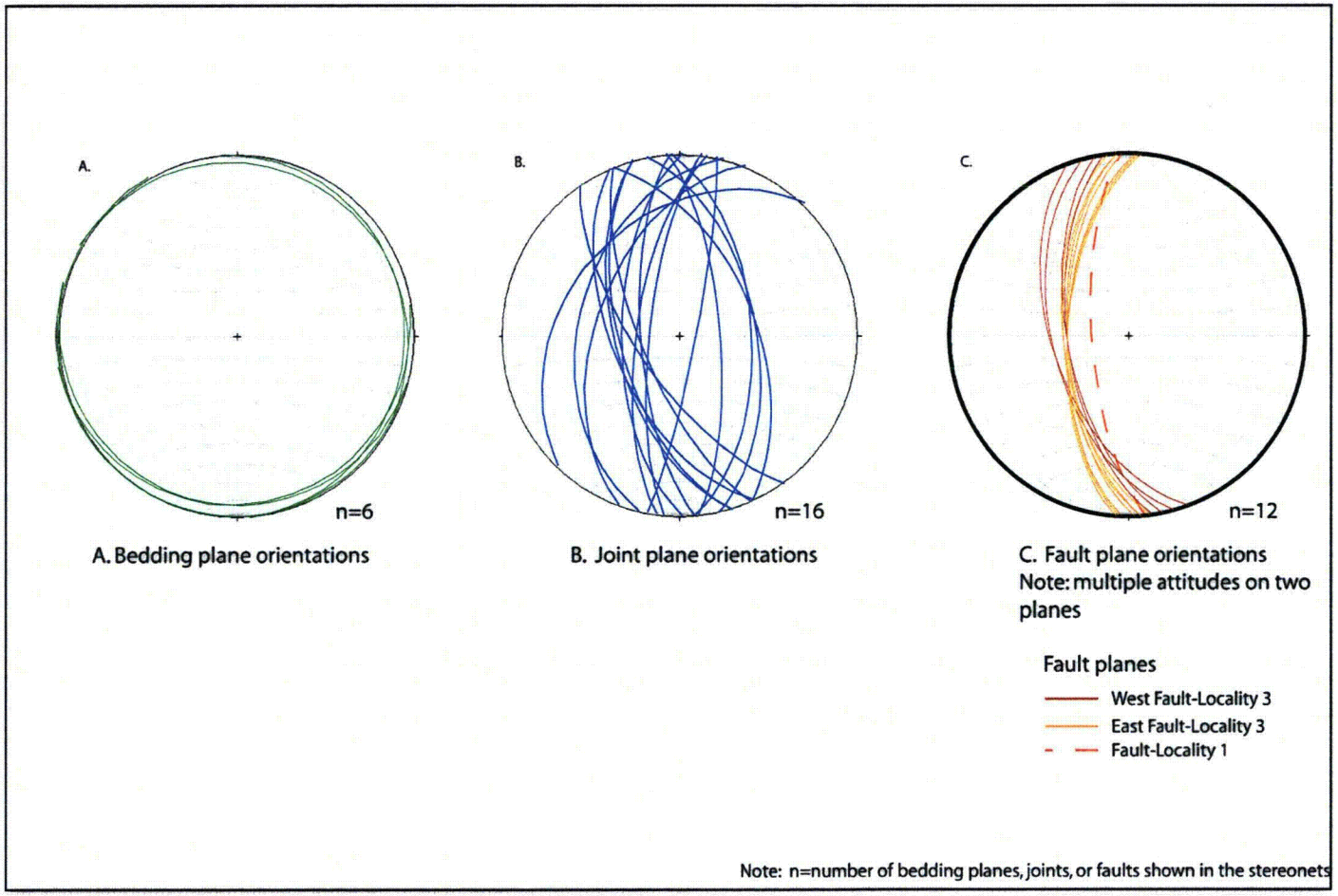

Figure 7. Orientations Estimated Using Ground-based LiDAR Survey (Localities 1, 2, and 3 Combined)

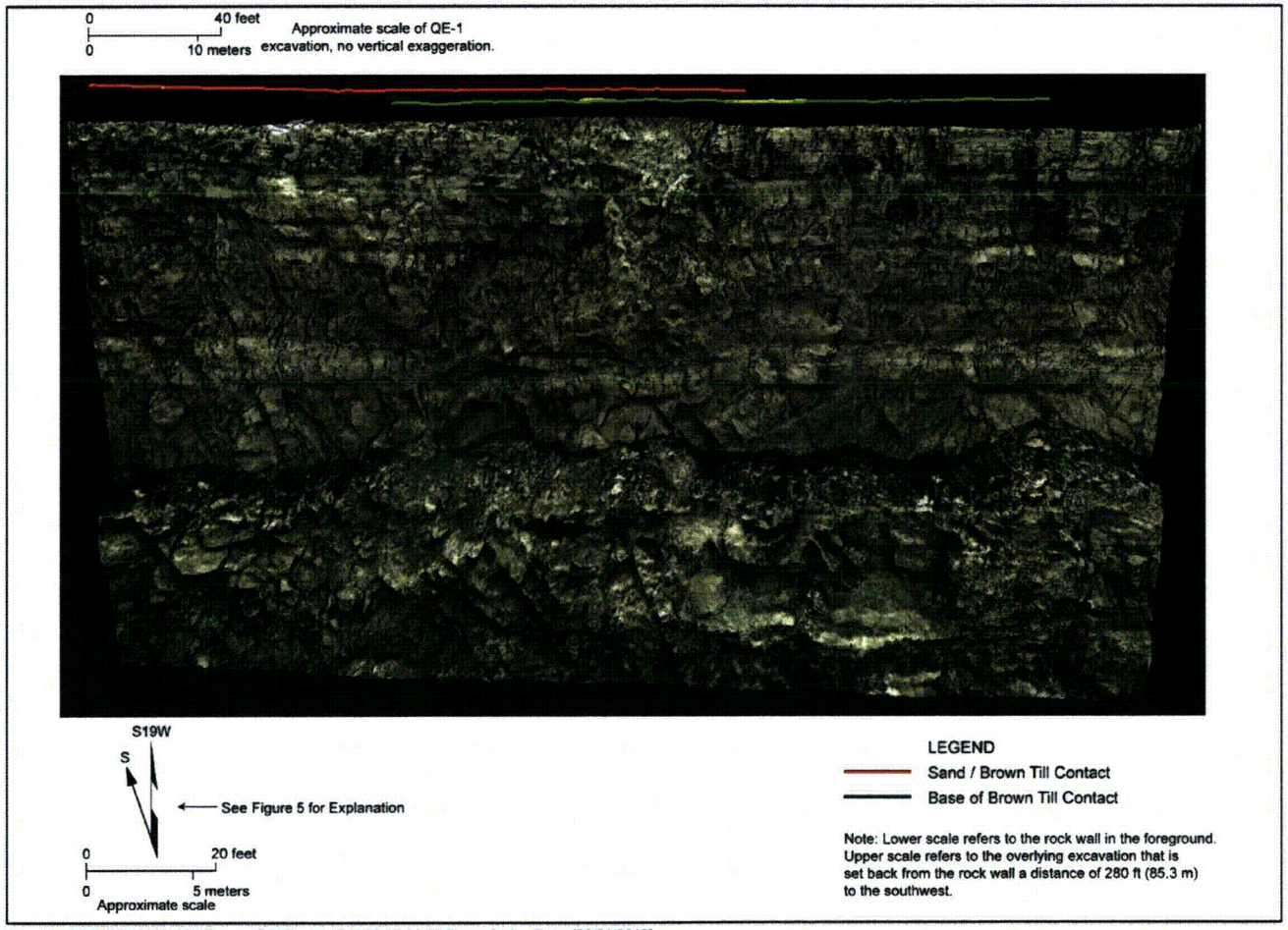

File path: S:\13300\13356_001\Figures\RAI Figures\RAI 02.05.01-29 Figure 8.ai; Date: [02/01/2010]

Figure 8. Denniston Quarry Locality 1 TIN with Draped Bedrock Photograph Relative to Quaternary Stratigraphic Contacts Mapped in Quaternary Excavation QE-1 Shown on Figure 2

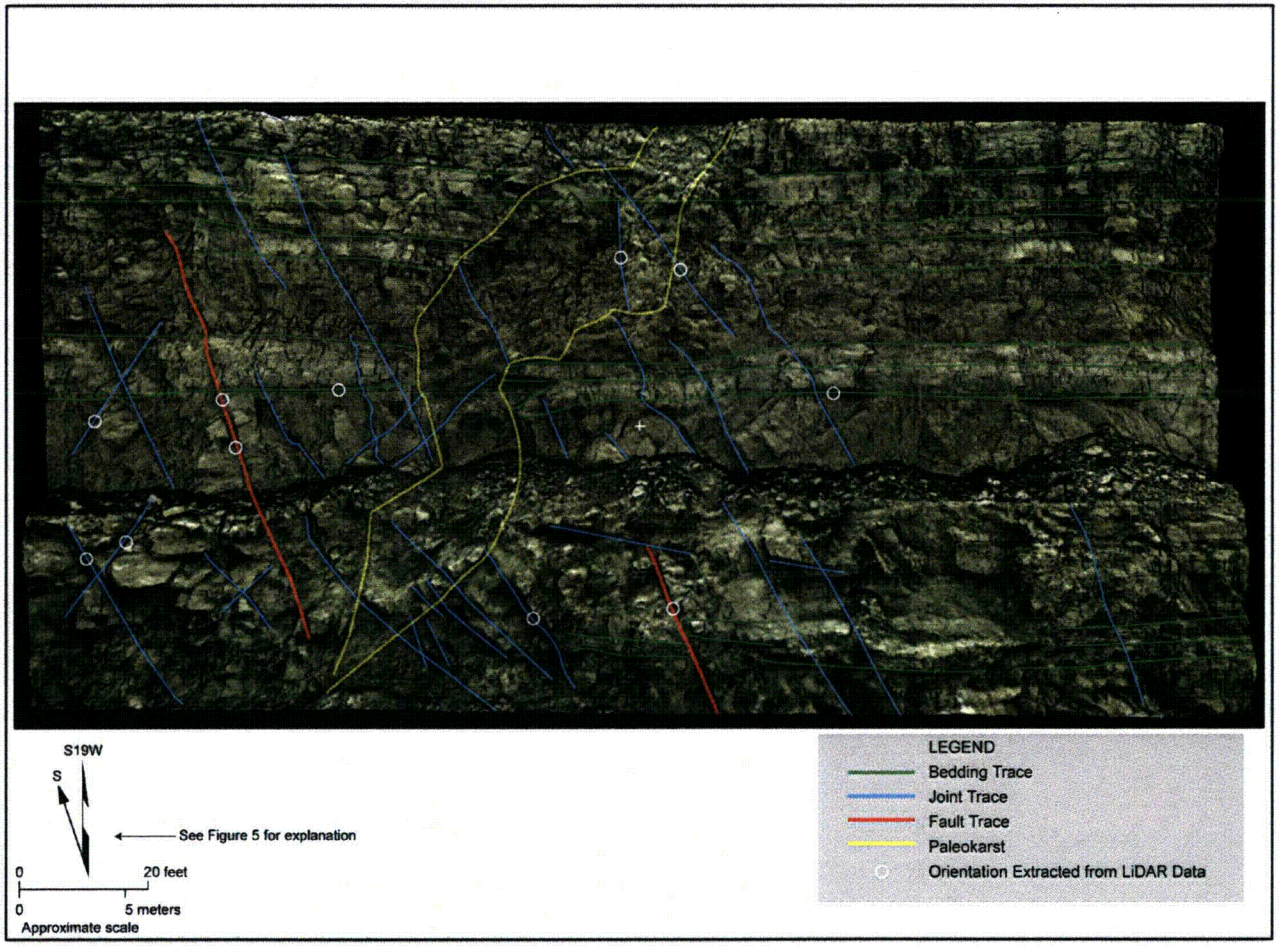

Figure 9. Denniston Quarry Locality 1 Interpreted TIN Constructed from LiDAR Data (Sheet 1 of 2)

Figure 9. Denniston Quarry Locality 1 Interpreted TIN Constructed from LiDAR Data (Sheet 2 of 2)

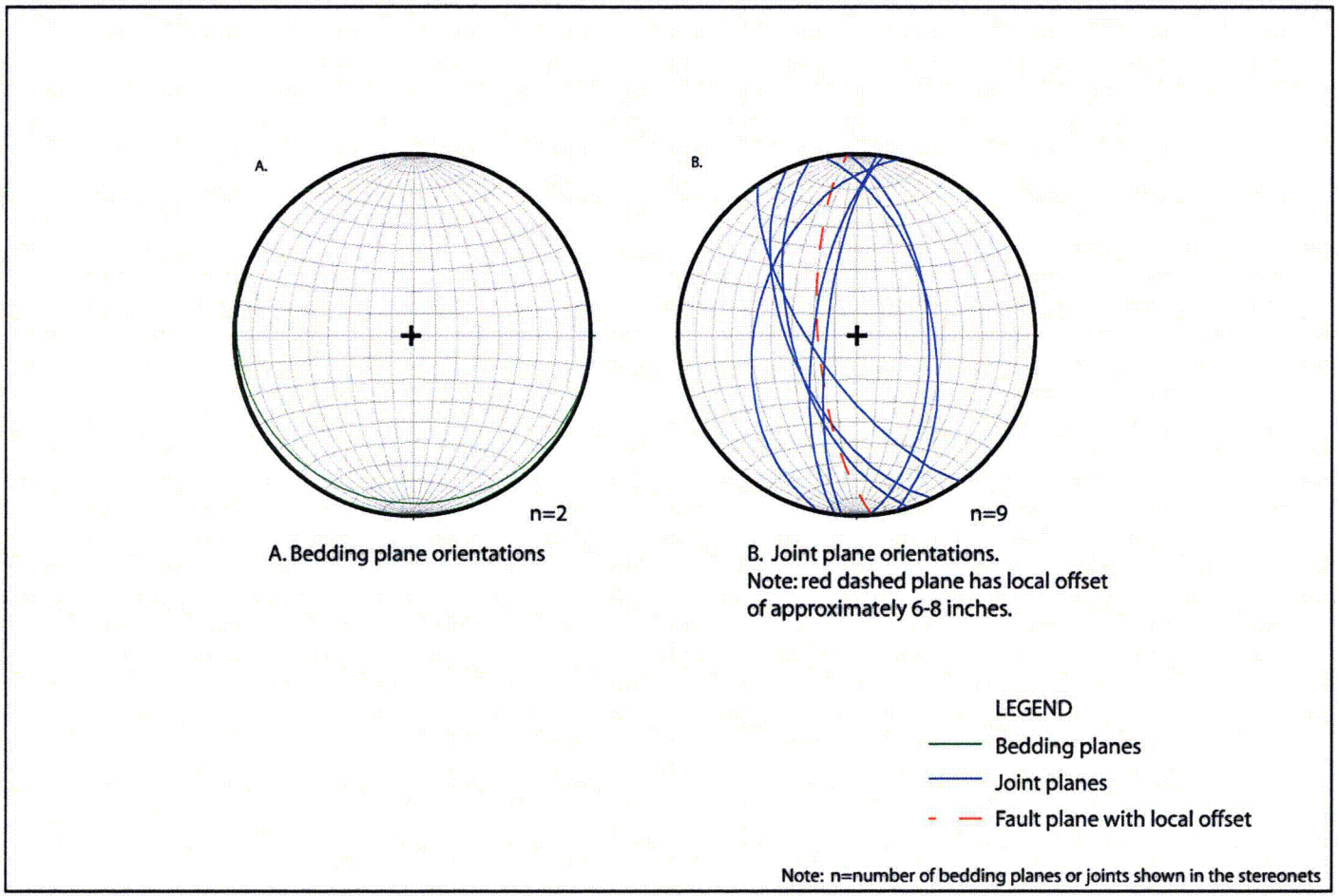

File path: S:\13300\13356_001\Figures\RAI Figures\RAI 02.05.01-29 Figure 9.ai; Date: [02/01/2010]

Figure 10. Orientations Estimated Using Ground-based LiDAR Survey at Locality 1

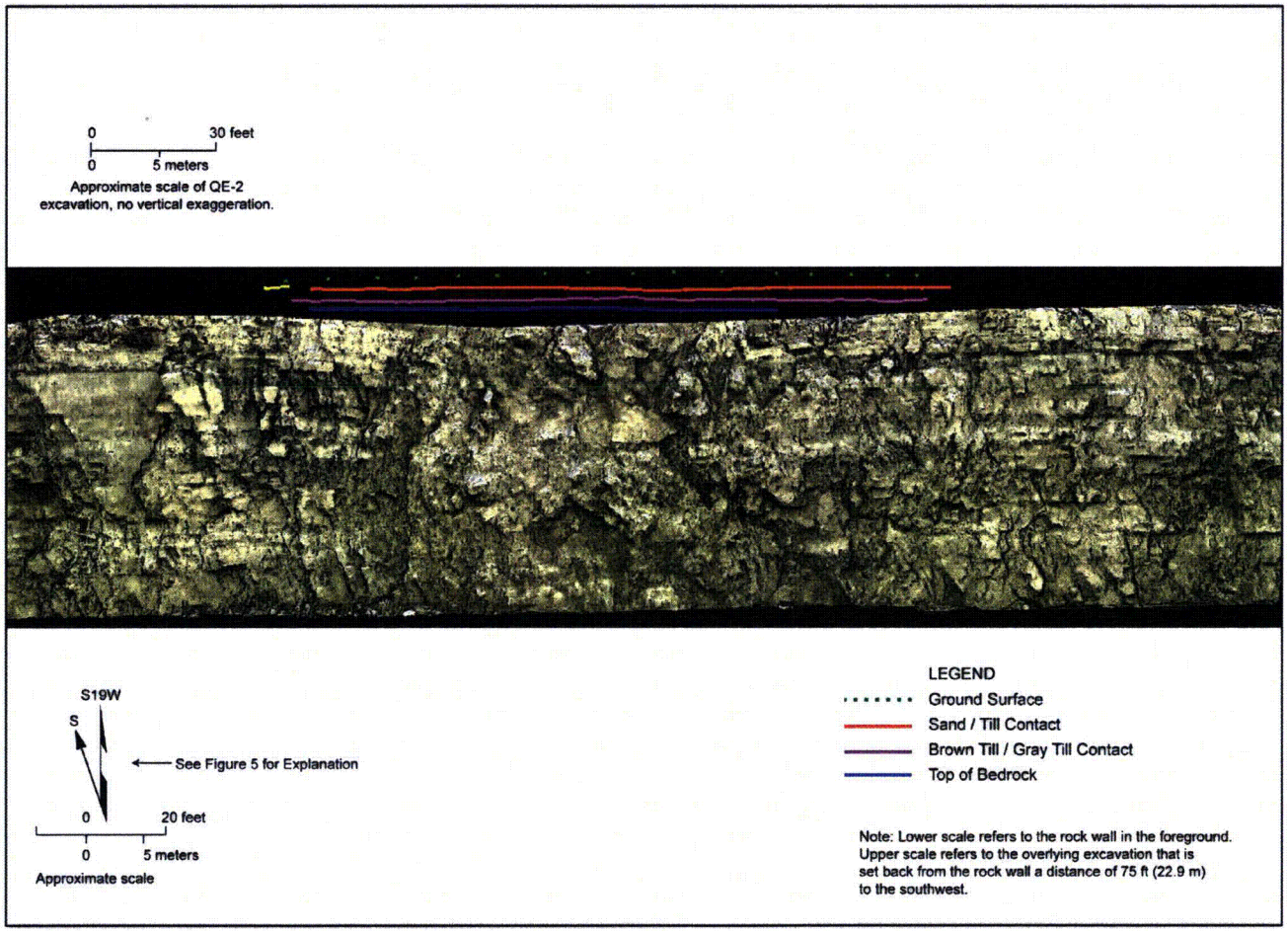

File path: S:\13300\13356_001\Figures\RAI Figures\RAI 02.05.01-29 Figure 11.ai; Date: [02/01/2010]

Figure 11. Denniston Quarry Locality 2 TIN with Draped Bedrock Photograph Relative to Quaternary Stratigraphic Contacts Mapped in Quaternary Excavation QE-2 Shown on Figure 2

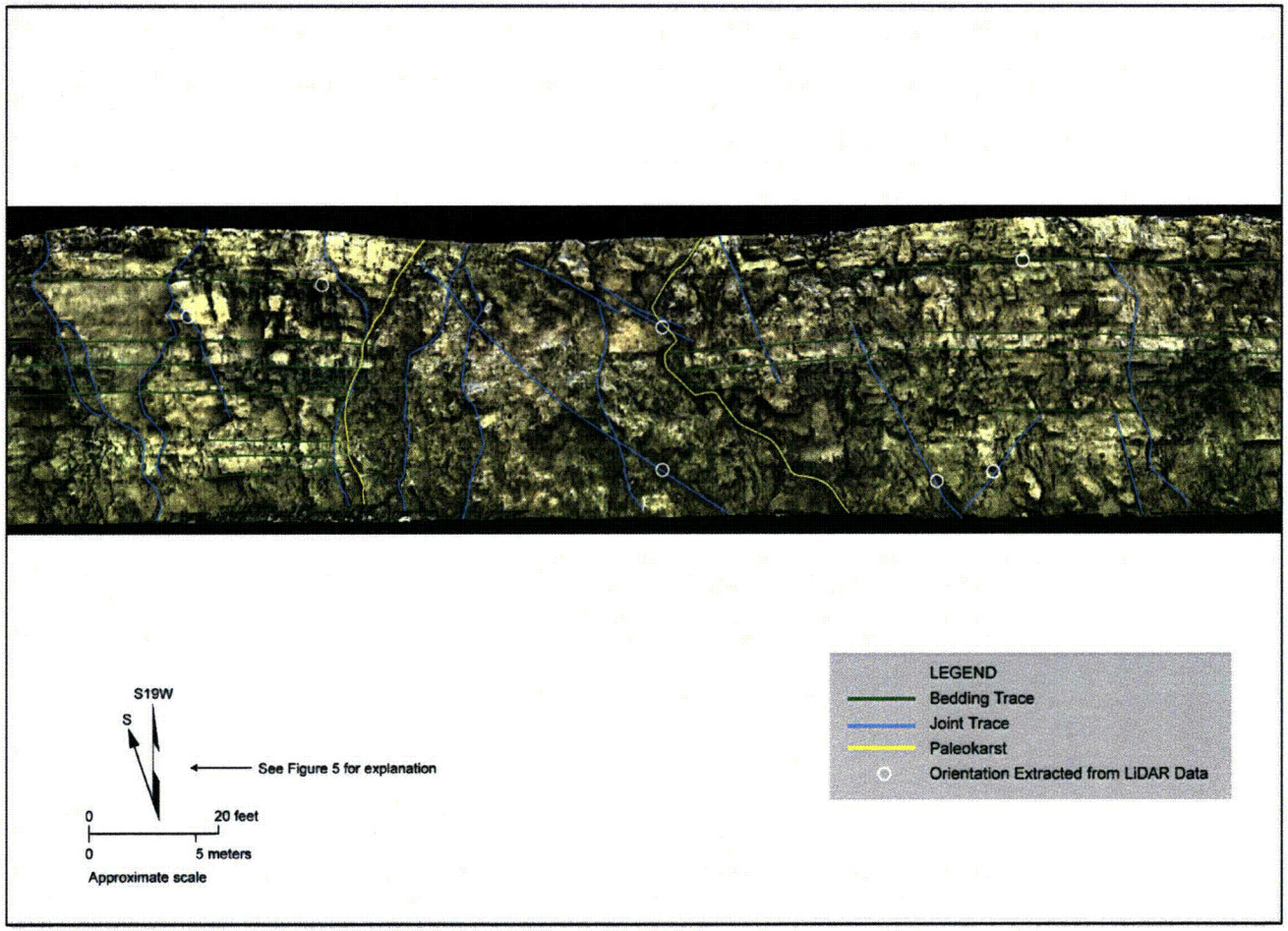

File path: S:\13300\13356_001\Figures\RAI Figures\RAI 02.05.01-29 Figure 12_Sheet 1.ai; Date: [02/01/2010]

Figure 12. Denniston Quarry Locality 2 Interpreted TIN Constructed from LiDAR Data (Sheet 1 of 2)

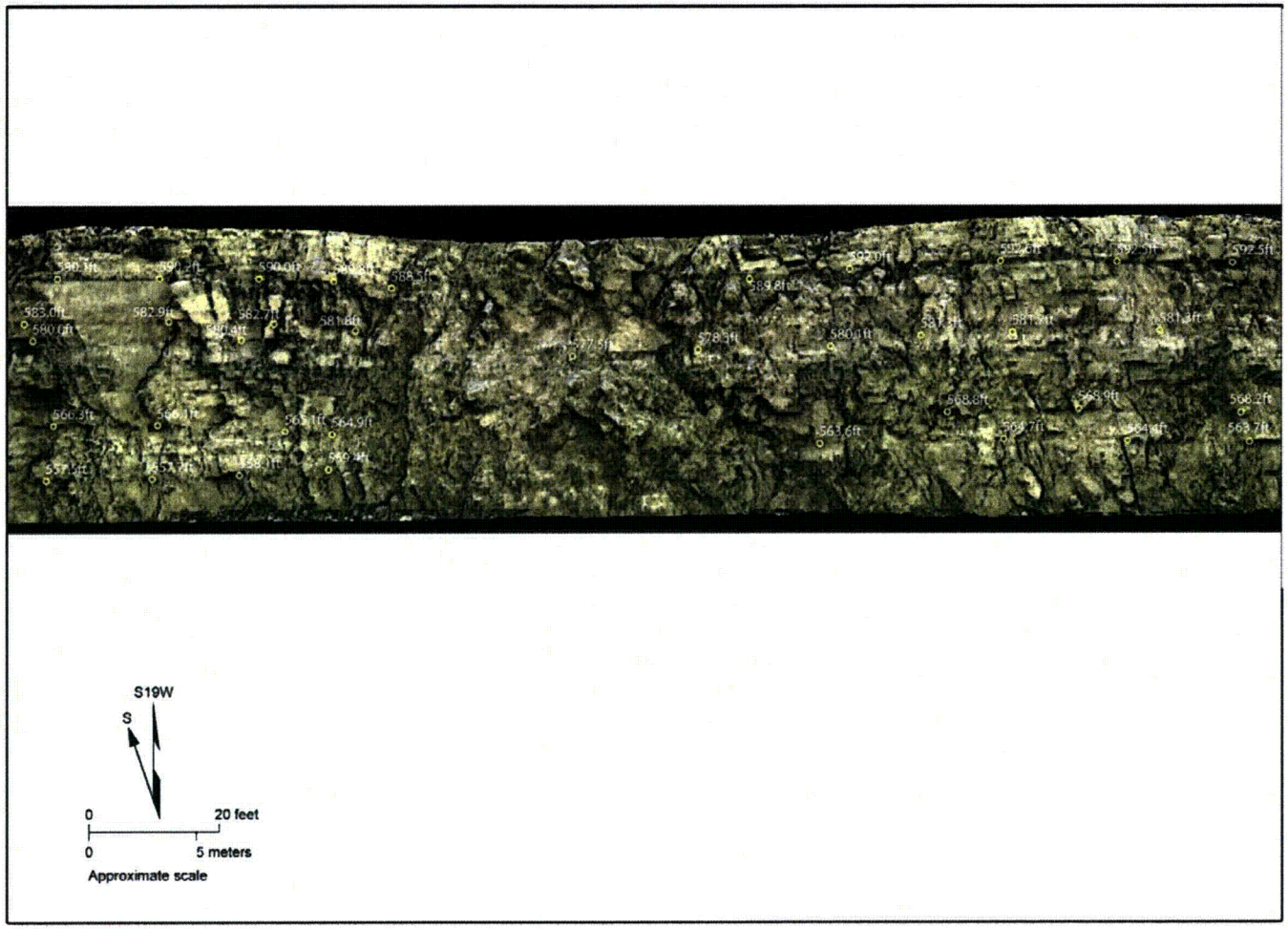

Figure 12. Denniston Quarry Locality 2 Interpreted TIN Constructed from LiDAR Data (Sheet 2 of 2)

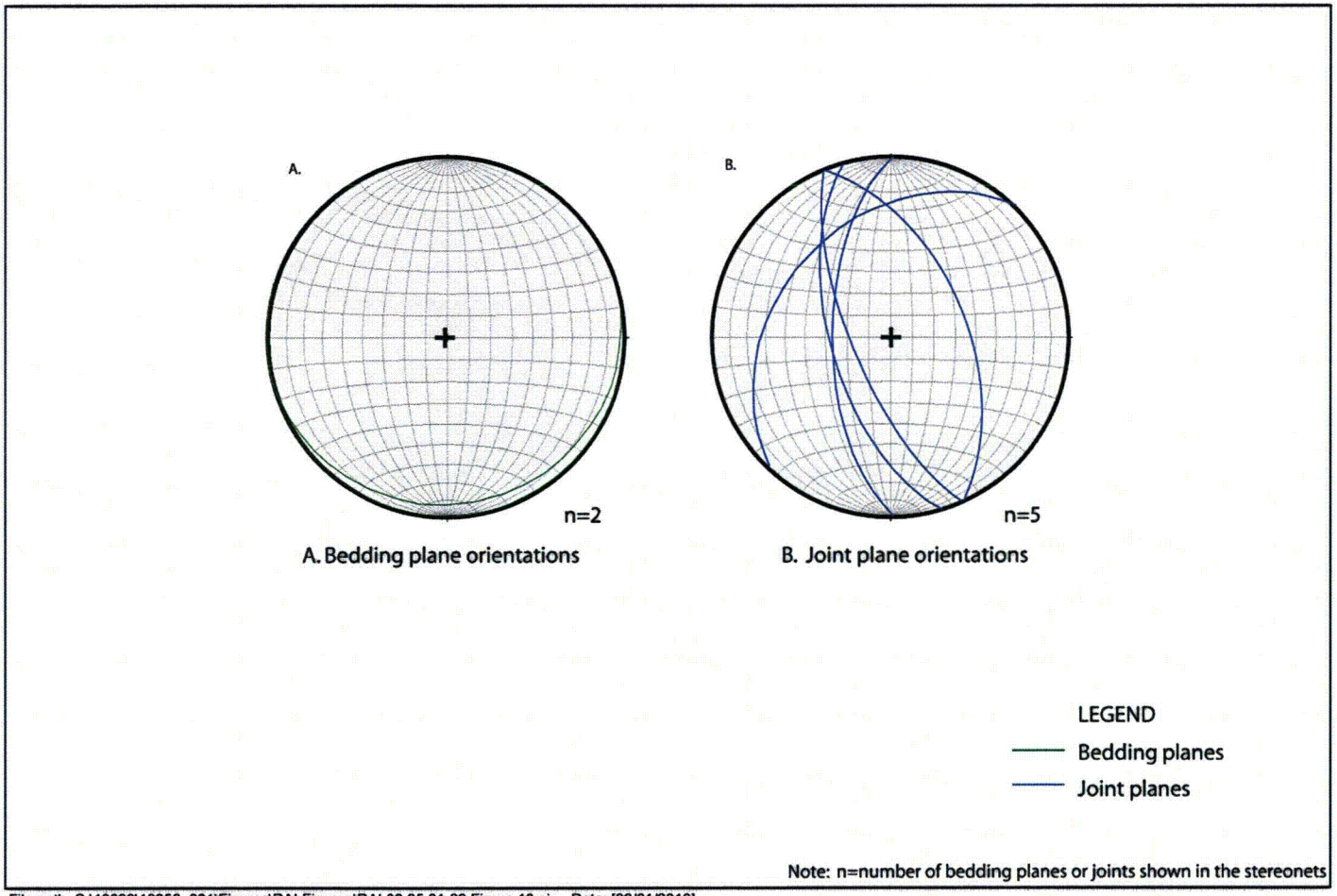

Figure 13. Orientations Estimated Using Ground-based LiDAR Survey at Locality 2

Figure 14. Photograph of Faulted Bedrock Exposed at the Denniston Quarry Locality 3

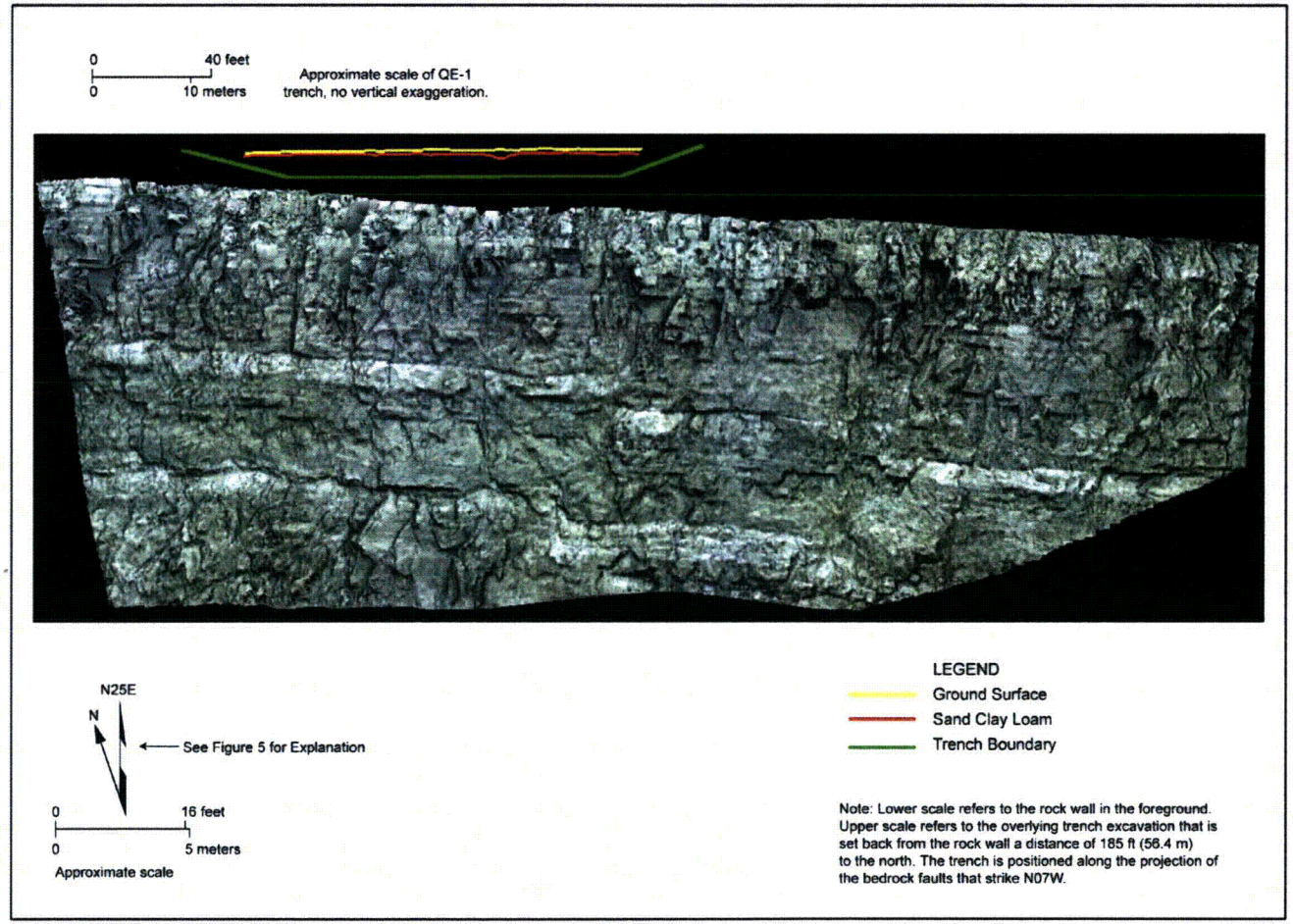

File path: S:\13300\13356_001\Figures\RAI Figures\RAI 02.05.01-29 Figure 15.ai; Date: [02/01/2010]

Figure 15. Denniston Quarry Locality 3 TIN with Draped Bedrock Photograph Relative to Quaternary Stratigraphic Contacts Mapped in Quaternary Excavation QE-3 Shown on Figure 2

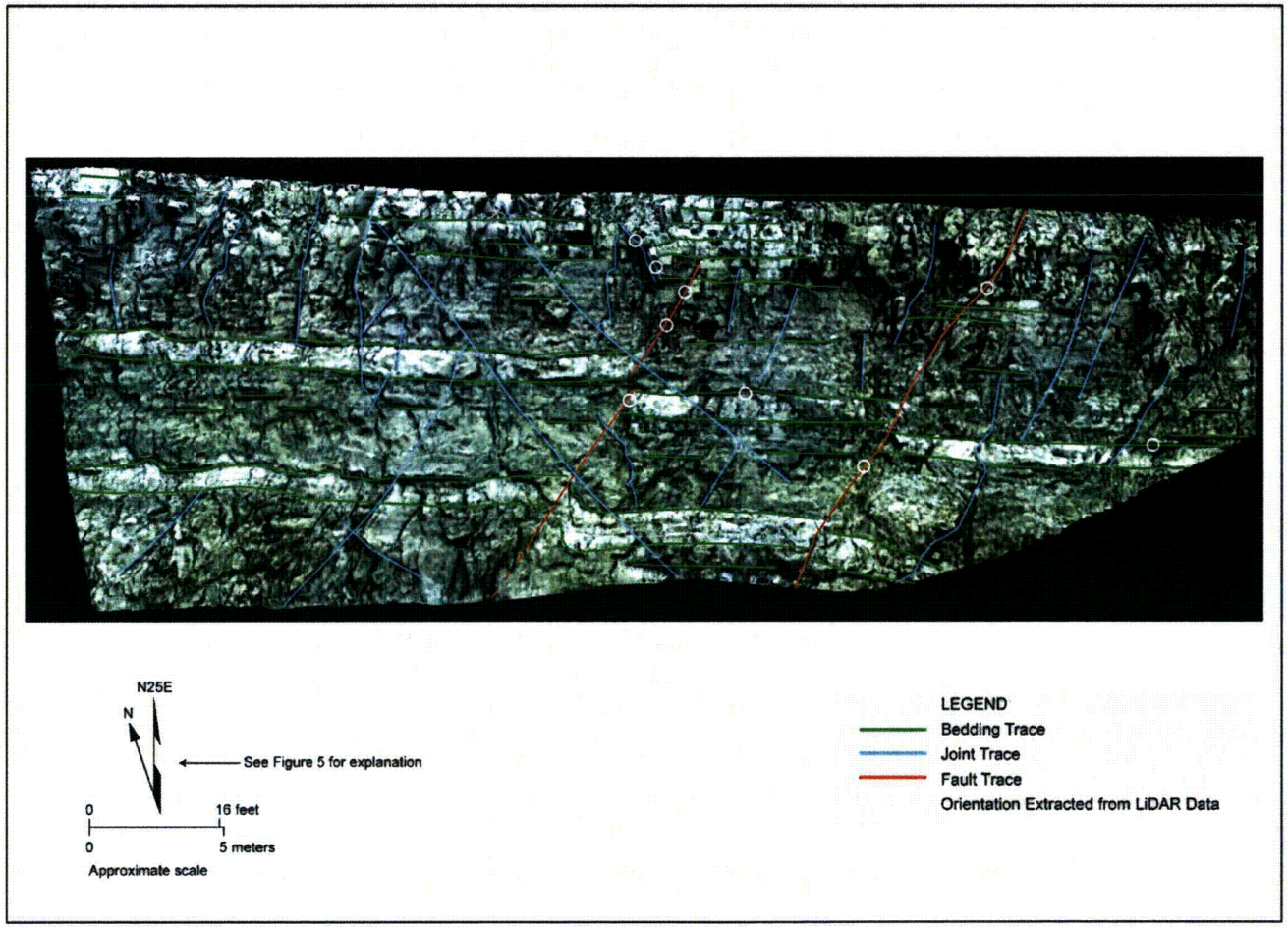

File path: S:\13300\13356_001\Figures\RAI Figures\RAI 02.05.01-29 Figure 17_Sheet 1.ai; Date: [02/01/2010]

Figure 16. Denniston Quarry Locality 3 Interpreted Tin Constructed from LiDAR Data (Sheet 1 of 2)

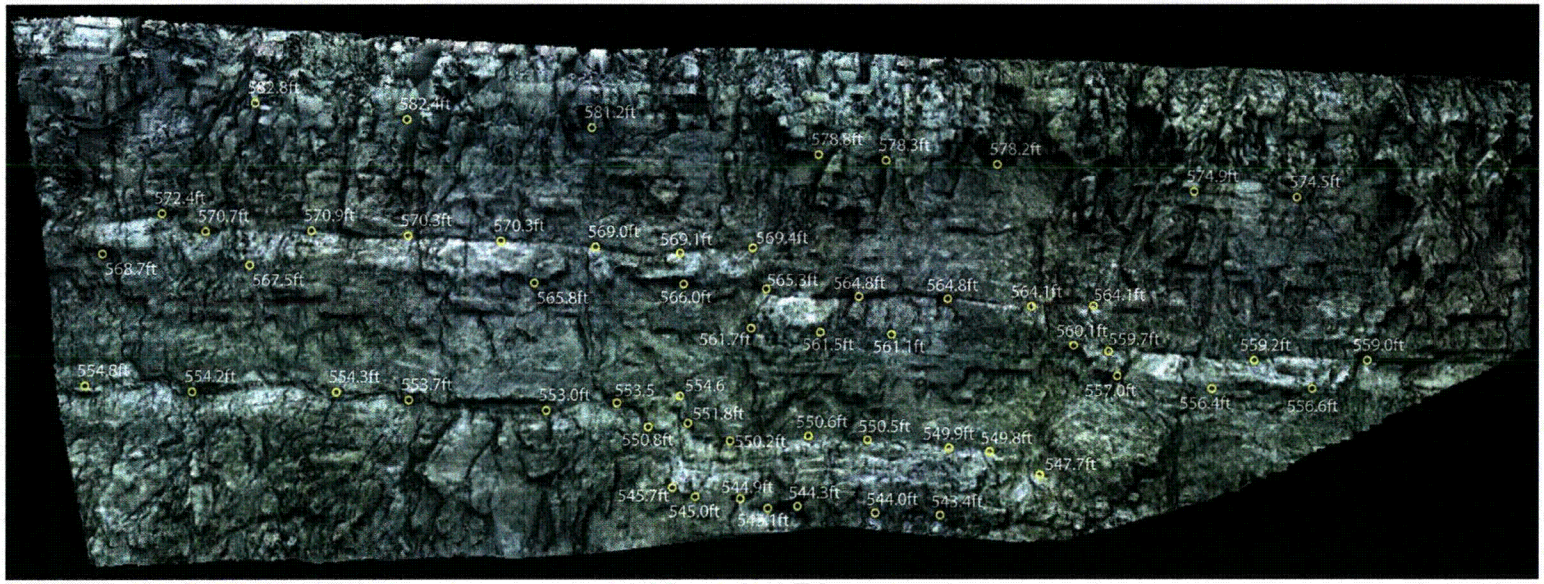

Figure 16. Denniston Quarry Locality 3 Interpreted Tin Constructed from LiDAR Data (Sheet 2 of 2)

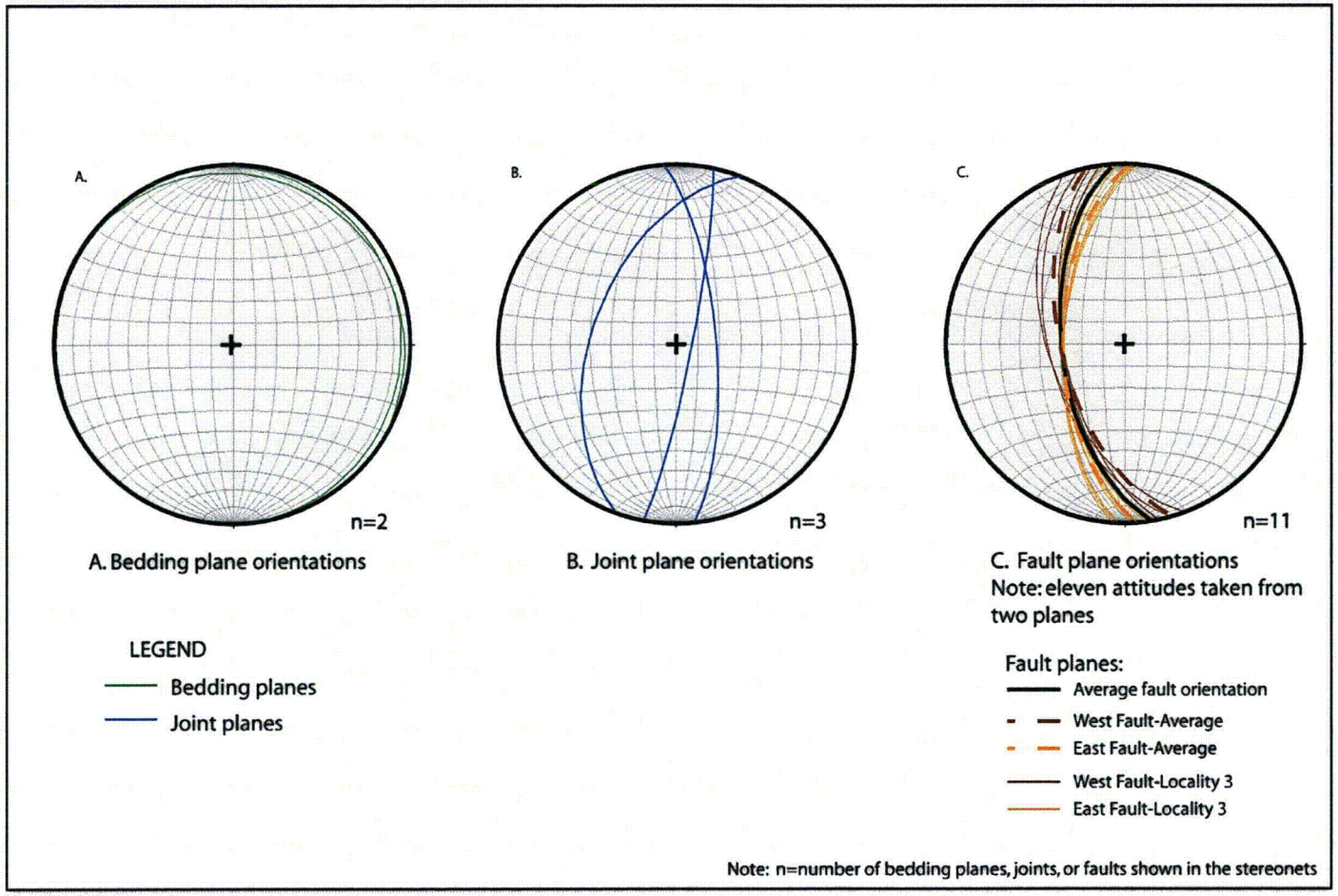

File path: S:\13300\13356_001\Figures\RAI Figures\RAI 02.05.01-29 Figure 16.ai; Date: [02/01/2010]

Figure 17. Orientations Estimated Using Ground-based LiDAR Survey at Locality 3

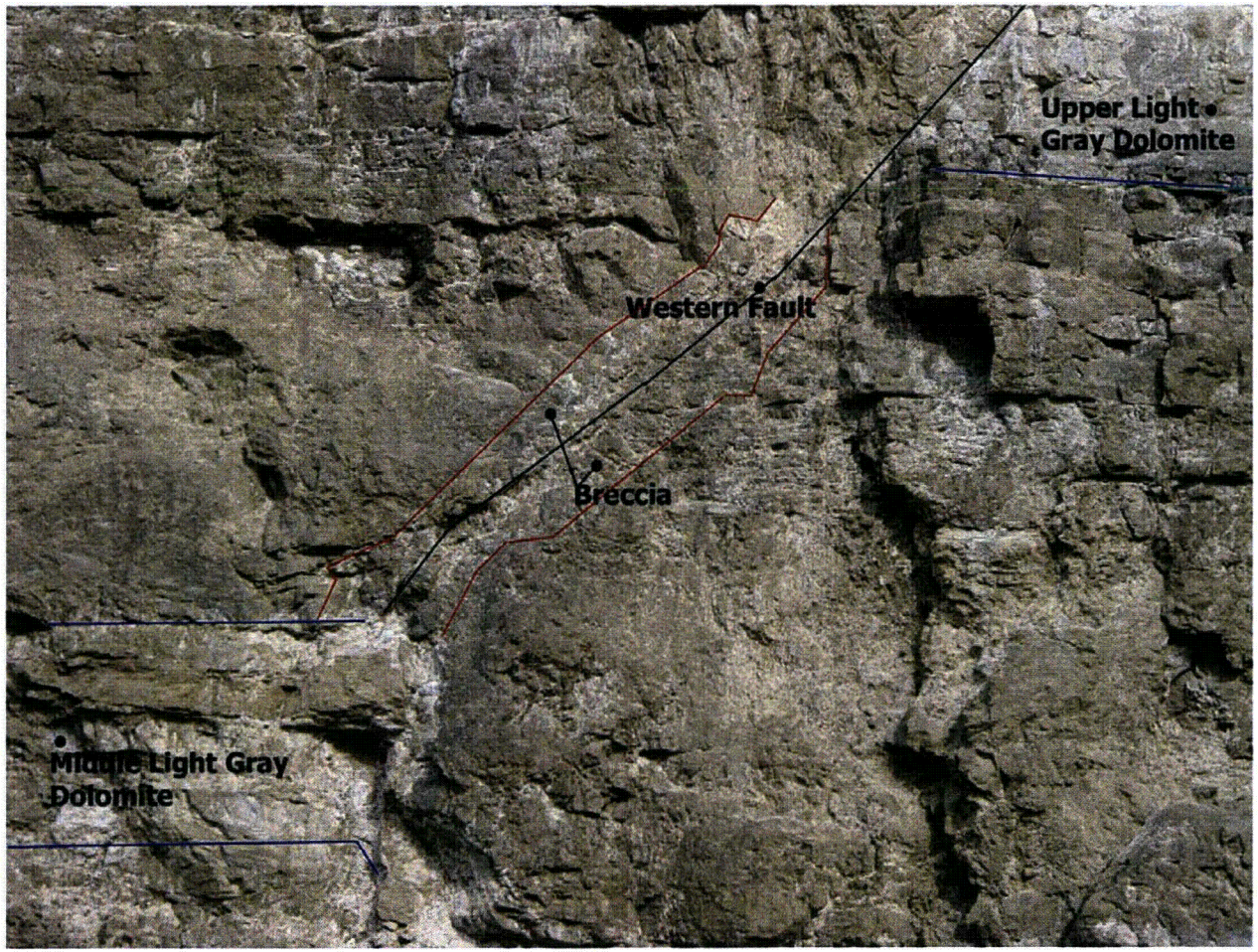

Figure 18. Photograph Showing Breccias (Possibly Paleokarst) Along the Western Fault at Locality 3

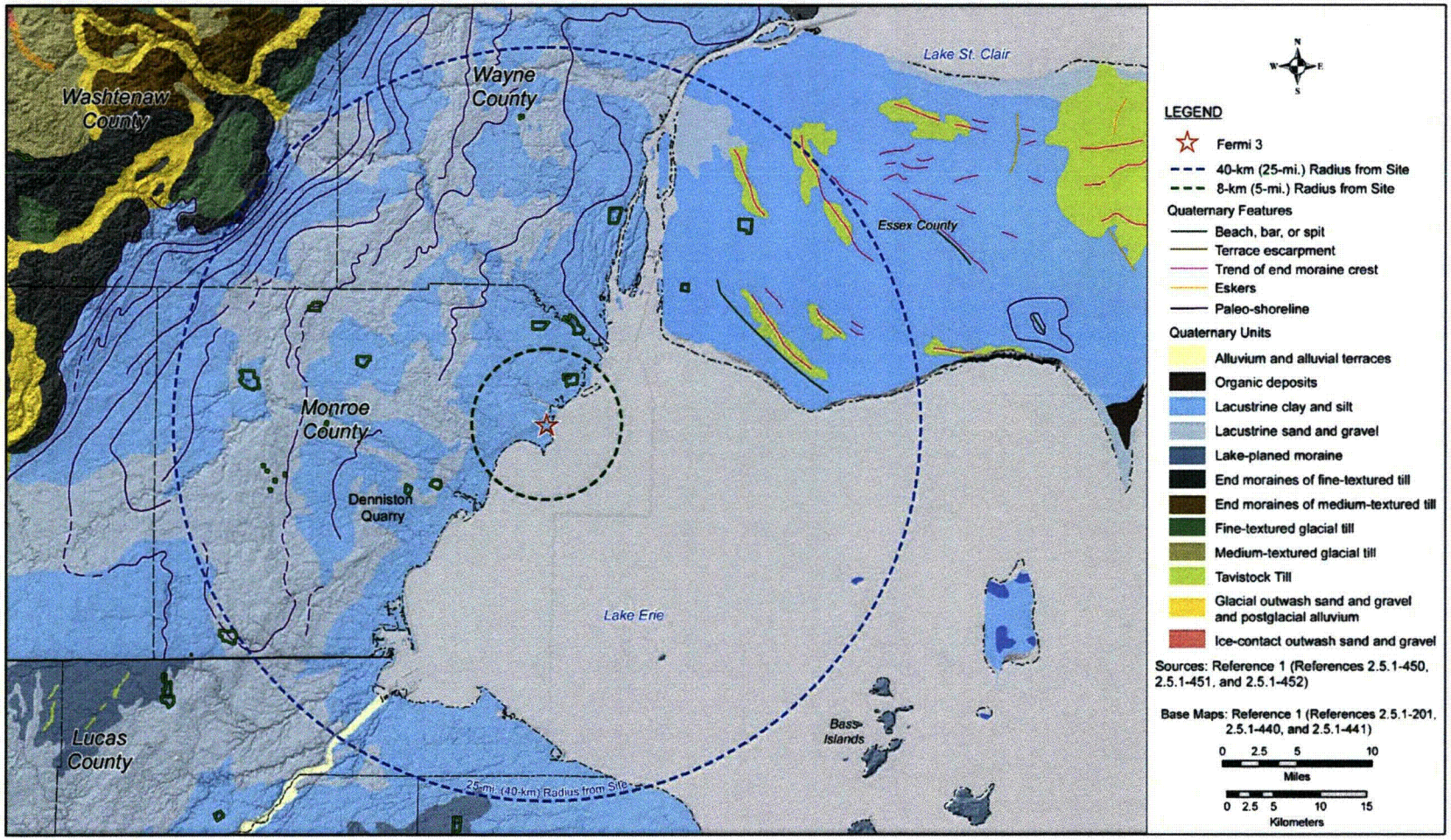

File path: S:\13300\13356_001\Figures\RAI Figures\RAI 02.05.01-29 Figure 19.mxd; Date: [01/19/2010]

Figure 19. Geologic Map Showing Quaternary Features of the Fermi 3 Site Vicinity

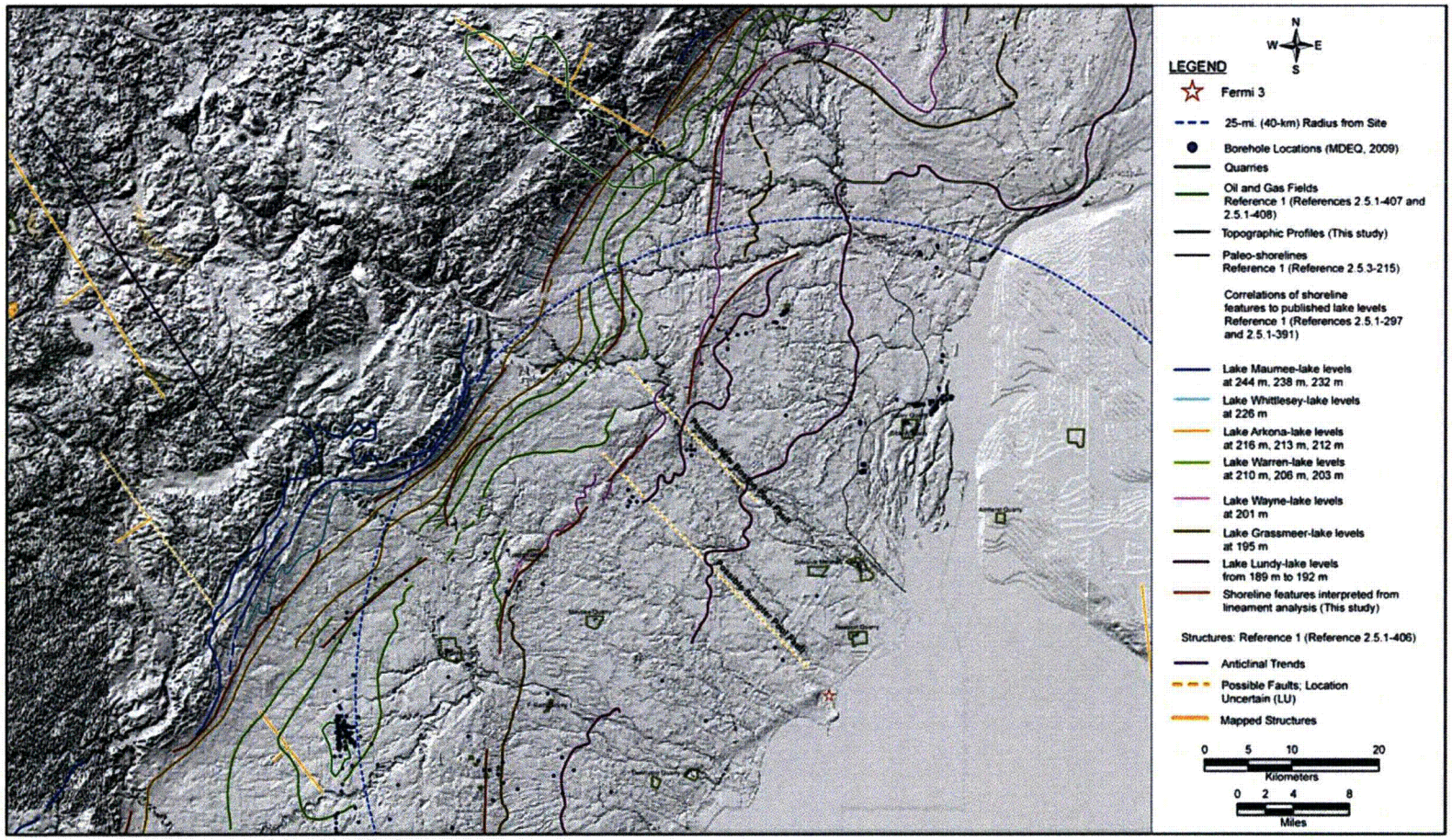

File path:S:\13300\13356_001\Figures\Revised_FSAR_Figures\DTE_FSAR_FIG02_05_01_256.mxd; Date: [02/01/2010]

Figure 20. Paleoshorelines and Structural Features in the Vicinity of the Fermi 3 Site

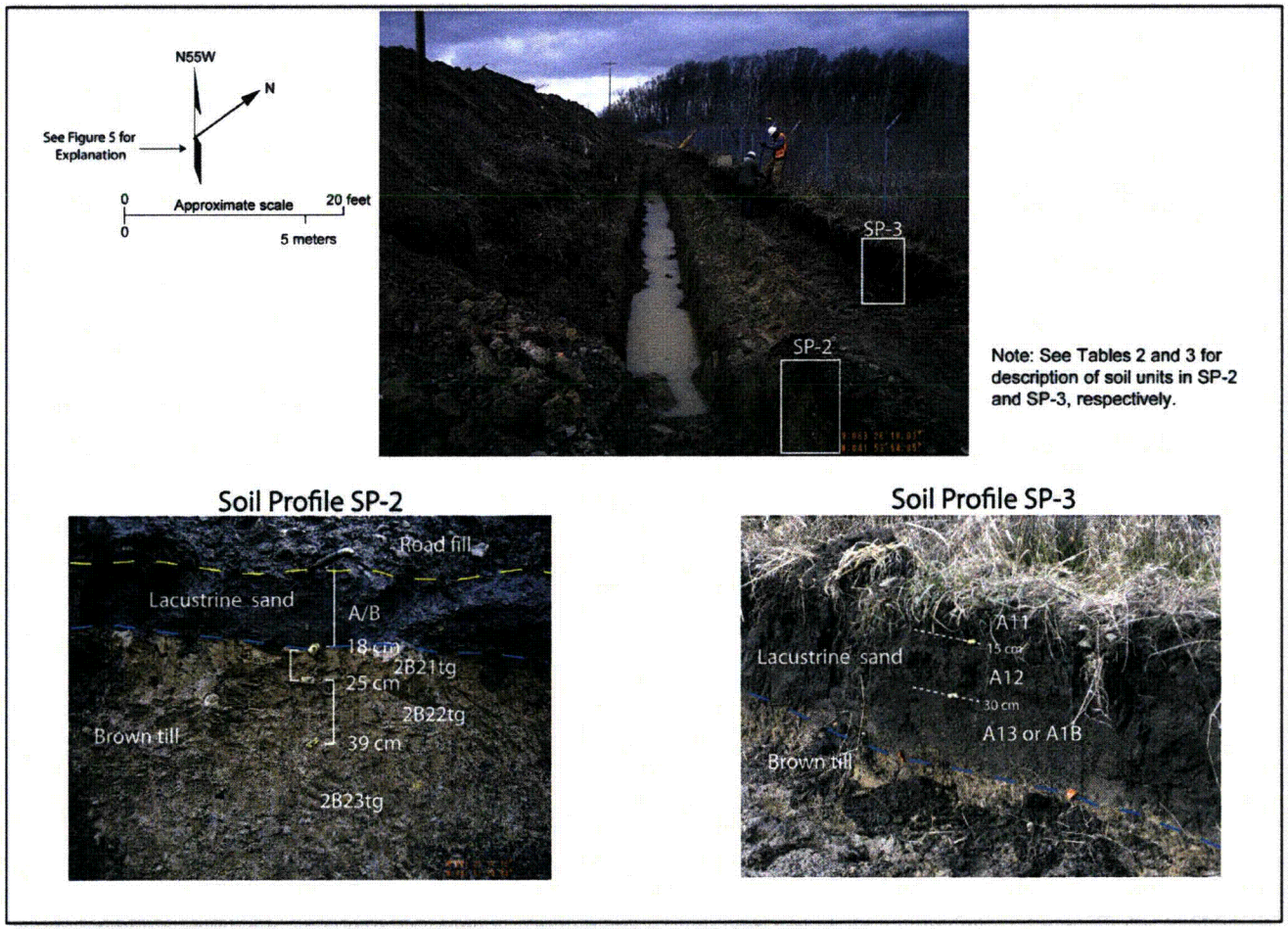

File path: S:\13300\13356_001\Figures\RAI Figures\RAI 02.05.01-29 Figure 21.ai; Date: [02/01/2010]; User:RC, AMEC Geomatrix, Inc.

Figure 21. Photographs Showing Quaternary Excavation QE-3 and Locations of Soil Profiles SP-2 and SP-3

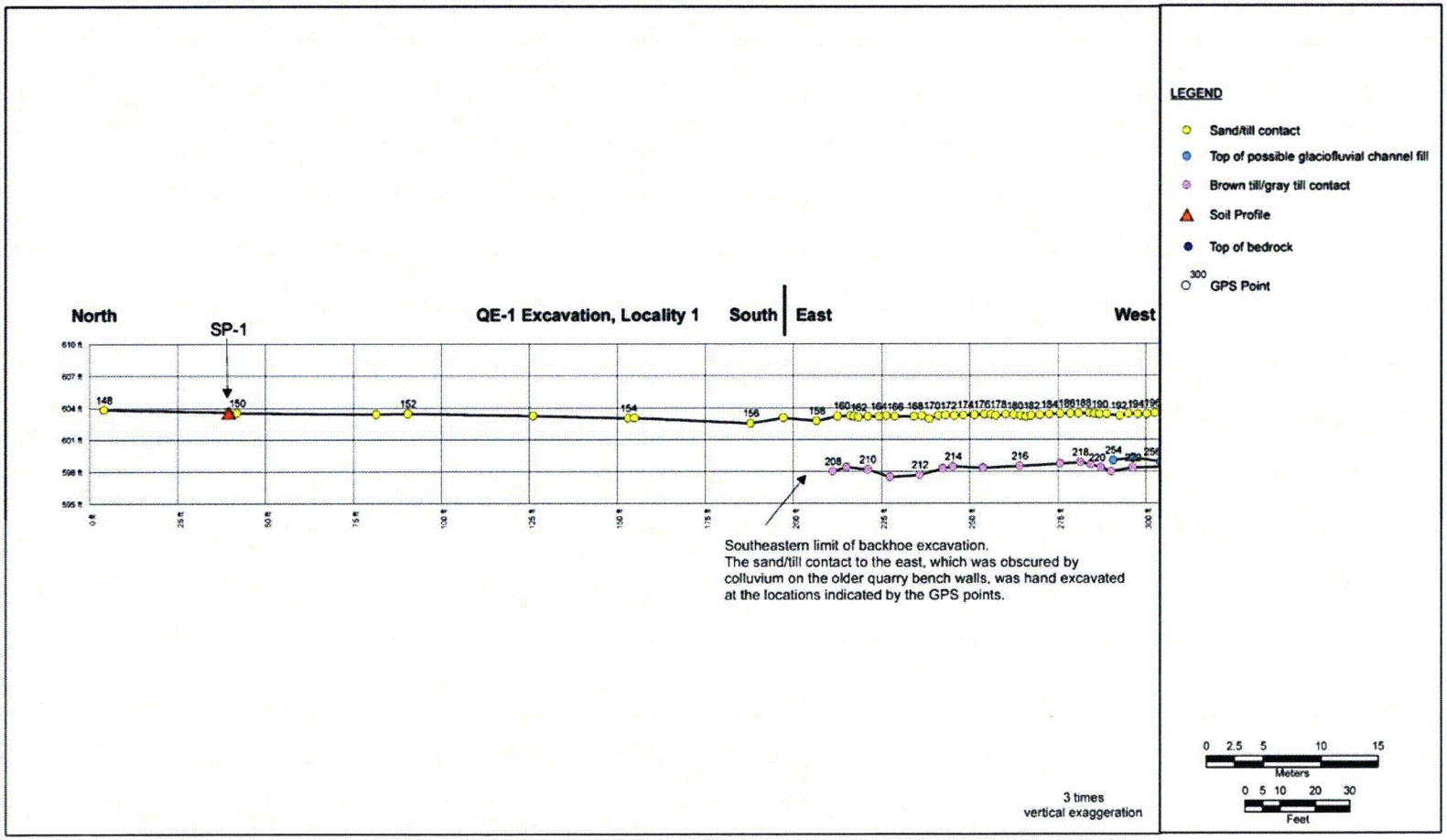

File path: S:\13300\13356_001\Figures\RAI Figures\RAI 02.05.01-29 Figure 22_Sheet 1.mxd; Date: [02/01/2010]; User:RC, AMEC Geomatrix, Inc.

Figure 22. Measured GPS Points for Stratigraphic Contacts in Quaternary Excavation QE-1, Locality 1 (Sheet 1 of 2)

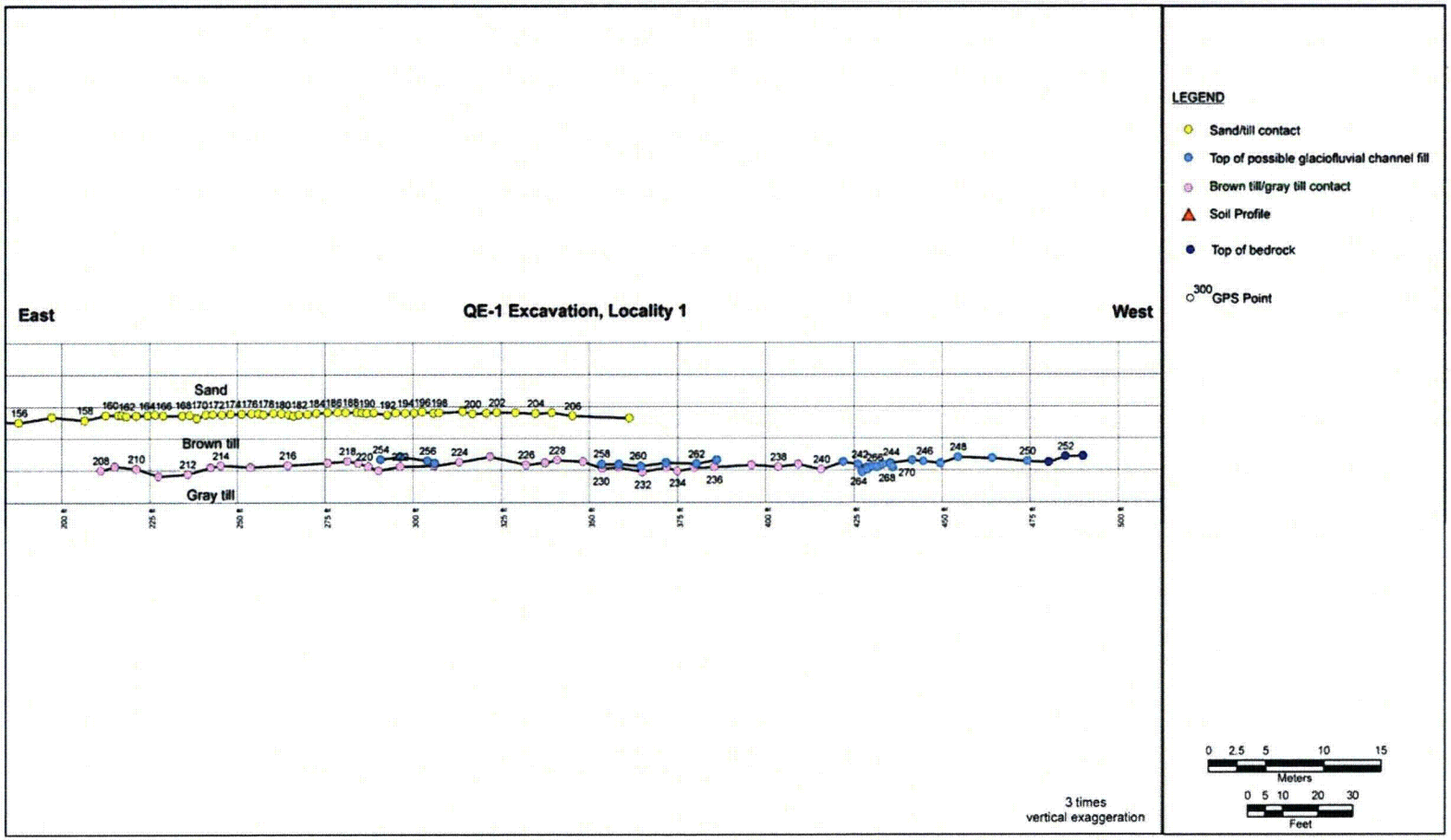

File path: S:\13300\13356_001\Figures\RAI Figures\RAI 02.05.01-29 Figure 22_Sheet 2.mxd; Date: [01/18/2010]; User:RC, AMEC Geomatrix, Inc.

Figure 22. Measured GPS Points for Stratigraphic Contacts in Quaternary Excavation QE-1, Locality 1 (Sheet 2 of 2)

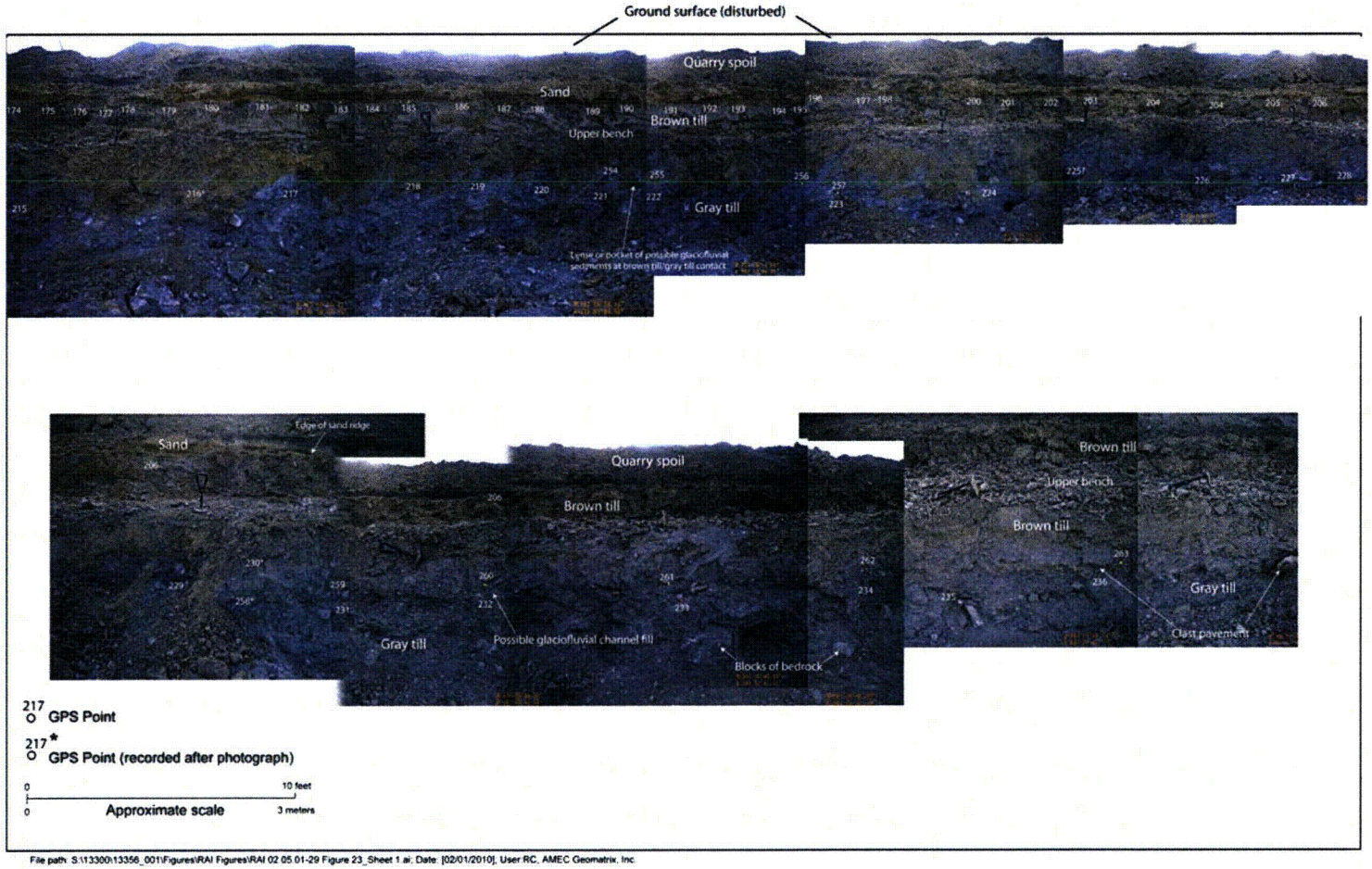

Figure 23. Photo-mosaic Showing Deposits Exposed in Quaternary Excavation QE-1 (Sheet 1 of 2)

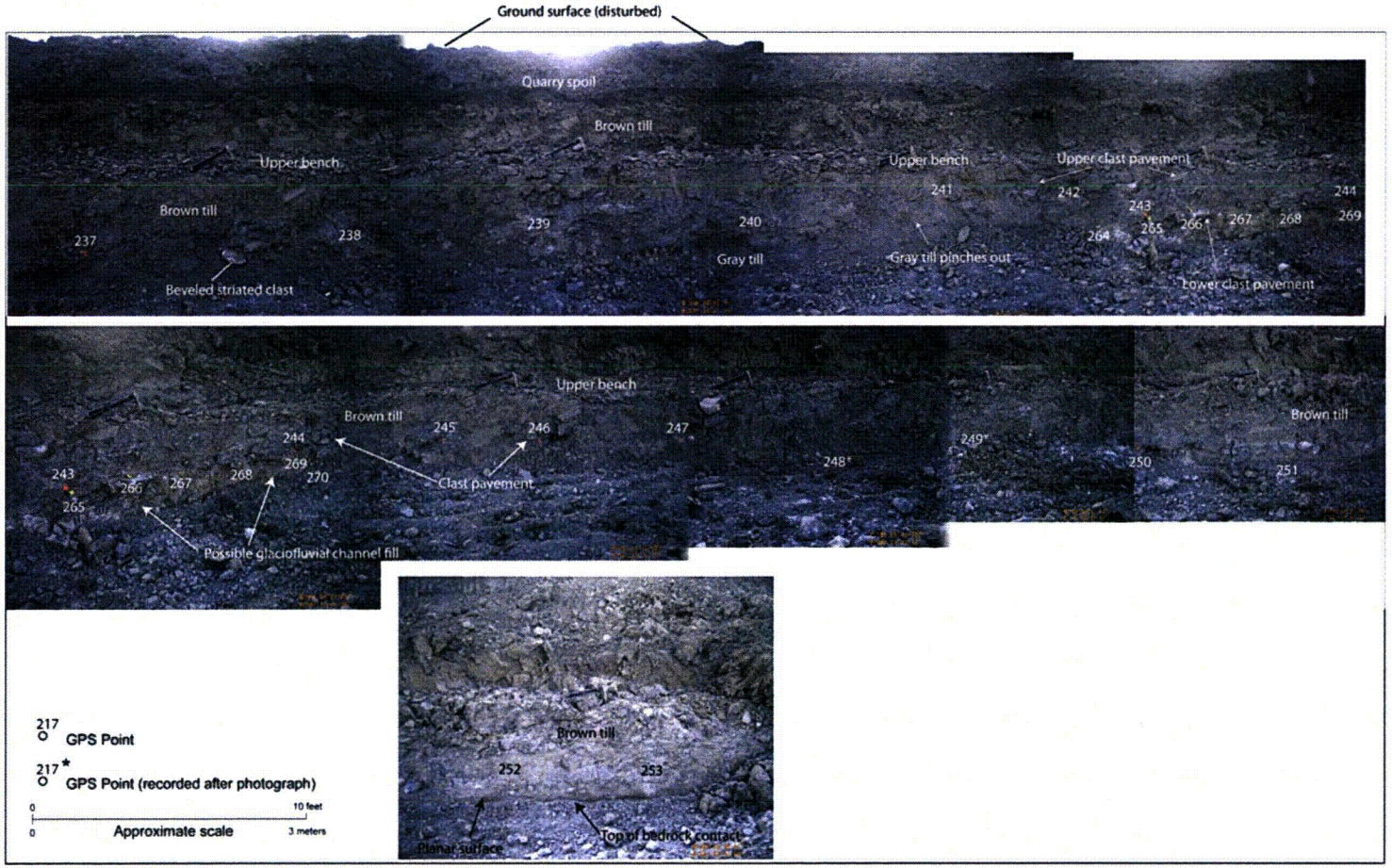

File path: S:\13300\13356_001\Figures\RAI Figures\RAI 02.05 01-29 Figure 23_Sheet 2.ai, Date: [01/18/2010], User RC, AMEC Geomatrix, Inc.

Figure 23. Photo-mosaic Showing Deposits Exposed in Quaternary Excavation QE-1 (Sheet 2 of 2)

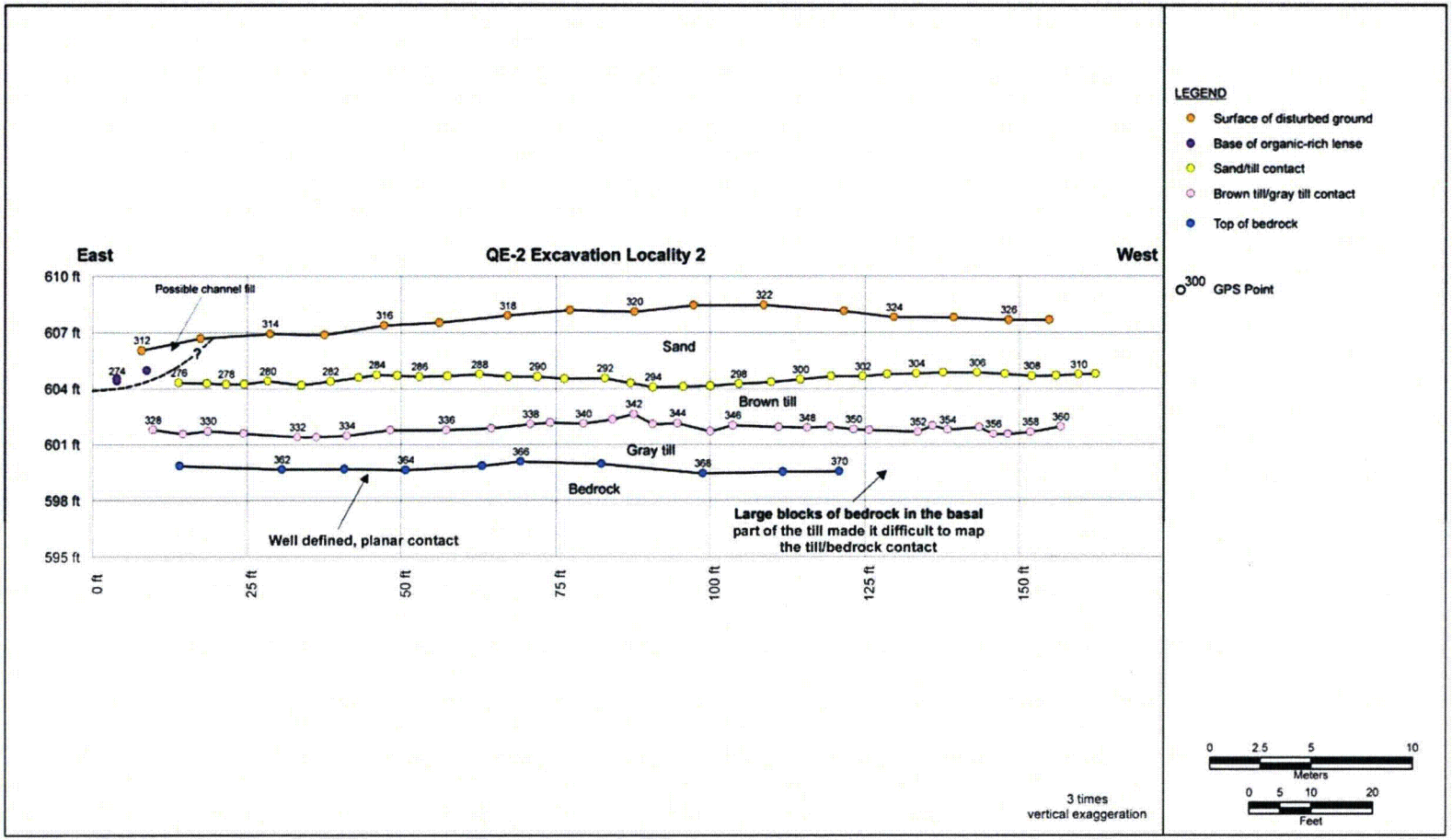

File path:S:\13300\13356_001\Figures\RAI Figures\RAI 02.05.01-29 Figure 24.mxd; Date: [02/01/2010]; User:RC, AMEC Geomatrix, Inc.

Figure 24. Measured GPS Points for Stratigraphic Contacts in Quaternary Excavation QE-2, Locality 2

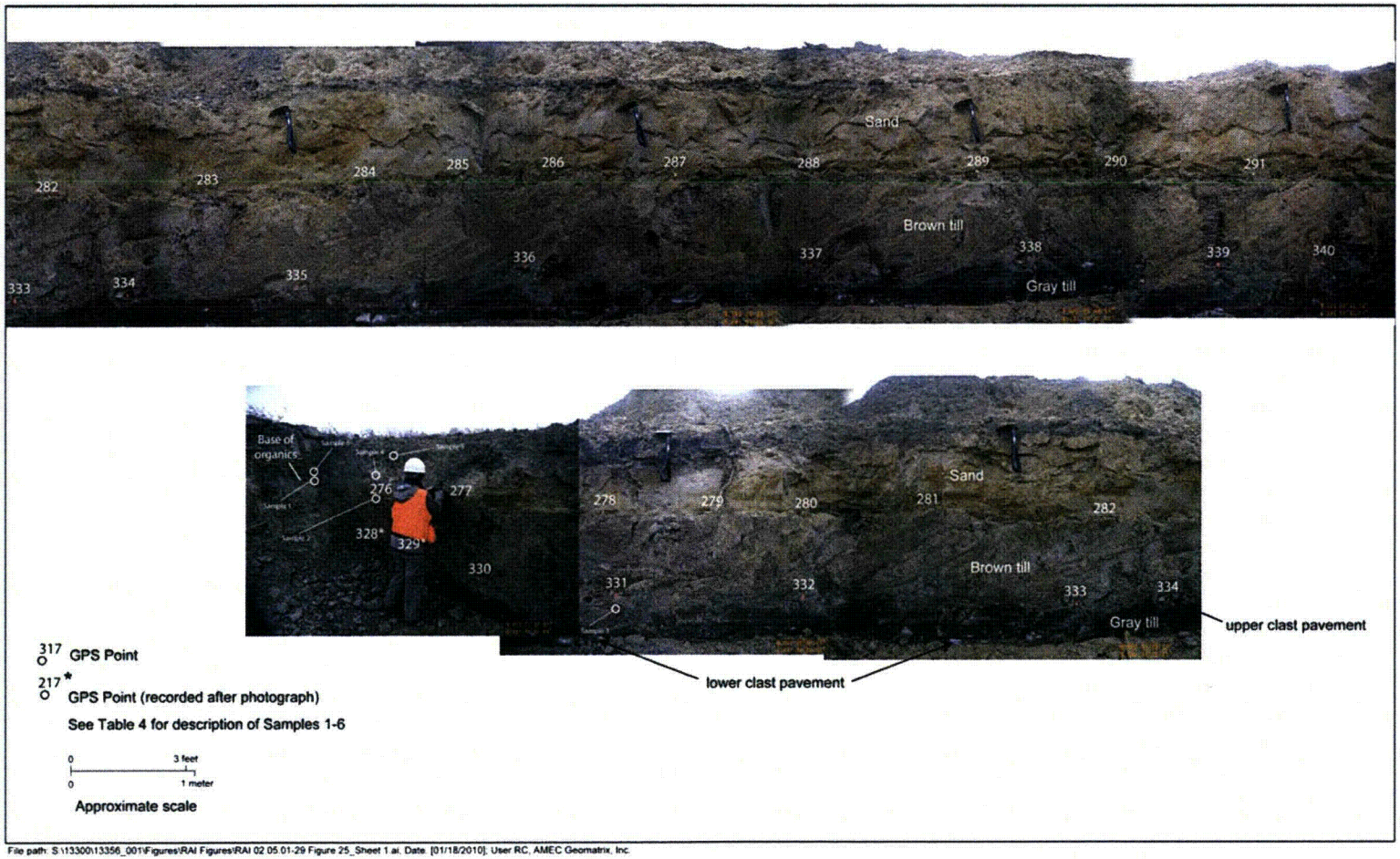

File path: S:\13300\13356_001\Figures\RAI Figures\RAI 02 05.01-29 Figure 25_Sheet 1 ai. Date: [01/18/2010]; User RC; AMEC Geomatrix, Inc.

Figure 25. Photo-mosaic Showing Deposits Exposed in Quaternary Excavation QE-2 (Sheet 1 of 2)

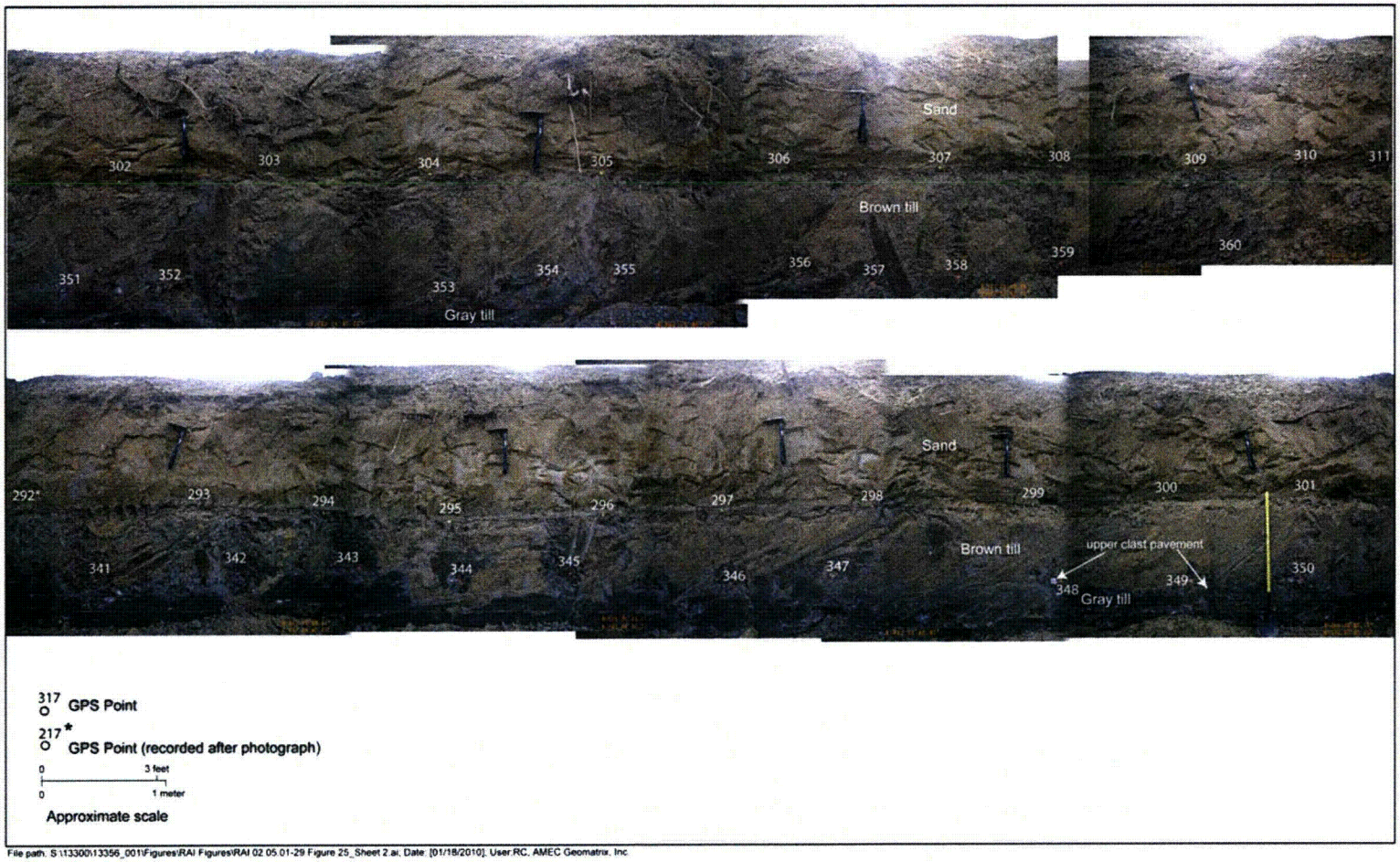

File path: S:\13300\13356_001\Figures\RAI Figures\RAI 02 05.01-29 Figure 25_Sheet 2.ai; Date: [01/18/2010]; User:RC; AMEC Geomatrix, Inc

Figure 25. Photo-mosaic Showing Deposits Exposed in Quaternary Excavation QE-2 (Sheet 2 of 2)

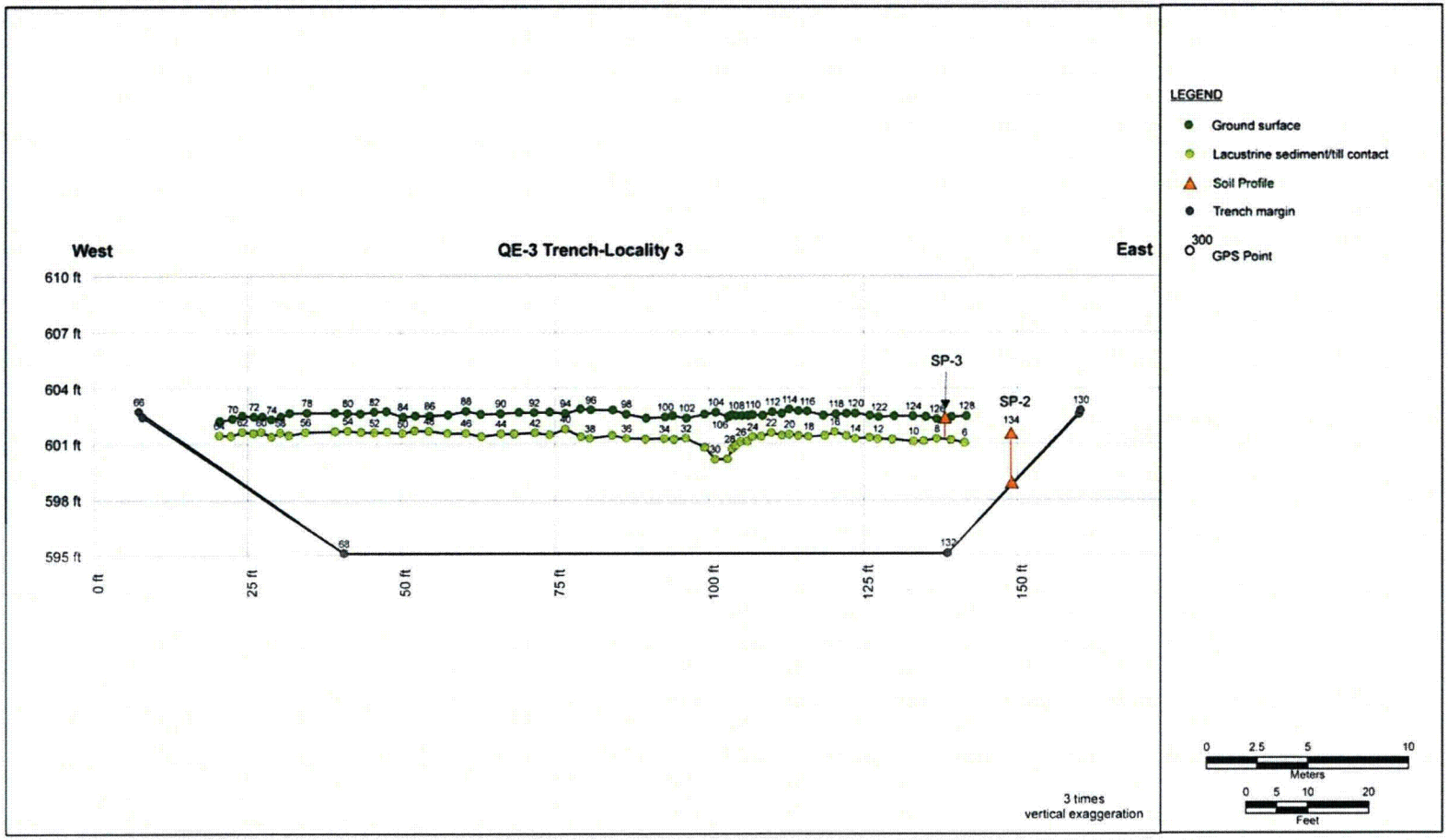

File path: S:\13300\13356_001\Figures\RAI Figures\RAI 02.05.01-29 Profile 3.mxd; Date: [02/01/2010]; User:RC, AMEC Geomatrix, Inc.

Figure 26. Measured GPS Points for Stratigraphic Contacts in Quaternary Excavation QE-3, Locality 3

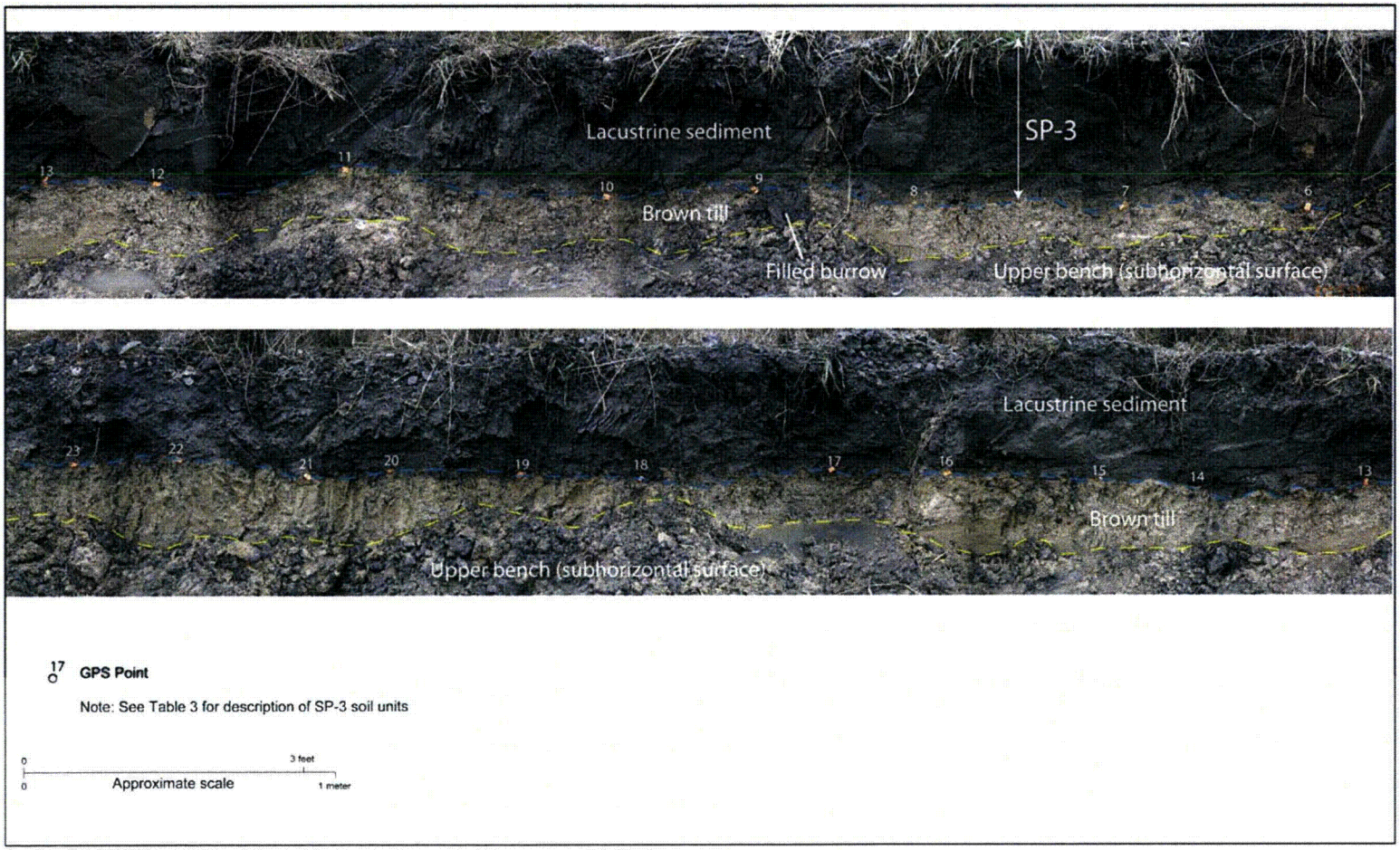

Figure 27. Photo-mosaic Showing Deposits Exposed in Upper Part of the Northern Wall of Quaternary Excavation QE-3 (Sheet 1 of 4)

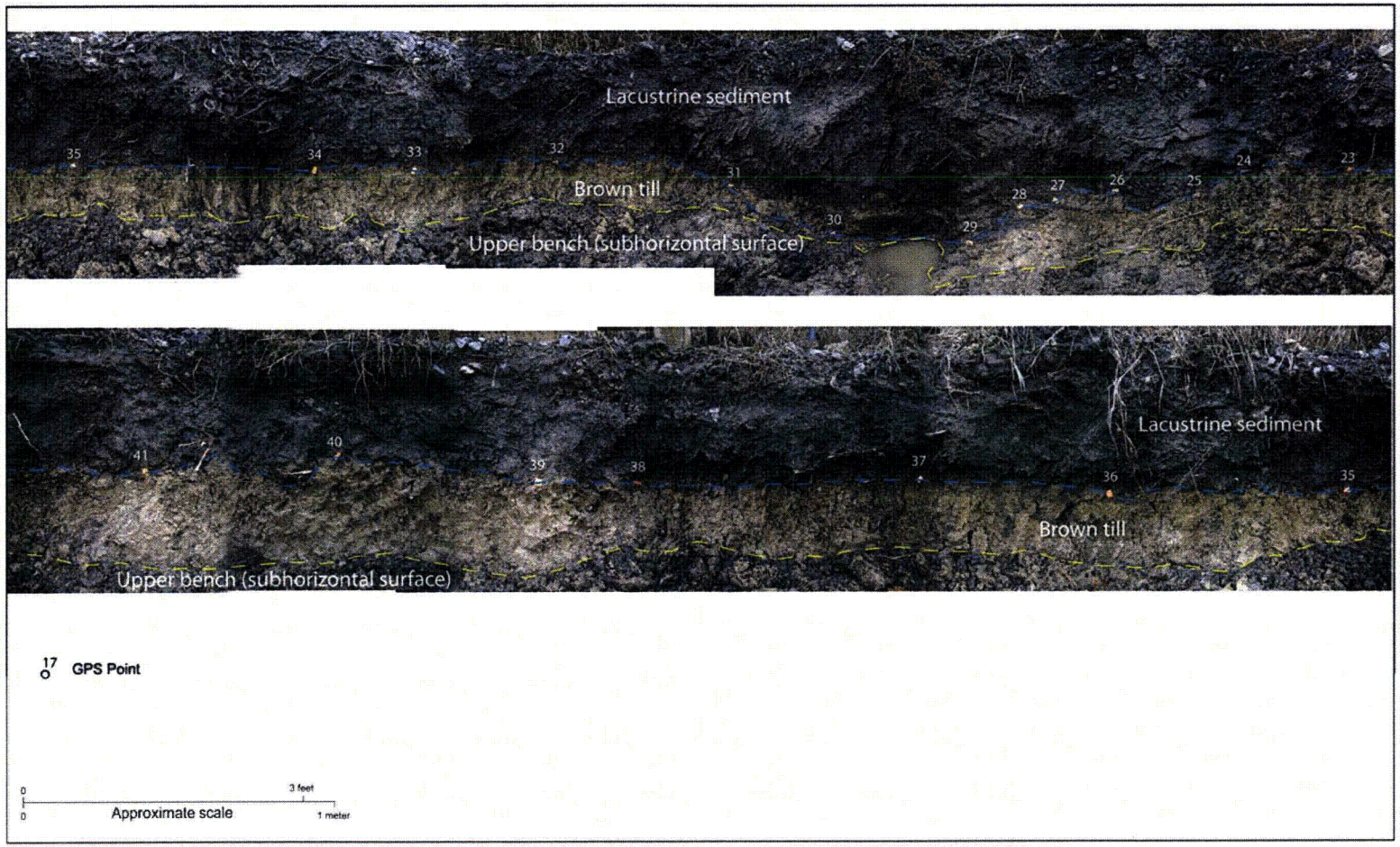

Figure 27. Photo-mosaic Showing Deposits Exposed in Upper Part of the Northern Wall of Quaternary Excavation QE-3 (Sheet 2 of 4)

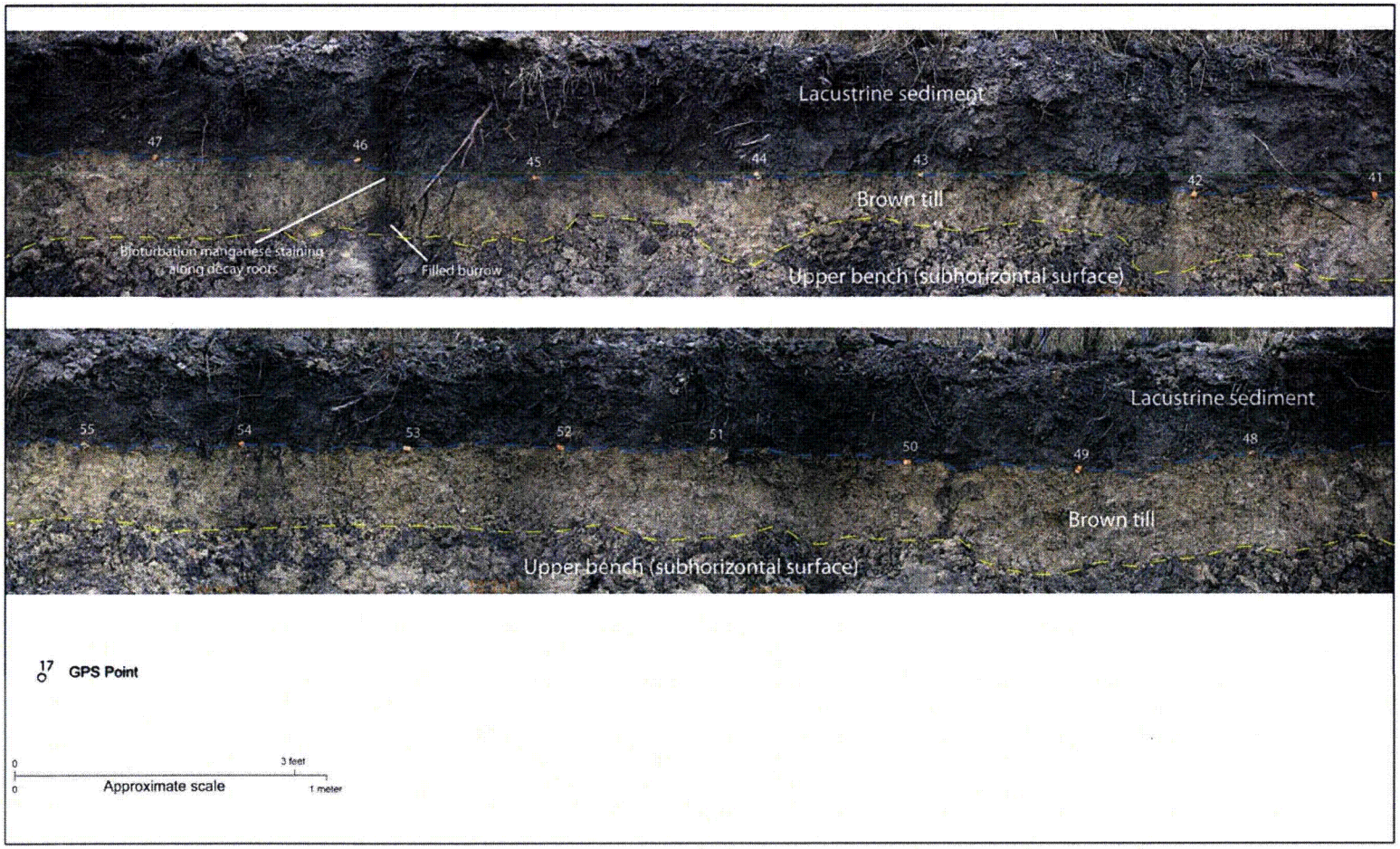

Figure 27. Photo-mosaic Showing Deposits Exposed in Upper Part of the Northern Wall of Quaternary Excavation QE-3 (Sheet 3 of 4)

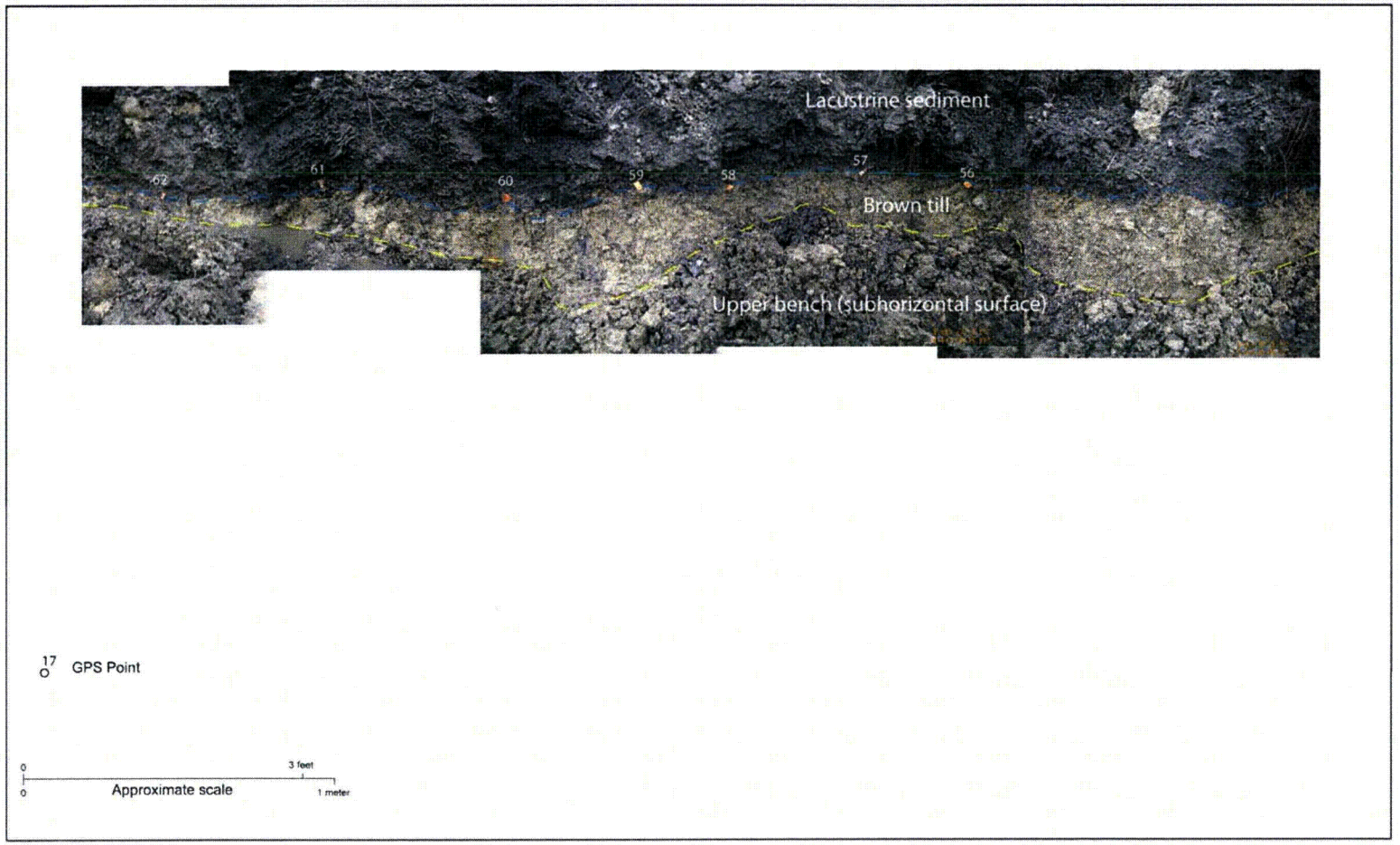

Figure 27. Photo-mosaic Showing Deposits Exposed in Upper Part of the Northern Wall of Quaternary Excavation QE-3 (Sheet 4 of 4)

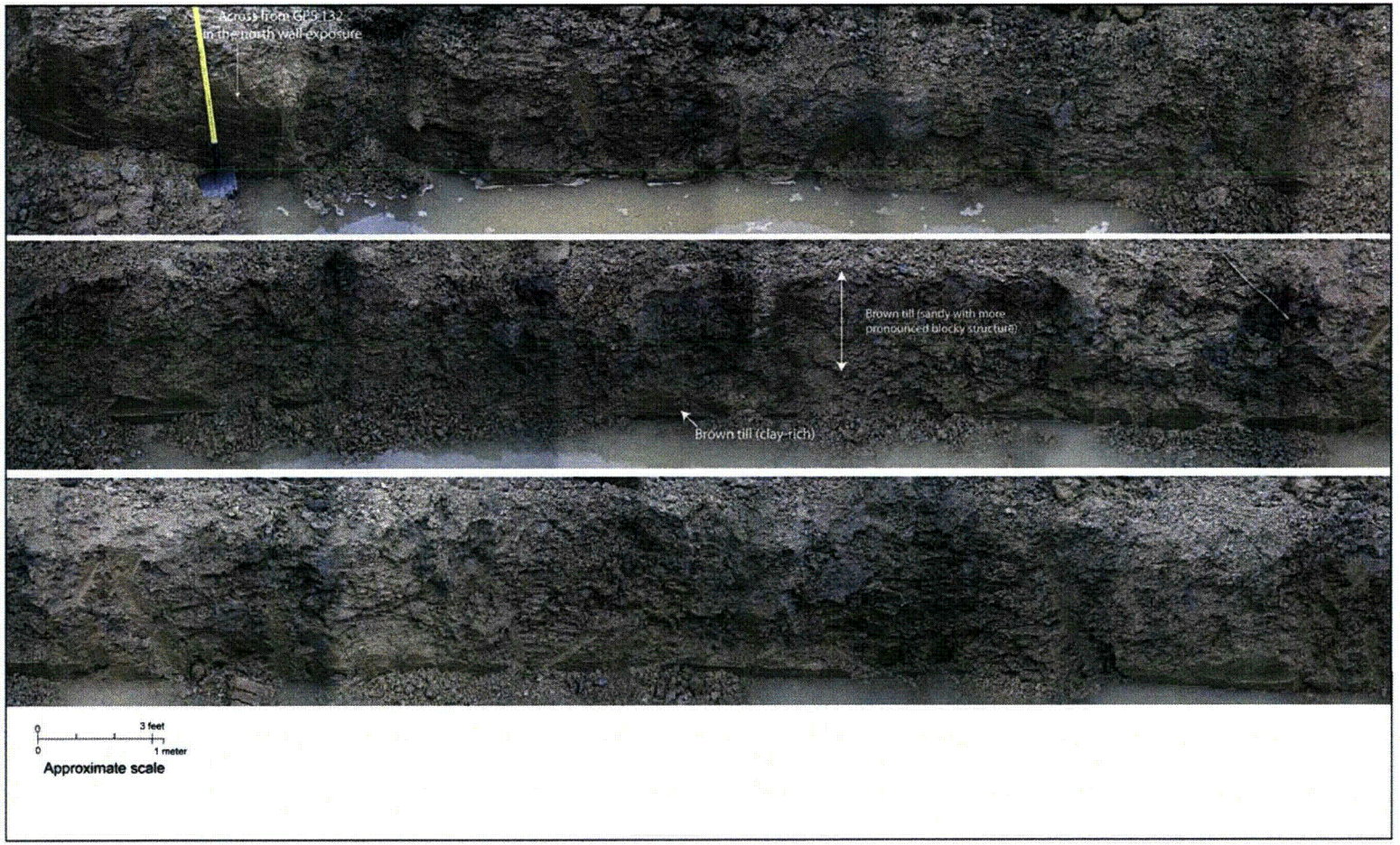

Figure 28. Photo-mosaic Showing Deposits Exposed in the South Wall of Quaternary Excavation QE-3 (Sheet 1 of 2)

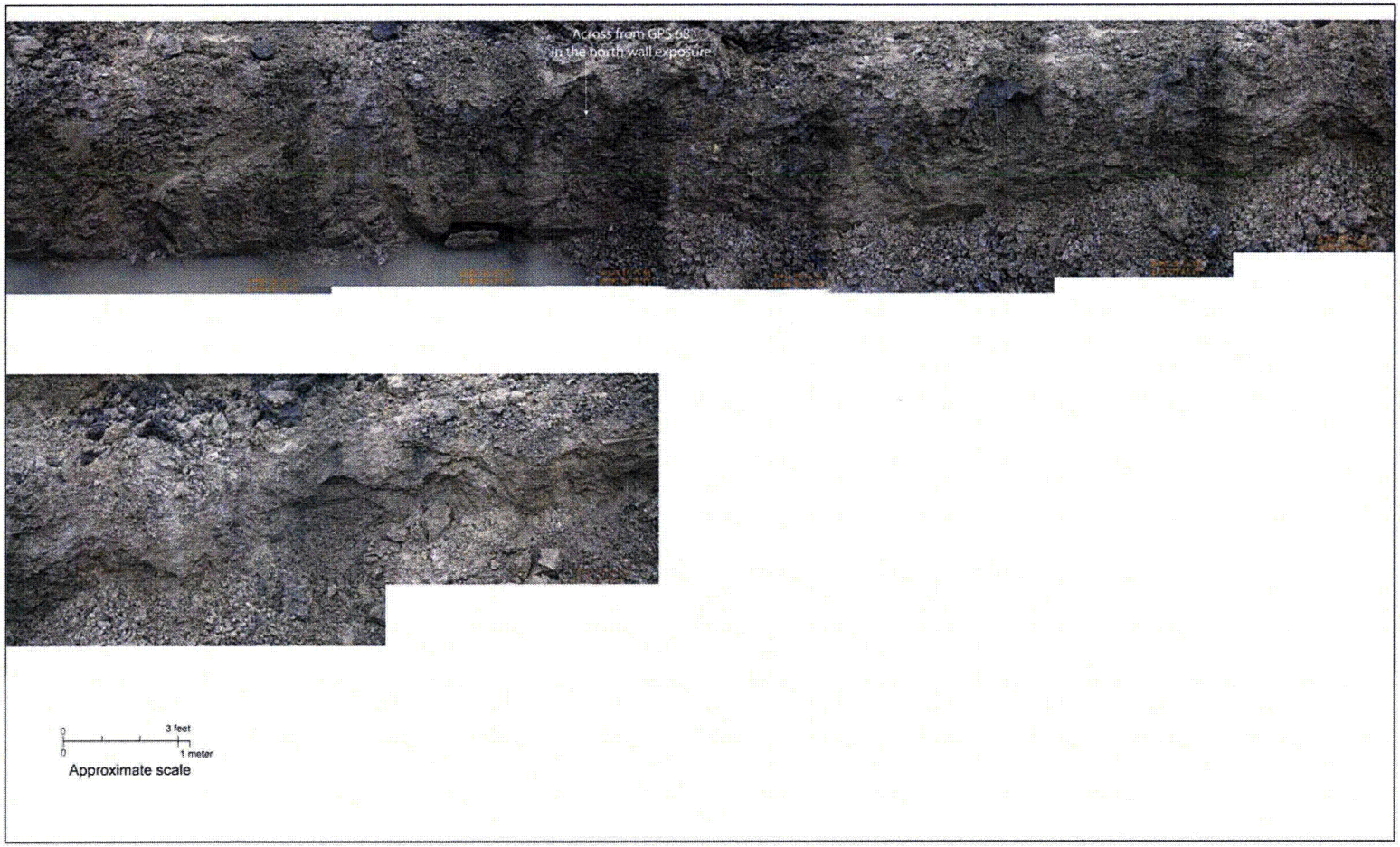

Figure 28. Photo-mosaic Showing Deposits Exposed in the South Wall of Quaternary Excavation QE-3 (Sheet 2 of 2)

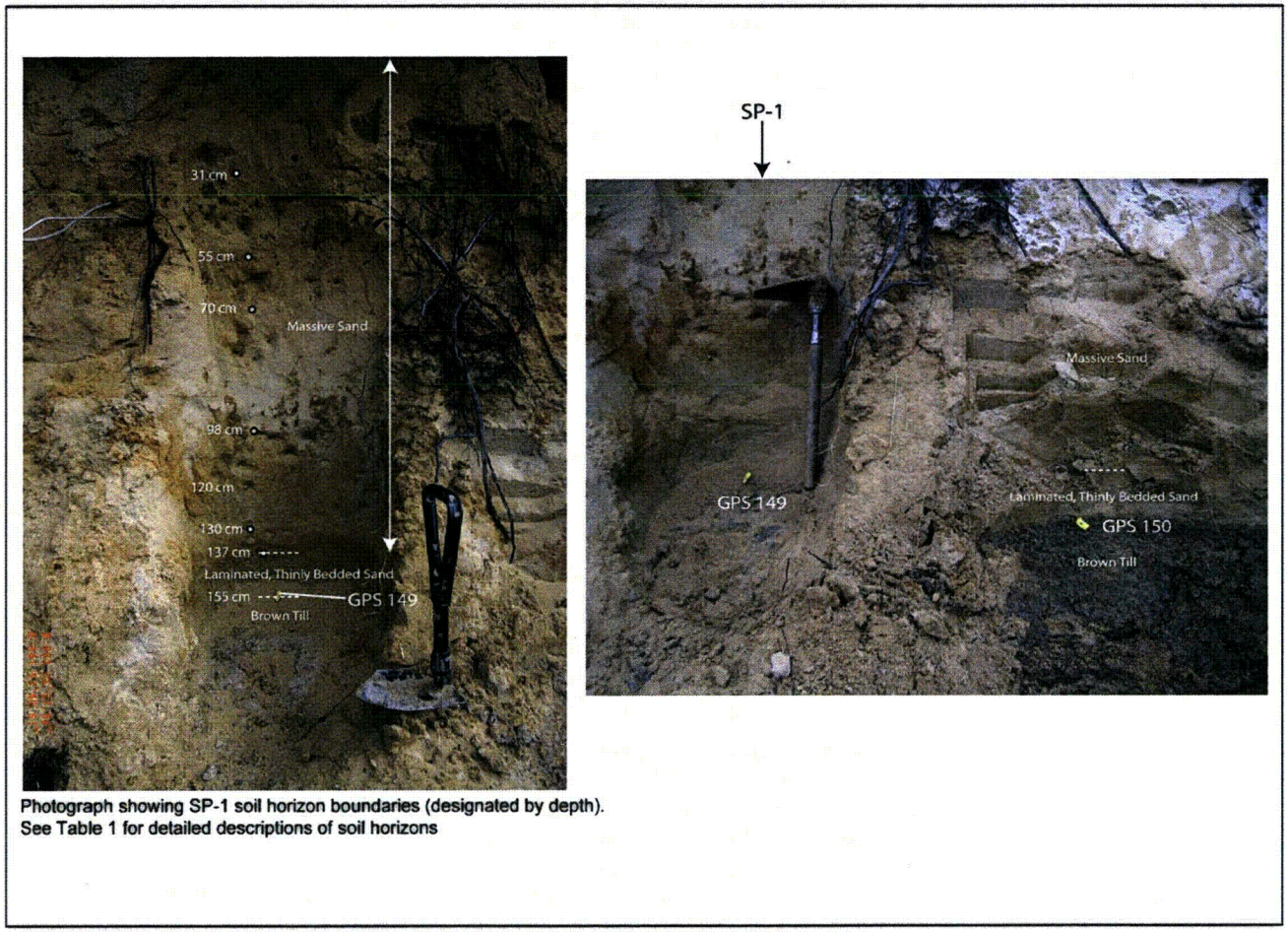

Photograph showing SP-1 soil horizon boundaries (designated by depth).
See Table 1 for detailed descriptions of soil horizons

File path: S:\13300\13356_001\Figures\RAI Figures\RAI 02.05.01-29 Figure 29.ai; Date: [02/01/2010]; User:RC, AMEC Geomatrix, Inc.

Figure 29. Photographs Showing Soil Profile SP-1 and the Sand/Till Contact at the Southeastern End of Quaternary Excavation QE-1 at Locality 1

Figure 30. Photograph Showing the North Wall of Quaternary Excavation QE-3